INTERACTIONS BETWEEN HIPPO, FGF, AND TGFβ SIGNALING REGULATE MORPHOGENESIS OF EARLY MOUSE EMBRYOS

By

Robin E. Kruger

A DISSERTATION

Submitted to
Michigan State University
in partial fulfillment of the requirements
for the degree of

Cell and Molecular Biology – Doctor of Philosophy

2023

ABSTRACT

Intercellular molecular signaling regulates every aspect of development, from the very first cell fate decisions to communication between complex organ tissues. Much of what we know about molecular regulation of development in mammals comes from studies of mouse embryos. In mice, the first cell fate decision, which separates the outer, multipotent trophectoderm cells from the pluripotent inner cell mass, is regulated by the Hippo signaling pathway. It is known that silenced Hippo signaling in the outer cells maintains the cells' polarity; however, my studies show that Hippo signaling does not direct the initiation of cell polarization in mouse embryos. The second cell fate decision in mouse embryos differentiates the inner cell mass into pluripotent epiblast and multipotent primitive endoderm. The Bone Morphogenic Protein (BMP) signaling pathway has been suggested to regulate preimplantation cell fate at this stage; however, I show that preimplantation lineage specification appears normal in mouse embryos that lack maternal and zygotic *Smad4*, an essential effector of canonical BMP signaling. Rather, my findings point to a previously unrecognized role for SMAD4 during early post-implantation stages, in which SMAD signaling restricts FGF signaling to promote epiblast growth and morphogenesis. In addition to these novel regulatory mechanisms in early cell fate, I present three technological advances in the study of early development, using recombinant fluorescent markers, more specific markers of pluripotency in reprogrammed stem cells, and ultra-low-input CUT&RUN to identify transcription factor binding sites in embryos. Altogether, these studies uncover novel mechanisms of cross-talk between regulatory pathways in development and present new strategies to investigate future questions in developmental biology.

ACKNOWLEDGEMENTS

First of all, I want to thank every member of the Ralston Lab for making my time in graduate school such a wonderful experience. I really could not have asked for a more supportive, fun, and smart group of people to spend five years with. Amy, you've taught me more than I thought possible. With your mentorship and guidance I've learned what it takes to be a scientist, but also what it takes to be a true mentor and a leader. Thank you for always being my advocate and for helping mold me into a well-rounded scientist. I hope I make you proud! Jenn, Alex, Tristan, and Dan, thank you for being my mentors and for teaching me the skills I needed to succeed in the lab. Barb, thank you for always being friendly and patient while fixing all my lab crises. And finally, my fellow labmates Tayler, Farina, Marcelio, Shannon, Ian, and Alyssa: you guys have been amazing friends through all of this. Every one of you have made me laugh, made me smile, helped me with experiments, debated science with me, and have helped me grow as a mentor, as a scientist, and as a person. I can't wait to see where all your successes take you in life!

I also want to thank the people who have made my professional development in graduate school a success. Thank you to the members of my guidance committee, Dr. Aitor Aguirre, Dr. Ingo Braasch, Dr. Chen Chen, and Dr. Almudena Veiga-Lopez, for your invaluable advice and support. Thank you to the Reproductive and Developmental Science Training Program (NIH T32 HD087166) to the directors, Dr. Keith Latham and Dr. Asgi Fazleabas, and to the coordinator Laurie Felton, for supporting my scientific training and giving me so many opportunities to share my work and improve as a

developmental biologist. A special thank you to the Cell and Molecular Biology program, my graduate director Dr. Peggy Petroff, and academic coordinator Alaina Burghardt. Thank you so much for your support, for handling all my crises, and for saying yes to all my crazy ideas. You do an incredible job making your students feel like they matter, and that is so critical in helping them succeed. I really felt like I found a home in CMB, and I wish all the best for everyone in the program!

I want to say a special thank you to the organizations I've been a part of during my time in graduate school for their support to my professional development: Graduate Women In Science Mid-Michigan, Cell and Molecular Biology Graduate Student Organization, and the Student Faculty Staff Hearing Board. Each one of these groups has taught me about what it takes to be a leader, to relate to people, to communicate effectively, and to take responsibility for a project from start to finish.

Last but not least, I need to thank my amazing friends and family who helped me get to this point in my life. I cannot tell you how much your love and support have meant to me. Mom and Dad, thank you so much for always believing that I could do anything. You are the world's best parents and I love you so much! Grandma and Grandpa, thank you so much for your love and support for everything I do. You've been a huge inspiration for me going into science, and I really appreciate how much you care about my work. Megan, you're the best sister anyone could ask for, thank you for all the things you do for me! My frieNDs, Bella, Cristina, Danielle, Emma, Laura, and Mara: you guys have been an amazing support system for me ever since we met, and the fact that we

are all still so close means the world to me. Skimble and Leia, thanks for sticking by me through everything and being my very best listeners. And finally, my wonderful husband, Adam Kruger. I truly would not have been able to do this if it were not for you. Thank you for everything, from moving with me to Lansing, to putting up with my unpredictable hours and weird nerdy science stuff, to just knowing how to cheer me up when things were tough. I hope you’re ready to be married to a doctor! To everyone mentioned and anyone else who has helped me through this journey, I can’t thank you enough for your guidance, love, and support.

TABLE OF CONTENTS

LIST OF ABBREVIATIONS

AP	Alkaline phosphatase
AVE	Anterior Visceral Endoderm
BMP	Bone Morphogenic Protein
BRE	BMP Response Element
BSA	Bovine Serum Albumin
CTB	Cytotrophoblast
DVE	Distal Visceral Endoderm
E	Embryonic Day
EMT	Epithelial-to-Mesenchymal Transition
EPI	Epiblast
ESC	Embryonic Stem Cell
EVT	Extravillous Trophoblast
ExE	Extraembryonic Ectoderm
FBS	Fetal Bovine Serum
FGF	Fibroblast Growth Factor
hCG	Human Chorionic Gonadotrophin
HuF	Human Stromal Fibroblasts
ICM	Inner Cell Mass
IFNT	Interferon Tau
iPSC	Induced Pluripotent Stem Cell
iXEN	Induced Extraembryonic Endoderm
LDN	LDN-193189, ALK3/6 inhibitor

m null	Maternal null
MenSC	Menstrual Stem Cell
mz null	Maternal-zygotic null
PE	Parietal Endoderm
pERK	Phosphorylated ERK protein(s)
PGC	Primordial Germ Cell
PrE	Primitive Endoderm
PS	Primitive Syncytium
pSMAD	Phosphorylated SMAD protein(s)
PV	Placental Villi
PVA	Polyvinyl alcohol
r-SMAD	Receptor-associated SMAD protein
RTK	Receptor Tyrosine Kinase
SSC	Spermatogonial Stem Cell
STB	Syncytiotrophoblast
T	Brachyury
TE	Trophectoderm
TGFβ	Transforming Growth Factor beta
VE	Visceral Endoderm
XEN	Extraembryonic Endoderm

CHAPTER 1.

MOLECULAR SIGNALING MECHANISMS REGULATING MURINE PRE- AND POST-IMPLANTATION EMBRYONIC CELL FATE DECISIONS

This study was supported by the National Institutes of Health R35 GM131759 and T32 HD087166.

Section 1.1. Abstract

The study of embryonic development is critical to understanding the basic functions of stem cells and to determine the factors which promote the birth of healthy offspring. Most current knowledge of mammalian embryogenesis has come from decades of study into the most widely-used model: the mouse embryo. In this chapter, I introduce the morphological and molecular changes that occur during the first week of embryonic development in mice, from fertilization to gastrulation. I focus on the regulation of these early developmental processes by molecular signaling pathways, with an emphasis on the roles of Hippo, Fibroblast Growth Factor, and Bone Morphogenic Protein signaling.

Section 1.2. Overview of mouse embryogenesis and early cell fate specification

1.2.1. Introduction to mouse development

The study of development is the study of life itself. All multi-cellular organisms must go through developmental processes to reach reproductive maturity and pass their genetic material to their progeny. For complex organisms such as mammals, this process requires a single cell, the zygote, to divide and differentiate to derive hundreds of specialized cell types. These cell types not only need to specify properly during development, but also communicate and organize with one another as they expand to generate highly organized tissues, organs, and organ systems. By studying development, researchers can begin to understand the etiology of developmental abnormalities such as congenital disorders, pre-term birth, miscarriage, and infertility. These can be used to improve strategies for assisted reproductive therapies. Similarly, information gleaned from studies of natural development can be used to improve stem

cell models of embryos, tissues, and organs for uses in research, stem cell therapies, and personalized medicine (Rosner et al., 2021; Wallingford, 2019).

Laboratory mice are the most common research models for the study of mammalian development. In humans, the process of embryonic development takes approximately 40 weeks; for mice, development from fertilization to birth takes 18-22 days (Murray et al., 2010). Despite the differences in timing, embryonic development in mice and humans is remarkably similar, going through similar processes in the same order and importantly, specifying many of the same cell types (Gupta et al., 2021; Taft, 2008). Developmental timepoints in mice are described by the number of days since fertilization, denoted by Embryonic Day (E). E0 is the moment of fertilization, which in nocturnal animals such as mice, typically occurs at night. After mating, male mice leave a waxy plug in the vaginal opening, allowing researchers to know when fertilization has occurred and to precisely determine the developmental stage of embryos developing internally. As a convention, mating is assumed to occur at midnight in laboratory tests, designating noon of the day the plug is detected as E0.5. This notation will be used throughout this work to designate developmental staging in mouse embryos.

In this chapter, I describe the developmental processes that occur during embryogenesis in mice (Fig. 1.1). In particular, I focus on the stem cell progenitor types which emerge in the earliest cell fate decisions of embryogenesis and the populations they give rise to during early post-implantation development. I also discuss the molecular signaling mechanisms that regulate stem cell fate specification and

differentiation, with an emphasis on Hippo, Fibroblast Growth Factor (FGF), and Bone Morphogenic Protein (BMP) signaling. Though I focus on mouse development, many of the cell types and processes are similar to human development, showing a high degree of evolutionary conservation between these two species in their developmental progression.

1.2.2. Molecular mechanisms regulating developmental stages and processes in murine preimplantation development

E0-E2.5: Cleavage divisions and zygotic genome activation

An overview of mouse preimplantation development is important not only because the processes are very similar in human embryos, but also to provide the necessary context for the discussions of molecular signals regulating development presented in Chapters 2 and 4 of this work. The developmental processes in mouse embryos before the embryo implants into the uterine wall (E0-E4.5) are very well-characterized. Preimplantation development begins at fertilization, when the gametes of sperm and egg fuse to create a diploid zygote. The murine zygote is surrounded by a protective glycoprotein layer called the zona pellucida, which persists around the outside of the embryo throughout preimplantation development (Rankin et al., 2000). Similar to other species, the genome of the murine zygote is initially silenced, and embryonic development relies on maternally-derived mRNA transcripts and proteins deposited into the oocyte for early cellular activity (Cockburn & Rossant, 2010). Zygotic genome activation (ZGA) occurs at E1.5 after the first cleavage division into a 2-cell embryo, and >90% of maternal transcripts are degraded at this point (L. Li et al., 2010). However,

maternally-derived proteins may persist to the blastocyst stage and the effects of maternal proteins, such as chromatin modifications, may direct development even after the proteins themselves have been degraded (F. Chen et al., 2022; Israel et al., 2019; L. Li et al., 2010; D. Wu & Dean, 2020; H. Zhang et al., 2023). This is important because it poses an added layer of redundancy for researchers to consider when examining gene function in early embryos; even if both copies of a gene are knocked out in the zygotic genome, early phenotypes may be masked by compensation from maternally-derived transcripts and proteins. To completely eliminate a gene at this stage, it is necessary to create a maternal and zygotic loss-of-function model (Cockburn & Rossant, 2010). One strategy to create such a model is described in Chapter 2.

E2.5-E3.0: Compaction, polarization, and the first cell fate decision regulated by Hippo signaling

After fertilization, successive cell divisions in the embryo lead to morphological changes and corresponding decreases in developmental potential. The single-celled zygote is totipotent, meaning it has the potential to give rise to all cells in the embryo, both embryonic and extraembryonic (Chazaud & Yamanaka, 2016). In mice, totipotency persists through three embryonic cleavage events until the embryo consists of 8 cells, or blastomeres. At that point, around E2.75, the 8-cell embryo undergoes a significant morphological change known as compaction. During compaction, cell-cell contacts between blastomeres increase dramatically. E-cadherin becomes enriched at adherens junctions between cells to form the basis of a basolateral domain toward the center of the embryo (Sozen et al., 2014). Accumulation of E-cadherin at the cell-cell contacts

displaces actin filaments, which accumulate at the cell-free surfaces on the outside of the embryo (Lim & Plachta, 2021). Simultaneously, proteins such as Par3, Par6, and aPKCζ are upregulated and targeted to the cell-free membrane, forming an outer apical domain around the embryo. The apical domain interacts with the accumulated actin to form an actomyosin ring at the cell-free surface of each blastomere, which contracts to pull the edges of the cells toward one another (Lim & Plachta, 2021). This causes the cells to visibly flatten against one another until the boundaries between blastomeres are no longer distinct. Blastomere polarization and compaction, including regulation by Hippo signaling, are further discussed in Chapter 4.

The process of compaction and cell polarization is the first developmental event that leads to symmetry breaking and cell differentiation in the embryo. Up until compaction, totipotent 8-cell blastomeres retain the ability to each give rise to a new blastocyst if separated (Tarkowski & Wróblewska, 1967). However, this potential is lost during the first cell division after compaction. During the 8-to-16-cell division, some compacted blastomeres divide asymmetrically so that not all daughter cells inherit the outer apical domain evenly. Those cells that lose the apical domain become apolar and move into the center of the embryo (Chazaud & Yamanaka, 2016). Apolar inner cells and polarized outer cells form the basis of the first cell fate decision in mouse embryos, which are driven to become inner cell mass (ICM) and trophectoderm (TE) cells, respectively (Chazaud & Yamanaka, 2016). Neither of these newly-formed cell populations retains their former totipotent state. The ICM cells are considered pluripotent, meaning they can still give rise to many, but not all, later cell types, while the TE cells are multipotent,

meaning that despite still being stem cell progenitors, their developmental potential is much more restricted (Rossant, 2001). ICM will eventually give rise to the fetus and extraembryonic tissues (discussed further below), while the TE lineage gives rise to embryonic placental cells (Chazaud & Yamanaka, 2016).

An extensive body of work suggests that Hippo signaling plays an integral role in regulating the ICM-TE cell fate decision in mouse embryos (Alarcon, 2010; Anani et al., 2014; Cao et al., 2015; Cockburn et al., 2013; Frum et al., 2018, 2019; Hirate et al., 2013, 2015; Home et al., 2012; Leung & Zernicka-Goetz, 2013; Lorthongpanich et al., 2013; Mihajlović & Bruce, 2016; Nishioka et al., 2008, 2009; Plusa et al., 2005; Ralston et al., 2010; Ralston & Rossant, 2008; Rayon et al., 2014; Wicklow et al., 2014; Yagi et al., 2007; Yamamura et al., 2020; M. Zhu et al., 2017, 2020). These studies and others are the subject of several reviews, which I recommend for further information on this topic (Alarcon & Marikawa, 2018; Hirate & Sasaki, 2014; Karasek et al., 2020; Lorthongpanich & Issaragrisil, 2015; Sasaki, 2015, 2017; J. Sharma et al., 2021; Z. Wu & Guan, 2021; Yildirim et al., 2021).

The collective model from these studies suggests that Hippo signaling is active in the apolar, inner cells of the morula which leads to an ICM fate, while the polarized outer cells silence Hippo signaling to induce a TE cell fate (Fig. 1.2). In the inner, apolar cells, the scaffolding protein Angiomotin (AMOT) localizes to adherens junctions on the cell membrane, and from there interacts with upstream Hippo family kinases LATS1/2 (Hirate et al., 2013). This interaction allows LATS1/2 to phosphorylate downstream

transcription factors YAP1 and WWTR1. Phosphorylation of YAP1 and WWTR1 prevents these factors from entering the nucleus and instead promotes their association with the 14-3-3 complex for degradation; therefore, phosphorylation of YAP1/WWTR1 downregulates their transcriptional activity (C. Y. Liu et al., 2010). In the TE of the preimplantation mouse embryo, YAP1/WWTR1 repress transcription of *Sox2*, the earliest marker of pluripotency (Frum et al., 2018, 2019). YAP1/WWTR1 degradation in the inner cells therefore upregulates *Sox2* and promotes a pluripotent, inner cell mass fate. By contrast, in outer, polarized cells, AMOT is restricted to the apical domain through interaction with the aPKC-Par system (Hirate et al., 2013). AMOT is unable to promote phosphorylation of LATS1/2 as effectively from the apical domain, and in turn inactive LATS1/2 does not phosphorylate YAP1/WWTR1. Unphosphorylated YAP1/WWTR1 are translocated into the nucleus where they partner with TEAD4 to promote transcription of trophectoderm-specific transcription factors *Cdx2* and *Gata3* (Nishioka et al., 2008; Ralston et al., 2010) and repress *Sox2* (Frum et al., 2018; Wicklow et al., 2014). Therefore, in mice, repression of Hippo signaling in the outer cells both actively promotes a TE cell fate and represses pluripotency.

E3.25-E3.75: Blastocyst formation and the second cell fate decision regulated by FGF signaling

This first cell fate decision coincides with the transition to the morula stage of development, which lasts from the 16-cell stage (at ~E3.0) to the 32-cell stage (at ~E3.25). At E3.25, tight junctions between outer TE cells allow the formation of a fluid-filled cavity within the embryo known as a blastocoel (Cockburn & Rossant, 2010). Once

the blastocoel is fully formed, around E3.5, the embryo is called a blastocyst. Inside the blastocyst, the apolar ICM cells are gathered to one side of the blastocoel, while the TE comprises an epithelial layer surrounding the outside. Soon after, at E3.75, the ICM undergoes a second cell fate decision to differentiate into pluripotent epiblast (EPI) and multipotent primitive endoderm (PrE) populations (Chazaud & Yamanaka, 2016). EPI cells will give rise to most of the eventual fetus as well as contribute to extraembryonic fetal membranes such as the chorion, amnion, and allantois. PrE gives rise primarily to the yolk sac endoderm, with some contribution to the definitive endoderm of the fetus (Kwon et al., 2008; Lu et al., 2001).

Regulation by FGF signaling plays a key role in the EPI-PrE cell fate decision. As this is the result of a large body of work (Arman et al., 1998; Azami et al., 2019; Bessonnard et al., 2017; Chazaud et al., 2006; Feldman et al., 1995; Frankenberg et al., 2011; Frum et al., 2013; Grabarek et al., 2012; Kang et al., 2013, 2017; Krawchuk et al., 2013; Le Bin et al., 2014; Messerschmidt & Kemler, 2010; Mistri et al., 2018; Molotkov et al., 2017; Nichols et al., 2009; Ohnishi et al., 2014; Plusa et al., 2008; Rappolee et al., 1994; Wicklow et al., 2014; Wigger et al., 2017; Yamanaka et al., 2010) and has been recently reviewed (Brewer et al., 2016; Dorey & Amaya, 2010; Lanner & Rossant, 2010; Soszyńska et al., 2019), the main points are summarized here (Fig. 1.3). FGF activity is detected in the ICM of the blastocyst as early as E3.25, and is gradually upregulated in PrE cells as they become specified in the mid-blastocyst stage (Azami et al., 2019; Morgani et al., 2018). During the early blastocyst stage, the ICM cells co-express the transcription factors *Nanog* and *Gata6*, regulators of EPI and PrE, respectively. *Nanog*

induces expression of the FGF ligand *Fgf4* (Frankenberg et al., 2011). Some bipotent ICM cells express higher levels of *Fgf4* than others, making *Fgf4* the first bimodally expressed gene among the ICM cells (Ohnishi et al., 2014). It is currently still unclear whether this asymmetry in *Fgf4* expression arises stochastically or if it is regulated in some way. Neighboring ICM cells receive this signal through the receptor FGFR1 (Molotkov et al., 2017), which stimulates the MEK/ERK pathway in the receiving cells. ERK activity downregulates expression of *Nanog,* which relieves repression and upregulates *Gata6* expression (Chazaud et al., 2006). *Gata6*-high cells upregulate expression of FGFR2, increasing the receptivity to FGF and reinforcing ERK activity and *Gata6* upregulation in these cells. By the mid-blastocyst stage *Gata6*-high cells have also upregulated *Pdgfrα, Sox17,* and *Gata4* to adopt a true PrE fate (Artus et al., 2012; Niakan et al., 2010). Meanwhile, upregulated *Nanog* expression in the *Fgf4*-high cells downregulates *Gata6* to solidify an EPI fate. By E3.75, *Gata6* and *Nanog* expression are mutually exclusive (Chazaud et al., 2006), although studies have shown that some ICM cells retain the potential to switch between EPI and PrE fates until E4.5 (Grabarek et al., 2012; Plusa et al., 2008; Wigger et al., 2017). In this manner, EPI and PrE cells arise in a “salt-and-pepper” distribution throughout the ICM, directed by localized high and low levels of FGF signaling (Fig. 1.3).

FGF signaling is necessary and sufficient to direct specification of PrE over EPI cell fate in the mouse ICM. The ability to modulate cell fate using exogenous factors that modulate FGF signaling has enabled the *in vitro* testing of models of ICM differentiation. Morula-stage embryos cultured with exogenous FGF4 and heparin to blastocyst stage

develop ICMs comprised entirely of *Gata6*-positive cells (Yamanaka et al., 2010). Similarly, treating embryos with a combination of FGFR and MEK inhibitors (PD173074 and PD0325901, respectively) for the same developmental duration directs the entire ICM to express *Nanog* (Nichols et al., 2009; Yamanaka et al., 2010). However, ICM cells become unresponsive to FGF4 around E4.0 (Yamanaka et al., 2010). This suggests that modulations in FGF are sufficient to direct PrE specification in the early ICM even in EPI-biased cells, but that it is not sufficient to change ICM cell fate once an EPI or PrE program is fully established. Whether other signaling pathways interact with FGF to reinforce PrE fate or regulate the timing of FGF sensitivity in ICM cells remains an open question. The potential of BMP signaling to interfere with PrE fate induction by FGF signaling will be discussed further in Chapter 2.

E4.0-E4.5: Embryo hatching and implantation

After the second cell fate decision, the embryo undergoes only a few more morphological changes before implantation. EPI and PrE cells initially arise in a “salt-and-pepper” distribution throughout the ICM, but by E4.0 they sort into separate populations with the PrE forming an epithelial layer between the EPI and the blastocoel (Cockburn & Rossant, 2010). Around this time, the embryo hatches out of the zona pellucida, allowing the exposed TE cells to attach to the mother’s uterine wall (Ma et al., 2024). Embryo attachment facilitates a massive proliferation process in the uterine stromal cells known as decidualization, which provides the embryo a protected place to grow and establishes a maternal-fetal interface (Rinkenberger et al., 1997). During this

period, TE cells begin to invade the decidua, forming the basis of the future placenta. Shortly after E4.5, the embryo is considered to be implanted (Rossant & Tam, 2009).

1.2.3. Molecular mechanisms regulating developmental stages and processes of murine post-implantation development through gastrulation

E4.75-E5.5: Egg cylinder formation and cell differentiation

Developmental and regulative processes become more complex after implantation as the embryo undergoes rapid proliferation and morphological changes as well as cell fate changes. The initial three cell types of EPI, PrE, and TE each begin to mature and differentiate as the embryo elongates into a cup-shaped structure known as the egg cylinder (reviewed in Arnold & Robertson, 2009; Filimonow & de la Fuente, 2022; Stower & Srinivas, 2018). These newly-differentiated cell types provide critical signals for the reorganization of the embryo and increase in complexity during gastrulation, and as such, their proper derivation and organization is crucial for further embryonic development. Several of these cell types and signaling pathways are discussed further in Chapter 2.

Many morphological and molecular changes in cell fate between embryonic implantation and gastrulation have been observed. The polar TE cells, adjacent to the EPI in the blastocyst, proliferate and expand to form the most proximal end of the egg cylinder. These differentiate into more mature cell types including the extra-embryonic ectoderm (ExE), which eventually gives rise to the main cell types that form the embryonic portions of the placenta. Just as importantly, the ExE plays an essential role in pre-

gastrulation embryonic patterning, particularly as the source of BMP4 that is necessary for mesoderm induction and primordial germ cell formation (Ben-Haim et al., 2006; Winnier et al., 1995, discussed further in Section 1.3).

The PrE also expands and differentiates after implantation, giving rise to the visceral endoderm (VE), which forms a single cell layer on the outside surface of the egg cylinder. These cells eventually give rise to the yolk sac endoderm (Filimonow & de la Fuente, 2022), as well as contribute to gut tube formation in the fetus (Kwon et al., 2008). Critically, the VE is the source of several essential extraembryonic signals to regulate embryonic axial patterning and gastrulation, including Nodal, BMP, and WNT (reviewed in S. M. Morgani & Hadjantonakis, 2020). EPI, although not referred to as a new cell type, undergoes significant changes during egg cylinder formation. In the blastocyst, expression of known pluripotency-promoting transcription factors such as *Nanog*, *Sox2*, and *Oct4* keep epiblast cells in a “naïve” state of pluripotency (Nichols & Smith, 2009). After implantation, EPI downregulates *Nanog, Klf4, Stella,* and other naïve markers to mature into a “primed” state of pluripotency. Possibly as a result of this molecular change, the EPI changes morphologically after implantation from round and apolar cells in the blastocyst to columnar, epithelialized cells by E5.0. The epithelized EPI organizes into a polarized rosette at the distal end of the growing egg cylinder (Bedzhov & Zernicka-Goetz, 2014). The VE cells overlying the EPI deposit a basement membrane between the VE and EPI, inducing a basolateral domain on the outer edge of the EPI rosette and an apical domain in the center (Bedzhov & Zernicka-Goetz, 2014; S. Li et al., 2003; Niakan et al., 2010; Shahbazi et al., 2017). Soon after EPI

polarization, a lumen opens in the rosette's center called the proamniotic cavity, forming the EPI into a single layer epithelium.

Importantly for my studies, there is some debate in the literature as to what induces epiblast cavitation at early post-implantation stages. Early studies in embryoid bodies (spherical structures grown *in vitro* from EPI-derived embryonic stem cells) proposed that the central EPI cells receive a cell death signal from the maturing VE which causes them to undergo apoptosis (Coucouvanis & Martin, 1995, 1999). This is supported by a recent study which detected cells undergoing apoptosis in the developing lumen of E5.5 embryos (Halimi et al., 2022). However, other studies have suggested that this mechanism is not sufficient to explain epiblast cavitation. An alternative mechanism was proposed by Bedzhov and Zernicka-Goetz in which EPI polarization is the driving force behind cavitation. According to this study, the central apical domain secretes anti-adhesion proteins like podocalyxin, which help force the apical ends of the cells away from one another (Bedzhov & Zernicka-Goetz, 2014). This mechanism is supported by studies which show that embryos which lack essential components of cell polarity like integrin and laminin also fail to cavitate (Smyth et al., 1999; Stephens et al., 1995). A model for how these two mechanisms may be working simultaneously to promote cavitation is discussed in Chapter 2.

E5.5-E7.5: Axial patterning and gastrulation

After the establishment of the egg cylinder at E5.5 and associated differentiation of cell types, the complexity of the embryo begins to increase dramatically, with various

signaling gradients directing cell differentiation and cell movement. These regulate the process of gastrulation, or the formation of embryonic germ layers. Importantly, prior to gastrulation the post-implantation embryo is considered morphologically and molecularly symmetrical, with the only apparent axis being the proximal-distal axis (Arnold & Robertson, 2009; Takaoka & Hamada, 2012). Anterior-posterior and dorsal-ventral patterning occur concomitantly with the onset of gastrulation, and these processes are tightly linked to one another. The morphological and molecular changes that occur during axial patterning and gastrulation, and the signaling pathways that regulate them (including Nodal, BMP, WNT, and FGF signaling), have been extensively reviewed, and I recommend these for further information on the subject (Arnold & Robertson, 2009; Beddington & Robertson, 1999; Filimonow & de la Fuente, 2022; Matsuo & Hiramatsu, 2017; Morgani & Hadjantonakis, 2020; Perea-Gomez et al., 2001; Rossant & Tam, 2009; Stower & Srinivas, 2018; Takaoka & Hamada, 2012).

The process of gastrulation and its regulation by BMP signaling will be discussed more thoroughly in Section 1.3. By E7.5, embryonic mesoderm is fully established, and more advanced structures begin to emerge, with the formation of the heart tube, head folds, amnion, and chorion. At this point, gastrulation is considered to be complete, and the dorsal-ventral and anterior-posterior axes are established. With the dorsal-ventral and anterior-posterior axes specified, the left-right axis becomes apparent, although the embryo does not show any overt left-right asymmetry until *Nodal* accumulates at the left side of the node ~E8.0 (Shiratori & Hamada, 2006). Thus, by the end of gastrulation, the embryo has specified all three germ layers and patterned the body axes, setting up the

more complex morphological and cell fate changes which occur in further stages of development.

Section 1.3. The roles for Bone Morphogenic Protein (BMP) signaling in early mammalian embryonic development are not fully understood

Bone Morphogenic Protein (BMP) signaling is essential for early mouse embryonic development and involved in many processes discussed in Section 1.2 (see highlighted processes in Fig. 1.1). BMP signaling is a highly conserved molecular signaling pathway, with homologs in all animals (Huminiecki et al., 2009), and its role in development has been studied for decades. The pathway is so named because it was first discovered as a factor which induced ectopic bone formation (E. A. Wang et al., 1988), but studies have since uncovered many other essential roles for BMP signaling regulating cell fate, cell survival, proliferation, and morphogenesis in both embryonic development and adult homeostasis (Reddi, 2003). Unsurprisingly, dysregulation of BMP signaling has also been implicated in a number of diseases, particularly congenital bone and heart defects (R. N. Wang et al., 2014). This section will focus on the roles of BMP signaling in pre- and peri-implantation mouse embryonic development, but many reviews discuss other important roles for BMP signaling (Bragdon et al., 2011; D. Chen et al., 2004; Reddi, 2003). Interestingly, studies of BMP signaling in mouse development disagree on the pathway's earliest role in embryogenesis. This is essential knowledge for the studies in Chapter 2, which endeavor to resolve this conflict within the literature.

1.3.1. Biochemical interactions of the Bone Morphogenic Protein Signaling Pathway

The biochemical interactions of BMP signaling have been well-described (Fig. 1.4). BMP is a subfamily of the TGFβ superfamily of signaling pathways, which also includes Activin, Nodal, and TGFβ signaling as well as Growth and Differentiation Factors, myostatin, and anti-Mullerian hormone (Reddi, 2003). BMPs may signal canonically through SMAD proteins or non-canonically through interaction with other pathways such as MEK/ERK, JNK/p38, or PI3K/Akt (Y. E. Zhang, 2009). Canonical BMP signaling is transduced through receptors known as activin-like kinases (ALKs) and internal effectors called SMAD proteins. BMPs, which are secreted proteins, form homo- or hetero-dimers to become biologically active. Dimerized ligands bind to membrane-bound ALK receptors on receiving cells. BMP signaling, as with other TGFβ pathways, requires two classes of protein to form an active receptor complex called Type I and Type II receptors. To induce a robust response, BMPs bind to heterodimers comprised of two Type I and two Type II receptor proteins. Both classes of protein are serine-threonine kinases, and upon assembly of the receptor complex the constitutively-active Type II receptors phosphorylate the Type I receptors to activate their kinase activity (Hari Reddi, 2003). Active Type I receptors can phosphorylate internal effector proteins called receptor-associated SMADs (r-SMADs). Many BMP receptors also transduce signals from Activin and Nodal signaling; however, Activin, Nodal, and TGFβ signals are transduced through the r-SMADs SMAD2/3 while BMP signals through SMAD1/5/9 (SMAD9 is also known as SMAD8) (Reddi, 2003). Phosphorylated r-SMADs can then bind a co-factor, SMAD4, which acts as a transcription factor. The completed SMAD

complex accumulates in the nucleus to bind DNA and affect gene expression. SMAD4 on its own has very weak binding affinity to DNA, and often requires co-factors such as p300 to initiate high-affinity and high-specificity DNA binding (Hill, 2016). It is important to note that SMAD4 is a shared co-factor for r-SMADs SMAD1/5/9 and SMAD2/3, making it an essential effector of both BMP and TGFβ/Activin/Nodal signaling (Weiss & Attisano, 2013). Also important is that while mammals express many different BMP ligands, receptors, and r-SMADs which may serve redundant or compensatory functions, SMAD4 is the only co-factor SMAD expressed in mammals (Huminiecki et al., 2009).

Nearly every level of this pathway is carefully regulated by agonists, co-factors, and antagonists (Reddi, 2003). Noggin, Chordin, and Gremlin are three well-studied antagonists that bind BMPs and prevent their interaction with receptors (Walsh et al., 2010). BAMBI is another BMP antagonist which acts as a non-functional pseudoreceptor (Reddi, 2003). SMAD6 and SMAD7 are inhibitory SMADs which compete with SMAD1/5/9, and their expression is often induced by BMP signaling as a form of negative feedback. These regulators play essential roles in embryonic development; in fact, loss of *Nog* (Noggin), *Grem1* (Gremlin), *Chd* (Chordin) and *Smad7* cause embryonic lethality (Bragdon et al., 2011; Q. Chen et al., 2009). Artificial small-molecule inhibitors of BMP signaling have also been produced, such as dorsomorphin (and derivatives), LDN (and derivatives), and VU5350 (Lowery et al., 2016). These generally inhibit the kinase activity of BMP receptors, with varying degrees of specificity for each ALK. As discussed in Chapter 2, these have often been employed to

investigate BMP loss-of-function phenotypes, though the possibility of off-target inhibition of other kinases may confound findings. Notably, despite the vast array of possibilities for regulation of individual TGFβ family signaling pathways *in vivo* and *in vitro,* SMAD4 presents as a convenient target to assess the requirement for all canonical TGFβ signaling.

1.3.2. BMP signaling is required after implantation in extra-embryonic tissues for gastrulation and mesoderm formation in mammals

Maternally-regulated BMP signaling gradients drive axis formation in non-mammalian models

BMP signaling has been extensively studied in the embryonic development of non-mammalian model systems for its role as a morphogen governing body axis development. The role of BMP signaling in amphibians is especially famous due to the classic developmental biology experiments performed by Spemann, Mangold, and colleagues (Spemann & Mangold, 1923). The Spemann-Mangold group discovered that a bisected blastula-stage frog embryo would only develop dorsal structures if it included part of the “gray crescent” organizer structure. Later, other groups identified that the dorsalizing components of the gray crescent were antagonists to BMP signaling, including Noggin and Chordin (Sasai et al., 1994; Smith & Harland, 1992). Dorsal expression of these inhibitors creates a gradient of BMP signaling across early frog embryos, with the highest BMP activity at the ventral side of the embryo (Plouhinec et al., 2013). Addition of BMP ligands or overexpression of downstream SMADs can induce formation of ventral tissues in frog embryos, demonstrating that BMP activity is

sufficient to induce ventral fate and suppress dorsal fate (Suzuki et al., 1997). In flies, *dpp* (a homolog of BMP2/4) expression is enriched on the future dorsal side of the blastula-stage embryo forming a dorsal-ventral gradient of BMP activity. Injecting embryos with *dpp* mRNA dorsalizes the embryo, while *dpp* mutant embryos are ventralized (Dorfman & Shilo, 2001; O'Connor et al., 2006). In zebrafish, the BMP antagonist Chordin is expressed specifically on the eventual dorsal side of the embryo, forming a gradient of BMP activity which is stronger on the ventral side (Ramel & Hill, 2013). All of these symmetry-breaking events occur very early in development in these model systems, occurring prior to, or coinciding with, the maternal-to-zygotic transition (Lee et al., 2014). Furthermore, the BMP activity gradient in these model systems is partially established by maternally-derived factors which are asymmetrically distributed in the oocyte and embryo prior to zygotic genome activation. In flies, maternal expression of *dorsal* in the dorsal region is required for asymmetric expression of *dpp* (Rushlow et al., 1987). In zebrafish, the dorsalized localization of zygotic Chordin is induced by asymmetric localization of maternal β-catenin (Ramel & Hill, 2013). Similarly, ventralized expression of *bmp2b* and *bmp4* in zebrafish is induced by asymmetric localization of maternally-derived *radar* and *pou2* transcripts (Reim & Brand, 2006; Sidi et al., 2003). In addition to directing BMP gradient formation, maternally-derived components of the BMP pathway have also been shown to have direct effects on embryonic development in these species (Das et al., 1998; Faure et al., 2000; Kramer et al., 2002; F. Zhang et al., 2020). Therefore, body axis formation in non-mammalian species is strongly regulated by both maternal and zygotic control of BMP signaling activity. This has prompted many groups to investigate if such a gradient of BMP activity

also exists to direct axis specification in early mammalian embryos, and whether BMP activity in mammalian embryos may be driven by maternally-derived factors.

BMP signaling is required for peri-implantation cell fate specification in mammals

In contrast to other model systems, regulation of axial patterning is not the earliest role for BMP signaling in mammalian embryogenesis. A key piece of evidence for this conclusion is the fact that maternal factors regulating the establishment of a BMP morphogenic gradient is not conserved in mammals. In fact, no intrinsic pattern of maternally-derived molecular components, either mRNA or protein, has been demonstrated in mammalian oocytes or zygotes. Although many studies have described molecular asymmetries in early embryos (Jedrusik et al., 2008; Lim et al., 2020; Piotrowska-Nitsche et al., 2005; Piotrowska et al., 2001; Plachta et al., 2011; Torres-Padilla et al., 2007), no such asymmetries been shown to be deterministic of cell fate during embryonic development (Kurotaki et al., 2007; Motosugi et al., 2005; Rossant & Tam, 2009; Takaoka & Hamada, 2012). Additionally, the mammalian embryo does not specify body axes until relatively late in development compared to non-mammalian model species (Arnold & Robertson, 2009). Instead, the first cell fate decisions of mammalian embryos are dedicated to setting up the extraembryonic structures that the embryo will need to implant into the uterine wall and develop in an internal environment: the placenta, yolk sac, amnion, and chorion. Since components of BMP signaling are expressed prior to body axes specification in mammals, it suggests that it plays a role in these earlier cell fate decisions.

Genetic studies of BMP signaling in mammals have shown that BMP signaling is absolutely required for embryonic development. Zygotic knockout of many BMP pathway members in mouse models results in embryonic lethality before mid-gestation. Several of these knockouts, including those for the genes encoding the ligand *Bmp4,* the Type I receptor *Bmpr1a*, the Type II receptor *Bmpr2,* the cofactor *Smad4*, and downstream target gene *Tlx2*, all show a similar phenotype where the embryos fail to undergo gastrulation and arrest at early egg cylinder stages (Beppu et al., 2000; Mishina et al., 1995; Sirard et al., 1998; Tang et al., 1998; Winnier et al., 1995; X. Yang et al., 1998). Other BMP knockouts, including those for the genes encoding the receptor-associated SMADs *Smad1* and *Smad5,* and the ligand *Bmp2*, are able to complete gastrulation and undergo turning, but die at early somite stages due to defects in mesoderm, heart development, and axial patterning (H. Chang et al., 1999; Hayashi et al., 2002; Tremblay et al., 2001; H. Zhang & Bradley, 1996). Additionally, many BMP knockout embryos display an obvious growth restriction at early egg cylinder stages and lack morphological distinction between the embryonic and extraembryonic parts of the embryo (Beppu et al., 2000; G. C. Chu et al., 2004; Di-Gregorio et al., 2007; Mishina et al., 1995; Sirard et al., 1998; Yamamoto et al., 2009; X. Yang et al., 1998; Ying et al., 2000). These phenotypes appear to result from a severe proliferation defect rather than an effect on cell survival, as several BMP knockout embryos show decreased BrdU incorporation or PCNA staining (Mishina et al., 1995; Sirard et al., 1998; X. Yang et al., 1998) and *Smad4*-null embryos did not display increased apoptosis as assessed by TUNEL staining (Sirard et al., 1998). This shows that BMP signaling is required for cell proliferation and cell fate specification after implantation.

BMP signaling regulates gastrulation and mesoderm formation in mouse embryos

There is abundant evidence to show that BMP signaling is required prior to body axis specification in mammals to initiate mesoderm formation and gastrulation. Gastrulation, or germ layer formation, usually occurs between E6.25-E7.5 in mice and can be visualized by the appearance of a morphologically distinct tissue known as the primitive streak, which arises from the proximal epiblast (Arnold & Robertson, 2009; Morgani & Hadjantonakis, 2020; Takaoka & Hamada, 2012). The primitive streak represents one of first symmetry-breaking structures in the mouse embryo proper and is essential to establishing the anterior-posterior and dorsal-ventral axes. EPI cells which delaminate from the egg cylinder epithelium and pass through the primitive streak give rise to extraembryonic mesoderm (which contributes to the allantois and part of the amnion and chorion), axial mesoderm and definitive endoderm, and to primordial germ cells (PGCs) (Morgani & Hadjantonakis, 2020; Senft et al., 2019). Knockouts of *Bmp4, Bmpr1a, Bmpr2, Acvr1a,* and *Smad4* completely fail to initiate mesoderm formation (Beppu et al., 2000; G. C. Chu et al., 2004; Di-Gregorio et al., 2007; Z. Gu et al., 1999; Mishina et al., 1995; Sirard et al., 1998; Winnier et al., 1995; X. Yang et al., 1998).These knockouts lack a visible primitive streak at E7.0 and do not express the mesoderm marker *Brachyury (T).* Other BMP-pathway knockouts, such as *Bmp2*, *Bmp8b, Smad1, Smad5,* and *Tlx2* are able to initially form mesoderm and a primitive streak, but these structures fail to differentiate properly (Bosman et al., 2006; Tang et al., 1998; Tremblay et al., 2001; Ying et al., 2000; H. Zhang & Bradley, 1996). Some of these mutants initiate *T* expression, but expression is either decreased or fails to expand distally to designate a fully functional primitive streak (Tang et al., 1998; Tremblay et al., 2001).

Crucially, in BMP mutants which are able to initiate gastrulation, many mesoderm-derived structures such as the amnion and allantois are visibly smaller than normal, mispatterned, and fail to properly fuse to create the amniotic cavity and exocoelom (Bosman et al., 2006; H. Chang et al., 1999; Hayashi et al., 2002; Tang et al., 1998; Tremblay et al., 2001; Ying et al., 2000; Ying & Zhao, 2001; H. Zhang & Bradley, 1996). BMP mutants also fail to properly specify primordial germ cells (Arnold et al., 2006; Chuva De Sousa Lopes et al., 2004; Hayashi et al., 2002; Lawson et al., 1999; Senft et al., 2019; Tremblay et al., 2001; Ying et al., 2000; Ying & Zhao, 2001), which are normally derived from a common precursor with mesoderm (Saitou & Yamaji, 2012). In some cases, BMP signaling has been shown to be functionally sufficient to induce PGC formation, as distal epiblast explants from E6.25 embryos (which do not normally specify PGCs) cultured with exogenous BMP8B and BMP4 produced recognizable PGCs (Ying et al., 2001). Altogether, this shows that SMAD-mediated BMP signaling is required for successful gastrulation and mesoderm progenitor specification in early post-implantation mouse embryos.

BMP signaling regulates axial patterning in mammals

BMP does play a role in the axial patterning in mammals. However, as previously noted, this is not from a maternally-deposited morphogen gradient unlike other model species. Instead, the regulation of axial patterning by BMP is secondary to the role of BMP in mesoderm specification. Anterior-posterior axis formation in mammals is induced by anterior factors secreted from the anterior visceral endoderm (AVE), which forms opposite the primitive streak. Therefore the distal expansion of the primitive streak

across from the AVE helps specify posterior fate (Morgani & Hadjantonakis, 2020). In BMP mutants, the primitive streak is often not specified or fails to elongate, which in turn leads to defects in anterior-posterior axis formation (Arnold et al., 2006; Beppu et al., 2000; Fujiwara et al., 2002; Lawson et al., 1999; Sirard et al., 1998). This is shown by a failure of posterior markers such as *Cripto* and *Fgf8* to show asymmetric expression in the epiblast by E7.5 in BMP knockouts (Beppu et al., 2000; Fujiwara et al., 2002).

As a second mechanism of BMP regulation of axial patterning, BMP activity is involved in specifying the dorsal-ventral axis, which mimics the proximal-distal axis of the early egg cylinder. BMP patterns the primitive streak by cross-inhibiting Nodal, possibly through competition for the shared downstream cofactor SMAD4 (Morgani & Hadjantonakis, 2020; Senft et al., 2019). As the primitive streak elongates, the most distal streak cells move farther away from the BMP signal in the ExE and inhibition of Nodal signaling is released. Nodal in the more distal (anterior) primitive streak induces expression of BMP inhibitors Noggin and Chordin, reinforcing the decreased BMP signaling in the distal streak. This establishes differential signaling environments in the distal and proximal epiblast which helps characterize the dorsal-ventral axis (Morgani & Hadjantonakis, 2020; Senft et al., 2019)

Finally, BMP may also be involved in specifying the left-right axis in mammals. *Nodal* is a right-side marker, since it is inhibited by *Lefty1/2* on the left side of the embryo, and in E8.5 *Bmp4*-null and *Smad1*$^{+/-}$*; Smad5*$^{+/-}$ embryos expression of *Nodal* is symmetrical, suggesting a defect in left-right patterning (Arnold et al., 2006; Fujiwara et al., 2002).

Possibly in support of this, several BMP mutants which survive to early somite stages display heart looping defects (Arnold et al., 2006; Bosman et al., 2006; H. Chang et al., 1999; Fujiwara et al., 2002; H. Zhang & Bradley, 1996). However, BMP signaling is known to be necessary for heart formation (Uchimura et al., 2009); therefore, it is difficult to determine whether the heart-looping failure is due to a left-right patterning defect or to a direct role for BMP in the heart (Fujiwara et al., 2002). As BMP mutants largely die *in utero* before any other left-right asymmetries are specified, it may be difficult to test this hypothesis further. However, we can conclude that any role for BMP signaling in left-right patterning is secondary to its earlier roles in gastrulation and embryo growth.

BMP regulation of epiblast morphogenesis is non-cell-autonomous

Although BMP is required for proliferation and mesoderm specification in the epiblast, several lines of evidence suggest BMP signaling is primarily active in the visceral endoderm. BMP activity has been visualized by several methods, including immunofluorescence or immunohistochemistry for pSMAD1/5/9 and transfection of reporter constructs which incorporate one or several “BMP response element” (BRE) motifs (Bosman et al., 2006; Chuva De Sousa Lopes et al., 2004; Di-Gregorio et al., 2007; Fernandes et al., 2016; Hayashi et al., 2002; Reyes de Mochel et al., 2015; Senft et al., 2019; Yamamoto et al., 2009). It is important to note that not all these reporters agree with one another on the extent of BMP activity in developing mouse embryos. Various studies report conflicting data on the earliest developmental timepoint at which BMP activity can be visualized, with some studies reporting BMP activity as early as the

4-cell stage (Reyes de Mochel et al., 2015) while others do not detect BMP activity until E6.5 (Chuva De Sousa Lopes et al., 2004). Similarly, studies do not agree on the cell type specificity of BMP signaling, with some reports claiming BMP activity is present nearly ubiquitously throughout the EPI and VE at early egg cylinder stages (Di-Gregorio et al., 2007) while others report it is restricted to the proximal EPI and extraembryonic VE (Chuva De Sousa Lopes et al., 2004) or to the proximal VE alone (Senft et al., 2019). Therefore, a consensus time course of BMP signaling in mouse embryos has not yet been constructed to date (I report one in Chapter 2). Nevertheless, several studies agree that BMP signaling is active in the VE, particularly around E6.5 when gastrulation is beginning (Chuva De Sousa Lopes et al., 2004; Di-Gregorio et al., 2007; Hayashi et al., 2002; Senft et al., 2019; Yamamoto et al., 2009). Additionally, BMP signaling is suggested to regulate VE maturation or patterning, as several BMP mutant models show disruption of VE morphology or molecular markers (Arnold et al., 2006; G. C. Chu et al., 2004; Z. Gu et al., 1999; Sirard et al., 1998; Tremblay et al., 2001; Yamamoto et al., 2009). Gain-of-function evidence is also available from studies of eXtraEmbryonic Endoderm (XEN) cells, a stem cell line derived from the preimplantation PrE (Kunath et al., 2005). These show that treating XEN cells with exogenous BMP4 upregulates differentiation markers for VE (Artus et al., 2012; Paca et al., 2012). This suggests an important role for BMP signaling in the VE.

Interestingly, there is considerable evidence to suggest that BMP signaling in the VE plays an important non-cell-autonomous role to regulate development of the epiblast. Several groups have shown that embryos which lacked expression of BMP pathway

members only in the extraembryonic tissues resemble full-body BMP knockouts, suggesting that BMP signaling in the EPI is unable to rescue the proliferation or mesoderm defects. (Z. Gu et al., 1999; Lawson et al., 1999; C. Li et al., 2010; Tremblay et al., 2001; Yamamoto et al., 2009). Similarly, wild-type E5.5 epiblasts stripped of extraembryonic tissues were unable to form PGCs in culture, even when supplemented with exogenous BMP4 in the media (de Sousa Lopes et al., 2004). On the other hand, embryo models where BMP signaling is intact in extraembryonic tissues but deleted in EPI generally developed further than those with full-body BMP knockouts or BMP-null extraembryonic cells (G. C. Chu et al., 2004; Fujiwara et al., 2001; Z. Gu et al., 1999; C. Li et al., 2010; Sirard et al., 1998). Some of these models with wild-type extraembryonic cells actually completed gastrulation and underwent turning, formed mesoderm-derived structures such as allantois, and specified PGCs. This suggests that BMP activity in extraembryonic tissues is sufficient for proper mesoderm formation in the epiblast. However, it is important to note that these embryos, which lack BMP signaling in EPI, still died *in utero* between E9.5-E10.5 (G. C. Chu et al., 2004; Z. Gu et al., 1999; Sirard et al., 1998). These observations suggest that while BMP signaling in the peri-implantation VE alone is sufficient for gastrulation, mesoderm formation, and PGC specification, cell-autonomous BMP signaling in EPI-derived tissues is still required for later embryonic development.

1.3.3. Proposed roles for BMP signaling in preimplantation mammalian development do not agree with post-implantation roles

The existing literature does not agree on the earliest role for BMP signaling in mammalian development. Most genetic BMP knockout studies did not report any phenotypes earlier than E5.5-E6.0, at which point *Bmp4*, *Bmp2, Bmp8b, Smad4, Acvr1a,* and *Bmpr1a* mutants appear morphologically normal (Di-Gregorio et al., 2007; Z. Gu et al., 1999; Mishina et al., 1995; Winnier et al., 1995; X. Yang et al., 1998; Ying et al., 2000; H. Zhang & Bradley, 1996). None of these studies conducted any molecular characterization of BMP knockout embryos at these peri-implantation stages; however, a few studies examined *Smad4*-null and *Bmpr2*-null blastocysts at E3.5 and reported that the knockout did not cause an apparent phenotype (Beppu et al., 2000; Sirard et al., 1998; X. Yang et al., 1998). Functionally, *Bmpr1a*-null and *Smad4*-null blastocysts were able to form recognizable EPI, PrE, and TE-derived cell types which were indistinguishable from controls (Mishina et al., 1995; Sirard et al., 1998; X. Yang et al., 1998). This suggests that without active BMP signaling, preimplantation embryos are able to specify all three cell lineages properly.

In contrast to these observations, more recent studies which focused specifically on preimplantation development have proposed that BMP signaling plays an important developmental role at these stages (Graham et al., 2014; Reyes de Mochel et al., 2015; Stuart et al., 2019). These studies detected pSMAD1/5/9 as early as the 4-cell stage in wild-type embryos and X-gal staining in *BRE-LacZ* reporter embryos at the morula stage (Graham et al., 2014; Reyes de Mochel et al., 2015), suggesting that BMP

signaling is active at preimplantation stages. Importantly, this contrasts with a finding published later that GFP is undetectable in *BRE:gfp* reporter embryos at E3.5 (Fernandes et al., 2016). To test the requirement for BMP signaling in preimplantation development, wild-type embryos were treated with a variety of inhibitors to block BMP receptor activity (Dorsomorphin, Noggin, (5Z)-7-Oxozeaenol, DMH2, and LDN-193189). As a complementary assay, these studies also knocked down BMP signaling by microinjecting wild-type embryos with mRNA to overexpress dominant-negative forms of BMPR1A, BMPR2, and SMAD4. Both dominant-negative receptors and all inhibitor treatments resulted in similar outcomes in both studies. BMP loss-of-function in preimplantation embryos decreased the total amount of TE and PrE cells at the blastocyst stage, resulting in embryos with significantly decreased total cell numbers (Graham et al., 2014; Reyes de Mochel et al., 2015; Stuart et al., 2019). These studies also reported that embryos treated with BMP inhibitors displayed changes in cell cycle time specifically in TE and PrE, which may account for the decreased amount of extraembryonic cells (Graham et al., 2014; Reyes de Mochel et al., 2015). Despite some differences in findings, these studies paint a fairly cohesive picture of a requirement for BMP signaling in preimplantation development, possibly for specification or maintenance of extraembryonic cell types. Notably, gain-of-function studies failed to show that exogenous BMP4 treatment during preimplantation development caused any change in extraembryonic cell fate specification, though they did report a slight decrease in EPI cells (Goissis et al., 2023). This study was also unable to replicate the earlier results and did not report any changes in cell number or cell fate when preimplantation embryos were treated with inhibitors to BMP signaling.

This questions the reproducibility of these results and means that the exact role for BMP signaling in preimplantation development has yet to be fully resolved.

It is unknown why none of the preimplantation defects described with BMP inhibitor treatment were observed in genetic knockouts of BMP signaling, though there are several possibilities which may explain this discrepancy. On the one hand, as with any small molecule treatment, it is possible that the “BMP” inhibitors have off-target effects which adversely affect preimplantation development. Indeed, many of these inhibitors have been shown to cause considerable off-target effects in vitro; dorsomorphin in particular can inhibit at least 30 other kinases in addition to BMPR1A at the concentrations used in these studies (Lowery et al., 2016). Overexpression of proteins at non-physiological levels and microinjection may also be detrimental to preimplantation embryos (Joris et al., 1998). This would suggest that the genetic knockout studies are a more reliable assay for BMP loss-of-function. However, as preimplantation embryos are known to contain maternally-derived transcripts for many BMP pathway components (Xie et al., 2010), it is possible that these could compensate for loss of the zygotic genes and mask potential preimplantation phenotypes in the genetic knockout studies. Furthermore, BMP4 is known to be produced in the maternal decidua and BMP signaling is active in this tissue during embryo implantation (Monsivais et al., 2021), meaning that essential downstream factors which are normally produced by BMP signaling in the embryo could be supplemented by the uterus. Thus, currently published studies do not clearly specify what role, if any, BMP signaling plays

in preimplantation mouse development. My studies in Chapter 2 address this gap in the literature.

Section 1.4. Conclusions

In summary, molecular signaling pathways dictate morphogenic and cell fate changes in many aspects of mouse embryonic development. Hippo signaling is crucial for regulating the first cell fate decision and polarization of blastomeres in preimplantation embryos. FGF signaling regulates the second cell fate decision between EPI and PrE cells within the preimplantation ICM. BMP signaling has well-described roles after implantation in regulating gastrulation, mesoderm formation, PGC specification, cell proliferation, and anterior-posterior patterning through development of the primitive streak. However, the role of BMP signaling at preimplantation stages is still unclear, as studies using BMP signaling inhibitors have proposed that BMP signaling regulates TE and PrE cell specification and cell cycle rate, but inconsistencies with genetic knockout studies calls these results into question. Thus, despite the depth of knowledge about molecular signaling pathways in mouse embryos, there are still many unanswered questions about their precise roles in development and how each of these pathways may interact with one another to direct proper embryogenesis.

FIGURES

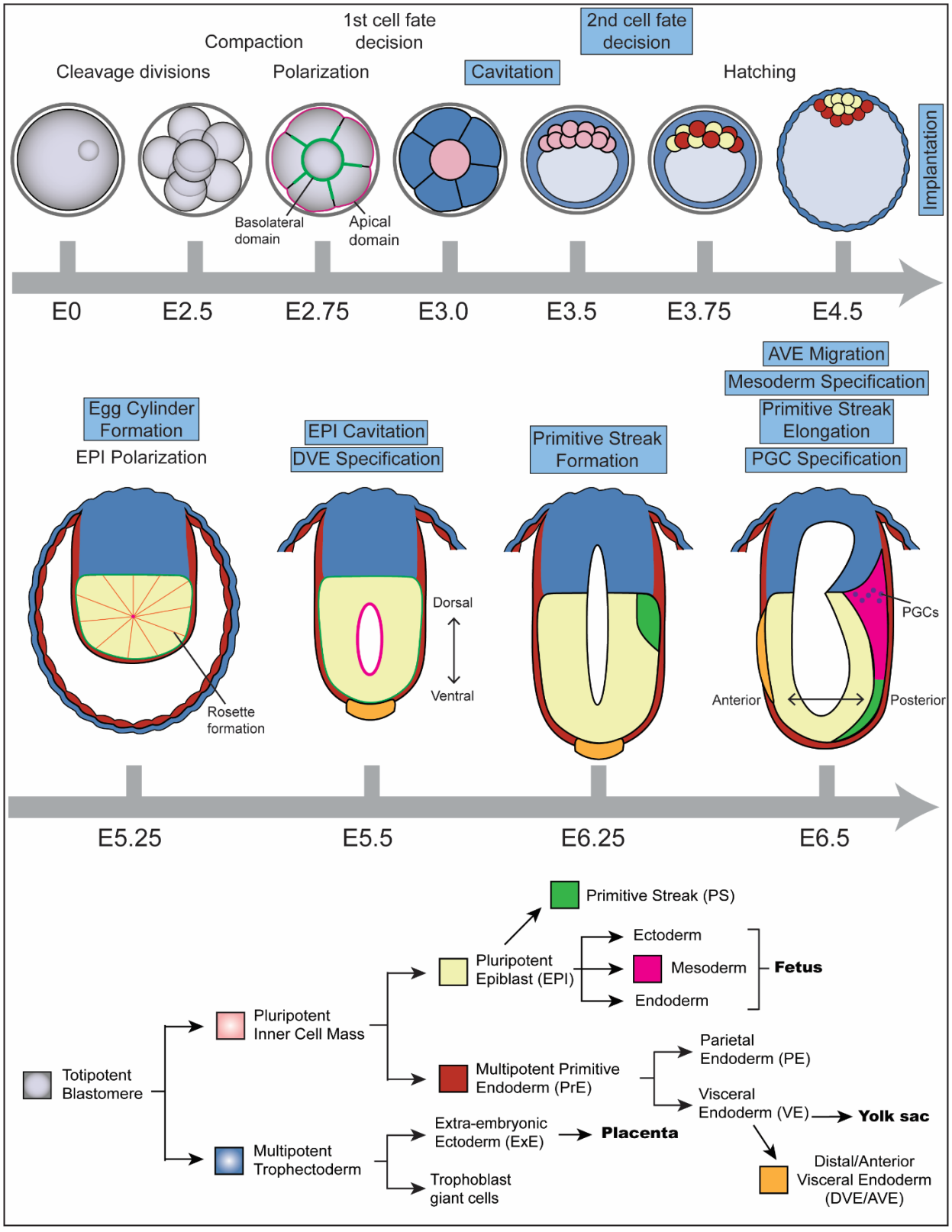

Figure 1.1. Key events in mouse development from zygote to gastrulation.

Figure 1.1 (cont'd).
The first week of embryonic development in mice can be divided into pre- and post-implantation stages. During pre-implantation, two cell fate decisions give rise to three important stem cell progenitor types: epiblast, primitive endoderm, and trophectoderm. After implantation, these cell types mature and differentiate to begin to pattern the embryo in preparation for germ layer formation and body axis specification during gastrulation. E = Embryonic Day. Blue boxes denote processes which are proposed to be regulated by BMP signaling.

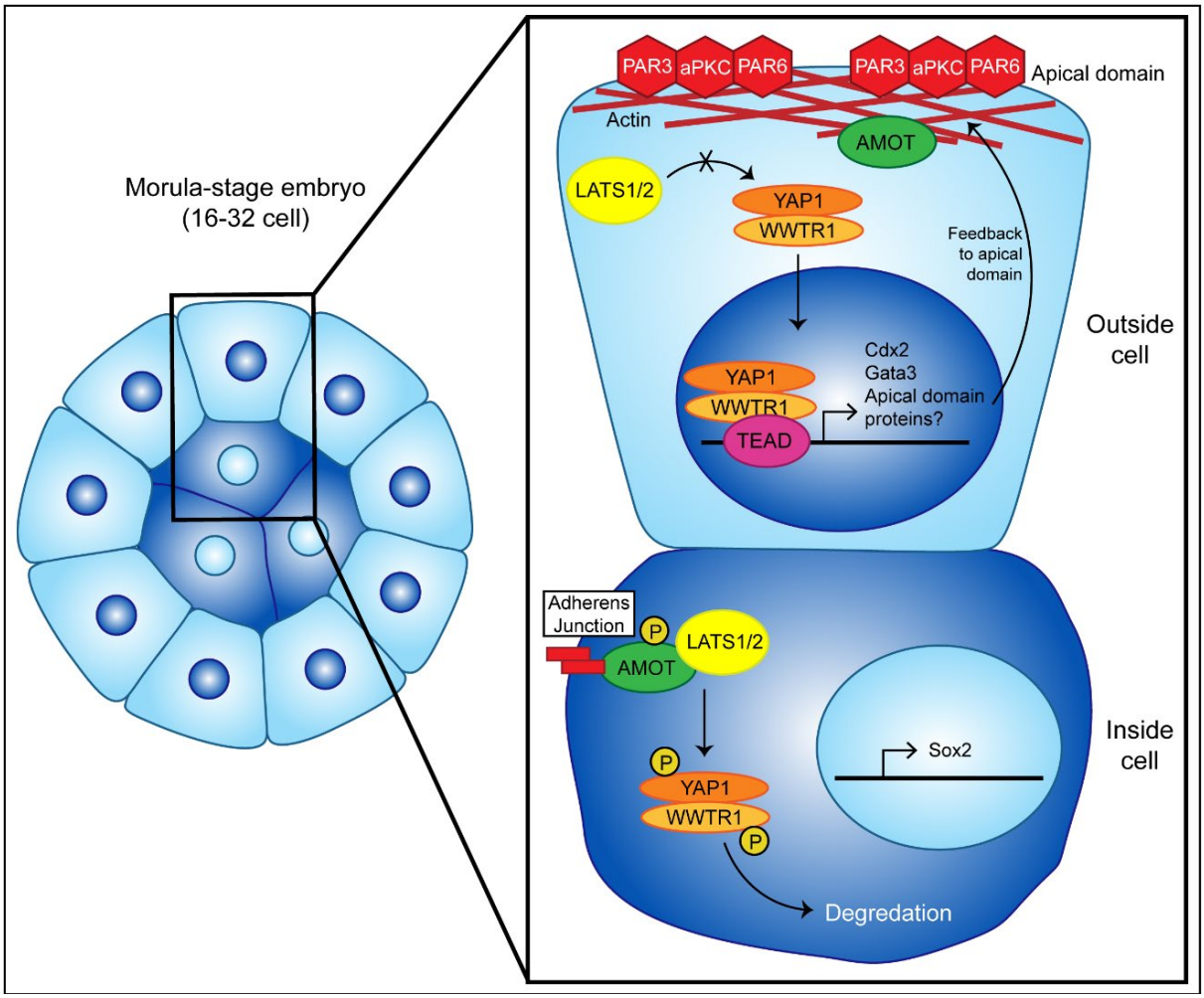

Figure 1.2. Hippo signaling regulates the first cell fate decision in mouse embryos. Beginning at the 16-cell stage in mouse embryonic development, the outer, polarized cells sequester AMOT at the apical domain and prevent its interaction with LATS1/2. This prevents LATS1/2 from phosphorylating YAP1/WWTR1, which are able to enter the nucleus and promote the transcription of TE genes. Inner cells do not have an apical domain, so LATS1/2 are able to phosphorylate YAP1/WWTR1 and prevent their translocation to the nucleus. Without YAP1/WWTR1 transcriptional activity, pluripotency genes are upregulated to establish an ICM cell fate.

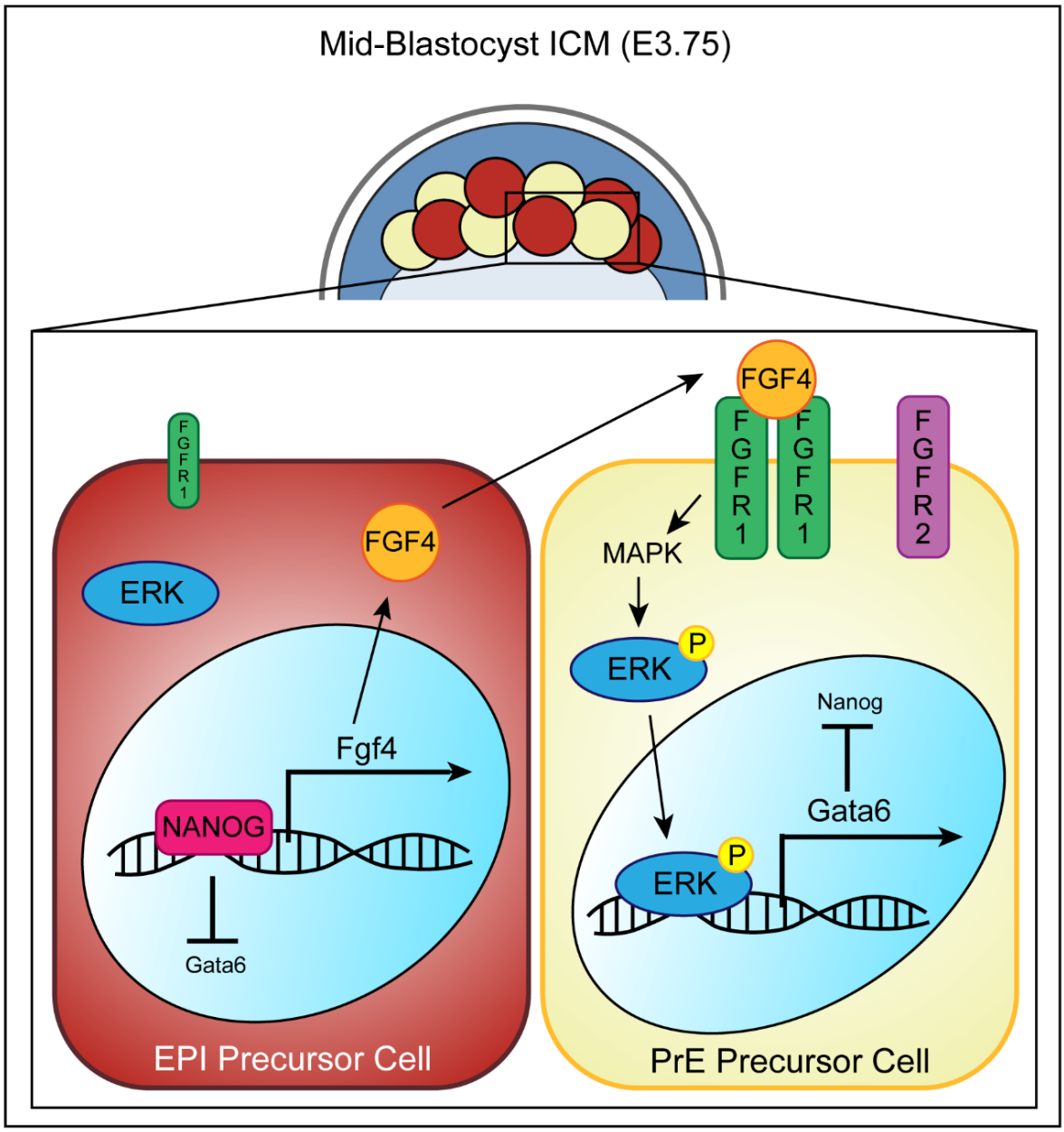

Figure 1.3. Fibroblast Growth Factor signaling regulates the second cell fate decision in mouse embryos. Within the ICM, cells with higher levels of *Fgf4* expression secrete the FGF4 ligand to neighboring cells. Active FGF signaling through MAPK and ERK promotes transcription of *Gata6*, promoting a PrE fate. Decreased signaling in the *Fgf4*-producing cells increases transcription of *Nanog*, promoting an EPI fate. GATA6 and NANOG mutually repress one another, creating feedback loops which solidify the cell fates.

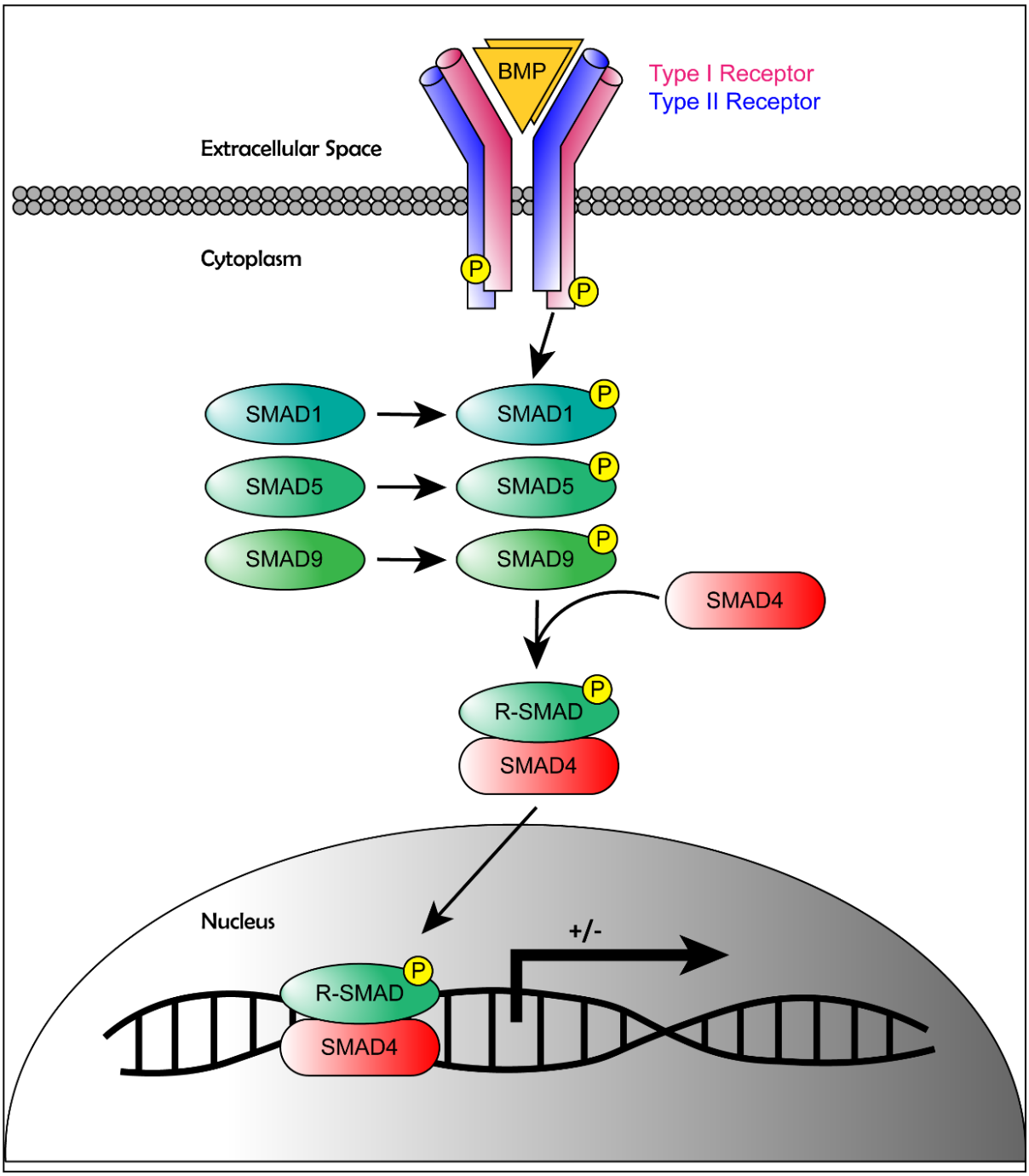

Figure 1.4. Biochemical interactions of BMP signaling in mammals. Dimerized BMP ligands bind heterotetramers of Type I and Type II serine-threonine kinase receptors. Activated receptor complexes phosphorylate internal receptor-associated SMAD proteins, which allows them to form complexes with the co-factor SMAD4. The completed SMAD complexes accumulate in the nucleus and regulate transcription, most often in conjunction with other transcription factors.

CHAPTER 2.

SMAD4 IS ESSENTIAL FOR EPIBLAST SCALING AND MORPHOGENESIS AFTER IMPLANTATION, BUT NONESSENTIAL PRIOR TO IMPLANTATION IN THE MOUSE

Robin E. Kruger[1,2], Tristan Frum[3,4], Stephanie L. Hickey[5], A. Sophie Brumm[6], Kathy K. Niakan[6,7,8,9], Farina Aziz[1], Marcelio A. Shammami[2,10], Jada G. Roberts[11], and Amy Ralston[2,3]

1) Cell and Molecular Biology Ph.D. Program, Michigan State University, East Lansing, MI, 48824, USA

2) Reproductive and Developmental Sciences Training Program, Michigan State University, East Lansing, MI, 48824, USA

3) Department of Biochemistry and Molecular Biology, Michigan State University, East Lansing, MI, 48824, USA

4) Current address: Department of Internal Medicine, University of Michigan Medical School, Ann Arbor, MI, 48109, USA

5) Research Technology Support Facility, Michigan State University, East Lansing, MI, 48824, USA

6) Human Embryo and Stem Cell Laboratory, The Francis Crick Institute; London, NW1 1AT, UK

7) The Centre for Trophoblast Research, Department of Physiology, Development and Neuroscience, University of Cambridge, Cambridge, CB2 3EG, UK

8) Wellcome Trust – Medical Research Council Stem Cell Institute, University of Cambridge, Jeffrey Cheah Biomedical Centre, Puddicombe Way, Cambridge, CB2 0AW, UK

9) Epigenetics Programme, Babraham Institute, Cambridge, CB22 3AT, UK

10) Genetics and Genome Sciences Ph.D. Program, Michigan State University, East Lansing, MI 48824, USA

11) Molecular, Cellular, and Integrative Physiology Ph.D. Program, Michigan State University, East Lansing, MI 48824, USA

This chapter is modified from Kruger *et al.,* submitted to *Development.* Figures and text pertaining to Figure 2.3, Supplemental Figure 2.3F-G, Supplemental Figure 2.5, and Supplemental Figure 2.6 are not included in the submitted manuscript.

This study was supported by the National Institutes of Health R35 GM131759 and T32 HD087166. Work in the laboratory of KKN was supported by the Wellcome (221856/Z/20/Z) and by the Francis Crick Institute (FC001120).

Section 2.1. Abstract

Bone Morphogenic Protein (BMP) signaling plays an essential and highly conserved role in axial patterning in embryos of many externally developing animal species. However, in mammalian embryos, which develop inside the mother, early development includes an additional stage known as preimplantation. During preimplantation, the epiblast lineage is segregated from the extraembryonic lineages that enable implantation and development *in utero*. Yet, the requirement for BMP signaling in mouse preimplantation is imprecisely defined. We show that, in contrast to prior reports, BMP signaling (as reported by SMAD1/5/9 phosphorylation) is not detectable until implantation, when it is detected in the primitive endoderm – an extraembryonic lineage. Moreover, preimplantation development appears normal following deletion of maternal and zygotic *Smad4,* an essential effector of BMP signaling. In fact, mice lacking maternal *Smad4* are viable. Finally, we newly uncover a requirement for zygotic *Smad4* in epiblast scaling and cavitation immediately after implantation, via a mechanism involving FGFR/ERK attenuation. Altogether, our results demonstrate no role for BMP4/SMAD4 in the first lineage decisions during mouse development. Rather, multi-pathway signaling among embryonic and extraembryonic cell types drives epiblast morphogenesis post-implantation.

Section 2.2. Introduction

In animal embryos, including mice, frogs, fish, and flies, the Bone Morphogenic Protein (BMP) signaling pathway oversees critical patterning events early in development. In non-mammalian species, BMP signaling is critical for specification of the dorsal/ventral

axis of the early embryo (De Robertis & Sasai, 1996; O'Connor et al., 2006; Zinski et al., 2018). However, the mammalian embryo has an additional developmental task immediately following fertilization: specification of the extraembryonic lineages that will give rise to placenta and yolk sac and enable development within the mother. Published studies support roles for BMP signaling in both extraembryonic lineage specification, prior to implantation, and subsequent axial patterning, which occurs after implantation (Graham et al., 2014; Reyes de Mochel et al., 2015; Senft et al., 2019; Yamamoto et al., 2009). However, differences in technical approaches used, as well as challenges intrinsic to mouse such as small embryo size and internal development, have limited origination of a universally accepted model of the role of BMP signaling in mouse embryos throughout pre- and post-implantation stages.

BMP is one of several related and highly conserved molecular signaling pathways belonging to the Transforming Growth Factor beta (TGFβ) superfamily of cytokines. The molecular mechanisms of TGFβ signaling have been carefully studied (C. Chang, 2016; Massagué & Sheppard, 2023). BMP proteins, like other members of the TGFβ pathway, are secreted ligands that elicit cellular responses by binding to heterodimeric, transmembrane serine-threonine kinase receptors. The activated receptor complex then phosphorylates members of a family of intracellular effectors known as receptor-associated SMADs (r-SMADs). Phosphorylation of r-SMADs allows their association with a co-factor SMAD and accumulation in the nucleus, where they impact chromatin and transcription (Hill, 2016). In mammals, r-SMAD activity is encoded by several *Smad* paralogues, with SMAD1, SMAD5, and SMAD9 (also known as SMAD8) primarily

transducing BMP signals and SMAD2 and SMAD3 primarily transducing Nodal, Activin, and TGFβ. Notably, the mammalian genome encodes a single co-factor Smad, SMAD4, which is shared by BMP, Nodal, Activin, and TGFβ signaling pathways.

Across species, BMP signaling has been visualized in embryos using antibodies that specifically recognize the phosphorylated form of the BMP-responsive r-SMAD(s). This approach has been used to observe gradients of BMP signaling activity that correspond with the dorsal/ventral axis in fly, fish, and frog embryos (Dorfman & Shilo, 2001; Plouhinec & De Robertis, 2009; Schohl & Fagotto, 2002; Tucker et al., 2008). In mouse, no graded pSMAD1/5/9 pattern has been reported. Prior to implantation, pSMAD1/5/9 is reportedly detected in all cell types of the embryo at multiple stages (Graham et al., 2014; Reyes de Mochel et al., 2015). After implantation, pSMAD1/5/9 is detected within a subdomain of extraembryonic cells, and not within the embryo itself until it is detected in emerging mesoderm during gastrulation (Senft et al., 2019). These observations suggest fundamental differences in the roles of BMP signaling between mammalian and non-mammalian animal embryos, but raise the need for additional, functional lines of evidence.

In mice, individual members of the BMP signaling pathway appear to be dispensable prior to embryonic day 6.5 (E6.5). Knockout of genes encoding the predominant ligand *Bmp4* (Lawson et al., 1999; Winnier et al., 1995), the receptors *Bmpr2* (Beppu et al., 2000), *Bmpr1a* (Mishina et al., 1995), *Actr1a* (Z. Gu et al., 1999), the r-SMADs encoded by *Smad1* (Tremblay et al., 2001) and *Smad5* (H. Chang et al., 1999), and the co-Smad

Smad4 (Sirard et al., 1998; X. Yang et al., 1998, 2002) all point to essential roles for BMP signaling in extraembryonic mesoderm, extraembryonic endoderm, and germ cell development. Mechanistically, BMP also interacts with Nodal to pattern the visceral endoderm and to specify distal, and then anterior visceral endoderm, structures required to spatially pattern the embryo and specify the primitive streak (Robertson, 2014; Waldrip et al., 1998; Yamamoto et al., 2009). These events define gastrulation and anterior/posterior axial patterning in mouse, processes which therefore rely on BMP signaling. None of these studies reported that BMP signaling loss-of-function had any effect on development prior to E5.5. However, maternal gene products provided within the oocyte could complicate interpretation of knockout phenotypes resulting from zygotic gene deletion only. Indeed, evidence exists that BMP pathway members are maternally supplied and functional in embryos of other animal species (Das et al., 1998; Faure et al., 2000; Kramer et al., 2002; Miyanaga et al., 2002; F. Zhang et al., 2020). Finally, mouse embryos are particularly challenging to recover between E4.5 and E6.5 and we lack an *in vitro* protocol that robustly recapitulates *in vivo* development during these stages, presenting a barrier to the facile testing of a possible role for BMP signaling during the peri-implantation period.

By contrast, preimplantation embryos are relatively easy to isolate and culture *in vitro*. Accordingly, several studies have suggested a role for BMP signaling in preimplantation development. Culturing preimplantation embryos in the presence of small-molecule BMP inhibitors led to decreased numbers and cell cycle rate of extraembryonic trophectoderm (TE) and primitive endoderm (PrE) cells, as well as changes in

expression of lineage-specific transcription factors, including markers of PrE (SOX17, GATA6), TE (CDX2), and inner cell mass (ICM, OCT4) (Graham et al., 2014; Reyes de Mochel et al., 2015; Stuart et al., 2019). Some of these observations were recapitulated following microinjection of siRNA against *Bmp4* or overexpression of dominant-negative forms of *Bmpr2* (Graham et al., 2014). Overexpression of dominant-negative *Smad4* reportedly phenocopied loss of the upstream signaling components. In principle, these approaches could interfere with the activities of both maternally and zygotically expressed signaling components and thereby achieve more extreme loss of function. However, pSMAD1/5/9 was not examined in these manipulated embryos, so the extent to which these manipulations disrupted BMP signaling is unclear. Moreover, inhibitors are prone to off-target effects, which could further confound interpretation of results (Lowery et al., 2016).

In the present study, we visualize pSMAD1/5/9 in wild-type and embryos in which *Bmp4* has been maternally and zygotically deleted, as well as lineage specification and morphogenesis in embryos lacking maternal and zygotic *Bmp4* or *Smad4* throughout preimplantation, peri- implantation, and early post-implantation stages. We report that, in contrast to previous studies, BMP signaling is apparently dispensable during mouse preimplantation development. However, we observed that SMAD4-mediated signaling is essential for peri-implantation epiblast morphogenesis shortly after implantation, when it helps attenuate FGF/ERK signaling to enable the timely execution of epiblast morphogenetic events.

Section 2.3. Materials and Methods

scRNA-seq Analysis

Single-cell RNA-seq data generated by Nowotschin et al. was used to analyze the expression of TGFβ genes in mouse E3.5, E4.5, E5.5, and E6.5 blastocysts (Nowotschin et al., 2019). The analysis was completed using R v4.1.0 with tools from Seurat v4.3.0 (R-core Team 2021) (Hao et al., 2021). We normalized the UMI counts using SCTransform and cells were visualized in 2D space using UMAP performed on the first 30 principal components (Choudhary & Satija, 2022; Hafemeister & Satija, 2019). After excluding TGFβ genes expressed in <10 cells, we used Seurat's FindAllMarkers function with the Wilcoxon rank-sum test to identify TGFβ genes enriched in each cell type versus all other cells. The p-values were corrected for multiple comparisons using the Bonferroni method. Genes with p-adj<0.01 and average log2 fold change<0.25 were considered cluster enriched. Heatmaps were generated using the pheatmap (v 1.0.12) after averaging the normalized expression for each gene in each cell type.

Mouse Strains and Genotyping

All animal research was conducted in accordance with the guidelines of the Michigan State University Institutional Animal Care and Use Committee under approved protocol 202300108. Wild type embryos were derived from CD-1 mice (Charles River). The following alleles were used in this study and maintained in a CD-1 background: *Bmp4*^{tm1Jfm}*/J* (W. Liu et al., 2004); *Smad4*$^{tm2.1Cxd}$*/J* (X. Yang et al., 2002); *Tg(Zp3-cre)93Knw* (De Vries et al., 2000). Null alleles were generated by breeding dams

carrying homozygous floxed alleles and the *Zp3Cre* allele to CD-1 males. Mouse genotypes were determined by PCR using genomic DNA extracted using the REDExtract-N-Amp kit (Sigma XNAT) according to the manufacturer's protocol. Embryo genomic DNA was extracted using the same kit scaled to 10 µL total volume. Genomic extracts (1–2 µL) were then subjected to PCR using allele-specific primers (see Table 2.3).

Embryo Collection and Culture

Mice were maintained on a 12 hour light/dark cycle. Preimplantation (E2.5-E4.5) embryos were collected by flushing the oviduct or uterus with M2 medium (Sigma M7167). Post-implantation (E4.75-E6.5) embryos were collected by dissecting the embryos from the decidua in ice-cold PBS containing 1% FBS (HyClone SH30396.02) or Bovine Serum Albumin (BSA, Sigma A7888). During embryo collection, dissected embryos were held in warm M2 media. For embryo culture, KSOM medium (Millipore MR-121-D) was equilibrated overnight prior to embryo collection. Where indicated, the following were included in the culture medium: 1 µM or 0.25 µM LDN-193189 in DMSO (Stemgent 04-0074-02); 1 µg/mL recombinant FGF4 in PBS with 0.1% BSA (R&D 235-F4); 1 µg/mL heparin (Sigma H3149); 100 ng/mL recombinant BMP4 in 4 mM HCl (R&D 314-BP); 1 µM PD173074 in DMSO (Selleckchem S1264); 5 µM PD0325901 in DMSO (Stemgent 04-0006); or 0.2% DMSO (New England BioLabs B0515A) as control. Embryos were cultured at 37°C in a 5% CO_2 incubator under light mineral oil (Millipore ES-005-C). For serum-free culture conditions (KSOM+PVA-BSA), embryos were cultured as described in Frum & Ralston, 2020.

Real-time PCR of Oocytes

Smad4 expression levels in oocytes were assessed by real-time PCR as previously described (Blij et al., 2012). *Smad4* levels were assessed in oocytes from three wild-type and three *Smad4* maternal null females. Oocytes collected from each female were pooled for mRNA extraction and cDNA synthesis. RT-PCR was performed in quadruplicate technical replicates for each cDNA sample. Primers were (5′-3′): *Actb*, CTGAACCCTAAGGCCAACC and CCAGAGGCATACAGGGACAG; *Smad4* (wild-type allele) CGCGGTCTTTGTACAGAGTTA and ACACTGCCGCAGATCAAAG; *Smad4* (deleted allele), CACAGGACAGAAGCGATTGA and CCAAACGTCACCTTCACCTT.

Immunofluorescence and Confocal Microscopy

Preimplantation embryos (E2.5-E4.75) were fixed with 4% formaldehyde (Polysciences 04018) for 10 minutes, permeabilized with 0.5% Triton X-100 (Sigma Aldrich X100) for 30 minutes, and then blocked with blocking solution (10% Fetal Bovine Serum (HyClone SH30396.02), 0.1% Triton X-100) overnight at 4°C. Embryos were incubated with primary antibody overnight at 4°C. The next day, embryos were washed in blocking solution for 30 minutes, incubated in secondary antibody diluted in blocking solution for 1 hour, washed in blocking solution for 30 minutes, then stained with nuclear stain diluted in block for 10 minutes or overnight.

Post-implantation embryos (E5.0-E6.5) were fixed with 4% formaldehyde for 1 hour, washed 3 times in 0.1% Tween-20 (Sigma Aldrich P9416), permeabilized for 4 hours in 0.5% Triton X-100, and then blocked with blocking solution (3% BSA (Sigma Aldrich

A7888); 0.3% Triton X-100 in PBS) overnight at 4°C. Embryos were incubated with primary antibody overnight at 4°C. The next day, embryos were washed three times in 0.1% Tween-20 for 5 minutes, then incubated in secondary antibody diluted in blocking solution overnight. The following day embryos were washed three times in 0.1% Tween-20 for 5 minutes, then stained with nuclear stain diluted in block for 10 minutes or overnight.

All embryos (preimplantation or post-implantation) which used antibodies against pSMAD1/5/9 were fixed with 4% formaldehyde for 1 hour, methanol dehydration-rehydration series (25%, 50%, 75%, 100%) for 5 minutes each, washed three times in freshly-made 1% Triton X-100 for 10 minutes, washed 20 minutes in ice-cold acetone at -20°C, washed three times in freshly-made 1% Triton X-100 for 10 minutes, then then blocked with blocking solution (10% Fetal Bovine Serum, 0.1% Triton X-100 in PBS) overnight at 4°C. Embryos were incubated with primary antibody overnight at 4°C. The next day, embryos were washed three times in freshly-made 0.1% Triton X-100 for 10 minutes, incubated in secondary antibody diluted in blocking solution for 2 hours, washed three times in freshly-made 0.1% Triton X-100 for 10 minutes, then stained with nuclear stain diluted in blocking solution for 10 minutes or overnight.

All embryos (preimplantation or post-implantation) which used antibodies against pERK were fixed with 4% formaldehyde for 1 hour, washed three times for 5 minutes in PBS, washed 20 minutes in ice-cold methanol at -20°C, permeabilized 30 minutes in 0.1% Tween-20, then blocked with blocking solution (3% Bovine Serum Albumin; 0.3% Triton

X-100 in PBS) overnight at 4°C. Embryos were incubated with primary antibody overnight at 4°C. The next day, embryos were washed three times in PBS for 5 minutes, incubated in secondary antibody diluted in blocking solution for 2 hours, washed three times in PBS for 5 minutes, then stained with nuclear stain diluted in block for 10 minutes or overnight. All solutions contained HALT protease inhibitor (Thermo Scientific 78430) and PhosSTOP phosphatase inhibitor (Roche 04906837001) diluted 1:500.

Antibodies used are listed in Table 2. Embryos were imaged using an Olympus FluoView FV1000 Confocal Laser Scanning Microscope system with 60X PlanApoN oil (NA 1.42) objective. For each embryo, z-stacks were collected, with 5 μm intervals between optical sections. All embryos were imaged prior to knowledge of their genotypes.

Embryo Analysis

For each embryo, z-stacks were analyzed using Fiji (ImageJ), which enabled the labeling, based on DNA stain, of all individual cell nuclei. Using this label to identify individual cells, each cell in each embryo was then assigned to relevant phenotypic categories, without knowledge of embryo genotype. Phenotypic categories included marker expression (e.g., OCT4 positive or negative) and marker localization (e.g., pSMAD1/5/9 nuclear, absent, or unlocalized). Statistical analysis was performed using GraphPad Prism (v. 9.5.1). Figure images were assembled using Adobe Illustrator.

Section 2.4. Results

Phosphorylated SMAD1/5/9 is first detectable in peri-implantation embryos

To determine when BMP signaling becomes active in the mouse embryo, we first developed a method to examine the localization of transcription factors SMAD1, 5, and 9, which are phosphorylated in response to ligand/receptor binding (Dijke & Hill, 2004). To achieve this, we used immunofluorescence and an antibody that recognizes phosphorylated SMAD1/5/9 (pSMAD1/5/9, Fig. 2.1) (Senft et al., 2019; Xu et al., 2019; Yuan et al., 2015). We did not detect pSMAD1/5/9 in preimplantation embryos flushed from uteri between E3.75-E4.25 (Fig. 2.1A, Supp. Fig. 2.1A). We first observed pSMAD1/5/9 in E4.5 peri-implantation embryos (Fig. 2.1A), when it was detected in nuclei of a few inner cell mass cells in 29% of embryos examined (Fig. 2.1B-C). By E4.75, when embryos have undergone implantation, we observed pSMAD1/5/9-positive cells in 87.5% of the embryos evaluated (Fig. 2.1A-C). Starting at E5.0, we observed pSMAD1/5/9- positive cells within 100% of embryos examined (Fig. 2.1A-C, Supp. Fig. 1A). The observed pSMAD1/5/9 overlapped with a sub-set of GATA6-expressing primitive endoderm (E4.5-E4.75) and visceral endoderm (E5.5-E5.75) cells (Fig. 2.1A).

To determine whether the observed pSMAD1/5/9 signal was specific, we treated E5.5 wild-type embryos with LDN-193189 (LDN hereafter) which has been used to disrupt BMP signaling in mouse embryos (Graham et al., 2014; Reyes de Mochel et al., 2015). A concentration of 1 μM LDN was reported as sufficient to inhibit BMP signaling in preimplantation mouse embryos (Reyes de Mochel et al., 2015). However, we found that treatment with 1 μM LDN was highly toxic to embryos (Supp. Fig. 2.1B).

Nevertheless, treatment with 0.25 μM LDN led to complete loss of pSMAD1/5/9 signal in E5.5 embryos (Supp. Fig. 2.1B). Altogether, these observations suggest that BMP signaling becomes active around the time of embryo implantation but is not active during preimplantation stages.

BMP pathway members are present, but largely inactive, prior to implantation

A prior report showed that BMP4 is sufficient to influence gene expression in preimplantation mouse embryos (Goissis et al., 2023), suggesting that preimplantation embryos can respond to exogenous BMP signals. We therefore examined expression dynamics of genes encoding BMP pathway members during preimplantation stages. We analyzed published single-cell RNA-seq data from mouse embryos at stages E3.5-E6.5 (Nowotschin et al., 2019). At E3.5, many core components of canonical BMP signaling were detectable, including the ligand *Bmp4,* Type I receptor *Bmpr1a*, Type II receptors *Bmpr2* and *Acvr2b,* receptor-associated SMAD *Smad5,* and co-factor SMAD *Smad4* (Fig. 2.1D and Supp. Fig. 2.2).

Next, we investigated whether pSMAD1/5/9 could be induced in preimplantation embryos treated with exogenous BMP. We cultured compacted 8-cell stage embryos (E2.75) in 300 ng/ml BMP4 for 36 hours to the blastocyst stage (equivalent in cell number to E3.75, as confirmed by cell counts). Although we did not observe pSMAD1/5/9 in any control embryos cultured in unsupplemented medium, we observed low, but detectable levels of pSMAD1/5/9 in 82% (n=14/17) of embryos treated with exogenous BMP4, further supporting the faithful detection of pSMAD1/5/9 by

immunofluorescence analysis (Fig. 2.1E-F). Notably, pSMAD1/5/9 was detected only in the ICM but did not preferentially colocalize with either SOX2-positive epiblast (EPI) or SOX2-negative PrE cells. Therefore, we conclude that BMP signaling is not highly active during preimplantation development, but ICM cells are competent to respond to exogenous BMP signals at these stages, consistent with published investigations (Graham et al., 2014; Reyes de Mochel et al., 2015).

We next analyzed the pSMAD1/5/9 in embryos shortly after implantation. Consistent with prior reports (Senft et al., 2019; Yamamoto et al., 2009), we detected pSMAD1/5/9 within a zone of the visceral endoderm (VE) that flanks the extraembryonic ectoderm (ExE) at E5.5 and E5.75 (Fig. 2.1A, Supp. Fig. 2.1A). This observation is also consistent with evidence that several key components, including *Bmp2, Smad1, Smad5,* and *Bmpr2,* are substantially upregulated around the time of implantation (E4.5-E5.5), particularly in the PrE/VE lineage (Fig. 2.1D, Supp. Fig. 2.1A- B). Notably, culturing E5.5 embryos in the presence of exogenous BMP4 for 6 hours was sufficient to expand the zone of pSMAD1/5/9 within the VE in a dose-dependent manner (Supp. Fig. 2.1C). Thus, the availability of ligand could limit the extent of pathway activation, during both pre- and post-implantation stages.

Finally, we evaluated pSMAD1/5/9 in *Bmp4*-null embryos at E5.5. We were unable to detect pSMAD1/5/9in *Bmp4*-null embryos, although it was observed at wild-type levels and localization in homozygous wild-type littermate controls (Fig. 2.1G-H). In *Bmp4* heterozygous embryos, we observed an intermediate phenotype where some

pSMAD1/5/9 was detectable but trended toward lower numbers of pSMAD1/5/9-positive cells than wild-type (Fig. 2.1H). This suggests that at E5.5, BMP4 plays a major role in initiating BMP signaling activity in the mouse, and that this function of BMP4 is dose-dependent.

Maternal *Bmp4* and *Smad4* are not required for development

Previous knockout studies of BMP signaling components did not report preimplantation phenotypes (Beppu et al., 2000; Mishina et al., 1995; Sirard et al., 1998; Winnier et al., 1995). However, other groups reported defects in preimplantation lineage specification using pathway inhibitors or microinjection of RNAi or mRNA for dominant-negative overexpression (Graham et al., 2014; Reyes de Mochel et al., 2015; Stuart et al., 2019). One way to reconcile these disparate findings is to invoke a model in which some components of the BMP pathway are maternally imparted to the oocyte and participate in preimplantation development to compensate for previously reported zygotic null mutations. To further investigate this possibility, we examined cell fate specification in embryos lacking both maternal (m) and zygotic (z) *Bmp4* or *Smad4* using the female germ line-expressed *Zp3-Cre* (De Vries et al., 2000) in combination with floxed alleles of either *Bmp4* or *Smad4* (see Supp. Fig. 2.3A for breeding scheme). RT-qPCR analysis confirmed the absence of detectable *Smad4* transcript in *Smad4* mz null embryos (Supp. Fig. 2.3B), as we have observed for many other loci deleted using this approach (Blij et al., 2012; Frum et al., 2013, 2018; Wicklow et al., 2014).

Remarkably, we were able to recover either *Bmp4* or *Smad4* mz null blastocysts at predicted rates, indicating no requirement for maternal *Bmp4* or *Smad4* on fertilization or embryo development. Moreover, both *Bmp4* and *Smad4* mz null embryos exhibited normal morphology, total cell number, and ratio of trophectoderm and ICM cells (Fig. 2.2, Supp. Fig. 2.3C-E). In addition, the ICM marker *Oct4* was detected at normal levels within the ICM, and CDH1 localization strongly suggested that the TE was properly polarized (Supp. Fig. 2.4). Finally, the expression of EPI and PrE cell fate markers at E3.75, E4.25, and E4.5 (Fig. 2.2, Supp. Fig. 2.3C-E) was unaffected in either *Bmp4* or *Smad4* mz null embryos at these stages, consistent with normal ICM differentiation. Our observations support the conclusion that canonical BMP signaling does not play a major role in preimplantation development.

As the embryos in these studies were fixed immediately after collection from the uterus, it is possible that uterine-derived signals compensated for loss of BMP4 in embryos. To eliminate potential exogenous BMP4 from the uterus, we collected *Bmp4* mz null embryos at E1.5 and cultured for 60 hours to blastocyst stage. As serum may contain BMP agonists or antagonists that can affect embryo development in culture, we conducted this experiment in serum-free conditions by supplementing KSOM media with polyvinyl alcohol without bovine serum albumin (Frum & Ralston, 2020). The cultured *Bmp4* mz null embryos again displayed normal morphology, and we did not observe any difference in total cell number or EPI:PrE ratio when compared to wild-type controls (Supp. Fig. 2.3F-G). In a parallel set of experiments, we allowed *Smad4* m null embryos to develop to term. Mice lacking m *Smad4* were born and developed

apparently normally to 4 months old (10/10 mice, two litters). We conclude that maternal *Bmp4* and *Smad4* are dispensable for development and that neither zygotic gene plays a predominant role prior to implantation.

Exogenous BMP4 is capable of inducing cell fate changes in preimplantation embryos

Because we were able to induce pSMAD1/5/9 expression in preimplantation embryos cultured with exogenous BMP4, we wanted to test the functional consequences of that induced signaling. BMP signaling has been suggested to affect preimplantation cell fate (Goissis et al., 2023; Graham et al., 2014; Reyes de Mochel et al., 2015). To test whether our induced BMP signaling could affect preimplantation cell fate, we cultured wild-type E2.75 embryos in 100 ng/ml or 300 ng/mL BMP4 for 36 hours to blastocyst stage. Examination of cell fate markers in these embryos by immunofluorescence did not reveal any significant differences in total cell number or the amount of EPI, PrE or TE cells (Fig. 2.3A-B, Supp. Fig. 2.5). This suggests that BMP4 treatment alone is not sufficient to induce changes in cell fate in preimplantation embryos.

To test this further, we cultured embryos with 100 ng/mL BMP4 in the presence of 1 ug/mL exogenous FGF4 and heparin, a treatment known to cause changes in preimplantation cell fate (Yamanaka et al., 2010). Treatment with FGF4/heparin alone directed the entire inner cell mass of treated embryos toward a PrE cell fate, as expected (Fig. 2.3A-B, Supp. Fig. 2.5C). Embryos treated with both exogenous BMP4 and exogenous FGF4/heparin did not rescue EPI specification, but instead showed a

significant increase in the amount of inner cell mass cells which did not express markers for either EPI or PrE cell fate (Fig. 2.3C, Supp. Fig. 2.5C). Importantly, this effect was not seen in *Smad4* mz null embryos cultured under the same conditions (Fig. 2.3C, Supp. Fig. 2.5C), suggesting that the increase in unspecified ICM cells relies on BMP signaling capability. Overall, these results suggest that although BMP signaling does not normally function in preimplantation cell fate specification, it has a capability to do so under specific culture conditions.

Smad4 is required for epiblast cavitation at E5.5 in a *Bmp4*-independent manner

Prior studies mainly focused on characterization of BMP signaling loss of function phenotypes at later stages (>E5.5) (Sirard et al., 1998; Winnier et al., 1995; X. Yang et al., 1998). However, we first observed BMP signaling activity in most embryos just after implantation at E4.75, prompting us to examine embryos lacking *Bmp4* or *Smad4* beginning at E4.75. At E4.75, *Smad4* null embryos were grossly morphologically normal (Fig. 2.4A). However, upon close examination, *Smad4* null embryos displayed a significant decrease in total cell number (Fig. 2.4B). We quantified the number of EPI, PrE, and TE cells in these embryos and discovered that the decreased cell number was most pronounced in EPI cells at this stage (Fig. 2.4B-C).

By E5.5, *Smad4* null embryos were visibly reduced in size and all displayed disorganization in EPI, VE, and ExE compartments, as expected from studies performed at E6.5 (Sirard et al., 1998; X. Yang et al., 1998) (Fig. 2.4D). Strikingly, the epiblast was greatly reduced in cell number (Fig. 2.4D-F) relative to controls, and had

not yet cavitated, as the proamniotic cavity was not present among most (>80%, n=7/9) *Smad4* null embryos examined (Fig. 2.4D, 2.4L). Notably, relative to extraembryonic lineages, the amount of EPI cells was disproportionately decreased in *Smad4* null embryos since the epiblast length was decreased even when normalized to proximal-distal embryo length (Fig. 2.4G-I, Supp. Fig. 2.6A). By contrast, the size of the ExE was appropriately scaled to the reduced size of *Smad4* null embryos at E5.5 (Fig. 2.4J-K). This suggests that *Smad4* is not only required for general embryonic growth, but also specifically required for epiblast growth relative to total embryo size. Notably, these phenotypes were not observed in E5.5 *Bmp4*-null embryos, which did not differ from wild-type in morphology, embryo size, or EPI or PrE cell number (Supp. Fig. 2.6B-E), suggesting that signaling pathways other than BMP signaling feed into SMAD4-regulation of epiblast growth and morphogenesis at this stage.

Defects in *Smad4*-null embryos are more widespread across cell types at E6.5

We next examined the epiblasts of *Smad4* mz null embryos at E6.5, which in other studies had been reported to display primarily extra-embryonic defects with relatively unaffected epiblasts (Sirard et al., 1998; X. Yang et al., 1998). Many of the defects we observed in E5.5 *Smad4*-null embryos were still observed at E6.5 (Supp. Fig. 2.7A). *Smad4*-null embryos showed a more significant reduction in total embryo size at this stage (Supp. Fig. 2.7B), as well as a highly disorganized and reduced EPI compartment (Supp. Fig. 2.7C). However, the difference in epiblast length as a percentage of total embryo length was no longer statistically significant between *Smad4*-null embryos and controls (Supp. Fig. 2.7D). Additionally, 60% of the observed E6.5 embryos had

cavitated (N=3/5) suggesting that loss of *Smad4* delays initiation of cavitation but does not prevent cavitation entirely. This is in agreement with previous studies, which did not report a specific defect in epiblast size or cavitation at E6.5 (Sirard et al., 1998; X. Yang et al., 1998). This observation suggests that by E6.5 the overall growth restriction of the entire embryo is so severe that the specific effect on the growth of the EPI is no longer apparent. None of the phenotypes observed in E6.5 *Smad4*-null embryos were as severe in E6.5 *Bmp4*-null embryos, although there was a slight significant decrease in total embryo length in E6.5 *Bmp4*-null embryos (Supp. Fig. 2.7E). The observed difference in total embryo size was not specific to the EPI (Supp. Fig. 2.7F-G). This suggests that there is a requirement for *Bmp4* at E6.5, but that the more severe effect of *Smad4* does not rely on *Bmp4*.

Epiblast cavitation requires SMAD4-dependent inhibition of FGF/ERK signaling

Having discovered that *Smad4* is required for epiblast cavitation and growth at E5.5, we began to investigate the mechanism underlying this role. We were struck by the observation that the ExE appeared disproportionately large, relative to the size of the EPI in E5.5 *Smad4* null embryos. To confirm the identity of the ExE cells, we examined markers of ExE, including phosphorylated ERK (pERK), which is elevated within the ExE (Corson et al., 2003). In *Smad4* null embryos, we observed pERK throughout putative ExE, consistent with their identity as ExE cells. However, we observed dramatically elevated levels of pERK within this region (Fig. 2.5A).

Since pERK in the ExE is known to be dependent on signaling by the Fibroblast Growth Factor (FGF) pathway (Corson et al., 2003), we therefore hypothesized that increased pERK could be due to elevated FGF signaling in *Smad4* null embryos. To test this hypothesis, we used a previously-published protocol to inhibit FGF signaling in embryos (Yamanaka et al., 2010), which effectively eliminated pERK in control embryos (Supp. 2.8A). Notably, inhibition of FGF signaling partially rescued epiblast defects in E5.5 *Smad4* null embryos (Fig. 2.5A). We observed a significant increase in epiblast scaling, as well as increased rates of cavitation (Fig. 2.5B-D). However, FGF inhibitor treatment did not rescue the overall growth restriction of *Smad4*-null embryos (Fig. 2.5E), nor was the number of OCT4-positive cells restored (Fig. 2.5F). These observations are consistent with SMAD4 repressing FGF signaling in the ExE during early post-implantation stages as a critical regulator of epiblast morphogenesis. Our observations also suggest that additional pathways regulate embryo growth downstream of SMAD4.

To determine whether elevated FGF signaling is sufficient to antagonize cavitation, we treated embryos with exogenous FGF4. In wild-type E5.5 embryos treated with exogenous 1 μg/mL FGF4, we observed elevated levels of pERK within the ExE and ectoplacental cone (Supp. Fig. 2.8A). However, we observed no impact on epiblast cavitation or epiblast size following this treatment (Supp. Fig. 2.8A-D). Altogether, these data suggest that pERK/FGF signaling antagonizes EPI cavitation, but upregulation of pERK alone is insufficient to induce cavitation defects in wild-type embryos, at least under the conditions tested here.

Section 2.5. Discussion

Despite being a highly conserved developmental signaling pathway, the role of BMP signaling in regulating peri-implantation mammalian development has not been fully elucidated. In part, this may be due to the technical challenges surrounding studying mammalian embryos at pre- and peri-implantation stages of development. Our study undertook a detailed examination of molecular markers of BMP signaling activity and the phenotypes of maternal-zygotic genetic knockout models of BMP signaling to identify the earliest role of BMP signaling in development. Although we failed to detect a role for BMP signaling in preimplantation embryos, we newly identified a role for *Smad4* in epiblast organization and cavitation at early post-implantation stages.

We focused our initial studies on defining the role of BMP signaling in preimplantation mouse development because there was not a consensus on this role in the existing literature. Previous studies of *Bmp4* and *Smad4* genetic knockouts in mice have largely focused on the more overt phenotypes which occur after implantation (G. C. Chu et al., 2004; C. Li et al., 2010; Senft et al., 2019; Sirard et al., 1998; Winnier et al., 1995; X. Yang et al., 1998). However, some studies have reported deleterious effects of BMP knockdown on *in vitro* cultured preimplantation embryos (Graham et al., 2014; Reyes de Mochel et al., 2015; Stuart et al., 2019). These studies found a range of effects, but largely reported a specific deficiency in extra-embryonic cell types, either by decreased cell numbers (Graham et al., 2014) or slower cell cycle (Reyes de Mochel et al., 2015). In contrast, our study did not uncover any defect in *Bmp4*- or *Smad4*-null preimplantation embryos, which did not differ from wild-type in morphology, cell type

specification, or expression of key developmental transcription factors even in *Bmp4*-null embryos cultured in defined media without BMP4 from E1.5 to blastocyst. These data suggest that the normal development of flushed embryos lacking BMP signaling factors is not due to replacement factors supplied by the uterus. Furthermore, in contrast to previous studies (Graham et al., 2014; Reyes de Mochel et al., 2015), we were unable to detect any pSMAD1/5/9 signal at preimplantation stages in flushed embryos, suggesting a lack of endogenous BMP signaling activity. Overall, our data strongly suggest that BMP signaling (or indeed, any signaling pathway mediated through SMAD4) does not play a role in preimplantation development or stem cell progenitor specification in mice.

Several differences exist between our current study and previous studies of BMP signaling in preimplantation development which may explain our failure to replicate the previous results. The earlier studies primarily examined preimplantation embryos in culture with serum. This may explain why they detected pSMAD1/5/9, as it is possible that the reported pSMAD1/5/9 signal was an artifact of culture conditions in undefined media. In support of this hypothesis, we were able to induce pSMAD1/5/9 when preimplantation embryos were cultured with exogenous BMP4. Differences in the embryo fixation or permeabilization protocols, the specificity of the antibodies used, or the genetic background of the embryos may also contribute to the differences in pSMAD1/5/9 expression or developmental phenotypes. Indeed, genetic background has already been shown to affect the severity of phenotypes in *Bmp4* knockout models (Winnier et al., 1995). Additionally, these earlier studies primarily modulated BMP

signaling with either pharmacological inhibitors or overexpression of dominant-negative receptors. As overexpressing proteins at above-physiological levels and off-target effects of chemical inhibitors have both been shown to induce detrimental phenotypes, it is also possible that the previously reported changes in preimplantation development were the result of non-specific effects. Several studies have reported that commonly-used BMP inhibitors such as dorsomorphin, LDN-193189, and DMH2 have the capability to inhibit dozens of non-specific kinases (Boergermann et al., 2010; Lowery et al., 2016; J. Vogt et al., 2011).

We report a novel requirement for *Smad4* in post-implantation development. Previous descriptions of *Smad4*-null embryos report growth restriction and disorganized VE beginning at E5.5, with embryonic lethality by E8.5 (G. C. Chu et al., 2004; Sirard et al., 1998; X. Yang et al., 1998). Our results are consistent with these findings, but also uncover a previously unappreciated defect specific to the epiblast. The proportion of EPI cells is decreased starting at E4.75, suggesting that in the absence of *Smad4* the number of EPI cells does not scale with embryo growth. The structure of the epiblast is also disrupted in these embryos, as *Smad4*-null embryos had largely disorganized epiblasts which failed to form a proamniotic cavity. It is unlikely that this defect is cell-autonomous, as embryos with an epiblast-specific knockout of *Smad4* do not display an observable defect until after gastrulation (G. C. Chu et al., 2004). Rather, it is likely that *Smad4* is required in the visceral endoderm to produce a signal that promotes EPI development non-cell-autonomously (Fig. 2.6A). This model is supported by the finding that VE-specific *Smad4*-knockout embryos fail to gastrulate properly and more closely

resemble whole-body *Smad4*-null embryos (C. Li et al., 2010). However, there was no defect reported in the VE-specific *Smad4*-KO embryos earlier than E6.5. It is possible that this discrepancy comes from the VE-specific *Cre* driver used to generate the knockout in this study, which is not active until E5.75. Since our study first observed an epiblast defect at E4.75, an earlier knockout of *Smad4* specific to the primitive endoderm lineage would be needed to test that the epiblast defect is in fact a non-cell-autonomous effect from the visceral endoderm. It is also interesting to note that a cavitation defect was not reported in previous *Smad4* knockout mouse models which targeted the same exon 8 (Sirard et al., 1998; X. Yang et al., 1998). It is possible that the phenotypic differences are due to differences in genetic background, as both of these studies were completed in C57/B6 mice, as opposed to the CD-1 background used in the current study. However, we also observed that some *Smad4* null embryos were cavitated at E6.5, so it is possible that the phenotypic discrepancies can be explained by a difference in developmental staging.

Our observations are consistent with prior observation that BMP signaling is necessary and sufficient for cavitation of embryoid bodies (Coucouvanis & Martin, 1999). In this context, BMP2 and BMP4 may be functionally redundant, and could explain why we observed normal cavitation in E5.5 *Bmp4*-null embryos. Alternatively, SMAD4 could regulate epiblast morphogenesis through another TGF-β pathway. Knockout of *Nodal* has been shown to decrease embryo size and expression of *Oct4* mRNA at early post-implantation stages (Brennan et al., 2001; Mesnard et al., 2006), but *Nodal*-null embryos cavitate normally and expression of OCT4 protein is apparently unaffected at E5.5 (Senft et al., 2019). As the cavitation defect and loss of OCT4-positive cells are

more severe in *Smad4*-null embryos than either *Bmp4*- or *Nodal*-null models alone, it suggests that *Smad4* may regulate epiblast morphogenesis through a combination of TGFβ pathways.

Our data also suggests that SMAD promotes cavitation by attenuating pERK levels. Inhibition of FGF/MAPK signaling rescued cavitation in *Smad4*-null embryos, even though the epiblast remained disproportionately small. This observation allows us to propose that cavitation is not dependent on epiblast size, but rather the embryo signaling environment. Our data suggest that ectopic upregulation of pERK resulting from loss of *Smad4* is detrimental to epiblast cavitation; however, the mechanisms of how these two pathways interact with one another and regulate cavitation remain unclear. SMAD4 could regulate several processes associated with epiblast cavitation, including epiblast cell apoptosis or epiblast cell polarization and lumenogenesis (Bedzhov & Zernicka-Goetz, 2014; Coucouvanis & Martin, 1995, 1999; Halimi et al., 2022) (Fig. 2.6B-C). In this model, *Smad4* is sufficient for initiation of cavitation, possibly through regulation of apoptosis by BMP signaling (Fig. 2.6A). Separately, *Smad4* also restricts MAPK signaling through ERK phosphorylation, which expands distally in the absence of *Smad4*. Meanwhile, FGF/MAPK partially regulates rosette formation, possibly through regulation of basement membrane formation by the emVE. In the presence of *Smad4*, when FGF/MAPK is restricted, rosette formation occurs properly, and cavitation is successful. In the absence of *Smad4*, the epiblast does not receive the signal for programmed cell death and does not initiate lumen formation. FGF/MAPK is also ectopically expanded, and rosette formation fails (Fig. 2.6B). By inhibiting ectopic

FGF/MAPK in *Smad4*-null embryos at the critical timepoint just before cavitation, basement membrane deposition occurs and rosette formation is allowed to proceed, forming a small proamniotic cavity. However, since the apoptotic signal from *Smad4* is still missing, cavitation is not completely rescued (Fig. 2.6C). This model suggests that the reason pERK upregulation was insufficient to compromise EPI cavitation in wild-type embryos is that by the time of treatment at E5.25, EPI polarization was already complete. In this way*, in vitro* modulation of FGF/MAPK signaling only affects cavitation in the absence of *Smad4*.

Although the above proposed mechanisms are consistent with our data, it is not proven from the current study that *Smad4* regulates cavitation through apoptosis or basement membrane deposition. Alternatively, SMAD4 could promote epiblast maturation, defined here as the transition from a naïve to primed state which normally occurs in epiblast cells between preimplantation and post-implantation stages (Boroviak et al., 2015; Nichols & Smith, 2009). Epiblast maturation has been shown to be critical in formation of proamniotic cavity (Carbognin et al., 2023; Shahbazi et al., 2017). Other mechanisms are also proposed to play a role in embryonic cavitation such as apical domain maintenance (Meng et al., 2017), tight junction formation (C. J. Chan et al., 2019), cellular adhesion through ECM interactions (Liang et al., 2005; Sakai et al., 2003), and establishment of an osmotic gradient (Dumortier et al., 2019). SMAD4 and pERK may regulate any or a combination of these factors. Further studies will be needed to interrogate the interaction of these pathways further, to identify the precise regulatory

mechanisms governing post-implantation epiblast morphogenesis downstream of SMAD4 and pERK.

Section 2.6. Acknowledgements

We thank the lab of Dr. David Arnosti for their generous loan of laboratory equipment. We also thank Barbara Makela and Ella Markley for technical support.

Section 2.7. Diversity and Inclusion Statement

The authors wholeheartedly support all efforts to increase the inclusion of scientists from underrepresented backgrounds (including, but not limited to, women, LGBTQIA+, people of color, Indigenous people, neurodivergent people, people with disabilities, and people from disadvantaged backgrounds) in developmental biology and related careers. This manuscript reflects the efforts of authors who identify as members of several of these groups. The authors believe that diverse perspectives are essential for scientific excellence and innovation, yet we acknowledge the continued existence of systemic barriers to success for scientists of underrepresented and marginalized communities. We support the development of initiatives to address disparities and biases in scientific publishing and encourage further efforts to implement inclusive practices.

TABLES

Allele	Common Allele Name	Strain, (*species*)	Source or Reference	Identifier(s)	Additional Information
CD-1	CD-1	CD-1 (*Mus musculus*)	Charles River Laboratories	Crl:CD1(ICR), Strain code: 022	Wild-type
Tg(Zp3-cre)93Knw/J	*Zp3Cre*	Mixed background (*M. musculus*)	De Vries et al, 2000 (PMID: 10686600)	RRID:IMSR_JAX:003651 MGI:J:67903	Presence of this allele assessed by genotyping for *Cre* and *Zp3Cre*
Bmp4^{tm1Jfm}/J	*Bmp4^{fl}*	Mixed background (*M. musculus*)	Liu et al, 2004 (PMID: 15070745; PMCID: PMC384774)	RRID:IMSR_JAX:016878 MGI:J:89237	*Bmp4^{del}* or *Bmp4* null refers to recombined allele
Smad4$^{tm2.1Cxd}$/J	*Smad4^{fl}*	Mixed background (*M. musculus*)	Yang et al, 2002 (PMID: 11857783)	RRID:IMSR_JAX:017462 MGI:J:75140	*Smad4^{del}* or *Smad4* null refers to recombined allele

Table 2.1. Animal Resources Table for Chapter 2.

Antibody/Stain	Source or reference(s)	Identifiers	Dilution	Additional Information
Goat-anti-hGATA6	R&D Systems	AF1700	1:100	
Goat-anti-GATA4	Santa Cruz Biotechnology	sc1237	1:2000	
Goat-anti-SOX17	R&D Systems	AF1924	1:2000	
Mouse-anti-CDX2	Abcam	CDX-88	1:500	
Rabbit-anti-CDX2	Abcam	ab76541	1:200	
Mouse-anti-OCT4	Santa Cruz Biotechnology	sc-5279	1:100	
Rabbit-anti-NANOG	Reprocell	RCAB002P-F	1:400	
Goat-anti-SOX2	Neuromics	GT15098	1:2000	
Rat-anti-CDH1	Sigma	U3254	1:500	
Rabbit-anti-Phospho-Smad1 (Ser463/465)/ Smad5 (Ser463/465)/ Smad9 (Ser465/467)	Cell Signaling	13820	1:50	
Rabbit-anti-Phospho-p44/42 MAPK (Erk1/2) (Thr202/Tyr204)	Cell Signaling	9101	1:100	
Donkey-anti-goat IgG	Invitrogen	A-11055	1:400	Alexa488
Donkey-anti-mouse IgG	Jackson Laboratories	715-165-150	1:400	Cy3
Donkey-anti-rabbit IgG	Jackson Laboratories	711-165-152	1:400	Cy3
Goat-anti-rabbit IgG	Invitrogen	A-11034	1:400	Alexa488
Goat-anti-mouse IgG	Invitrogen	A-11029	1:400	Alexa488
DRAQ5	Cell Signaling	4084	1:400	

Table 2.2. Antibody Table for Chapter 2.

Allele	Forward Primer	Reverse Primer
Bmp4^{WT}, Bmp4^{fl}	GAGCTAAGTTTTGCTGGTTTGC	GCCCATGAGCTTTTCTGAGA
Bmp4^{del}	GCTAAGTTTTGCTGGTTTGC	TGACTAGGGGAGGAGTAGAAGGTG
Smad4^{WT}, Smad4^{fl}	TAAGAGCCACAGGGTCAAGC	TTCCAGGAAAAACAGGGCTA
Smad4^{del}	TAAGAGCCACAGGGTCAAGC	GACCCAAACGTCACCTTCAG
Cre	CTAGGCCACAGAATTGAAAGATCT	GTAGGTGGAAATTCTAGCATCATCC
Zp3Cre	CGAGATTGAGGGAAGCAGAG	CAGGTTCTTGCGAACCTCAT

Table 2.3. Allele-specific primers for PCR genotyping for Chapter 2.

FIGURES

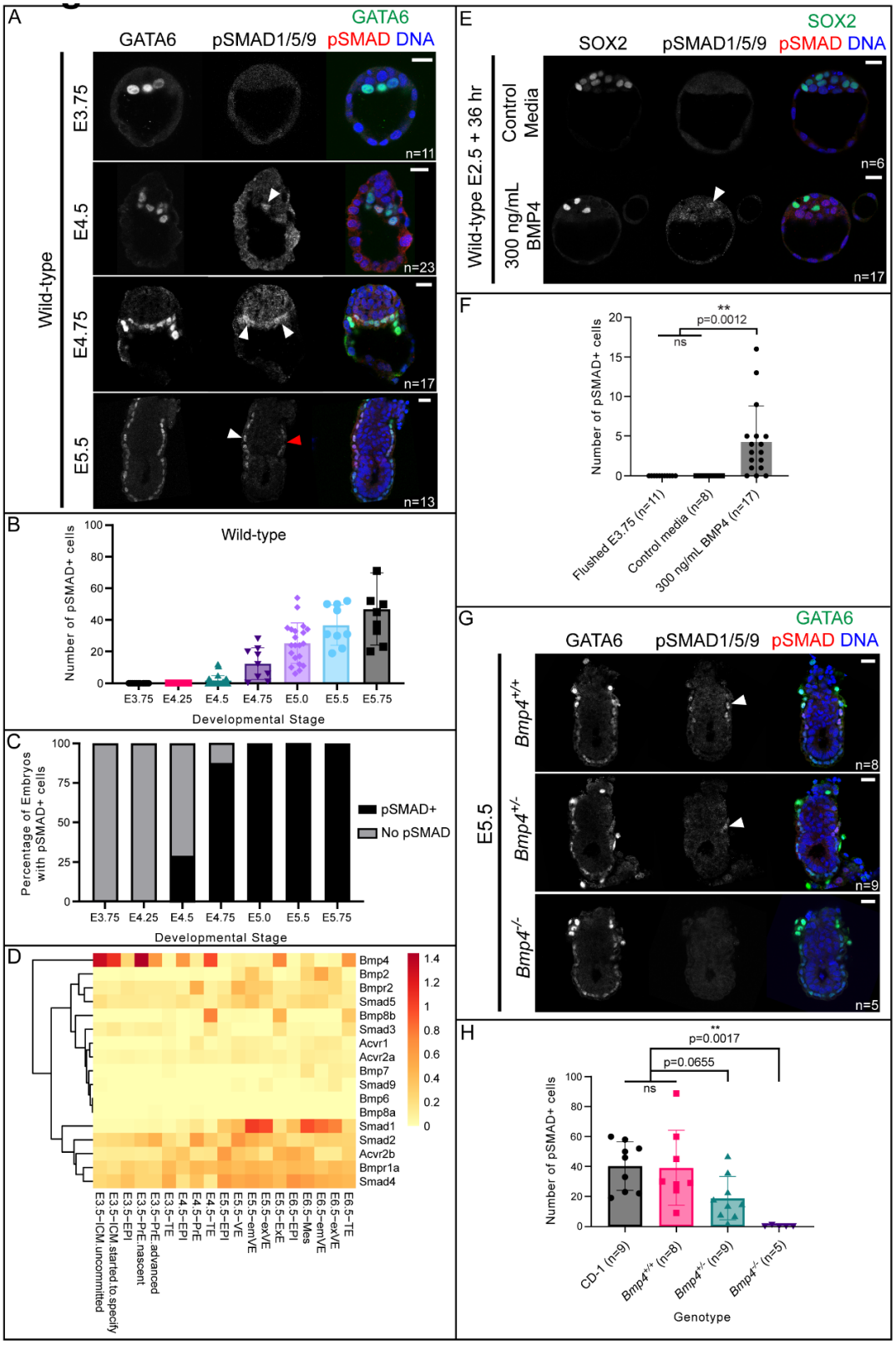

Figure 2.1. BMP signaling becomes active in primitive endoderm at implantation.

Figure 2.1 (cont'd).
A) SMAD1/5/9 phosphorylation (pSMAD) in wild-type CD-1 embryos at E3.75, E4.5, E4.75, and E5.5. In all cases, positive pSMAD signal co-localizes with GATA6 as a marker of primitive endoderm and visceral endoderm. **B)** Quantification of total number of pSMAD-positive cells in wild-type embryos in A and Supplemental Figure 2.1A. **C)** Quantification of the percentage of embryos from A and Supplemental Figure 2.1A which display any pSMAD-positive cells versus no pSMAD-positive cells. **D)** Heat map of the mean normalized expression of BMP pathway genes from scRNA-seq data from Nowotschin et al., 2019. **E)** pSMAD in wild-type embryos collected at E2.75 and cultured for 36 hours in media containing 300 ng/mL exogenous BMP4. **F)** Quantification of the total number of pSMAD-positive cells in embryos from E revealed significantly more pSMAD-positive cells in BMP4-treated embryos. **G)** pSMAD staining is absent in *Bmp4* z null embryos at E5.5. **H)** Quantification of total number of pSMAD-positive cells in wild-type and *Bmp4*-null embryos at E5.5 revealed significantly fewer pSMAD-positive cells in *Bmp4*-null embryos. All pairwise comparisons were assessed by analysis of variance (ANOVA) with Tukey's post-hoc test. White arrowheads indicate positive pSMAD signal. Red arrowhead indicates a GATA6-positive cell which does not express pSMAD. Scale bars represent 10 μm.

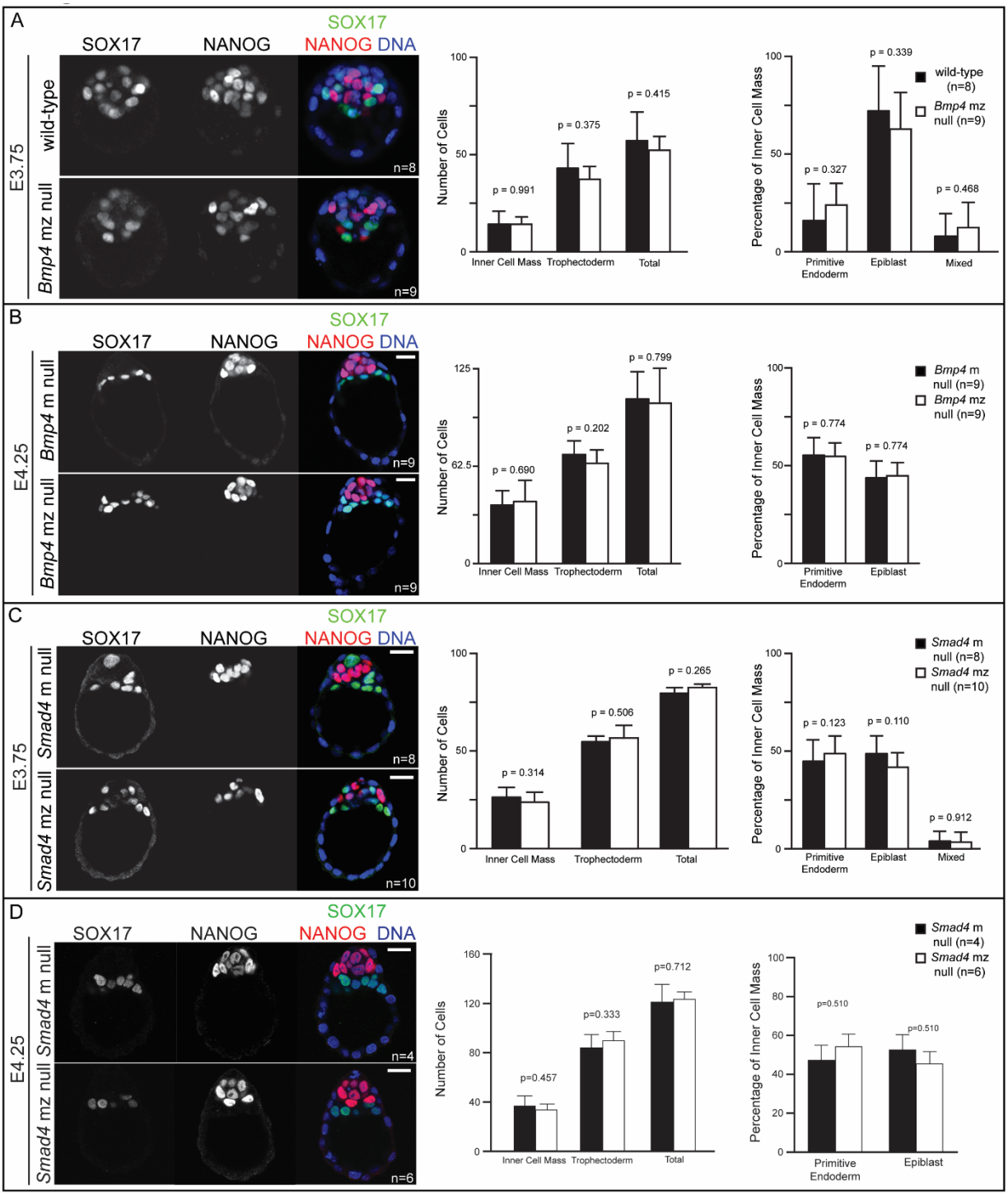

Figure 2.2. Maternal and zygotic *Smad4* and *Bmp4* are dispensable for blastocyst formation and preimplantation cell fate specification. A) Immunofluorescence for SOX17 and NANOG as respective markers of primitive endoderm (PrE) and epiblast (EPI) in flushed E3.75 wild-type CD-1 embryos and embryos lacking maternal and zygotic *Bmp4* (mz null). Quantification did not reveal any significant difference in cell number or cell fate between *Bmp4* mz null embryos and controls.

Figure 2.2 (cont'd).
"Mixed" indicates co-expression of SOX17 and NANOG. **B)** Immunofluorescence for SOX17 and NANOG in flushed E4.25 embryos lacking maternal *Bmp4* only (m null) and *Bmp4* mz null embryos. Quantification did not reveal any significant difference in cell number or cell fate between *Bmp4* mz null embryos and controls. "Mixed" indicates co-expression of SOX17 and NANOG. **C)** Immunofluorescence for SOX17 and NANOG in flushed E3.75 *Smad4* m null and *Smad4* mz null embryos. Quantification did not reveal any significant difference in cell number or cell fate between *Smad4* mz null embryos and controls. **D)** Immunofluorescence for SOX17 and NANOG in flushed E4.25 *Smad4* m null and *Smad4* mz null embryos. Quantification did not reveal any significant difference in cell number or cell fate between *Smad4* mz null embryos and controls. All pairwise comparisons were assessed by Student's t-test. Scale bars represent 10 μm.

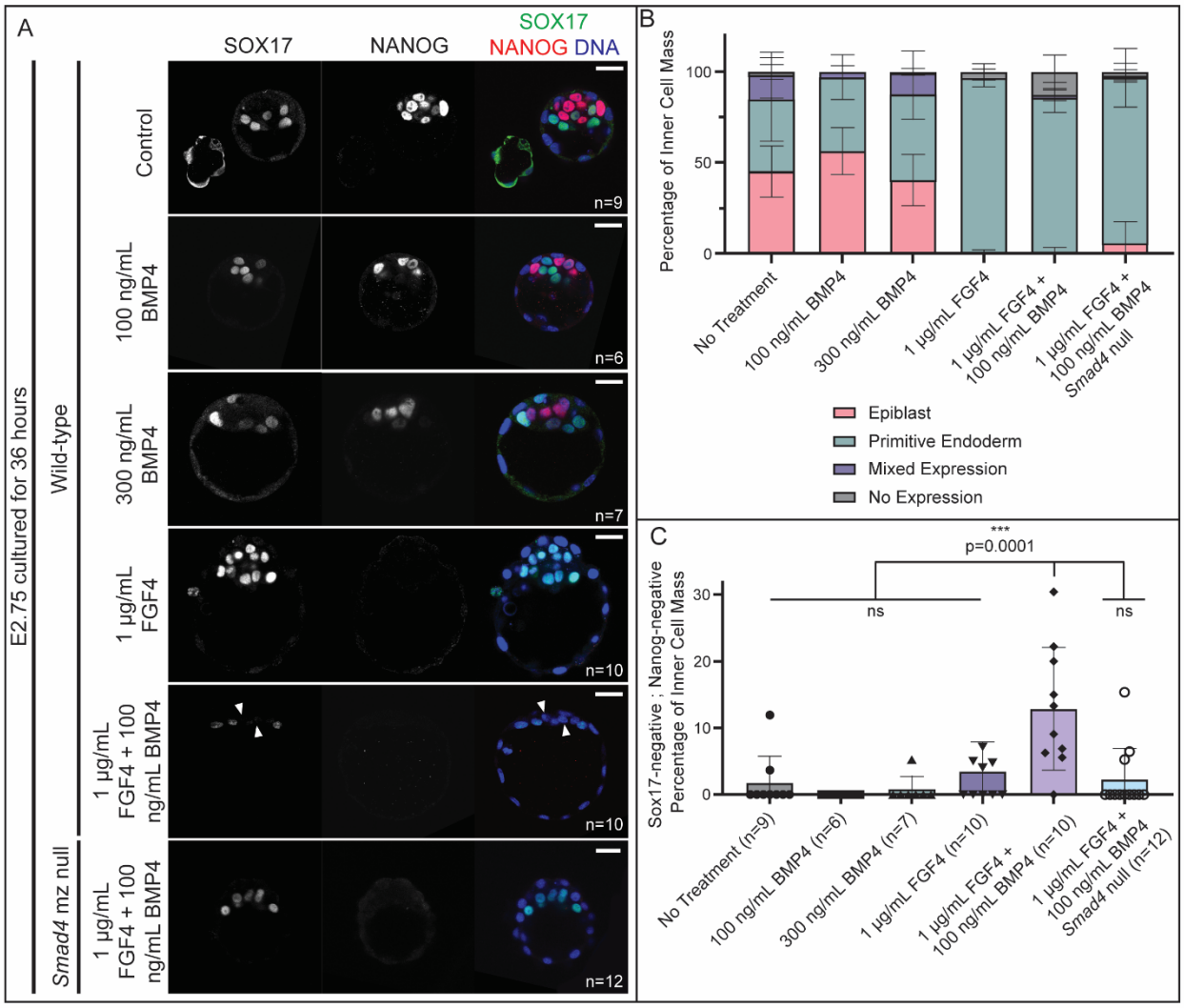

Figure 2.3. Exogenous BMP4 is capable of inducing cell fate changes in preimplantation embryos. A) Wild-type embryos collected at E2.75 and cultured for 36 hours in untreated control media, 100 ng/mL BMP4, 300 ng/mL BMP4, 1 ug/mL FGF4 + heparin, or both 100 ng/mL BMP4 and 1 ug/mL FGF4 + heparin. *Smad4* mz null embryos collected at E2.75 and cultured for 36 hours in both 100 ng/mL BMP4 and 1 ug/mL FGF4 + heparin. Embryos were stained by immunofluorescence for NANOG and SOX17 as markers of EPI and PE, respectively. **B)** Quantification of the amount of EPI, PE, mixed, and no expression cells as a percentage of total ICM cells in embryos from A. EPI=NANOG-positive only, PE=SOX17-positive only, mixed=NANOG/SOX17 double-positive, no expression=NANOG/SOX17 double-negative. **C)** Quantification of NANOG/SOX17 double-negative cells as a percentage of ICM cells in embryos from A. Comparisons were assessed by analysis of variance (ANOVA) with Tukey's post-hoc test.

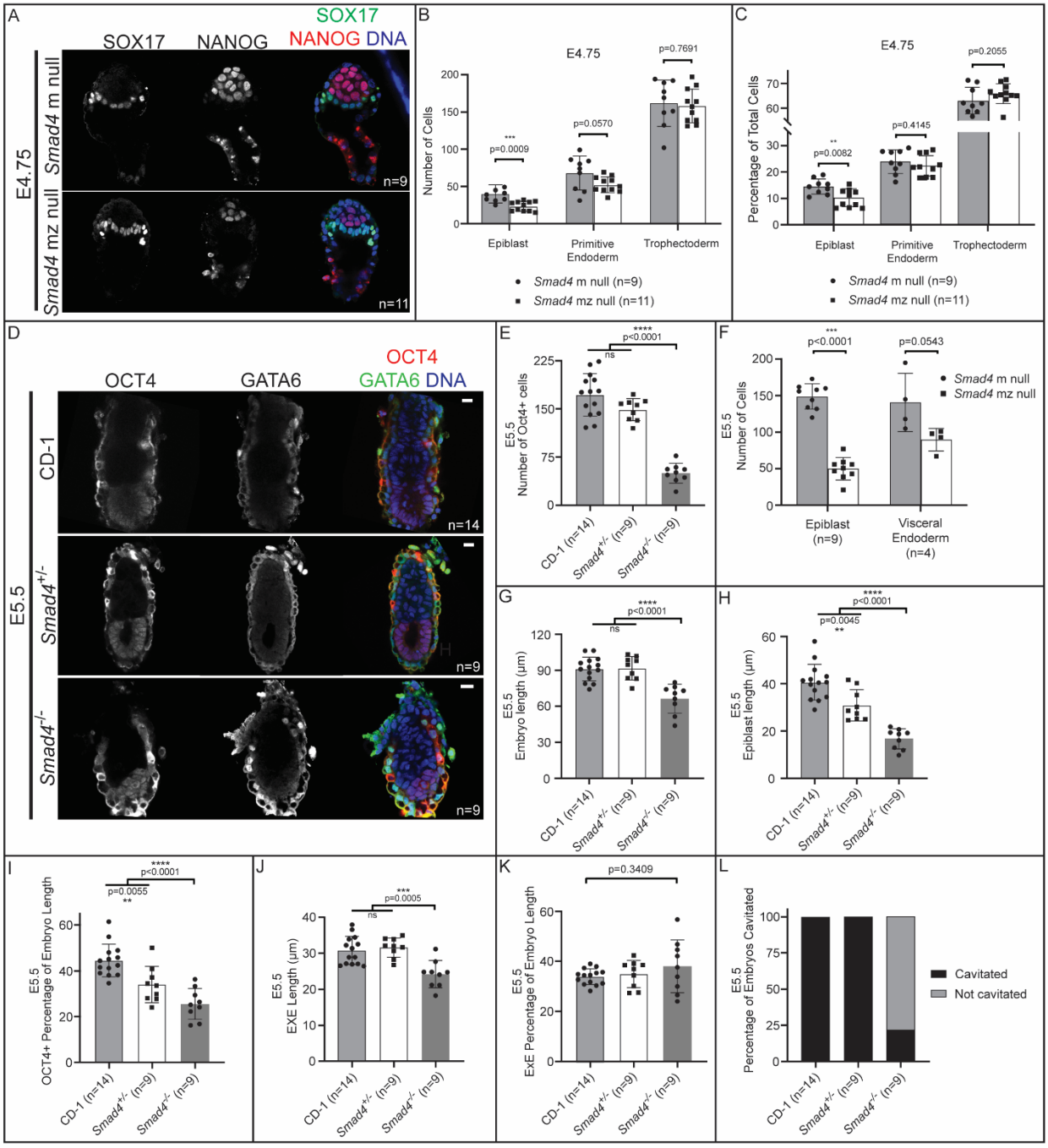

Figure 2.4. BMP-independent function of *Smad4* is required for post-implantation epiblast organization and maintenance. A) E4.75 *Smad4* mz null embryos stained by immunofluorescence for SOX17 and NANOG. **B)** Quantification of EPI, PrE, and TE cell numbers from embryos in A revealed a significant decrease in EPI cells in *Smad4* mz null embryos when compared to controls. **C)** Quantification of the EPI, PrE, and TE cells as a percentage of total cell number from embryos in A revealed a significant decrease in EPI percentage in *Smad4* mz null embryos. **D)** E5.5 *Smad4*$^{-/-}$ embryos stained by immunofluorescence for OCT4 and GATA6 as markers of EPI and VE, respectively.

Figure 2.4 (cont'd).
Smad4$^{-/-}$ refers to combined *Smad4* z null and *Smad4* mz null embryos. **E)** Quantification of the number of OCT4-positive cells in wild-type, *Smad4*$^{+/-}$, and *Smad4*$^{-/-}$ embryos. **F)** Quantification of EPI and PrE cell numbers from *Smad4*$^{+/-}$ and *Smad4*$^{-/-}$ embryos at E5.5 revealed a specific, significant decrease in epiblast cell number in *Smad4* mz null embryos when compared to controls ($p<0.05$ by Student's t-test). The difference in VE cell numbers was not significant ($p>0.05$). **G)** Quantification of the proximal-distal length wild-type, *Smad4*$^{+/-}$, and *Smad4*$^{-/-}$ embryos at E5.5. **H)** Quantification of the proximal-distal length of the EPI of wild-type, *Smad4*$^{+/-}$, and *Smad4*$^{-/-}$ embryos at E5.5. **I)** Quantification of the proximal-distal length of the EPI as a percentage of total length of wild-type, *Smad4*$^{+/-}$, and *Smad4*$^{-/-}$ embryos at E5.5. **J)** Quantification of the proximal-distal length of the ExE of wild-type, *Smad4*$^{+/-}$, and *Smad4*$^{-/-}$ embryos at E5.5. **K)** Quantification of the proximal-distal length of the ExE as a percentage of total length of wild-type, *Smad4*$^{+/-}$, and *Smad4*$^{-/-}$ embryos at E5.5. **L)** Quantification of the proportion of *Smad4*$^{+/-}$ and *Smad4*$^{-/-}$ embryos with a proamniotic cavity at E5.5. Comparisons in B,C, F were assessed by Student's t-test. Comparisons in E, G-K were assessed by analysis of variance (ANOVA) with Tukey's post-hoc test.

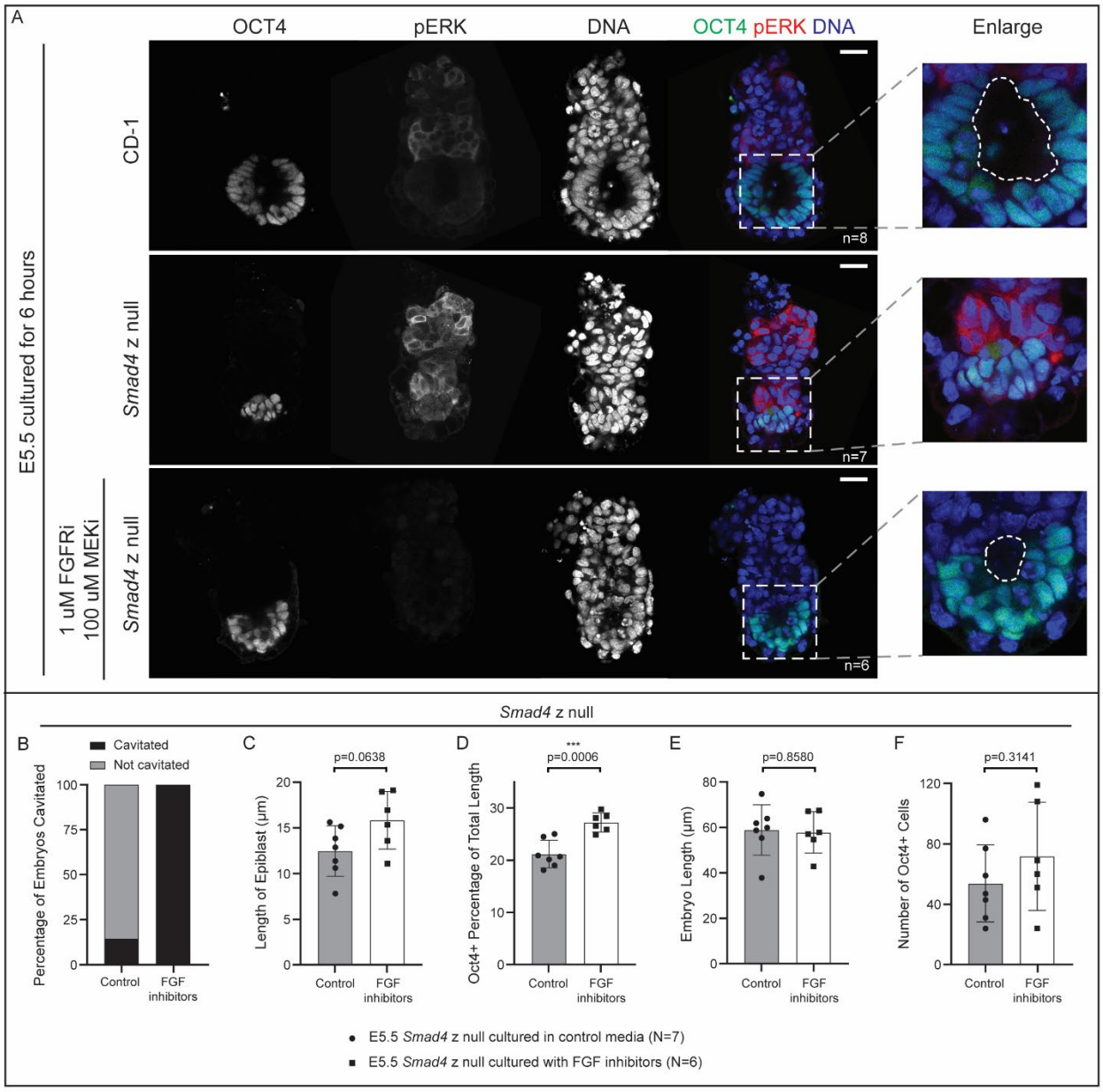

Figure 2.5. Inhibition of FGF signaling partially rescues epiblast cavitation in E5.5 *Smad4* null embryos. A) Wild-type and *Smad4* z null embryos collected at E5.5 and cultured for 6 hours after dissection in control media or media containing FGFR/MEK inhibitors (see Methods), then stained by immunofluorescence for OCT4 and phosphorylated ERK (pERK). Dashed line in enlargement notates the proamniotic cavity. **B)** Quantification of the proportion of treated and untreated *Smad4*$^{-/-}$ embryos with a proamniotic cavity at E5.5. **C)** Quantification of proximal-distal length of the EPI, **D)** proximal-distal length of the EPI as a proportion of total length, **E)** total proximal-distal length, and **F)** OCT4-positive cell number in treated and untreated E5.5 *Smad4*$^{-/-}$ embryos.

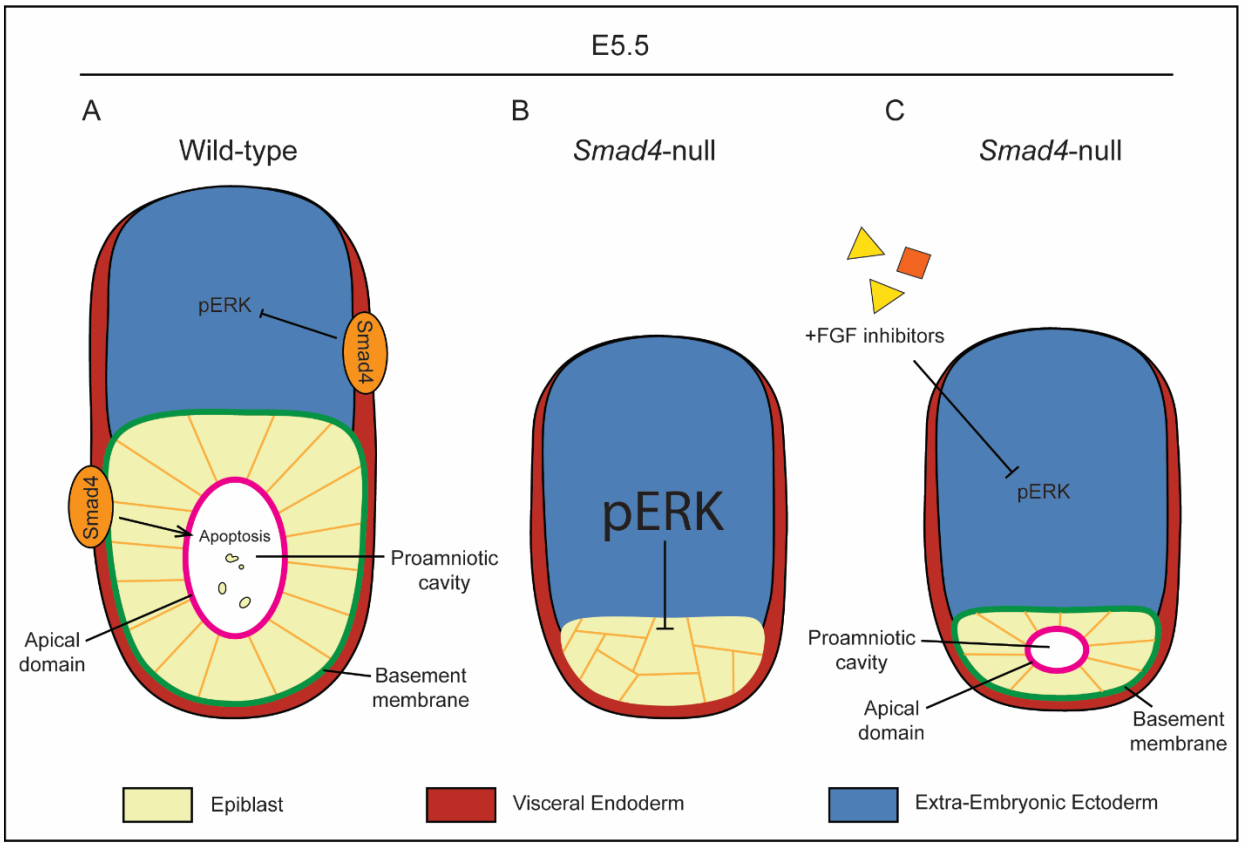

Figure 2.6. Possible model of FGF inhibition rescuing rosette formation but not embryo growth in *Smad4*-null embryos. A) In wild-type embryos, SMAD4 in the visceral endoderm promotes lumen formation in the epiblast by regulating a pro-apoptotic signal. Separately, SMAD4 also inhibits ERK phosphorylation in the ExE, which allows for polarization and rosette formation in the epiblast. **B)** In *Smad4*-null embryos, pERK is upregulated, causing an ectopic increase in pERK and preventing epiblast polarization. The pro-apoptotic signal is also lost. The combination of these two factors lead to epiblast disorganization and a failure to cavitate. **C)** Treatment with FGF inhibitors prevents upregulation of pERK in *Smad4*-null embryos. Repressed pERK levels allow epiblast polarization to proceed, resulting in a small proamniotic cavity.

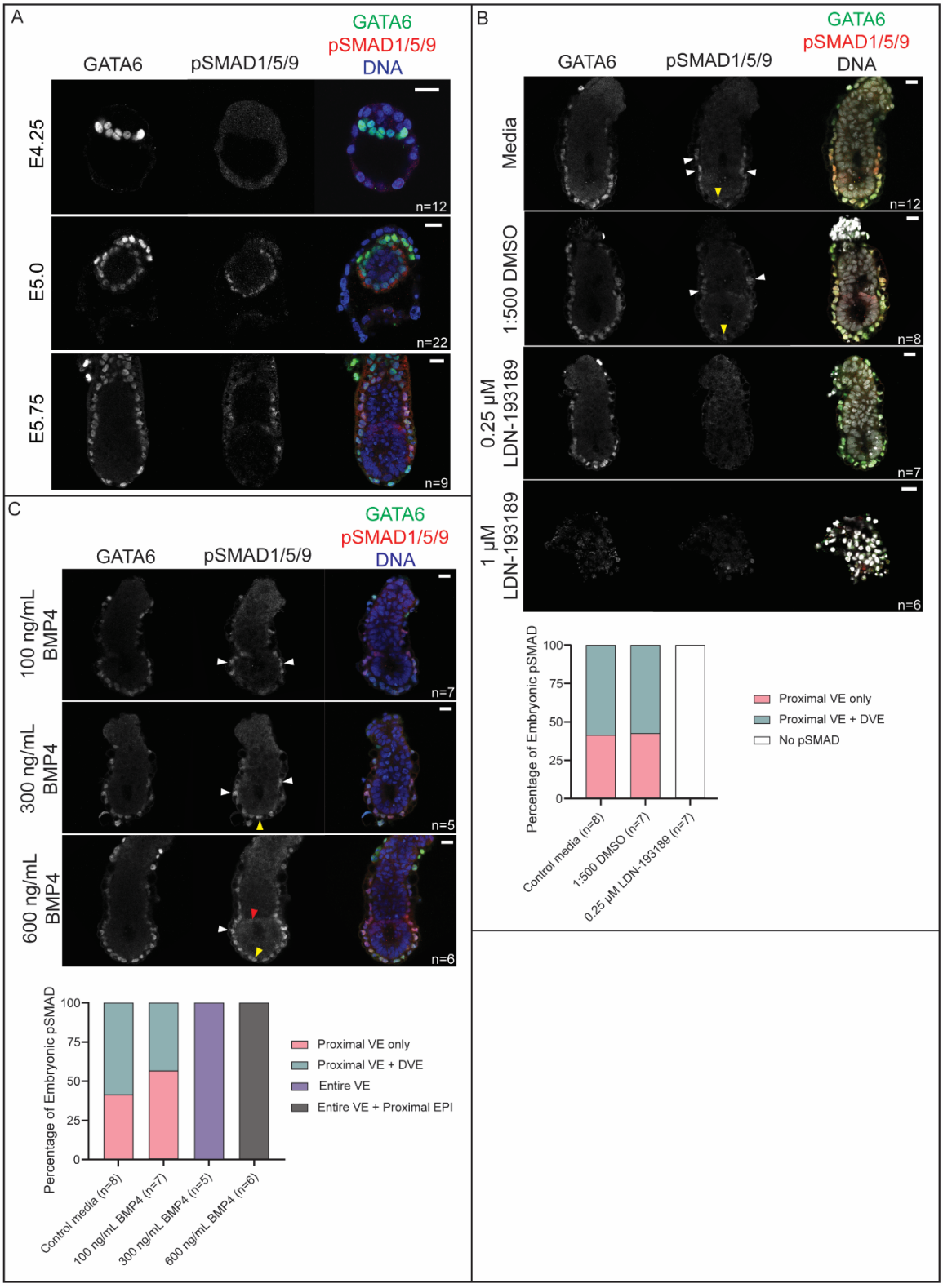

Supplemental Figure 2.1. SMAD1/5/9 phosphorylation in post-implantation embryos can be modulated. A) Immunofluorescence for GATA6 and SMAD1/5/9 phosphorylation (pSMAD) in wild-type E4.25, E5.0, and E5.75 embryos.

Supplemental Figure 2.1 (cont'd).
B) Immunofluorescence for GATA6 and pSMAD in wild-type E5.5 embryos after 6 hours of culture in control media or BMP inhibitor treatments. Note the lack of pSMAD with 0.25 μM LDN-193189 treatment. 1 μM LDN-193189 resulted in severe toxicity to the treated embryos. Graph represents quantification of the proportion of embryos displaying unique SMAD1/5/9 phosphorylation patterns. **C)** Immunofluorescence for GATA6 and pSMAD in wild-type E5.5 embryos after 6 hours of culture in indicated concentrations of exogenous BMP4 treatment. pSMAD showed a dose-dependent increase as BMP4 concentration increased. Graph represents quantification of proportion of embryos displaying unique SMAD1/5/9 phosphorylation patterns. "Proximal VE only" and "Proximal VE and DVE" refer to pSMAD signal in some cells in those tissues, while "Entire VE" refers to pSMAD signal in every observed VE cell. pSMAD signal in proximal VE is indicated by white arrowheads. pSMAD signal in DVE is indicated by yellow arrowheads. pSMAD signal in proximal EPI is indicated by red arrowhead.

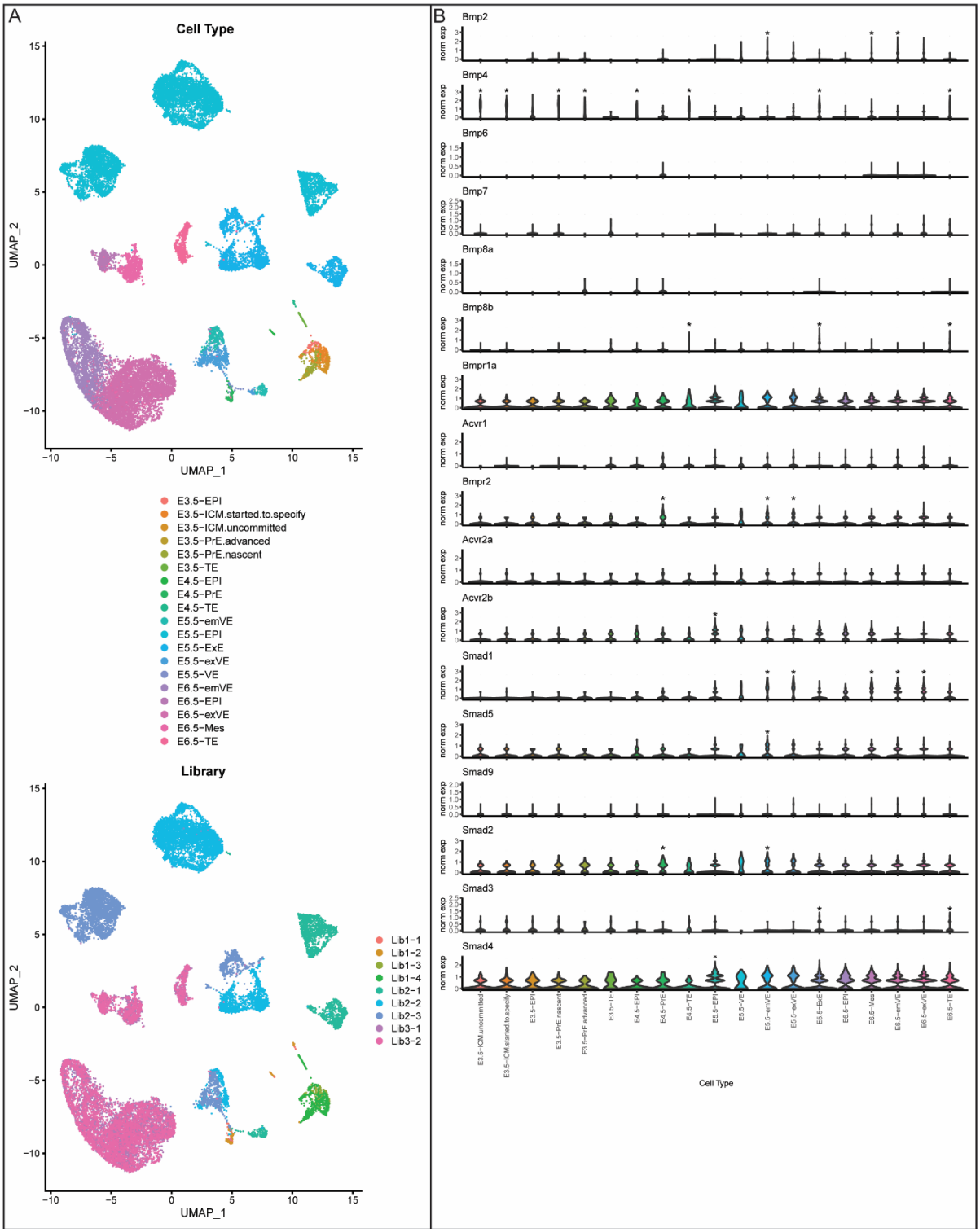

Supplemental Figure 2.2. BMP pathway genes are upregulated after implantation. **A)** Single-cell RNA-seq data generated by Nowotschin *et al*. reclustered using Seurat and identified by cell type. **B)** BMP ligand genes enriched in identified cell types and stages. Genes with p-adj<0.01 and average $\log_2$ fold change <0.25 were considered cluster enriched (*).

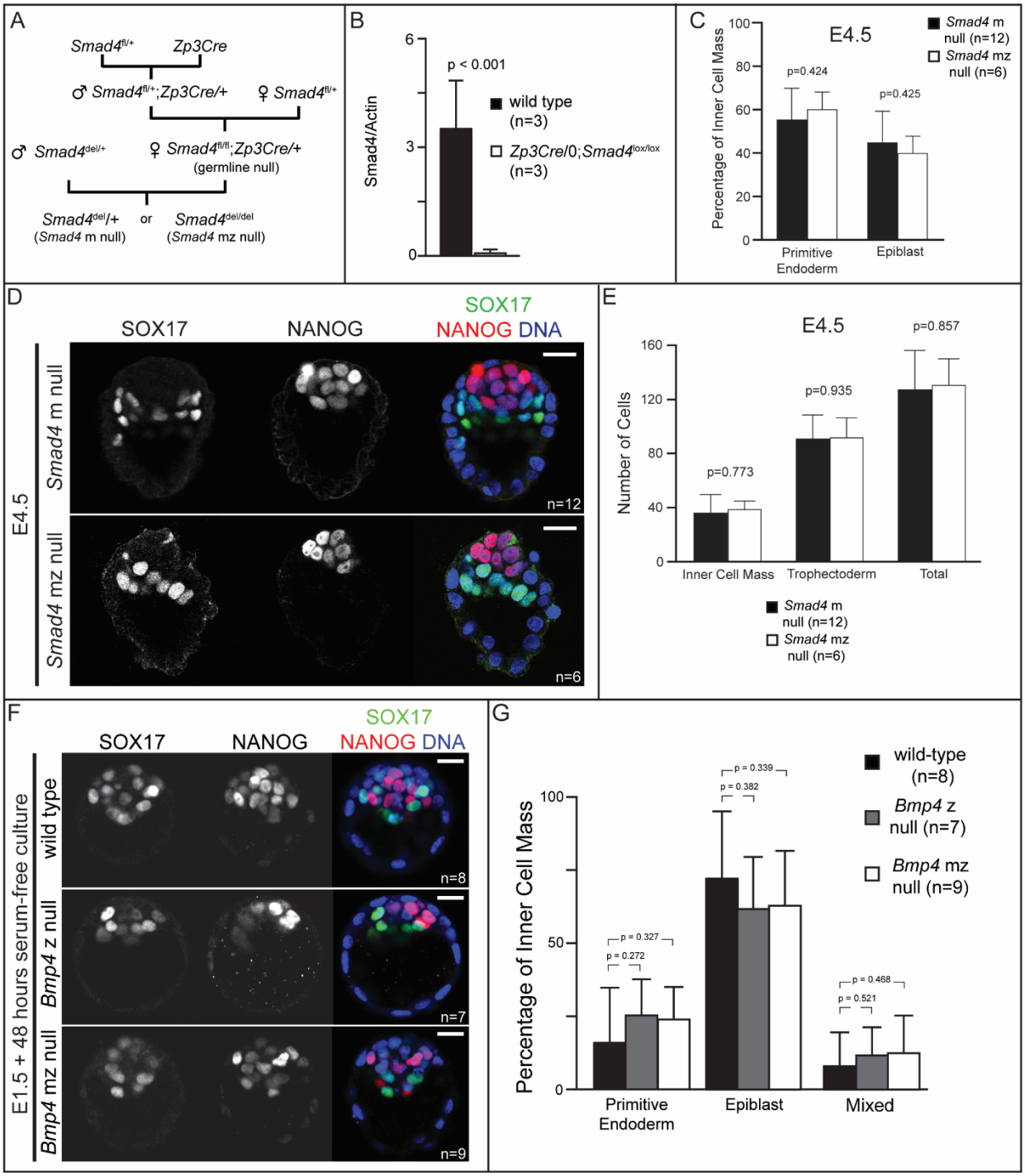

Supplemental Figure 2.3. Maternal and zygotic *Smad4* and *Bmp4* are dispensable for blastocyst formation and preimplantation cell fate specification. A) Breeding scheme for the generation of *Smad4* maternal-zygotic (mz) null embryos using the *Zp3Cre* allele described in de Vries *et al*, 2000. The same strategy was applied to generate *Bmp4* mz null embryos. **B)** Level of *Smad4* mRNA detected in wild-type and *Zp3Cre*; *Smad4*$^{fl/fl}$ oocytes by qPCR, normalized to *Actin* mRNA level.

Supplemental Figure 2.3 (cont'd).
C) Quantification of the ratio of EPI and PrE cells in the inner cell mass of embryos from D. **D)** Immunofluorescence for SOX17 and NANOG in dissected E4.5 *Smad4* m null and *Smad4* mz null embryos. **E)** Quantification of the number of cells occupying the inner cell mass or trophectoderm and total cell number in embryos from D. **F)** Immunofluorescence for SOX17 and NANOG in wild type, *Bmp4* zygotic (z) null and *Bmp4* mz null embryos cultured in KSOM +PVA -BSA (see Methods) from E1.5 to E3.75. **G)** Quantification of EPI and PrE cell numbers from F did not reveal any significant difference in ICM composition between *Bmp4* mz null embryos and controls. "Mixed" indicates co-expression of SOX17 and NANOG. Pairwise comparisons were evaluated by Student's t-test.

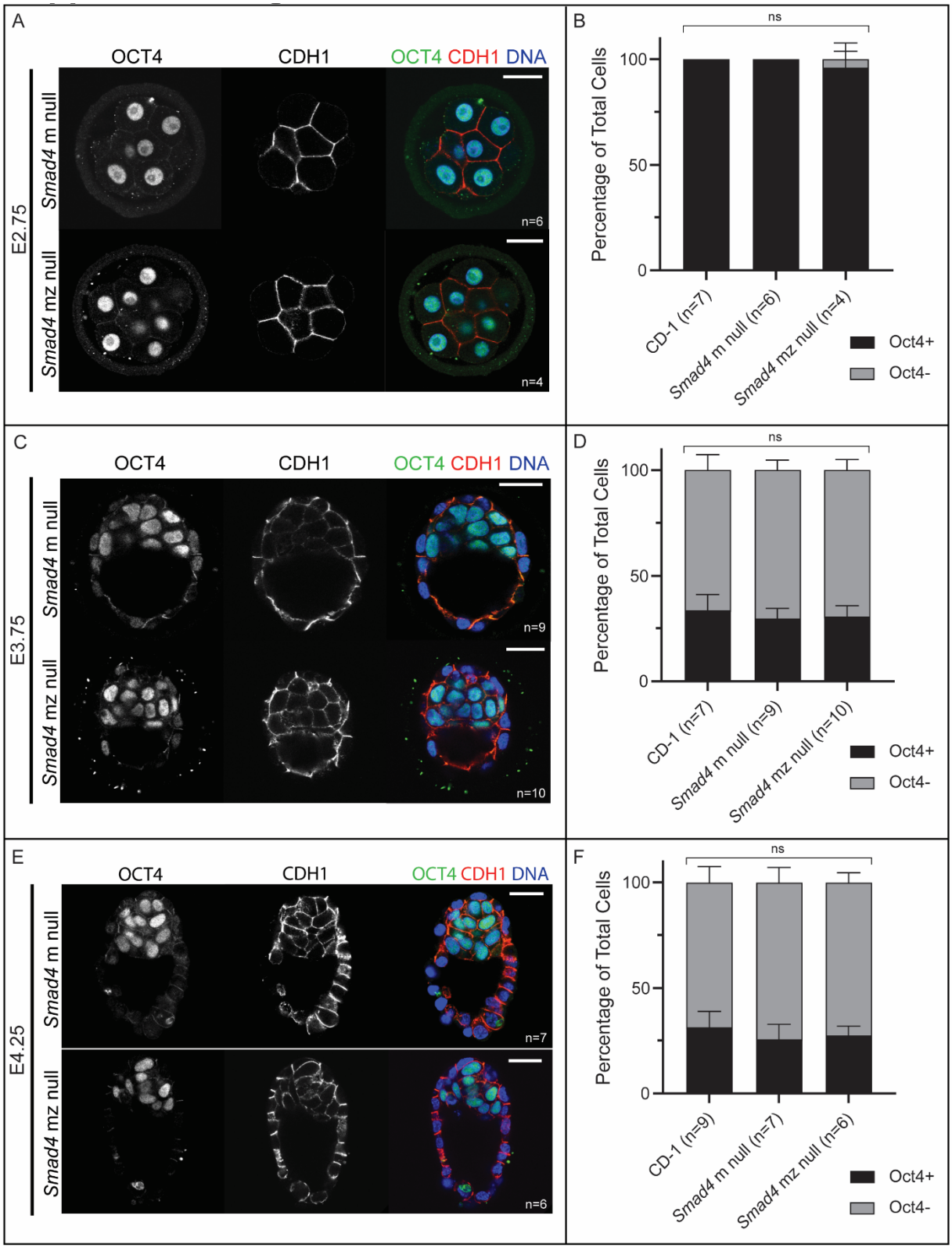

Supplemental Figure 2.4. Maternal and zygotic *Smad4* are dispensible for OCT4 expression in preimplantation mouse embryos.

Supplemental Figure 2.4 (cont'd).
A) Immunofluorescence for OCT4 and CDH1 in E2.75 *Smad4* m null and *Smad4* mz null embryos. **B)** Quantification of the number of OCT4-positive cells as a percentage of total cells in embryos from A. **C)** Immunofluorescence for OCT4 and CDH1 in E3.75 *Smad4* m null and *Smad4* mz null embryos. **D)** Quantification of the number of OCT4-positive cells as a percentage of total cells in embryos from B. **E)** Immunofluorescence for OCT4 and CDH1 in E4.25 *Smad4* m null and *Smad4* mz null embryos. **F)** Quantification of the number of OCT4-positive cells as a percentage of total cells in embryos from E. All comparisons were assessed by analysis of variance (ANOVA).

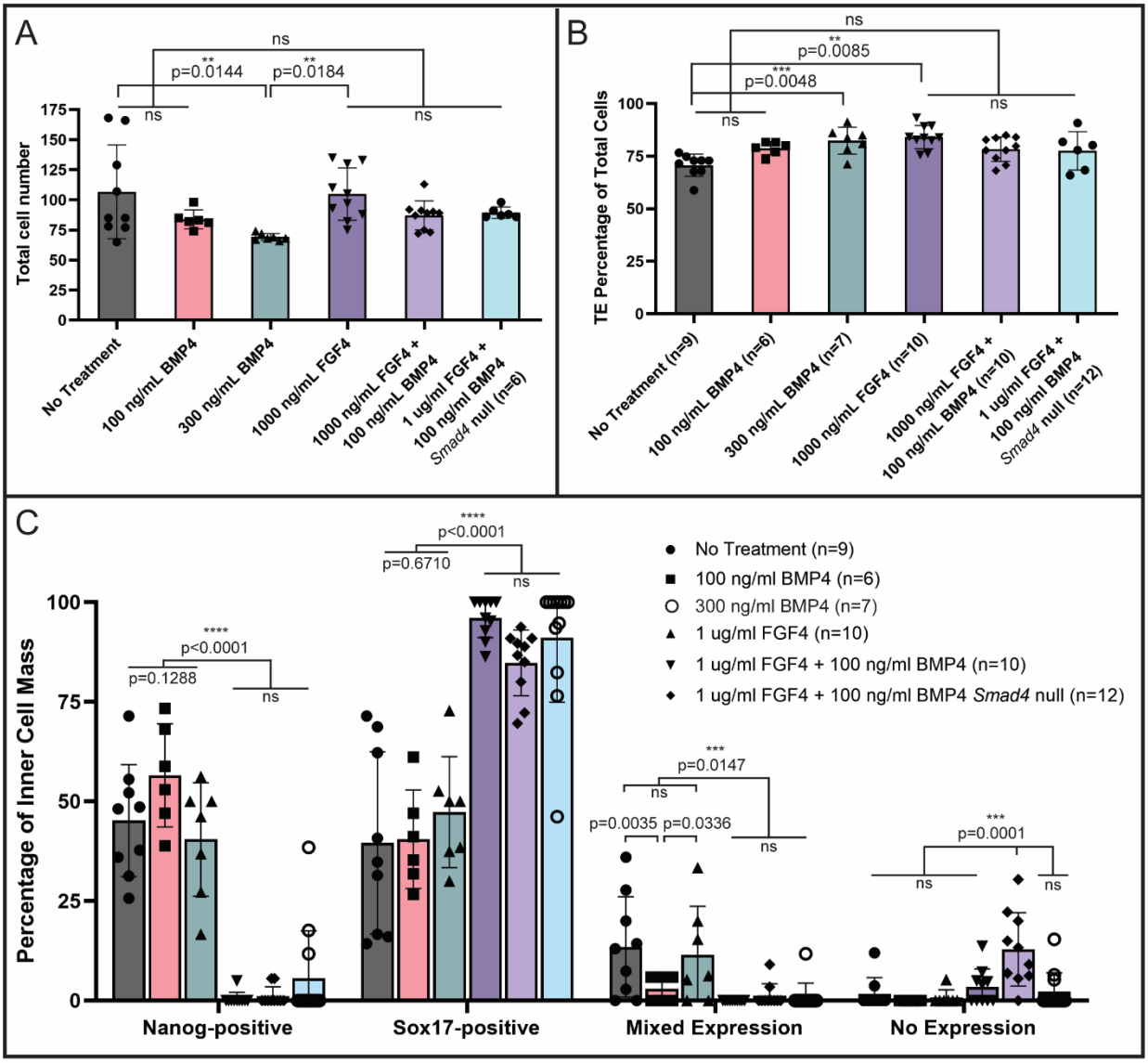

Supplemental Figure 2.5. Additional data for the effect of BMP4 treatment on preimplantation cell fate. A) Quantification of total cell numbers for embryos from Fig. 2.3A. **B)** Quantification of TE cell numbers for embryos from Fig. 2.3A. **C)** Percentage of ICM cells with EPI, PE, mixed, and no expression from Fig. 2.6B represented as individual data points. EPI=NANOG-positive only, PE=SOX17-positive only, mixed=NANOG/SOX17 double-positive, no expression=NANOG/SOX17 double-negative. All comparisons were assessed by analysis of variance (ANOVA) with Tukey's post-hoc test.

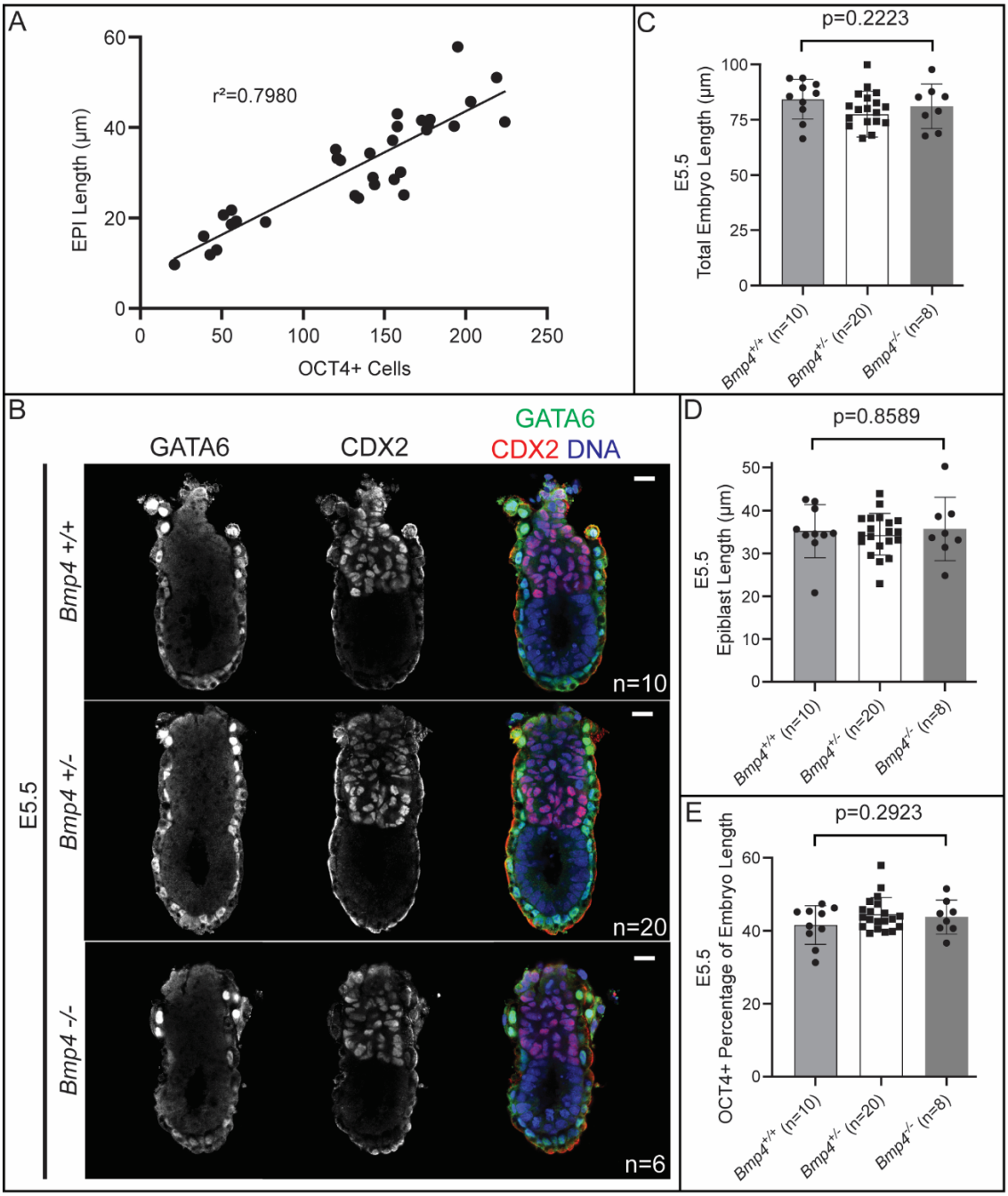

Supplemental Figure 2.6. *Bmp4* is dispensable for embryo growth and organization at E5.5. **A)** Correlation between the number of OCT4+ cells and proximal-distal length of the EPI in wild-type, *Smad4*$^{+/-}$, and *Smad4*$^{-/-}$ embryos at E5.5 from Fig. 2.4 and Fig. 2.5. Correlation assessed by Pearson's coefficient. **B)** Immunofluorescence for GATA6 and CDX2 as respective markers of visceral endoderm and extra-embryonic ectoderm in E5.5 wild-type, *Bmp4*$^{+/-}$, and *Bmp4*$^{-/-}$ embryos. **C)** Quantification of the proximal-distal length of embryos from B. **D)** Quantification of the proximal-distal length of the EPI in embryos from B. **E)** Quantification of the proximal-distal length of the EPI as a percentage of total length in embryos from B.

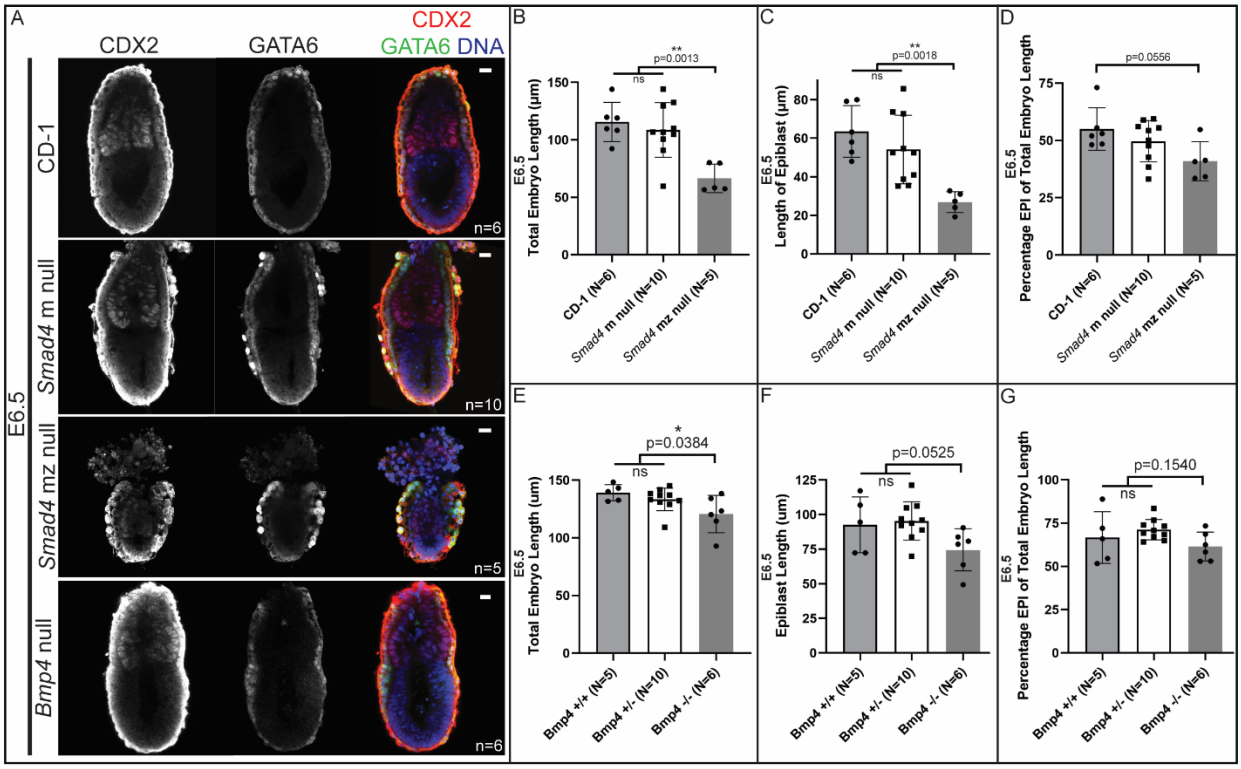

Supplemental Figure 2.7. Defects in *Smad4*-null embryos are more widespread across cell types at E6.5. A) E6.5 *Smad4* mz null and *Bmp4* z null embryos stained by immunofluorescence for CDX2 and GATA6. Epiblast length was inferred from the unstained cells distal to the CDX2-positive compartment in these embryos. **B)** Quantification of the proximal-distal length of wild-type, *Smad4* m null, and *Smad4* mz null embryos at E6.5. **C)** Quantification of the proximal-distal length of the EPI of wild-type, *Smad4* m null, and *Smad4* mz null embryos at E6.5. **D)** Quantification of the proximal-distal length of the EPI as a percentage of total length of wild-type, *Smad4* m null, and *Smad4* mz null embryos at E6.5. **E)** Quantification of the proximal-distal length of wild-type, *Bmp4*$^{+/-}$, and *Bmp4*$^{-/-}$ embryos at E6.5. **F)** Quantification of the proximal-distal length of the EPI in wild-type, *Bmp4*$^{+/-}$, and *Bmp4*$^{-/-}$ embryos at E6.5. **G)** Quantification of the proximal-distal length of the EPI as a percentage of total length in wild-type, *Bmp4*$^{+/-}$, and *Bmp4*$^{-/-}$ embryos at E6.5. All comparisons were assessed by analysis of variance (ANOVA) with Tukey's post-hoc test.

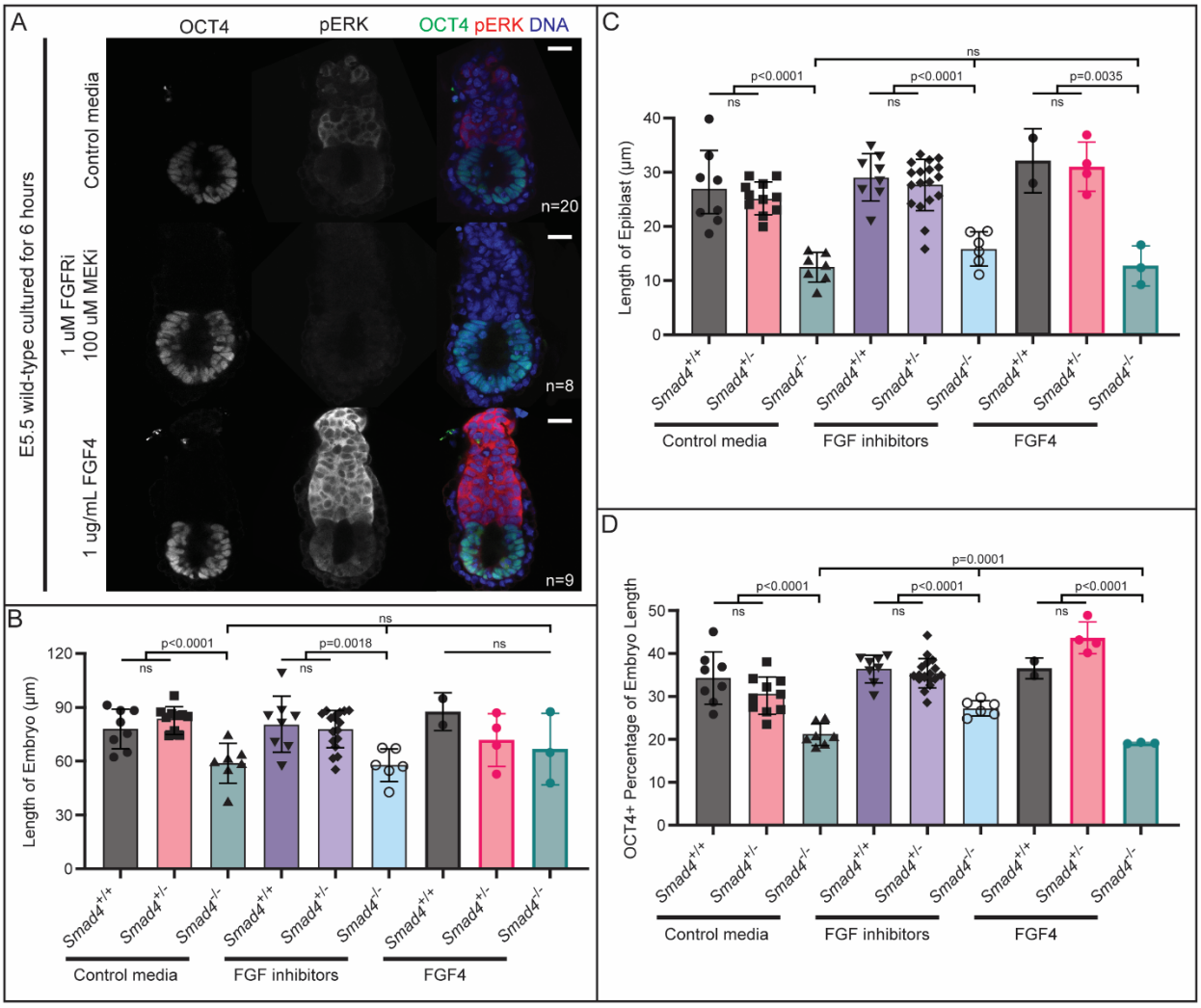

Supplemental Figure 2.8. ERK phosphorylation is responsive to modulation of FGF signaling. A) Wild-type embryos collected at E5.5 and cultured for 6 hours in control media, 1 µg/mL FGF4 + heparin, or media containing FGFR/MEK inhibitors (see Methods), then stained by immunofluorescence for OCT4 and phosphorylated ERK (pERK). Note decreased pERK in inhibitor-treated embryos and increased pERK in FGF4-treated embryos. **B)** Quantification of proximal-distal length of all embryos from Figure 2.5A and Supplemental Figure 2.8A. **C)** Quantification of proximal-distal length of the EPI in all embryos from Figure 2.5A and Supplemental Figure 2.8A. **D)** Quantification of proximal-distal length of the EPI as a percentage of total length in all embryos from Figure 2.5A and Supplemental Figure 2.8A. All comparisons were assessed by analysis of variance (ANOVA) with Tukey's post-hoc test.

CHAPTER 3.

ESSENTIAL ROLES FOR HIPPO SIGNALING IN MAMMALIAN REPRODUCTION

Robin E. Kruger[1,2], Farina Aziz[1], and Amy Ralston[2,3]

1) Cell and Molecular Biology Ph.D. Program, Michigan State University, East Lansing, MI, 48824, USA

2) Reproductive and Developmental Sciences Training Program, Michigan State University, East Lansing, MI, 48824, USA

3) Department of Biochemistry and Molecular Biology, Michigan State University, East Lansing, MI, 48824, USA

This chapter is a completed manuscript that will be submitted for publication in *Reproduction.*

This study was supported by the National Institutes of Health R35 GM131759 and T32 HD087166.

Section 3.1. Abstract

Hippo signaling, a highly conserved molecular signaling pathway with well-known functions in development, has long been known to be essential for mammalian fertility. In this review, we discuss recent advances which have uncovered the functions of Hippo signaling in key reproductive organs such as the testes, ovaries, uterus, and placenta. We also discuss human reproductive disorders whose etiology may be related to dysregulation of Hippo signaling and possible therapies which have been proposed to correct this dysregulation. Finally, we highlight current gaps in knowledge where further studies of Hippo signaling may uncover new insights into molecular regulation of reproduction and fertility.

Section 3.2. Introduction to the Hippo signaling pathway

The Hippo signaling pathway is a highly conserved pathway which is known to play essential roles in both development and adult homeostasis. The biochemical interactions of this pathway have been well-described in several model systems (M. Fu et al., 2022). The pathway is so named because loss-of-function mutations caused massive organ overgrowth in fruit flies, causing a bloated appearance reminiscent of a hippopotamus (Harvey et al., 2003). Subsequent studies using biochemical and genetic approaches uncovered core components of the Hippo pathway, including inputs and outputs. Unlike many signaling pathways, Hippo signaling relies on a large variety of upstream signals to initiate its activity. In addition to extracellular ligands, initiation of this pathway is often regulated by mechanical cues from changes in the extra-cellular matrix

or cytoskeleton. Hippo signaling may also be modulated by soluble factors such as steroids, or in response to stress (reviewed in Fu et al., 2022).

The main output of Hippo signaling is modulation of the transcriptional activity of homologous transcription factors YAP1 and WWTR1. In the absence of Hippo signaling, these proteins complex with other transcription factors (particularly TEAD factors) to bind DNA and effect changes in gene expression. Active Hippo signaling initiates a phosphorylation cascade in which upstream kinases MST1/2 phosphorylate and activate downstream kinases LATS1/2. Activated LATS proteins form a complex with the scaffolding protein Angiomotin (AMOT), which facilitates their ability to phosphorylate YAP1 and WWTR1. Phosphorylation prevents YAP1/WWTR1 from entering the nucleus, and instead targets these proteins for degradation. In this way, active Hippo signaling prevents the transcriptional activity of YAP1/WWTR1 (see Fig. 1.2).

Several excellent review articles have described Hippo roles in homeostasis, disease, development, and regeneration, in model organisms and humans (Davis & Tapon, 2019; M. Fu et al., 2022; Misra & Irvine, 2018; Moya & Halder, 2016; Zheng & Pan, 2019). Yet, the roles of Hippo signaling in reproduction have not been comprehensively reviewed. Relying heavily on studies in mice, we summarize known roles for Hippo signaling in reproduction, beginning with the adult testis, ovary, and uterus, which then sets the stage for understanding Hippo signaling during early development and formation of the extraembryonic tissues.

Section 3.3. Hippo signaling in male reproduction

Male reproduction processes and cell types

In male mammalian reproduction, Hippo signaling is greatly involved in the regulation of spermatogenesis. Spermatogenesis takes place within the seminiferous tubules of the testes, where immature, self-renewing spermatogonial stem cells (SSCs) reside on the inner edge of the tubule. These germ cells gradually mature as they move inward toward the tubule lumen. SSCs first differentiate into spermatogonia, which can divide by mitosis to produce meiotically-capable spermatocytes. After completing meiosis, haploid spermatocytes differentiate further into spermatids, where they undergo the morphological changes to become mature sperm in the process of spermiogenesis. During spermiogenesis, the spermatids develop an acrosomal head, intermediate mid-piece, and flagellar tail. Finally, the mature spermatid enters the lumen of the seminiferous tubule as a fully-developed spermatozoon. Spermatozoa travel from the seminiferous tubule to the epididymis, where they undergo final maturation before ejaculation.

The somatic cells of the testis, Sertoli cells, Leydig cells, and structural interstitial cells, are essential to the process of spermatogenesis. Leydig cells function primarily to produce testosterone, which among several other targets is received by Sertoli cells. Sertoli cells act as “nurse” cells for the developing germ cells within the seminiferous tubules, providing nutrients, structural support, and aiding in waste removal. Tight junctions between Sertoli cells help form the blood-testes barrier, providing a favorable microenvironment for spermatogenesis. Finally, Sertoli cells produce anti-Mullerian

hormone and inhibin, both key molecules in supporting male sexual development. Proper function of Sertoli and Leydig cells is essential for spermatogenesis and male fertility.

Hippo signaling maintains testicular somatic cell identity and promotes spermatogenesis non-cell-autonomously

Hippo signaling is essential to male fertility, as demonstrated by the decreased fertility in Hippo genetic knockout models in mice (Hossain et al., 2007; St John et al., 1999). Several knockouts, including those of *Lats1, Lats2,* and *Yap1;Wwtr1* report decreased testis size (Abou Nader et al., 2022; Levasseur et al., 2017; St John et al., 1999). However, although YAP1 and WWTR1 protein are expressed and localized to the nucleus in germ cells after puberty (Levasseur et al., 2017), the direct, cell-autonomous effect of Hippo signaling on spermatogenesis appears to be limited. Conditional knockout of *Yap1* in mouse germ cells had no apparent effect on the expression of germ cell markers, spermatogonial stem cell formation, or sperm count *in vivo* (Abou Nader et al., 2019). Neither knockdown of *fat, expanded, hippo, salvador,* or *warts,* nor overexpression of *yorkie,* had any discernible effect on germ cell cyst formation in *Drosophila* (S. Sun et al., 2008). However, in sheep, Mst2, Lats1/2, and Yap1 mRNA and protein are all strongly upregulated in mature, ejaculated sperm as opposed to immature spermatozoa recovered from the cauda epididymis, suggesting that Hippo signaling may play a role in adult sperm function even if it is not required cell-autonomously in spermatogenesis (G.-M. Zhang et al., 2019).

Although Hippo signaling is apparently dispensable in germ cells, it is essential to maintain the cell identities of Sertoli and Leydig cells. Conditional double knockout of *Lats1* and *Lats2* in murine testicular somatic cells (using a *Nr5a1-Cre* strain, which drives Cre expression in a common progenitor cell population for Sertoli cells and fetal Leydig cells as well as adrenal precursors), led to smaller and disorganized testes as early as embryonic day E14.5 (Abou Nader et al., 2022). These knockouts showed decreased expression of many Sertoli cell markers including *Sox9.* More strikingly, testes in these animals showed severe dysgenesis, marked by a progressive increase in spindle-shaped, fibroblast-like cells and corresponding decrease in Sertoli and Leydig cells (Abou Nader et al., 2022). Further analysis revealed a loss of polarity markers in Sertoli cells, suggesting that without *Lats1/2* these cells undergo an epithelial-to-mesenchymal transition resulting in fibrosis of the testis interstitium (Abou Nader et al., 2022). On the other hand, conditional double knockout of *Yap1* and *Wwtr1* in Sertoli cells decreased expression of male-specific genes such as *Dhh, Dmrt1, Sox9,* and *Wt1* at pre-pubertal stages (Levasseur et al., 2017). The fact that loss of *Lats1/2* resulted in a more detrimental phenotype than loss of *Yap/Wwtr* is consistent with a requirement for active Hippo signaling in Sertoli cell differentiation.

Similar results were reported with loss of cell identity and transdifferentiation in Leydig cells in the *Lats1/2* conditional knockout model, showing that Hippo signaling is necessary for maintenance of cell identity in both of these cell types. It is, of course, possible that the two cell identities are not independent from one another; for example, if loss of Hippo signaling prevented Leydig cell differentiation, decreased

steroidogenesis could indirectly compromise Sertoli cell identity. However, knockdown of *Yap1/Wwtr1* in Sertoli cells did not impact testosterone levels, suggesting that YAP1/WWTR1 transcriptional activity in Sertoli cells does not compromise Leydig cell function (Levasseur et al., 2017). It is important to note that the loss of cell identity in Sertoli and Leydig cells does not result in sex reversal, as neither *Yap1/Wwtr1* knockout or *Lats1/2* knockout resulted in upregulation of granulosa cell genes *in vivo* (Abou Nader et al., 2022; Levasseur et al., 2017). Altogether, these data suggest that active Hippo signaling is required for maintenance of somatic testicular cell types.

The requirement for Hippo signaling in somatic cell identity leads to an essential, non-cell-autonomous role in spermatogenesis. This role was first observed in *Drosophila,* where deletion of *expanded* (a *hippo* co-factor) in germ cells themselves did not have an effect on germ cell cyst formation; however, *expanded* deletion in the surrounding somatic cells led to overproliferation of spermatogonia (S. Sun et al., 2008). Later, several studies showed that disruption of Hippo signaling in Sertoli cells disrupts spermatogenesis (Abou Nader et al., 2022; Ni et al., 2019; S. Sen Sharma & Majumdar, 2017). Conditional double knockout of *Lats1* and *Lats2* in mouse Sertoli cells results in small, disorganized testes with very few observable seminiferous tubules, and germ cells in this model were mostly apoptotic by E17.5 (Abou Nader et al., 2022). Similarly, knockout of *Yap1* and *Wwtr1* in Sertoli cells does not impair early spermatogenesis (Levasseur et al., 2017). This suggests that active Hippo signaling, or silenced YAP1/WWRT1 activity, is specifically required in Sertoli cells for early spermatogenesis.

The specific transcriptional targets of YAP1/WWTR1 and exact mechanisms by which Hippo signaling regulates Sertoli cell fate remain to be identified. One study suggested that Hippo signaling may be required for stabilization of cilia, as kidney cells with increased nuclear localization of YAP1 also showed increased expression of AURKA, a cilia disassociation protein (W. H. Shi et al., 2023). In support of this hypothesis, *Wwtr1* knockout mice which survive to birth also display cilia malformations in renal cells (Hossain et al., 2007). This possibility is intriguing as patients with autosomal dominant polycystic kidney disease, which affects cilia formation, also commonly display male infertility and sperm motility defects (W. H. Shi et al., 2023). Another study suggested that *Yap1* regulates the response of Sertoli cells to cAMP (S. Sen Sharma & Majumdar, 2017). As cAMP signaling in mature Sertoli cells regulates follicle stimulating hormone (FSH) response, this suggests a mechanism for *Yap1* regulation of Sertoli cell fate (S. Sen Sharma et al., 2019). It was also shown that FSH treatment could upregulate YAP1 and increase YAP1 nuclear localization in Sertoli cells, suggesting a regulatory feedback loop in which increased FSH induces YAP1 nuclear localization, and then transcriptional targets of YAP1 increase cAMP signaling, which in turn allows for a stronger response to FSH. Excess YAP1 is kept controlled by increased expression of Hippo kinases and increased YAP1 phosphorylation (S. Sen Sharma et al., 2019). This model positions Hippo signaling and YAP1 as master regulators in Sertoli cell maturation and function, making them essential factors for male reproduction.

Section 3.4. Hippo signaling in the ovary

Ovarian structure and cell types

Many processes critical to female mammalian reproduction, including oogenesis, ovulation, and production of female sex hormones such as estrogens and progesterone occur in the ovaries. The ovary is a non-ductal structure composed of two layers of tissue. The internal medulla is a highly vascularized collagenous support matrix for the outer cortex, which itself contains the ovarian functional units known as follicles.

Follicles contain all the essential pieces necessary for ovulation. Each follicle has a single germ cell at its center (which becomes a mature oocyte during ovulation) and several surrounding layers of somatic cells including theca cells and granulosa cells. These cells grow and differentiate through several stages of follicular maturity. Follicle formation commences when pre-granulosa cells surround the early germ cell to form the primordial follicle. As the follicle matures, the granulosa cells differentiate into cumulus cells, which provide nutrients and growth factors for the maturing oocyte, and mural granulosa cells, which are responsible for estrogen production. Following ovulation, granulosa cells luteinize and form the bulk of the corpus luteum, a temporary endocrine structure which produces progesterone during early pregnancy. In addition to their hormone-producing capabilities, granulosa cells are also non-vascularized and separated from surrounding cells by a basal lamina, creating a blood-follicle barrier between the oocyte and potential toxins.

Theca cells become associated with the follicle at the primary follicle stage, forming the final vascularized layer outside of the basal lamina. The primary role of the theca cells is to produce androgens, which are secreted to the aromatase-expressing granulosa cells to be converted into estrogens. After ovulation, the theca cells also contribute to the corpus luteum as theca lutein cells and continue to play a steroidogenic role until the corpus luteum is resorbed. These somatic cells are essential to the reproductive process; loss of any of these cell types will result in oocyte death, failed ovulation, or pregnancy loss.

Hippo signaling is essential for proper ovarian function

The Hippo pathway has been shown to play an essential role in female fertility, particularly through regulation of ovarian cell growth, follicle maturation, and key ovarian functions such as ovulation and steroidogenesis. The first evidence of a Hippo requirement in female reproduction was produced by St John et al., 1999, who showed that 60% of female mice with a full-body knockout of *Lats1* were completely sterile and did not progress through the estrus cycle. Further studies have shown that Hippo signaling activity through LATS1/2 is necessary in granulosa cells for key ovarian processes such as follicle maturation (L. L. Hu et al., 2019; St John et al., 1999; S. Sun et al., 2015; Ye et al., 2017), ovulation (Ji et al., 2017; Plewes et al., 2019; T. Sun & Diaz, 2019), steroidogenesis (M. Fu et al., 2022; Lv et al., 2020; Plewes et al., 2019; Tsoi et al., 2019), maintenance of granulosa cell fate (Lv et al., 2020; Tsoi et al., 2019), and granulosa cell proliferation (M. Fu et al., 2022; Lv et al., 2020; Plewes et al., 2019; T. Sun & Diaz, 2019). Similarly, changes in Hippo signaling have been associated with

defects in ovarian function such as polycystic ovarian syndrome (Cheng et al., 2015; Jiang et al., 2017; Kawamura et al., 2013; T. Li et al., 2012; Maas et al., 2018), primary ovarian insufficiency (Ye et al., 2017), and simple age-related ovarian functional decline (J. Li et al., 2015; Xiang et al., 2015). Further information may be found in several recent reviews on this topic (Clark et al., 2022; Hsueh et al., 2015; Maas et al., 2018; Xia & Du, 2022; M. Zhu et al., 2023).

A point we want to emphasize is that collective evidence supports a model in which a balance of Hippo signaling activity is needed for proper ovarian function. Studies show that both YAP1 inactivation (by *Yap1* knockdown) and YAP1 hyperactivation (by *Lats1* knockout) both resulted in decreased follicle formation (L. L. Hu et al., 2019; St John et al., 1999; S. Sun et al., 2015; Ye et al., 2017). Similar studies have reported ovulation defects and decreased steroidogenesis both when Hippo signaling is overactive and when it is underactive (D. Fu et al., 2014; Lv et al., 2020; Plewes et al., 2019; Tsoi et al., 2019). Furthermore, a need for balanced Hippo signaling in granulosa cells has been demonstrated, which is important because studies have demonstrated that Hippo signaling in the ovary is primarily required in granulosa cells rather than in the oocyte itself (Abbassi et al., 2016; Yu et al., 2016). Too little Hippo activity in granulosa cells, as in the loss of *Lats1/2,* causes them to transdifferentiate into a variety of cell types, leading to loss of steroidogenesis function and disruption of the follicular structure (Tsoi et al., 2019). This in turn leads to a deficiency in follicle abundance, ovulation defects, and a severe decrease in fertility. Interestingly, all previous studies of *Lats* KO in the ovary reported growth of ovarian tumor- or cyst-like structures (St John et al., 1999; S.

Sun et al., 2015). It is possible that these phenomena may have actually been transdifferentating cell populations which had not been fully characterized, though more work in this area is needed to test this hypothesis. Too much Hippo activity, as in the case of *Yap1* knockdown, prevents proper maturation and proliferation of granulosa cells to result in a decrease in mature follicles and compromised fertility. Further research is required to elucidate how this balance of Hippo activity is maintained.

Model for Differential Regulation of Hippo in Follicle Maturation

Altogether, the evidence suggests that there is an essential but dynamic role for Hippo signaling in follicle maturation. The requirements for Hippo activity change over the lifespan of a follicle. Early follicles have higher expression of Hippo kinases (*Mst1/2, Lats1/2*), decreased nuclear localization of YAP1, and more Hippo activity in early granulosa cells which helps to prevent premature follicle activation (De Roo et al., 2020; L. L. Hu et al., 2019; Lv et al., 2019; S. Sun et al., 2015; Xiang et al., 2015). Active Hippo signaling also prevents unrestricted granulosa cell proliferation and maintains granulosa cell identity (S. Sun et al., 2015; Tsoi et al., 2019). However, as follicles begin to mature they downregulate Hippo signaling to allow YAP1 to induce granulosa cell proliferation and maturation (J. Li et al., 2015). As further evidence of a stage-dependent role for Hippo signaling in granulosa cells, functional studies of YAP1 were conducted in cell-specific *Yap1* knockouts in both proliferating and mature granulosa cells (Lv et al., 2019). In mature cells, YAP1 localized in the cytoplasm and loss of *Yap1* in these cells produced no functional or morphological differences. In proliferating granulosa cells, however, loss of *Yap1* led to small ovaries and significantly fewer

follicles. It is possible that this differential regulation of YAP1 activity is partially regulated by mechanical signals, as the stiffer ECM of the outer ovarian cortex may induce Hippo activity in primordial follicles. As the maturing follicles move inward to the less stiff ovarian medulla, the mechanical signal may relax to silence Hippo signaling and allow YAP1 nuclear entry (Hsueh et al., 2015). In support of this hypothesis, strips of ovarian tissue have been shown to have less pYAP and more advanced follicles near the edges of the strip, where the ECM has been disrupted (Grosbois & Demeestere, 2018). After ovulation, Hippo turns back on (possibly in response to endocrine signals such as LH or hCG) to limit proliferation and induce corpus luteum formation (Ji et al., 2017; T. Sun & Diaz, 2019). Therefore, Hippo signaling serves as a possible master regulator for the changes in granulosa cells through the whole lifetime of a follicle.

Remaining questions about Hippo signaling in the ovary

Despite the abundant reported studies, there remain some unanswered questions which are needed to put together a full picture of Hippo signaling in the ovary. Though the requirement for and effects of Hippo signaling in granulosa cells are clear, it is still unknown what regulates Hippo signaling activity in granulosa cells. It would be especially interesting to discover the mechanism by which granulosa cells modulate Hippo signaling throughout follicle maturation. Similarly, many of the direct genetic targets of YAP1/WWTR1 which regulate granulosa cell fate, proliferation, and follicle maturation have not been reported.

Much remains to be discovered on the role of Hippo signaling in the oocyte as well. It is known that both *Yap1* and *Wwtr1* mRNA are maternally loaded in the oocyte (Xie et al., 2010). However, YAP1 protein localization is strictly cytoplasmic and *Yap1* is apparently dispensable for follicle formation, follicular maturation, and ovulation (Abbassi et al., 2016; L. L. Hu et al., 2019; S. Sun et al., 2015; Yu et al., 2016). WWTR1, by contrast, appears to be strongly nuclear in the oocyte (S. Sun et al., 2015). This functional localization of WWTR1 suggests a difference between *Yap1* and *Wwtr1* in regard to their respective roles in the oocyte. Since maternal *Wwtr1* KO embryos develop into adult mice when fertilized by wild-type sperm (although these offspring are subfertile), it appears that its function in the oocyte may be dispensable (Hossain et al., 2007). However, all developmental studies with *Wwtr1* have been done in whole-body knockouts; no oocyte-specific knockouts of *Wwtr1* have been examined to date. Oocyte-specific knockout models of *Lats* or other Hippo kinases have not been examined either. Though full-body knockout of *Lats1* resulted in high rates of oocyte apoptosis, it is possible that this is caused by loss of granulosa cells (and thereby loss of growth factors and sex hormones essential for oocyte development), rather than any direct impact on the oocyte itself (S. Sun et al., 2015). More cell-type-specific knockout models are essential to determine the direct effect of active Hippo signaling in ovarian germ cells.

Section 3.5. Hippo signaling in the uterus

Uterine tissues and processes

Hippo signaling is known to have a profound effect on the uterus, particularly in the process of decidualization. The uterus is comprised of three tissue layers, with an outer perimetrium, middle, muscular myometrium, and inner endometrium. The endometrium is the site of embryo attachment during pregnancy, and as such, this layer has been the focus of most studies regarding Hippo signaling in reproduction. During early pregnancy, the endometrium undergoes drastic morphological and functional remodeling to accommodate the incoming blastocyst for the duration of the pregnancy; this process is known decidualization. Decidualization takes place around four days after fertilization in mouse while in human it begins during the secretory phase of the menstrual cycle (Okada et al., 2018). One of the hallmarks of decidualization is the differentiation of elongated, fibroblast-like endometrial stromal cells to rounded, epithelial-like decidual cells. These cells secrete hormones such as prolactin that are fundamental for embryo implantation and development of the invading trophoblasts to form the placenta. Thus, decidualization is critical for the success of a pregnancy and impairment to this process leads to multitude of pregnancy disorders including infertility and miscarriage.

Hippo signaling is required for uterine decidualization

The components of the Hippo signaling pathway have been implicated in modulating the decidualization process in mammals. Several groups have reported changes in the expression of Hippo pathway members during decidualization. Strakova et al. reported

a decrease in the expression of nuclear WWTR1 after inducing *in vitro* decidualization in human stromal fibroblast cells (Strakova et al., 2010). Increased phosphorylation of LATS1 and WWTR1 have been reported in human endometrial stromal cells cocultured in conditioned media from menstrual stem cells (H. Zhu et al., 2019). Consistent with the upregulation of LATS kinase activity during decidualization, there was decreased expression of WWTR1 in the uterine stroma during the secretory phase of the menstrual cycle in humans (Strakova et al., 2010). Interestingly, the ability of endometrial stromal cells to undergo decidualization was not compromised with the loss of *Lats1* and *Lats2* which might suggest the dispensability of Hippo signaling in this context (St-Jean et al., 2019). It could also mean that *Lats1/2* become dispensable once the decidual cell fate has been established. Taken together, these suggest that Hippo signaling is active during decidualization in uterine stromal cells.

The mechanism by which Hippo regulates decidualization is still under investigation. Interestingly, treatment with a commonly used decidualization inducer, cAMP, did not affect WWTR1 protein level in human stromal fibroblast cells, which suggests that the expression of WWTR1 in decidualization is controlled more by hormones (progesterone/PGR signaling) than by cAMP/PKA signaling (Strakova et al., 2010). In contrast to Wwtr1, both mRNA and protein level of Yap1 is upregulated in human decidual tissue compared to the non-pregnant endometrial stromal cells. Consistent with that, an increase in both YAP1 and TEAD1 mRNA and protein levels has been reported during decidualization in cultured human endometrial cells (H. Chen et al., 2017). Knockdown of *Yap1* using shRNA in these cells showed lack of typical decidual

morphology along with decreased expression of decidua-specific markers and TEAD1, indicating that YAP1 might regulate decidualization in endometrial stromal cells through TEAD1 (H. Chen et al., 2017). The contrasting role of YAP1 and WWTR1 in this context suggests that these homologous proteins play distinctive roles in regulating decidualization.

Hippo disruption may lead to development of endometrial disorders

In addition to their role in regulating decidualization, dysregulation of YAP1/WWTR1 levels has been reported to be involved in the development of endometriosis and endometrial fibrosis (Pei et al., 2019, 2022; Song et al., 2016; H. Zhu et al., 2019). YAP1 mRNA and protein level is significantly higher in endometrial stem cells in women with endometriosis compared to women without endometriosis (Song et al., 2016). YAP1-TEAD1 complex causes increased proliferation and decreased autophagy of endometrial stromal cells from endometriosis via interaction with the negative regulator of autophagy, mTOR (Pei et al., 2019, 2022). This suggests that disrupted Hippo signaling in endometriosis leads to YAP1 overactivation and overproliferation of endometrial cells. Moreover, phosphorylated WWTR1 causes downregulation of the expression of fibrotic genes in endometrial fibrosis, suggesting that disruption of Hippo signaling may also be a driving factor in the etiology of this disease (H. Zhu et al., 2019). These data indicate a connection between the Hippo pathway and the development of endometrial disorders, though more research is needed to thoroughly define this relationship. Taken together, published studies indicate that Hippo signaling

is involved in the dynamic changes occurring in the uterine endometrium during the reproductive cycle and is essential to establishing a healthy pregnancy.

Section 3.6. Hippo signaling in the trophoblast and placenta lineage

Cell types and mechanisms of placental development

After a pregnancy is established, Hippo signaling plays a vital role in the specification and development of the placental lineage. The placenta is a large reproductive organ which acts as an exchange barrier between the mother and the developing fetus. It is comprised of both maternal and fetal components, with the key functional cell type being the trophoblast cells (Rossant & Cross, 2001). The maternal components of the placenta arise from the uterine decidual cells and maternal vasculature, while chorion-derived epithelial cells and allantois-derived vascular cells generate the fetal vascular compartment (Rossant & Cross, 2001). Placentation is characterized by invasion of multipotent, fetal trophoblasts into the maternal endometrium and establishing direct contact between trophoblasts and maternal blood (Cross et al., 1994; Simmons et al., 2007). Placental villi, the functional unit of the human placenta, are generated when rows of fetal trophectoderm-derived cytotrophoblast (CTB) cells break though the expanding primitive syncytium. As this process continues, the villous CTBs continue to expand and differentiate into two principal trophoblast cell types: syncytiotrophoblasts (STBs) and extravillous trophoblasts (EVTs). STBs are responsible for secreting crucial pregnancy hormones, such as human chorionic gonadotrophin (hCG) to maintain the corpus luteum after ovulation (Costa, 2016). The invasive EVT lineage is involved in remodeling the uterine vasculature to enhance maternal blood supply to support the

growing fetus (Knöfler et al., 2019). EVTs also express nonclassical human leukocyte antigen-G to promote immune tolerance to the fetus (PrabhuDas et al., 2015). Any change in this developmental program of the placenta can cause substantial effects on the fetus and its ability to cope with the *in utero* environment (Perez-Garcia et al., 2018; Rossant & Cross, 2001). Therefore, proper development of the trophoblast lineage (i.e., the synchrony between self-renewal and differentiation ability of the trophoblast progenitors) is crucial for successful placentation.

Hippo signaling regulates trophoblast specification and placentation

The Hippo pathway is a critical regulator of many steps of placental development, beginning with an essential role in the differentiation of placental progenitors. As discussed in Chapter 1, the Hippo pathway is well known to regulate a global gene expression program to establish TE lineage in preimplantation mouse embryos (Nishioka et al., 2008; Ralston et al., 2010; Yagi et al., 2007). Interestingly, YAP1 and TEAD4 continues to support trophectoderm lineage development even after implantation. In early post implantation mouse embryo, it has been demonstrated that conditional deletion of *Tead4* in trophoblast stem cell-like progenitor cells leads to impaired placentation together with the repression of trophoblast stem state specific genes, such as *Esrrb*, *Tfap2C* and *Gata3* (Saha et al., 2020). Moreover, both mouse and human TSCs undergo differentiation and display loss of stem state colony morphology with *Tead4*-knockdown, signifying a requirement for TEAD4 to maintain self-renewal ability and stemness in mouse TSCs (Saha et al., 2020). Another study showed that depletion of WWTR1 in CTB-derived human TSCs led to loss of stem-state

colony morphology together with a strong reduction in cell proliferation (Ray et al., 2022). Thus, the transcriptional activity of Hippo effectors is critical to maintain the progenitor state of early trophoblasts.

After implantation, upregulation of Hippo signaling activity and silencing of YAP1/WWTR1 is essential to allow differentiation of more mature trophoblast lineages. YAP1 protein expression level is higher in first-trimester human placentae compared to those of the full-term group, showing that *Yap1* is downregulated after placentation is complete. (Sudol et al., 1995; M. Sun et al., 2018). Furthermore, loss of TEAD4 in human TSCs promotes expression of differentiated STB specific genes such as *CGA*, *CGB* isoforms and *PSG*s. Similarly, YAP1-knockout trophoblastic JEG3 carcinoma cells (representing early pregnancy trophoblasts with TSC-like properties) showed decreased expression of stemness/proliferation associated genes such as cyclin A (*Ccna*), *Cdk6*, *Cyr61*, *Itga6* and *Tead4* whereas overexpression of YAP1 led to induced expression of these genes (Meinhardt et al., 2020). Consistently, overexpression of YAP1 caused downregulation of STB markers such as *Cgβ*, *Gcm1*, *Ovol1, Endou and Gdf15.* As a proposed mechanism to explain YAP1-mediated inhibition of STB differentiation, the YAP1/TEAD4 complex has been shown to interact with the genomic regions of cell cycle regulators such as *Ccna2* and *Cdk6* as well as the promoter regions of the STB specific genes such as *CGB5* and *CGB7* (Meinhardt et al., 2020; Saha et al., 2020). Depletion of *Wwtr1* in human TSCs also resulted in strong upregulation of STB-specific genes and extended culture of this cells led to a STB fate in a culture medium that otherwise supported the maintenance of TSC stem state (Ray et al., 2022). This shows

that YAP1/TEAD4 and WWTR1 are key factors in promoting cell proliferation and in maintaining a self-renewing stem state in trophoblast cells, which must be downregulated for trophoblast differentiation to STBs. However, YAP1 and WWTR1 may not necessarily work together to complete these roles. Overexpression of YAP1 in villous CTBs led to decreased WWTR1 while YAP1 knockout led to increased WWTR1 expression (Meinhardt et al., 2020). This YAP1 mediated alteration of WWTR1 expression suggests a regulatory link between them and suggests that these proteins may work via independent mechanisms to regulate trophoblast differentiation. Taken together, the roles of YAP1, WWTR1 and TEAD4 maintain a balance between CTB self-renewal and differentiation establishes Hippo as a critical regulator of human trophoblast development.

In addition to the roles in maintenance, self-renewal, and differentiation of trophoblasts, downstream mediators of the Hippo pathway have been implicated as critical regulators of placentation and embryo implantation (Bai et al., 2018; Kusama et al., 2016; Meinhardt et al., 2020; Ray et al., 2022; Saha et al., 2020). During placentation, YAP1/WWTR1 are essential for proliferation and invasion of trophoblasts. In support of this, TEAD4 and YAP1 shows strong overlapping expression in the nuclei of proliferative villous CTBs in the first trimester placenta, whereas WWTR1 is abundant in the nuclei of EVTs (Meinhardt et al., 2020; Ray et al., 2022; Saha et al., 2020). Overexpression of YAP1 protein in human trophoblast cell line HTR-8/SVneo led to increased invasive ability of the cells whereas knockdown of YAP1 yielded the opposite outcome (M. Sun et al., 2018). Together, this suggests that YAP1 enhances human trophoblast invasion.

Hippo signaling is also involved during conceptus attachment into the bovine endometrium. Interferon tau (IFNT) is the pregnancy recognition protein in ruminants and is secreted by trophoblast cells of peri-implantation conceptuses (Imakawa et al., 1987). IFNT exerts an anti-luteolytic activity to maintain the integrity of corpus luteum and secretion of progesterone, and thus essential for maintenance of pregnancy (Antoniazzi et al., 2013; Roberts et al., 1992). Bovine IFNT level peaks during peri-attachment period and the level decreases soon after the initiation of the conceptus attachment to the endometrium (Hansen et al., 1999; Kusama et al., 2016). Notably, this downregulation of IFNT in bovine conceptuses has been associated with a decrease in *Yap1* mRNA expression level together with an increase in phosphorylated YAP1 level (Kusama et al., 2016). Consistent with this, nuclear localization of both TEAD2 and TEAD4 was lower during the conceptus attachment period compared to the peri-attachment period. Taken together, these studies suggest that activation of Hippo causes downregulation of IFNT to promote bovine conceptus attachment. Additionally, YAP1-TEAD complex downregulates bovine OVOL2, a transcription factor essential for mesenchymal-to-epithelial transition, concurrently with conceptus implantation. This downregulation of OVOL2 subsequently induces trophectoderm epithelial-to-mesenchymal progression and aids in the non-invasive type of trophoblast implantation in the endometrium (Bai et al., 2018). Therefore, Hippo signaling is crucial for early gestational processes beginning with trophoblast invasion to conceptus attachment among mammals.

Hippo dysregulation is implicated in complications of pregnancy

The Hippo pathway has been implicated in several pregnancy associated complications, such as preeclampsia, intrauterine growth retardation, recurrent pregnancy loss, and preterm birth (Ray et al., 2022; Saha et al., 2020; St John et al., 1999; M. Sun et al., 2018). Abnormal placentation due to shallow trophoblast invasion is central to the pathogenesis of preeclampsia during pregnancy (Fisher, 2015; Goldman-Wohl & Yagel, 2002). It was shown that both YAP1 mRNA and protein expression level is decreased in preeclamptic human placentae compared to the control first trimester and full-term group (M. Sun et al., 2018). Since invasion ability of trophoblasts depends on the enhanced YAP1 expression level, the decreased YAP1 level in preeclamptic placentas might be associated with loss of invasion and thus leading to a disease state (M. Sun et al., 2018). This YAP1-mediated trophoblast invasion defect could be related to microRNA-21 (miR-21) mediated modulation of Hippo signaling. miR-21 is upregulated in preeclamptic human placentae compared to the matched normal placentae (M. Hu et al., 2022; Zhou et al., 2020). Transfection of human trophoblast line HTR-8/SV neo with miR-21 mimic resulted in significant inhibition of both the invasion and migration of the cells (M. Hu et al., 2022). It has been shown that PP2A Bβ, the regulatory subunit of the highly conserved serine threonine phosphatase enzyme PP2A, dephosphorylates LATS1 and leads to increased nuclear YAP1 (M. Hu et al., 2022). Consequently, abnormal level of miR-21 during placentation interferes with the PP2A Bβ activity which leads to Hippo pathway activation and subsequent sequestration of YAP1 in the cytoplasm. In addition, loss of TEAD4 has been associated with defective development of placental villi, particularly defective formation of CTB/STB layer, and thus leading to

idiopathic recurring pregnancy loss in patients (Saha et al., 2020). Finally, placentae from pregnancies complicated with extreme preterm birth showed drastically low level of WWTR1 expression in CTB layer indicating the dysregulation of Hippo effectors as a factor in poor placentation (Ray et al., 2022). Thus, Hippo pathway members orchestrate an intricate developmental program during early human placentation and improper activation of the pathway may result in poor placentation leading to adverse pregnancy outcomes.

Section 3.7. Conclusions

In conclusion, Hippo signaling is a critical regulator of many aspects of mammalian reproduction. In particular, the transcriptional activity of YAP1/WWTR1 appears to regulate many of the reproductive processes involving cellular proliferation, such as spermatogenesis, follicle growth, decidualization, and placentation. Similarly, repression of YAP1/WWTR1 through activation of Hippo signaling kinases is crucial to prevent overproliferation and allow differentiation of reproductive cell types. Thus, precise activation and repression of Hippo signaling is essential to promote fertility and successful pregnancy in mammals. Dysregulation of Hippo signaling can lead to many detrimental reproductive disorders, whether from Hippo hyperactivity causing poor placentation in preeclampsia to Hippo hypoactivity leading to overproliferation of uterine stromal cells in endometriosis. The position of Hippo signaling as such a key regulator in these disorders makes it an attractive therapeutic target; however, there are some drawbacks. The fact that most reproductive processes appear to require a balance of Hippo signaling activity, neither too much nor too little, means that strategies inhibiting

or stimulating the Hippo pathway itself are likely to cause severe side effects. Similarly, since Hippo signaling regulates similar processes of cell proliferation and differentiation in many other tissues, the therapeutic targeting to the reproductive system would need to be very precise. One way to address this would be to look more deeply into factors upstream and downstream of Hippo signaling in reproductive tissues, many of which have yet to be elucidated. These factors may be more specific to reproduction than the Hippo pathway itself and may present more attractive therapeutic targets. There is still much to be learned about Hippo signaling regulation in reproduction, and this field represents exciting opportunities for further discovery and abundant applications in human health and disease.

CHAPTER 4.

HIPPO SIGNALING EFFECTORS MAINTAIN BUT DO NOT REGULATE INITIATION OF CELL POLARIZATION IN MOUSE BLASTOMERES

Robin E. Kruger and Amy Ralston

This study was supported by the National Institutes of Health R35 GM131759 and T32 HD087166.

Section 4.1. Abstract

Hippo signaling effectors YAP1 and WWTR1 are key regulators of polarization in mammalian morula-stage embryos; however, it is unknown whether these factors regulate the initiation of embryo polarization or the maintenance of polarization. In this study, I examined the localization of apical domain markers aPKCζ and PARD6B in wild-type and *Yap1;Wwtr1* maternal-zygotic null embryos at early compaction stages to assess whether *Yap1* and *Wwtr1* were required for the initiation of blastomere polarization. I found that polarization initiated at wild-type rates in the absence of *Yap1* and *Wwtr1.* This suggests that Hippo effectors are required to maintain polarization in late morula and blastocyst-stage embryos after initial formation of the apical domain at the 8- to -16-cell stage.

Section 4.2. Introduction

Hippo signaling is a critical regulator of the first cell fate decision in mammalian embryogenesis. Active Hippo signaling in the inner cells of morula-stage embryos induces expression of inner cell mass (ICM) factors such as *Sox2*, while silenced Hippo in the outer cells allows transcription of key trophectoderm (TE) factors such as *Cdx2* and *Gata3* (see Chapter 1, Fig. 1.2).

One of the key upstream factors governing differential Hippo activity in inside and outside cells of preimplantation embryos is the presence or absence of apical-basal cell polarity. Formation of the apical domain first arises during compaction of blastomeres at the late 8-cell stage (E2.75) (Vinot et al., 2005). The apical domain is characterized by

localization of PAR complex (composed of PAR3, PAR6, and aPKC proteins) and p-ERM to the cell membrane (Alarcon, 2010; Plusa et al., 2005; M. Zhu et al., 2017). These proteins help direct the formation of an apical F-actin “cap”, which further assists in blastomere compaction (Maître et al., 2016; Zenker et al., 2018). Recently, keratin proteins have also been suggested to accumulate at the apical domain and help direct F-actin assembly (Lim et al., 2020). Meanwhile, the nascent basolateral domain is characterized by upregulation of E-cadherin and EMK1 and forms adherens junctions between neighboring cells, which also help maintain apicobasal polarity (Shirayoshi et al., 1983; Stephenson et al., 2010; Vinot et al., 2005). Following compaction and polarization, asymmetric cell divisions cause some cells to inherit the apical domain proteins and remain outside cells, while those that do not inherit an apical domain lose their polarity and are directed to the inside of the embryo (Johnson & Ziomek, 1981; Korotkevich et al., 2017; Lim et al., 2020). This leads to transcriptional and morphological differences between inside and outside cells.

The presence or absence of an apical domain heavily regulates the activity of Hippo signaling in blastomeres. Single, dissociated blastomeres lose apical domain expression and concomitantly display Hippo signaling activity (Lorthongpanich et al., 2013). Hippo signaling is also active in blastomeres cultured in media containing Ca^{2+}, which prevents polarization and cell-cell contact (Anani et al., 2014). In embryos lacking maternal and zygotic E-cadherin, aPKCζ is ectopically localized to the membrane of inner cells, and in these embryos Hippo signaling is inactive (Stephenson et al., 2010). Finally, if a section of apical domain is added to an initially apolar blastomere, the cell

will move to the outside of the embryo and typically adopt a trophectoderm identity (Korotkevich et al., 2017). This shows that cell polarization upstream of Hippo signaling is necessary and sufficient for regulating ICM and TE cell fate at early morula stages.

Interestingly, evidence suggests that polarization may also be downstream of Hippo signaling, forming a feedback mechanism to direct the first cell fate decision. At the blastocyst stage, dual loss of Hippo effector proteins YAP1 and WWTR1 leads to a loss of apical aPKC, PAR3, and ZO-1 (Frum et al., 2018). This suggests that Hippo signaling is partially responsible for ensuring the proper apical localization of these proteins, which is critical to embryonic development as loss of either *aPKC* or *Pard6b* causes blastomeres to adopt an inside position (Hirate et al., 2015; Plusa et al., 2005). However, it is unknown whether YAP1/WWTR1 are required for the initial localization of these factors at the apical domain or simply for their maintenance at that localization.

To test the hypothesis that YAP1/WWTR1 are essential for initiating blastomere polarization, I examined apical domain markers aPKCζ and PARD6B at early morula stages in wild-type and *Yap1;Wwtr1* mz null embryos. I found that, surprisingly, polarization appears normal in *Yap1;Wwtr1* mz null embryos at the 16-cell stage, suggesting that Hippo signaling regulates the maintenance but not the initial localization of these apical domain factors.

Section 4.3. Materials and Methods

Mouse Strains and Genotyping

All animal research was conducted in accordance with the guidelines of the Michigan State University Institutional Animal Care and Use Committee under approved protocol 202300108. Wild type embryos were obtained from CD-1 mice (Charles River). The following alleles were used in this study and maintained in a CD-1 background: *Yap1*$^{tm1.1Eno}$ (Xin et al., 2011); *Wwtr1*$^{tm1.1Eno}$ (Xin et al., 2013); *Tg(Zp3-cre)93Knw* (De Vries et al., 2000). Null alleles were generated by breeding dams carrying homozygous floxed alleles and the *Zp3Cre* allele to wild-type CD-1 males. Mouse genotypes were determined by PCR using genomic DNA extracted using the REDExtract-N-Amp kit (Sigma XNAT) according to the manufacturer's protocol. Embryo genomic DNA was extracted using the same kit scaled to 10 µL total volume. Genomic extracts (1–2 µL) were then subjected to PCR using allele-specific primers (see Table 4.1).

Immunofluorescence and Confocal Microscopy

Preimplantation embryos (E2.5-E3.0) were fixed with 4% formaldehyde (Polysciences 04018) for 10 minutes, permeabilized with 0.5% Triton X-100 (Sigma Aldrich X100) for 30 minutes, and then blocked with blocking solution (10% Fetal Bovine Serum (HyClone SH30396.02), 0.1% Triton X-100) overnight at 4°C. Embryos were incubated with primary antibody overnight at 4°C. The next day, embryos were washed in blocking solution for 30 minutes, incubated in secondary antibody diluted in blocking solution for 1 hour, washed in blocking solution for 30 minutes, then stained with nuclear stain diluted in block for 10 minutes or overnight.

Antibodies used are listed in Table 4.2. Embryos were imaged using an Olympus FluoView FV1000 Confocal Laser Scanning Microscope system with 60X PlanApoN oil (NA 1.42) objective. For each embryo, z-stacks were collected, with 5 mm intervals between optical sections. All embryos were imaged prior to knowledge of their genotypes.

Embryo Analysis

For each embryo, z-stacks were analyzed using Fiji (ImageJ), which enabled the labeling, based on DNA stain, of all individual cell nuclei. Statistical analysis was performed using GraphPad Prism (v. 9.5.1). Figure images were assembled using Adobe Illustrator.

Section 4.4. Results

Apical domain formation is first initiated at the 8-cell stage (Vinot et al., 2005). Therefore, I first investigated polarization in wild-type embryos at this stage. Apical aPKCζ was detectable in all 8-cell embryos, consistent with previous reports (Frum et al., 2018; Vinot et al., 2005). However, in most 8- to 10-cell embryos only ~60% of outer blastomeres expressed apical aPKCζ. Furthermore, most embryos still did not express apical PARD6B (Fig. 4.1A). This suggested that although outer blastomere polarization had initiated at the 8-cell stage, it was not yet complete. I therefore performed a time course to determine the first stage where polarization was complete in all embryos. At the 16- to 18-cell stage, I observed that nearly 100% of outer cells expressed apical aPKCζ and PARD6B, a significant upregulation from previous stages (Fig. 4.1B). The

percentage of polarized cells remained at nearly 100% after this stage (Fig. 4.1B). From these observations, I concluded that polarization of outer blastomeres (as defined by apical localization of aPKCζ and PARD6B) is normally complete at the 16-cell stage.

Having identified the developmental stage at which apical domain formation is normally complete in mouse embryos, I then assessed whether the loss of Hippo effectors YAP1 and WWTR1 would result in decreased or delayed apical domain formation. *Yap1* and *Wwtr1* have been shown to have partially redundant roles in early mouse embryos (Nishioka et al., 2009), and maternally-derived transcripts of both are present and functional in oocytes and early embryos (Frum et al., 2018; Varelas et al., 2010; Xie et al., 2010; Yu et al., 2016). Therefore, to avoid potential compensation from any source of genetic material, I generated embryos lacking maternal and zygotic *Yap1* and *Wwtr1* (*Yap1/Wwtr1* mz null, see breeding scheme in Fig. 4.2). If my hypothesis that YAP1/WWTR1 are required to initiate blastomere polarization was correct, I expected to see decreased initial apical localization of aPKCζ and PARD6B in *Yap1/Wwtr1* mz null embryos. In contrast to this hypothesis, I detected apical localization of aPKCζ and PARD6B in 16-cell *Yap1/Wwtr1* mz null embryos at a similar level to wild-type (Fig. 4.3A). The percentage of outer blastomeres which were polarized did not differ between *Yap1/Wwtr1* mz null embryos and wild-type or single-knockout controls (Fig. 4.3B). This suggests that initial apical localization of aPKCζ and PARD6B does not depend on *Yap1* and *Wwtr1.*

Section 4.5. Discussion

Hippo signaling effectors YAP1 and WWTR1 have been shown to be necessary for outer cell polarization in mouse blastocysts (Frum et al., 2018); however, the mechanism of this requirement is still unknown. My data suggest that YAP1 and WWTR1 do not regulate the initial formation of an apical domain at the 8- to 16-cell stages, as marker proteins aPKCζ and PARD6B show normal apical localization in *Yap1/Wwtr1* mz null embryos at this stage. Rather, it appears that YAP1 and WWTR1 are required for apical domain maintenance between the early morula and blastocyst stages.

It is unknown how YAP1/WWTR1 may be regulating apical domain maintenance in early embryos. YAP1/WWTR1 generally induce molecular changes by binding to TEAD family transcription factors in order to regulate gene expression (Zheng & Pan, 2019). TEAD4 is canonically considered the main transcriptional binding partner for YAP1/WWTR1 in mouse embryos, as *Tead4*-null embryos largely recapitulate the phenotypes associated with *Yap1*;*Wwtr1* loss-of-function and *Lats1/2* gain-of-function (Nishioka et al, 2008; 2009; Frum et al 2018). Interestingly, however, *Tead4* z null embryos retain normal apical localization of aPKCζ at late morula stage (exact timepoint not reported), indicating that polarization is maintained properly (Nishioka et al., 2008). This suggests that YAP1/WWTR1 may regulate apical domain maintenance through partnership with proteins other than TEAD4 (Frum et al 2018).

Likewise, the exact mechanism by which targets of YAP1/WWTR1 and their binding partner(s) may regulate apical domain maintenance is still unknown. However, there is evidence to suggest that regulation of the actin cytoskeleton may be a good candidate. Actin remodeling is an essential part of blastomere compaction at the late 8-cell stage, a process largely concomitant with cell polarization (M. Zhu & Zernicka-Goetz, 2020). During compaction, F-actin is excluded from cell-cell contacts and accumulates at the cell-free, outer membranes. Increased tension from unequal actomyosin contractility helps drive compaction of blastomeres (Maître et al., 2016). Shortly afterward, polarization initiates and accumulation of Par complex proteins helps remodel the actomyosin network into a characteristic apical ring (Zenker et al., 2018). Interestingly, initial localization of apical domain proteins is unperturbed when actomyosin contractility is decreased by inhibiting myosin II activity, suggesting initiation of polarization may be independent of actin dynamics (M. Zhu et al., 2017). However, polarization is not maintained in embryos where actin nucleation is inhibited (S. C. Sun et al., 2013). Significantly, there is abundant evidence that actin polymerization can regulate Hippo signaling activity in mammalian and fly systems (Hirate et al., 2013, reviewed in Matsui & Lai, 2013; Reddy et al., 2013), and this regulation is not one-sided; in flies, Hippo pathway kinase activation can also downregulate F-actin accumulation (Matsui & Lai, 2013). If F-actin accumulation is essential for the maintenance of blastomere polarization but not its initiation, it is possible that *Yap1;Wwtr1* mz null embryos fail to maintain polarity by inappropriate downregulation of F-actin. More studies are needed to determine the validity of this model and define the factors which maintain blastomere polarity downstream of Hippo signaling.

Section 4.6. Acknowledgements

I thank Drs. Tristan Frum and Jennifer Watts for their technical assistance in this study.

TABLES

Allele	Forward Primer	Reverse Primer
Yap1^{WT}, Yap1^{fl}	ACATGTAGGTCTGCATG CCAGAGGAGG	AGGCTGAGACAGGAGG ATCTCTGTGAG
Yap1^{del}	ACATGTAGGTCTGCATG CCAGAGGAGG	TGGTTGAGACAGCGTGC ACTATGGAG
Wwtr1^{WT}, Wwtr1^{fl}	GGCTTGTGACAAAGAAC CTGGGGCTATCTGAG	CCCACAGTTAAATGCTT CTCCCAAGACTGGG
Wwtr1^{del}	TGACAAAGAACCTGGGG CTA	AACTGCTAACGTCTCCT GCC
Cre	CTAGGCCACAGAATTGA AAGATCT	GTAGGTGGAAATTCTAG CATCATCC
Zp3Cre	CGAGATTGAGGGAAGCA GAG	CAGGTTCTTGCGAACCT CAT

Table 4.1. Allele-specific primers for PCR genotyping for Chapter 4.

Antibody/Stain	Source	Identifiers	Dilution	Fluorophore
Mouse-anti-aPKCζ	Santa Cruz Biotechnology	sc-17781	1:100	
Rabbit-anti-PARD6B	Novus Biologicals	NBP1-87337	1:100	
Goat-anti-mouse IgG	Invitrogen	A-11029	1:400	Alexa488
Donkey-anti-rabbit IgG	Jackson Immuno Research	711-165-152	1:400	Cy3
DRAQ5	Cell Signaling	4084	1:400	

Table 4.2. Antibody Table for Chapter 4

FIGURES

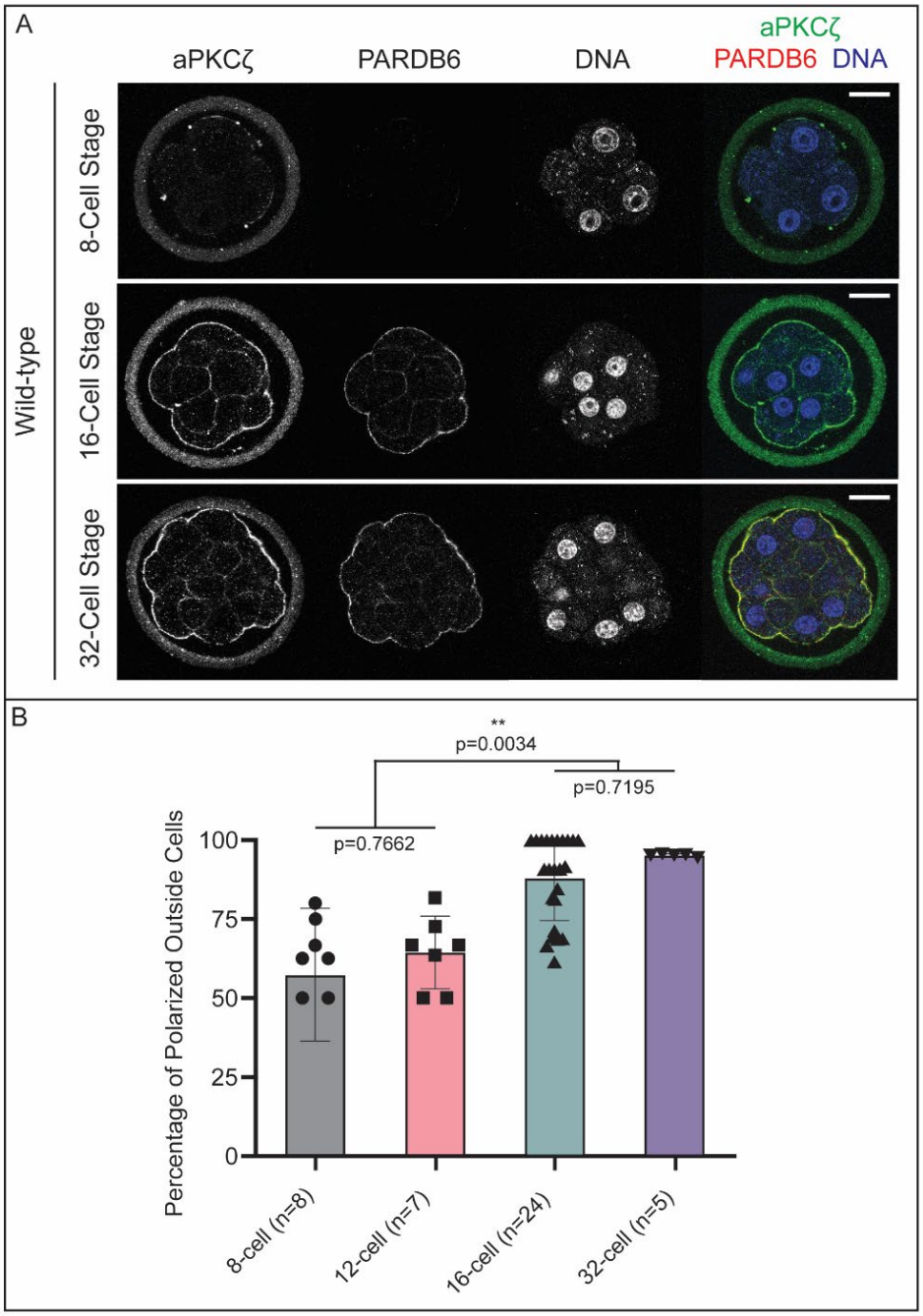

Figure 4.1. Polarization of outer blastomeres is complete at the 16-cell stage. A) Immunofluorescence for aPKCζ and PARD6B in wild-type preimplantation mouse embryos collected at designated timepoints. **B)** Quantification of the percentage of outside blastomeres in embryos from A which display apical localization of aPKCζ. Statistical analysis was performed using analysis of variance (ANOVA) with Tukey's post-hoc test.

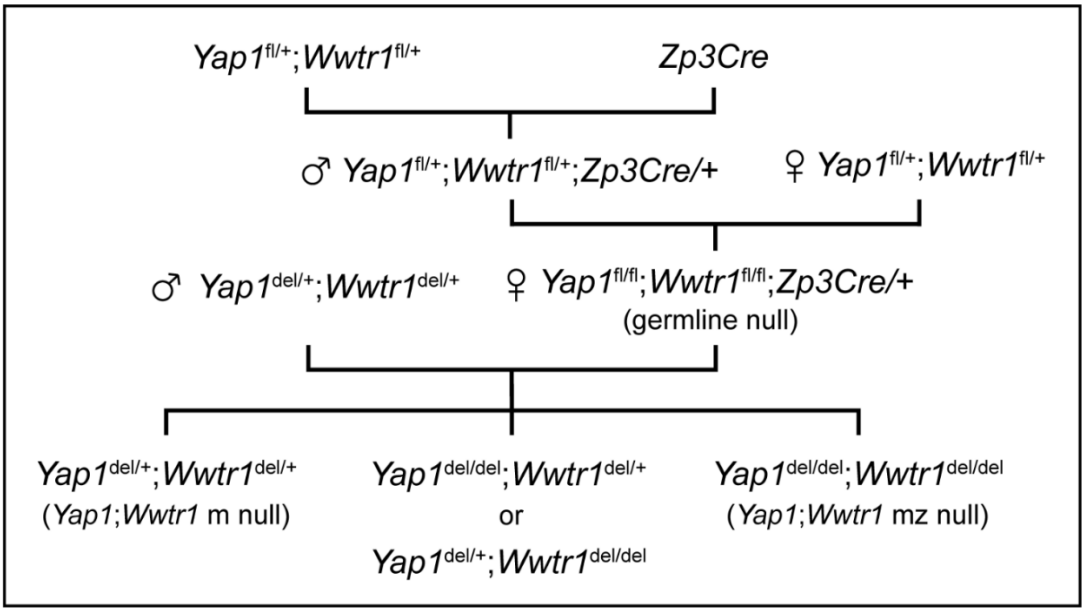

Figure 4.2. Breeding Scheme for *Yap1;Wwtr1* maternal-zygotic (mz) null embryos. *Yap1;Wwtr1* mz null embryos were generated using the *Zp3Cre* allele described in De Vries *et al.,* 2000. *Yap1;Wwtr1* mz null embryos lacked zygotic expression of both genes and did not have maternally-derived transcripts of either gene deposited in the oocyte before fertilization.

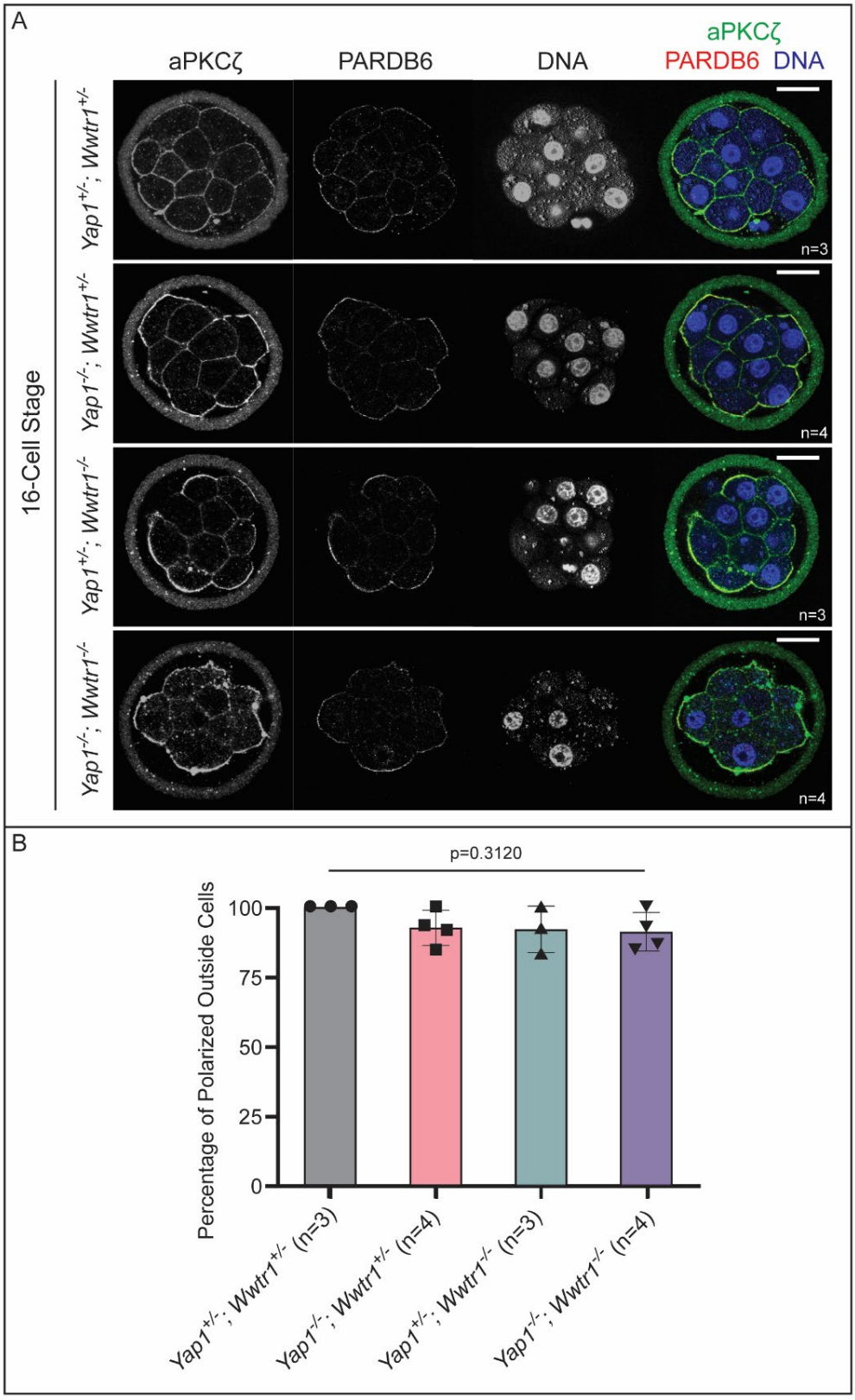

Figure 4.3. Initial polarization of outer blastomeres does not depend on *Yap1/Wwtr1*.

Figure 4.3 (cont'd).
A) Immunofluorescence for aPKCζ and PARD6B in 16-cell mouse embryos lacking maternal *Yap1;Wwtr1* and either heterozygous or null for zygotic *Yap1;Wwtr1.* **B)** Quantification of the percentage of outside blastomeres from embryos in A which display apical localization of aPKCζ. Statistical analysis was performed using analysis of variance (ANOVA) with Tukey's post-hoc test.

CHAPTER 5.

EFFICIENT GENERATION OF ENDOGENOUS PROTEIN REPORTERS FOR MOUSE DEVELOPMENT

Daniel O'Hagan[1], Robin E. Kruger[2], Bin Gu[3,4], and Amy Ralston[1,2]

1) Department of Biochemistry and Molecular Biology, Michigan State University, East Lansing, MI, 48824

2) Reproductive and Developmental Sciences Training Program, Michigan State University, East Lansing, MI, 48824

3) Department of Obstetrics, Gynecology and Reproductive Biology, Michigan State University, East Lansing, MI, 48824

4) Institute for Quantitative Health Science and Engineering, Michigan State University, East Lansing, MI, 48824

This chapter is modified from O'Hagan *et al.,* published in *Development* on May 20, 2021.

This study was supported by the National Institutes of Health R35 GM131759 and T32 HD087166.

Section 5.1. Abstract

Fluorescent proteins and epitope tags can reveal protein localization in cells and animals, yet the large size of many tags hinders efficient genome targeting. Accordingly, many studies have relied on characterizing overexpressed proteins, which might not recapitulate endogenous protein activities. Here, we present two strategies for higher throughput production of endogenous protein reporters in mice, focusing on the blastocyst model of development. Our first strategy makes use of a split fluorescent protein mNeonGreen2 (mNG2). Knock-in of a small portion of the *mNG2* gene, in frame with gene coding regions of interest was highly efficient in embryos, potentially obviating the need to establish mouse lines. When complemented by the larger portion of the *mNG2* gene, fluorescence was reconstituted and endogenous protein localization faithfully reported in living embryos. Our second strategy achieves in-frame knock-in of a relatively small protein tag, which provides high efficiency and higher sensitivity protein reporting. Together, these two approaches provide complementary advantages and enable broad downstream applications.

Section 5.2. Introduction

Mouse models are essential tools for research to uncover human disease mechanisms. To produce new mouse lines, embryos are collected and genetically manipulated during the preimplantation stage, and are then transferred to surrogate mothers for gestation. Thus, preimplantation embryos are the starting point for many studies. Within preimplantation, the blastocyst stage of development is also an alluring model in its own right. This is in part because the blastocyst provides technical advantages, including

optical transparency, the capacity to develop *ex vivo* in a cell culture incubator, and the ease of collecting dozens of embryos at a time. These properties have enabled discovery of the molecular mechanisms of the first steps in mammalian development. Moreover, embryonic stem cells (ESC) are derived from blastocysts, providing additional models for basic and applied research. Thus, technological advances using the blastocyst can impact broader areas of biomedical research.

One powerful approach to elucidating the molecular mechanisms of development and disease has been live imaging of fluorescent reporters *in vivo*, which enables time-resolved analysis of gene expression at the cellular level (Nowotschin & Hadjantonakis, 2014). Live imaging of gene expression *in vivo* is often achieved by knocking in genes encoding *Green Fluorescent Protein* (*GFP*) and other fluorescent proteins downstream of gene promoters, to create a gene reporter. This approach requires establishing and breeding new mouse lines. An alternative method of protein detection is to use antibodies to localize endogenous proteins, for example by immunofluorescence. However, immunofluorescence does not allow visualization of dynamic processes. Moreover, identification of reliable and specific antibodies can also be time-intensive and, for some antigens, may not exist.

Our goal was to help overcome some of these challenges by developing an alternative, streamlined pipeline for the detection or screening of endogenous proteins *in vivo*. We focus on preimplantation mouse embryos, where we present two complementary approaches to enhance the efficiency of detecting endogenous proteins *in vivo*. We

provide guidelines for implementation of these approaches in broader experimental settings.

Section 5.3. Materials and Methods

Animal Use

All animal research was conducted in accordance with the guidelines and approval of the Michigan State University Institutional Animal Care and Use Committee. Most experiments were performed using male or female CD-1 mice, at least 6-8 weeks of age, maintained on a 12-hour day/night cycle with food and water *ad libitum*.

Plasmid construction

The pR26-CAG-mNG2(∆11) targeting vector was cloned by insertion of a synthesized dsDNA fragment encoding mNG2(∆11) (Table 5.4) into the previously published vector pR26-AsisI/MluI (Addgene #74286) (V. T. Chu et al., 2016) via restriction/ligation with AsisI and MluI. After cloning, the Lox-Stop-Lox site was removed by exposure to recombinant Cre recombinase (NEB), using the NEB standard protocol. The *in vitro* transcription plasmids for *Clta-mNG2(11)*, *mNG2(∆11)*, and *Cdx2-mNG2(11)* were cloned by inserting a synthesized dsDNA fragment (Table 5.4) containing the respective coding sequence into a pcDNA3.1-poly(A)83 vector (K. Yamagata et al., 2005) downstream of the T7 promoter via restriction ligation with HindIII and NotI. pX459-sgRosa26-1 was generated by inserting the guide RNA sequence targeting *Rosa26* (Table 5.3) into pSpCas9(BB)-2A-Puro (PX459) V2.0 (Addgene #62988) via restriction ligation with BbsI.

mRNA synthesis

In vitro transcription (IVT) was performed using the T7 mMessage mMachine kit (Life Technologies). Each IVT construct was digested with XbaI, followed by ethanol precipitation, and was then used in the IVT reaction per manufacturer's instructions. Resulting mRNA was purified using the MEGAclear kit (Ambion). mRNA quantity and quality were assessed by Nanodrop spectrophotometer and by agarose gel, respectively.

Zygote and 2-cell embryo microinjection

Target-specific crRNA and non-variable tracrRNA obtained from Integrated DNA Technologies were each suspended in injection buffer (1 mM Tris HCl, pH 7.5; 0.1 mM EDTA), mixed at a 1:1 molar ratio and annealed in a thermal cycler by ramping down from 95 ºC to 25 ºC at 0.1 ºC/second. The annealed RNAs were then mixed with recombinant Cas9 Protein at a 5:1 RNA:Cas9 molar ratio and allowed to form RNPs for 15 minutes at room temperature. RNPs were mixed with donor ssODN synthesized as Ultramers from Integrated DNA Technologies (Table 5.2) and diluted to working concentrations (Table 5.5) by addition of injection buffer. For mRNA injections, each mRNA was diluted in injection buffer to 350 ng/µl and injected either into one pronucleus of the mouse zygote or into one blastomere of the 2-cell mouse embryo. Injection mixes and mRNAs were aliquoted and stored at -80 ºC, avoiding freeze/thaw cycles.

Zygotes were harvested from naturally mated pregnant mice on the day that copulatory plugs were detected. Oviducts were flushed with M2 medium (Millipore Sigma), and

then injection mix was delivered into one pronucleus or the nucleus of one blastomere via microinjection (Nagy et al., 2003). Injected zygotes were cultured in KSOM + amino acids (Millipore Sigma) for up to five days before being either fixed or imaged live. Only embryos that survived injection and appeared to have cavitated or to be attempting cavitation were included in the analysis.

Generation of R26-mNG2(∆11) Mouse Line

The *R26-mNG2(∆11)* mouse line was generated by zygote microinjection at the Michigan State University Transgenic and Genome Editing Facility. *Rosa26* sgRNA was synthesized by *in vitro* transcription (IVT) of PCR-amplified region of PX459-sgRosa26-1 using the Life Technologies MEGAshortscript T7 kit. Transcripts were subsequently purified using the MEGAclear kit. A mixture containing 5 ng/µl circular pR26-CAG-mNG(∆11) and 125 ng/µl Cas9 RNP complexed with *sgRosa26* guide RNA was injected into one pronucleus of C57BL/6J mouse zygotes. Zygotes were then transferred to CD-1 recipient mice. After birth, tail tips were screened by PCR for successful integration of the *R26-CAG-mNG(∆11)* allele.

Immunofluorescence and Confocal Microscopy

V5 was detected by mouse anti-V5 antibody (Thermo Fisher, R96025). Embryos were fixed with 4% formaldehyde (Polysciences) for 10 minutes, permeabilized with 0.5% Triton X-100 (Millipore Sigma) for 30 minutes, and then blocked in 10% Fetal Bovine Serum (Hyclone) with 0.1% Triton X-100 for 1 hour at room temperature. Embryos were then incubated in anti-V5 at a dilution of 1:400 in blocking solution at 4 ºC overnight.

The next day, embryos were stained with goat anti-mouse Alexa488 (Invitrogen, A-11030) at a 1:400 dilution in blocking solution for 1 hour at room temperature. Embryos were then stained for 10 minutes at room temperature in 50 μM Hoechst nucleic acid stain (Thermo Fisher) or DRAQ5 (Cell Signaling, 4084S, 1:400 dilution). Rabbit-anti-Nanog, (Reprocell, RCAB002P-F) was used at 1:400 dilution, with Cy3-conjugated donkey-anti-rabbit IgG (Jackson Laboratories, 711-165-152) at 1:400 dilution. Split mNG2 embryos were imaged either fixed or live after Hoechst staining. Imaging was performed using an Olympus FluoView FV1000 Confocal Laser Scanning Microscope system with 20x UPlanFLN objective (0.5 NA) and 5x digital zoom or with 60x PlanApoN oil (NA 1.42) objective. For each embryo, z-stacks were collected with 3 μm intervals between optical sections. Optical sections are displayed as an intensity projection over the Z axis. Figures were prepared using FIJI, Adobe Photoshop, and Adobe Illustrator.

Genotyping

To genotype embryos, genomic DNA was extracted from single blastocysts by placing each blastocyst in a microtube containing 4.4 μl Extraction buffer (REDExtract-N-Amp Tissue PCR Kit, Millipore Sigma) mixed with 1.1 μl of Tissue Prep Buffer, and then incubating tubes at 56 ºC for 30 minutes, 24 ºC for 5 minutes, and 95 ºC for 5 minutes. After incubation, 5 μl Neutralization buffer was added to each tube. In subsequent reactions, 1 μl of embryo extract was used as PCR template, and locus-specific primers (Table 5.1). To genotype adult mice, genomic DNA was extracted from ear punch

biopsies using the Wizard SV Genomic DNA Purification System (Promega), and PCR was performed using Herculase II Polymerase (Agilent).

Sequencing

To confirm the identity of select PCR products, the products were directly cloned into pCR2.1 TOPO using the Invitrogen TOPO TA Cloning Kit (Invitrogen). Plasmids containing the PCR product were prepped with the Spin Miniprep Kit (Qiagen) and then sequenced by RTSF Sanger method at the Genomics Core at Michigan State University.

mNG2(Δ11) ES Cell Derivation

R1/E ES cells (ATCC) were cultured on CF-1 feeder MEFs (Applied Stem Cell) in ES cell medium [DMEM supplemented with 1000 U/mL leukemia inhibitory factor (Millipore Sigma), 15% (v/v) fetal bovine serum (Hyclone), 2 mM L-Glutamax (Thermo Fisher), 0.1 mM beta-mercaptoethanol (Millipore Sigma), 0.1 MEM non-essential amino acids (Millipore Sigma), 1 mM Sodium Pyruvate (Millipore Sigma), and 1% (v/v) penicillin/streptomycin (Gibco)]. Passage 13 R1/E ES cells were cultured to approximately 70% confluence in a 10 cm dish, and then electroporated with pX459-sgRosa26-1 and pR26-CAG-mNG2(Δ11) as follows: pelleted cells were resuspended in 800 µl Embryo-Max Electroporation Buffer (Millipore Sigma) containing 20 µg each plasmid, and cells were then electroporated in a 0.4 cm electrode gap electroporation cuvette (Bio-Rad) using Bio-Rad Gene Pulser XCell electoporator (250 V, 500 µF, infinite Ω). Subsequently, 400 µl electroporated cells were then diluted in 10 mL ES cell

medium, and then plated on a 10 cm dish on puromycin-resistant DR4 feeder MEFs (Applied Stem Cell). After 24 hours, selection was started with ES cell medium containing 1.25 µg/mL puromycin (Gibco). After 12 days, colonies were picked into 96-well plates and expanded over several more passages. Cell lines were genotyped by PCR using R26F3 and SAR primers to detect insertion of *mNG2(∆11)* in the *Rosa26* locus (Table 5.1).

Section 5.4. Results

A mouse line to enable *in vivo* implementation of a split fluorescent protein

Like GFP, the yellow-green, monomeric fluorescent protein mNeonGreen (mNG), derived originally from the marine invertebrate *Branchiostoma lanceolatum*, is an eleven-stranded beta-barrel, but is up to three times brighter than GFP (Shaner et al., 2013). The mNG derivative, mNG2 can be split into two separate coding units, mNG2(∆11), which lacks the eleventh beta-strand, and mNG2(11), which is the eleventh beta-strand (Feng et al., 2017). Individually, the two resulting proteins lack appreciable fluorescence. However, when the larger protein mNG2(∆11) is complemented by the 16-amino acid mNG2(11), fluorescence is reconstituted (Fig. 5.1A), and the two proteins are capable of self-assembly through non-covalent intermolecular interactions (Cabantous et al., 2005).

We sought to make use of this fluorescence complementation strategy to evaluate localization of endogenous proteins in mouse embryos because we reasoned that tagging endogenous proteins with the smaller, 16-amino acid *mNG2(11)* coding region

would be more efficient than knocking in the full-length gene encoding the full-length, 236 amino acid fluorescent protein. Then, to provide the complementary protein, we aimed to establish a mouse line capable of constitutive expression of *mNG2(Δ11)*. Our goal was to introduce an expression construct including cytomegalovirus enhancer, chicken beta-actin promoter, rabbit beta-globin splice acceptor (CAG) sequences, and the *mNG2(Δ11)* coding region into the *Rosa26* (*R26*) locus by homologous recombination (Fig. 5.1B), which would enable constitutive, ubiquitous expression of *mNG2(Δ11)* throughout mouse tissues and development (Friedrich & Soriano, 1991). However, prior to attempting knock-in in mouse zygotes, we first established an *R26-mNG2(Δ11)* embryonic stem (ES) cell line using a Cas9/CRISPR-mediated knock-in strategy (V. T. Chu et al., 2016) (see Methods). These *R26-mNG2(Δ11)* ES cells provided a renewable source of positive control genomic DNA for subsequent experiments.

To produce a mouse line capable of expressing *mNG2(Δ11)*, we subsequently introduced the *mNG2(Δ11)* expression construct into the *Rosa26* (*R26)* locus in zygotes, following the strategy we had used in ES cells. Injected zygotes were transferred to recipient females, allowed to gestate, and then founder mice carrying *mNG2(Δ11)* were identified by PCR genotyping (Fig. 5.1C-D) and genomic sequencing (not shown). A single founder mouse was then expanded, and bred to homozygosity to establish *R26-mNG2(Δ11)*/*R26-mNG2(Δ11)* mice. In principle, providing *mNG2(11)* in trans to *R26-mNG2(Δ11)* would lead to reconstitution of the green fluorescent protein. For simplicity, we called this the GOGREEN system.

As an initial evaluation of the GOGREEN system, our first test was to determine if we could detect fluorescence complementation in embryos by epifluorescence microscopy (Fig. 5.2A). For this test, we generated mRNA encoding *mNG2(11)*-tagged *Clathrin, light polypeptide* (*Clta*). For negative controls, mRNA encoding either *mNG2(Δ11)* or *mNG2(11)-Clta* were injected individually into wild type embryos (Fig. 5.2B). For a positive control, wild type zygotes were co-injected with mRNAs encoding both *R26-mNG2(Δ11)* and *mNG2(11)-Clta*, and these exhibited greatly elevated fluorescence over both negative controls. Finally, *R26-mNG2(Δ11)*/+ zygotes were injected with mRNA encoding *mNG2(11)-Clta*, which led to elevated fluorescence at the blastocyst stage, demonstrating functionality of the GOGREEN system *in vivo* using epifluorescence and an exogenous *mNG2(11)*-tagged protein.

Fluorescence reconstitution by split fluorescent protein knock-in

We next aimed to evaluate the performance of the GOGREEN system when *mNG2(11)* was endogenously expressed from several genomic loci. Our goal was to derive *R26-mNG2(Δ11)*/+ zygotes and, in these, perform CRISPR/Cas9-mediated knock-in of *mNG2(11)* in frame with proteins of interest (Fig. 5.3A) to produce mNG2(11) fusion proteins capable of complementing mNG2(Δ11) and reporting endogenous protein patterns.

To achieve in-frame *mNG2(11)* knock-in, we designed targeting constructs encoding the 16 amino acid mNG2(11), plus a three-amino acid linker, flanked by genomic locus-specific homology arms of 30 nucleotides each (Fig. 5.3B). Resulting targeting

constructs ranged from 117-120 nucleotides in length, permitting their synthesis as a single stranded oligodeoxyribonucleotides (ssODN) by a commercial vendor (see Methods). For our first knock-in attempts, we targeted cytoskeletal proteins, including intermediate filaments and beta-actin, because their subcellular localizations in mouse preimplantation have long been known (Chisholm & Houliston, 1987; Coonen et al., 1993; Reima & Lehtonen, 1985).

We designed CRISPR reagents to knock *mNG2(11)* in-frame with *Keratins* (*Krt*) *Krt8* and *Krt18*, as well as *Actin, beta* (*Actb).* Following injection of the knock-in mixture into *R26-mNG2(⊿11)*/+ zygotes, embryos were cultured to the blastocyst stage, and then imaged by confocal microscopy. For each knock-in, we observed the very unique fluorescent meshwork of cortical filamentous proteins expected, in accordance with published observations (Coonen et al., 1993; Lim et al., 2020; Ralston & Rossant, 2008; Reima & Lehtonen, 1985). These observations are indicative of faithful protein reporting. Individual embryos were then harvested, and gene targeting evaluated by PCR (Fig. 5.3D) and sequencing (not shown). In all cases, monoallelic targeting was highly efficient (Fig. 5.3E). These observations demonstrate the utility of the GOGREEN system for efficiently reporting localization of endogenous proteins *in vivo*. Given that the dynamics of cytoskeletal protein localization and turnover during preimplantation development are actively studied (Anani et al., 2014; Schwarz et al., 2015; Zenker et al., 2018), the GOGREEN system could provide new tools since these proteins are usually visualized either in fixed embryos or by injection of mRNAs encoding tagged proteins, both of which could introduce unwanted artifacts.

Fluorescence complementation in the nuclear compartment

Thus far, we had evaluated the ability of the GOGREEN system to report endogenous cytoplasmic proteins *in vivo*. However, we were uncertain whether the GOGREEN system could effectively report the dynamics of endogenous nuclear protein expression, owing to the possibility that the two components of the GOGREEN system might end up separated by the nuclear membrane.

To investigate the performance of the GOGREEN system in visualizing nuclear proteins *in vivo*, we evaluated fluorescence in embryos after targeting the genes *Nucleophosmin* (*Npm1*) and *NOP58 ribonuclear protein* (*Nop58*), which both encode nucleolar proteins. As for previous experiments, we targeted *mNG2(11)* in frame with target genes in the *R26-mNG2(⊿11)*/+ genetic background. Remarkably, were able to detect fluorescence within the nuclear compartment (Fig. 5.4A) in embryonic cells following *mNG2(11)* knock-in (Fig. 5.4B, C). *Npm1* fluorescence recapitulated the pattern reported by immunofluorescence (E. J. Vogt et al., 2012), while the observed *Nop58* pattern is novel. These observations indicate that the nuclear envelope does not necessarily present a barrier to fluorescence complementation, in spite of fact that the GOGREEN components lack nuclear localization sequences.

Robust detection of low abundance endogenous proteins

Having observed that the GOGREEN system can detect both cytoplasmic and nuclear proteins, we next tested its performance in reporting transcription factor localization, since there is great interest in imaging transcription factor dynamics in living

preimplantation embryos (B. Gu et al., 2018; McDole et al., 2011; Posfai et al., 2017; Saiz et al., 2013, 2015). We next evaluated CDX2, YAP1, GATA6, and NANOG, four transcription factors with essential activities during preimplantation development (Frum et al., 2018; Mitsui et al., 2003; Schrode et al., 2014; Strumpf et al., 2005). However, we were unable to detect appreciable fluorescent signal in embryos of any of these four *mNG2(11)* knock-ins in the *mNG2(Δ11)* background (Fig. 5.4D and data not shown). We therefore developed a second and alternative knock-in tagging strategy for detecting endogenous transcription factors.

We selected the V5 epitope, a 14 amino acid protein derived from the simian virus 5 (SV5) paramyxovirus because its small size promised high knock-in efficiency and because of the existence of low background, commercially available, monoclonal anti-V5 antibody that could be used for immunofluorescent detection of V5-tagged proteins in embryos. We then designed V5-encoding targeting constructs for generating in-frame V5 fusion proteins (Fig. 5.5A,B).

We targeted the V5 tag in frame with key transcription factors in zygotes, and then observed immunofluorescence patterns in blastocysts by confocal microscopy. We were able to detect V5 signals that were clear and specific after targeting the nuclear factors such as GATA3, CTCF, and NANOG (Fig. 5.5C-E). Importantly, the patterns of V5-tagged GATA3, NANOG, and CTCF recapitulated their reported expression patterns in blastocysts (Home et al., 2009; Marcho et al., 2015; Ralston & Rossant, 2008; Strumpf et al., 2005). In a parallel set of experiments, we harvested embryos prior to blastocyst

stage and then costained these with anti-V5 and anti-NANOG antibodies. In these embryos, we detected NANOG expression in every V5-expressing cell (Supp. Fig. 5.1), confirming the utility of the V5 knock-in approach for faithfully reporting gene expression, even at preimplantation stages prior to blastocyst. These observations highlight the utility of the V5-tagging system to evaluate the endogenous expression patterns of known or novel transcription factors.

Having observed that V5 outperformed the GOGREEN system, in terms of transcription factor detection, we hypothesized that protein abundance could be the limiting factor for detection using the GOGREEN system. Consistent with this hypothesis, we were able to detect the transcription factor CDX2 using GOGREEN when *Cdx2-mNG2(11)* was overexpressed by mRNA injection (Fig. 5.6A,B). Finally, we evaluated the abundance of transcripts encoding proteins evaluated in this study, as measured by RNA sequencing of individual blastocysts (Aksoy et al., 2013). Remarkably, transcript abundance predicted protein detectability using the GOGREEN system (Fig. 5.6C). Moreover, proteins of extremely low abundance could still be detected using the V5 system. This analysis therefore provides a guideline for informing subsequent experimental design and in selecting the optimal protein tagging approach. Ultimately, the GOGREEN and V5 systems together enable detection of endogenous proteins across the range of protein expression levels, facilitating multiple downstream applications, and opening doors for new discoveries.

Section 5.5. Discussion

Split GFP and V5 epitope tagging have been used for protein detection in cell lines and in some animal models (Hefel & Smolikove, 2019; Kamiyama et al., 2016; Kim et al., 2012; Leonetti et al., 2016; To et al., 2016; M. Yamagata & Sanes, 2012; H. Yang et al., 2013), but their use as knock-in mouse reporters has not been systematically compared across diverse genomic loci. Here, we presented a systematic comparison of their performance, sensitivity, and efficiency of endogenous protein reporting. We note that both approaches are similarly efficient, averaging ~60% knock-in efficiency across more than a dozen loci tested. This rate is much higher than targeting full-length fluorescent proteins by zygote injection. For example, we observed a 6% knock-in efficiency at the *Rosa26* locus with the nearly full-length fluorescent protein mNG2(∆11). In fact, we observed upwards of 75-100% knock-in efficiency for multiple loci, which exceeds allele inheritance rates in most mating strategies. Moreover, the relatively short length of the ssODN enables higher efficiency targeting and ease of synthesis, bypassing traditional molecular cloning methods required for producing longer donors. Finally, tagging with GOGREEN and V5 enables efficient detection of endogenous proteins, thereby circumventing artifacts caused by imaging fluorescently tagged, overexpressed proteins.

We note opportunities for applying biochemical and molecular techniques *in vivo*. V5 is commonly used for purifying proteins from cells and tissues for the downstream identification of protein or nucleotide interactions, including immunoprecipitation-western blotting or mass spectrometry, chromatin-immunoprecipitation or ribonucleotide

pulldown and sequencing (ChIP-seq, RIP-seq) or Cleavage Under Targets and Release Using Nuclease (CUT&RUN) (Hainer et al., 2019; Skene & Henikoff, 2017). We therefore envision that the approaches described here could be used to generate stable mouse lines that enable anti-V5 antibody-mediated discovery of protein localization patterns, protein and RNA binding partners and DNA binding sites throughout the genome.

Both GOGREEN and V5 systems present exciting opportunities for biological investigation outside of preimplantation mouse development as well. For example, *V5* or *mNG2(11)* knock-in embryos could be transferred to recipient females to allow for postimplantation development so that protein localization can be evaluated in later developmental processes or in adult tissues and organs. Additionally, both the GOGREEN and V5 systems could be adaptable to viral transduction (Yoon et al., 2018), which could extend applications to adult organs and tissues. Our studies thus provide guidelines, molecular reagents, and genotyping assays to enable these applications.

In considering endogenous protein tagging applications, we identify several key considerations. First, care should be given to the design of the tagged protein, and whether the location and nature of the tag interfere with protein function. Validation for protein function and localization can be confirmed using appropriate strategies, including mouse genetics and, if possible, by confirming protein localization by immunofluorescence. Second, guide RNA design should follow best practices so as to minimize the chance of on/off-target indel alleles; targeting protein c-termini may help

avoid unwanted phenotypes caused by frame-shift mutations. Third, the genotyping strategy should confirm that the tag has been knocked in in-frame with the target protein at the sequence level. Related to this, strategies for identifying random ssODN insertions should be considered (Lanza et al., 2018). Finally, if microinjection is to be used as the delivery method, consultation with institutional transgenic facility with proper technical expertise should be sought, when available to ensure optimal experimental design.

Finally, both the GOGREEN and V5 systems could also be used in embryos from species such as humans or other primates, where breeding to establish knock-in lines is either inappropriate or impractical. There would be additional advantages to applying either system to emerging mammalian models, such as marsupials, where protein-specific antibodies have not yet been developed. For live imaging, *mNG2(Δ11)* could be provided by mRNA injection, while *mNG2(11)* would be knocked in frame into genes of interest. If fixed imaging of low abundance proteins is preferred, then V5 could be knocked in. Either system promises new opportunities for discovery of developmental principles in mouse as well as understudied mammalian species.

Section 5.6. Acknowledgements

We thank Dr Kristin Parent for comments on the manuscript; current and former members of the Ralston Laboratory, especially Dr Michael Halbisen and Dr Tristan Frum, for helpful discussions and training; Axel Schmitter for assistance in the

laboratory; and Drs Elena Demeriva and Huirong Xie at the MSU Transgenic and Genome Editing Facility for the R26 mouse knock-in line.

TABLES

Allele	Forward	Reverse
R26- mNG2(Δ11)	CTGCCCGAGCGGAAAC GCCACTGAC	CCTGGACTACTGCGCCC TACAGA
Krt18- mNG2(11)	GGCTGTTTATAACTAAGG CTTGGTC	GGACAGTCATATCTCCTA CTTCGTC
Krt8- mNG2(11)	TGTGGTTGTGAAGAAGA TTGAAACC	ATACAACTGAATTGGGTT TGGATGG
mNG2(11)- Actb	CCAGCGTTTGCCTTTTAT GGTAATA	CACTCCCAAAGTAACAG GTCACTT
Npm1- mNG2(11)	GGCAACACTGGCCATAA AGTATTTA	CAAACACAGTAGGGAAA GTTCTCAC
mNG2(11)- Nop58	GATATTTTAAGGCCGTCT CTTTCCG	CAACAACTCCATCTCAC CTACCTTA
Ctcf-V5	CAGAATACAGGTGCAAT TGAGAACA	CATCCTTGAAGTTTTCGT TCTCAGT
V5-Gata3	CTTTTGCTAAACTATCCC GCAAAGA	TTGCCTTGACCATCGAT GTTAAAAA
Nanog-V5	CCACTAGGGAAAGCCAT GCGCATTT	GGAAGAAGGAAGGAAC CTGGCTTTGC
Cdx2- mNG2(11)	GAGAGGAAAATCAAGAA GAAGCAGC	GAGGAATCTCTTCTGAG GATTCTCG

Table 5.1. Genotyping primers used in Chapter 5.

Allele	Sequence 5’ to 3’
Krt18-mNG2(11)	T*TCCCAGGGGTTCCCTCCTTCTCTGCCTCACATCATATCGG TAAAGGCCTTTTGCCACTCCTTGAAGTTGAGCTCGGTGCCA GAGCCGTGC CTCAGAACTCTGGTGTCATTAGTCT*C
Krt8-mNG2(11)	G*TGTCCGAGTCTTCTGATGTCGTGTCCAAGGGCTCTGGCA CCGAGCTCAACTTCAAGGAGTGGCAAAAGGCCTTTACCGAT ATGATGTGAA TGGCCACTGAAGTCCTTGCCAGCCT*G
mNG2(11)-Actb	G*ACGACCAGCGCAGCGATATCGTCATCCATGCCACCTCCC ATCATATCGGTAAAGGCCTTTTGCCACTCCTTGAAGTTGAGC TCGGTCATG GCGAACTATCAAGACACAAAAGAAGGCT*A
Npm1-mNG2(11)	C*AAGATCTCTGGCAGTGGAGGAAATCTCTTGGCTCTGGCA CCGAGCTCAACTTCAAGGAGTGGCAAAAGGCCTTTACCGAT ATGATGTAAG AAAAGGGTTTAAACAGTTTGAAATA*T
mNG2(11)-Nop58	C*GCGTAGCGCCGCCCTGACCTGGTCTCATCATGACCGAGC TCAACTTCAAGGAGTGGCAAAAGGCCTTTACCGATATGATG GGAGGTGG CATGTTGGTCCTGTTTGAAACGTCCGTTGG*C
Ctcf-V5	C*CTGAGATGATCCTCAGCATGATGGACCGGGGCTCTGGCG GCAAGCCGATCCCTAACCCTCTGCTGGGCCTGGACAGCAC TTGATGCTG GGGCCTTGCTCGGCACCAGGA*C
V5-Gata3	G*GGCGAGAGGGCGCGAGCACAGCCGAGGACATGGGCAA GCCGATCCCTAACCCTCTGCTGGGCCTGGACAGCACTGGA GGTGGCATGG AGGTGACTGCGGACCAGCCGCGCTG*G
Nanog-V5	A*CTTTAAGCCCAGATGTTGCGTAAGTCTCAAGTGCTGTCCA GGCCCAGCAGAGGGTTAGGGATCGGCTTGCCGCCAGAGCC TATTTCACC TGGTGGAGTCACAGAGTAGT*T
Cdx2-mNG2(11)	C*GCCGCCGCTTCAGACCACGGGAGGGGTCACATCATATCG GTAAAGGCCTTTTGCCACTCCTTGAAGTTGAGCTCGGTGCC AGAGCCCT GGGTGACAGTGGAGTTTAAAACCCCTC*C

Table 5.2. Synthesized ssODN sequences used in Chapter 5. Phosphorothioate bonds (indicated by *) were added during oligo synthesis to enhance oligo resistance to endogenous exonuclease degradation.

Allele	Guide Sequence (5’ to 3’)
R26-mNG(Δ11)	ACTCCAGTCTTTCTAGAAGATGG
Krt18-mNG2(11)	ACCAGAGTTCTGAGGCACTGAGG
Krt8-mNG2(11)	TGATGTCGTGTCCAAGTGAATGG
mNG2(11)-Actb	TGTGTCTTGATAGTTCGCCATGG
Npm1-mNG2(11)	GAGGAAATCTCTTTAAGAAAAGG
mNG2(11)-Nop58	CTGACCTGGTCTCATCATGTTGG
Ctcf-V5	GAGCAAGGCCCCAGCATCACCGG
V5-Gata3	GAGCACAGCCGAGGACATGGAGG
Nanog-V5	CGTAAGTCTCATATTTCACCTGG
Cdx2-mNG2(11)	CAGACCACGGGAGGGGTCACTGG

Table 5.3. CRISPR Guides used in Chapter 5. Underlined sequence = Protospacer Adjacent Motif (PAM).

Purpose	Sequence 5’ to 3’
mNG2(D11) Synthesized dsDNA Fragment	gccagctaggccttgaccaaagttcctctggaattgcgatgcgatcgcggagaattct ccacgcgtcgccaccATGGTGAGCAAGGGTGAGGAGGATAACAT GGCCTCTCTCCCAGCGACTCATGAGTTACACATCTTTGGC TCCATCAACGGTGTGGACTTTGACATGGTGGGTCAGGGTA CCGGCAATCCAAATGATGGTTATGAGGAGTTAAACCTGAA GTCCACCAAGGGTGACCTCCAGTTCTCCCCCTGGATTCTG GTCCCTCATATCGGGTATGGCTTCCATCAGTACCTGCCCTA CCCTGACGGGATGTCGCCTTTCCAGGCCGCCATGGTAGAT GGCTCCGGATACCAAGTCCATCGCACAATGCAGTTTGAAG ATGGTGCCTCCCTTACTGTTAACTACCGCTACACCTACGAG GGAAGCCACATCAAAGGAGAGGCCCAGGTGATGGGGACT GGTTTCCCTGCTGACGGTCCTGTGATGACCAACACGCTGA CCGCTGCGGACTGGTGCATGTCGAAGAAGACTTACCCCA ACGACAAAACCATCATCAGTACCTTTAAGTGGAGTTACACC ACTGTAAATGGCAAACGCTACCGGAGCACTGCGCGGACC ACCTACACCTTTGCTAAGCCAATGGCGGCTAACTATCTGAA GAACCAGCCGATGTACGTGTTCCGTAAGACGGAGCTCAAG CACTCCATGGGAACAGGTGGCGGCGGAAGTTAGagcgatcg cactccaatgccctggatcgcacgcgtaaatgattgcagatccactagttctagag
Clta-mNG2(11) Synthesized dsDNA Fragment for *in vitro* transcription (IVT)	ctagttaagcttgctgtcgccaccATGACCGAGCTCAACTTCAAGGAG TGGCAAAAGGCCTTTACCGATATGATGGGAGGTGGCATGG CCGAGCTTGACCCTTTTGGAGCTCCAGCAGGCGCACCAG GTGGTCCTGCTCTGGGTAATGGTGTTGCCGGGGCAGGTG AGGAAGACCCTGCTGCAGCATTTCTTGCCCAGCAAGAATC TGAGATAGCTGGGATCGAAAATGACGAGGCATTTGCCATT CTCGACGGTGGAGCCCCCGGACCCCAACCTCATGGGGA GCCTCCTGGCGATGCAGTTGACGGGGTTATGAACGGAGA ATACTATCAGGAGTCTAACGGCCCCACAGATAGCTACGCC GCCATATCAGAGGTTGATAGACTTCAATCAGAGCCAGAGA GCATACGAAAATGGCGCGAAGAACAGACCGAGCGATTGG AAGCTCTTGATGCTAACAGTCGCAAGCAAGAAGCCGAATG GAAGGAAAAAGCCATCAAAGAACTGGAGGAATGGTATGCC AGACAGGATGAGCAGTTGCAAAAGACAAAGGCAAATAATA GAGCCGCAGAGGAGGCTTTTGTCAATGATATAGACGAGTC CAGCCCCGGAACCGAGTGGGAACGGGTCGCTAGACTCTG TGATTTCAATCCAAAATCCAGCAAGCAGGCCAAAGACGTG TCACGAATGCGGTCAGTGCTTATCTCATTGAAGCAAGCAC CACTGGTTCATTGAagagccgcggccgctcgact

Table 5.4. dsDNA fragments synthesized for Chapter 5. Coding sequences are capitalized.

Purpose	Sequence 5' to 3'
mNG2(D11) Synthesized dsDNA Fragment for IVT	ctagttaagcttgctgtcgccaccATGGTGAGCAAGGGTGAGGAGGAT AACATGGCCTCTCTCCCAGCGACTCATGAGTTACACATCTT TGGCTCCATCAACGGTGTGGACTTTGACATGGTGGGTCAG GGTACCGGCAATCCAAATGATGGTTATGAGGAGTTAAACCT GAAGTCCACCAAGGGTGACCTCCAGTTCTCCCCCTGGATT CTGGTCCCTCATATCGGGTATGGCTTCCATCAGTACCT GCCCTACCCTGACGGGATGTCGCCTTTCCAGGCCGCCAT GGTAGATGGCTCCGGATACCAAGTCCATCGCACAATGCAG TTTGAAGATGGTGCCTCCCTTACTGTTAACTACCGCTACAC CTACGAGGGAAGCCACATCAAAGGAGAGGCCCAGGTGAT GGGGACTGGTTTCCCTGCTGACGGTCCTGTGATGACCAA CACGCTGACCGCTGCGGACTGGTGCATGTCGAAGAAGAC TTACCCCAACGACAAAACCATCATCAGTACCTTTAAGTGGA GTTACACCACTGTAAATGGCAAACGCTACCGGAGCACTGC GCGGACCACCTACACCTTTGCTAAGCCAATGGCGGCTAAC TATCTGAAGAACCAGCCGATGTACGTGTTCCGTAAGACGG AGCTCAAGCACTCCATGGGAACAGGTGGCGGCGGAAGTT AGagagccgcggccgctcgact
Cdx2-mNG2(11) Synthesized dsDNA Fragment for IVT	ctagttaagcttgctgtcgccaccATGTACGTTTCATACTTGCTGGACA AGGACGTCAGTATGTATCCCAGTAGTGTTCGCCACTCAGG GGGATTGAATTTGGCCCCCCAAAATTTCGTTAGCCCCCCT CAATACCCTGACTATGGCGGCTATCATGTAGCCGCCGCAG CAGCCGCAACTGCTAACTTGGATAGTGCCCAATCTCCCGG GCCCTCCTGGCCAACAGCATACGGGGCTCCCCTCCGAGA AGATTGGAATGGGTATGCTCCTGGGGGTGCAGCAGCAGC AAATGCTGTGGCCCACGGTCTGAATGGGGGCAGTCCTGC TGCCGCTATGGGGTATTCTAGTCCTGCCGAATACCATGCC CATCACCACCCACATCACCATCCACACCATCCCGCCGCCT CTCCATCCTGTGCAAGCGGGCTGCTCCAAACCCTGAACCT CGGACCCCCAGGTCCTGCTGCCACTGCAGCTGCAGAACA ACTCTCACCAAGTGGTCAGCGGCGAAATCTGTGCGAATG GATGCGAAAACCAGCACAACAGTCACTCGGCTCTCAAGTC AAAACCCGCACCAAAGACAAGTACAGGGTCGTTTATACCG ATCATCAGCGGTTGGAACTGGAGAAAGAGTTCCATTTTAG CAGGTATATAACTATTCGACGCAAATCTGAGCTTGCTGCAA CTTTGGGGTTGTCAGAGCGGCAAGTTAAGATCTGGTTTCA AAACCGACGAGCTAAGGAAAGAAAAATTAAGAAAAAGCAA CAACAACAGCAGCAACAGCAACAGCAGCAACCCCCCCAA CCTCCTCCACAGCCATCCCAACCACAGCCAGGGGCATTG CGCAGTGTACCTGAGCCATTGAGCCCAGTGACCAGCCTC CAGGGTTCTGTACCAGGAAGCGTTCCCGGTGTGCTGGGG CCCGCTGGTGGCGTGCTTAACTCAACAGTGACACAGGGC TCTGGCACCGAGCTCAACTTCAAGGAGTGGCAAAAGGCC TTTACCGATATGATGTGAagagccgcggccgctcgact

Table 5.4. (cont'd).

Gene Targeted	Tag	Cas9 RNP (ng/μL)	ssODN (ng/μL)
Krt8	mNG2(11)	100	20
Actb	mNG2(11)	100	20
Krt18	mNG2(11)	100	20
Nop58	mNG2(11)	100	20
Npm1	mNG2(11)	100	10
Ctcf	V5	25	5
Gata3	V5	100	20
Nanog	V5	100	20

Table 5.5: Concentrations of Cas9 RNP and ssODN used for targeting each gene in Chapter 5.

FIGURES

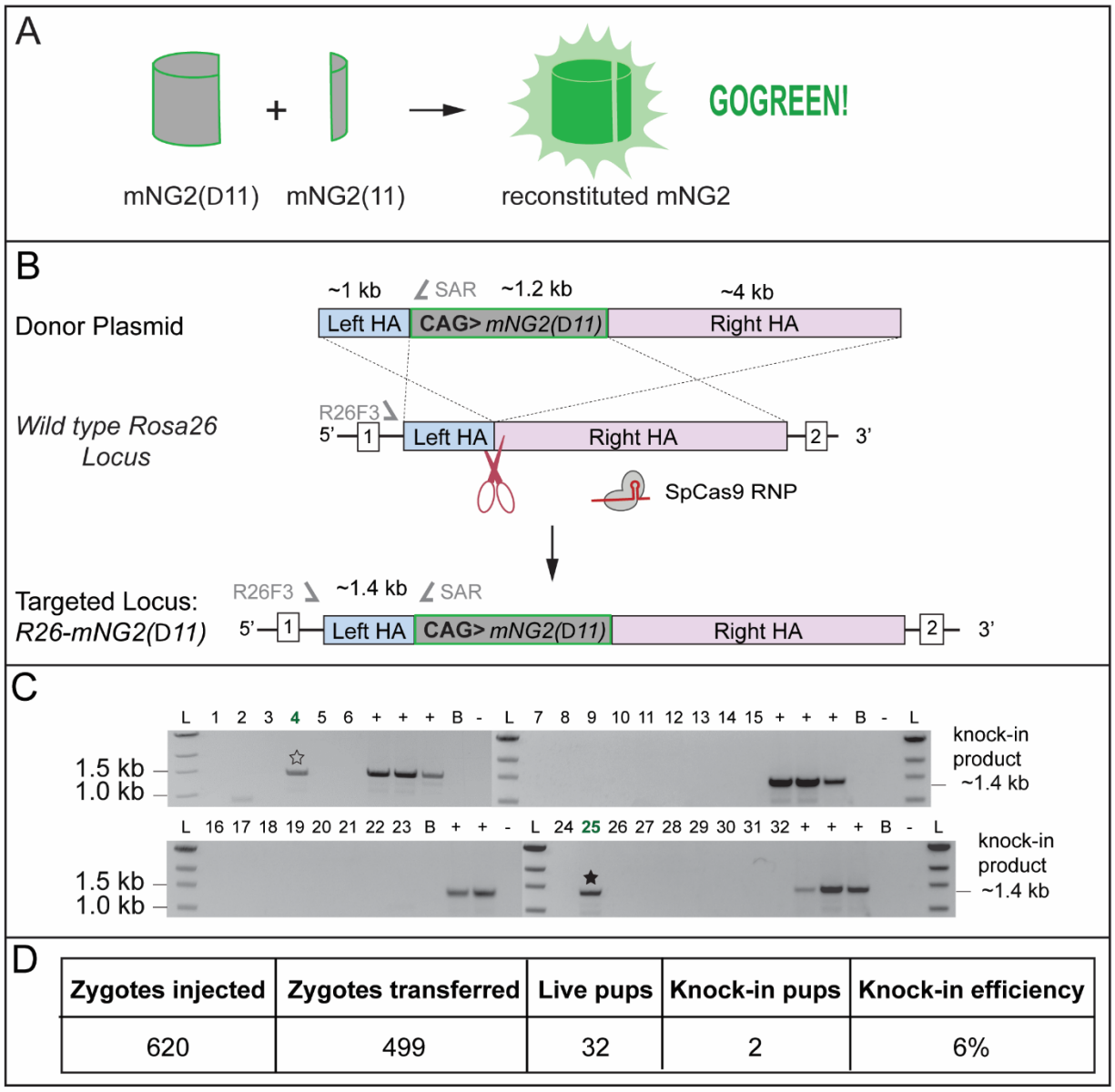

Zygotes injected	Zygotes transferred	Live pups	Knock-in pups	Knock-in efficiency
620	499	32	2	6%

Figure 5.1. A mouse line for fluorescence complementation *in vivo*. (A) Deletion of mNG2(11), the 11th beta-strand of the fluorescent protein mNeonGreen2 (mNG2), eliminates its fluorescent properties. However, complementation by co-expression of *mNG2(Δ11)* and the 11th beta-strand *mNG2(11)* enables non-covalent association of the two proteins and reconstitution of the mNG2 fluorescent properties. (B) Strategy for CRISPR/Cas9 knock-in of the *mNG2(Δ11)* expression construct into the mouse *Rosa26 (R26)* locus. Sequence of single-guide RNA (sgRNA), location of genotyping primers (*R26F3* and *SAR*) and predicted Cas9 cut site are shown. HA, homology arm; RNP, ribonucleoprotein. (C) PCR genotyping of tail tip biopsies from offspring born following zygote injection of CRISPR/Cas9 reagents to target the *CAG-mNG2(Δ11)* expression construct to the R26 locus in zygotes.

Figure 5.1 (cont'd).
Successful homologous recombination suggested by PCR amplification of a 1.389 kb band from genomic DNA. B, C57BL/6 wild-type genomic DNA; L, DNA ladder; +, positive control (targeted embryonic stem cells); −, negative control (no DNA template). Numbers indicate individual mice screened by PCR; stars indicate potential founders (D) Summary of *R26* targeting with *mNG2(Δ11)* expression construct.

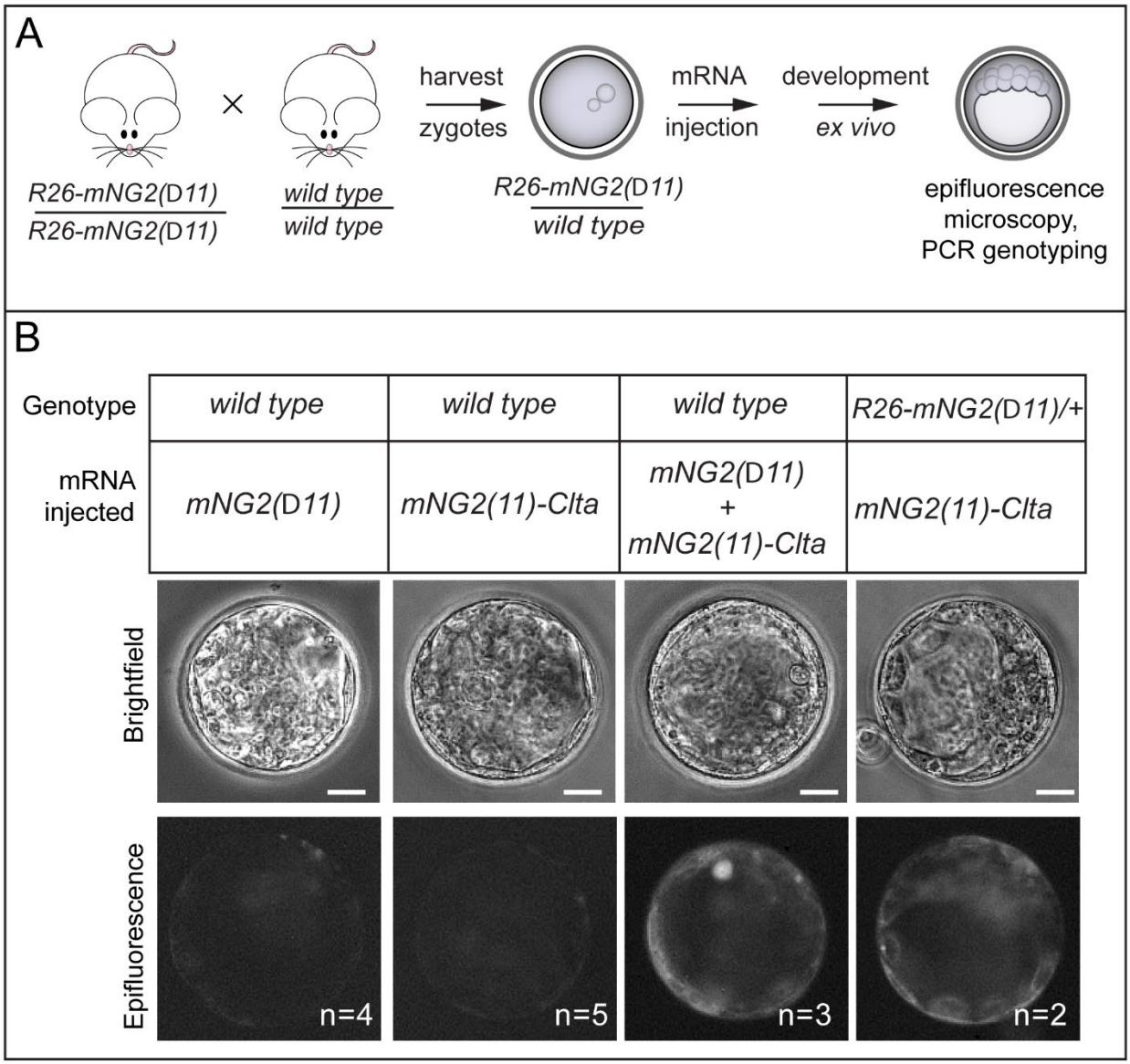

Figure 5.2. Fluorescence complementation *in vivo* using the GOGREEN system. (A) Strategy for testing fluorescent complementation in early embryos. Zygotes carrying *mNG2(Δ11)* were harvested and then injected with mRNA encoding mNG2(11)-tagged clathrin (CLTA). Zygotes were subsequently cultured *ex vivo* to later stages and fluorescence examined in individual embryos. Individual embryo genotypes were determined by PCR. In control experiments, zygotes were produced harvested from wild-type parents. (B) Fluorescence reconstitution can be detected by epifluorescence. Negative controls, wild type embryos injected with mRNA encoding only *mNG2(Δ11)* or *mNG2(11)*-tagged *Clta* exhibit background levels of fluorescence (columns 1 and 2); positive control, wild-type embryos co-injected with *mNG2(Δ11)* and *mNG2(11)-Clta* exhibit reconstituted fluorescence (column 3); test of *R26-mNG2(Δ11)* mice, heterozygous knock-in embryos injected with mRNA encoding *R26-mNG2(11)-Clta* also exhibit reconstituted fluorescence above background (column 4). n, number of embryos evaluated in the experiment. Scale bars: 20 μm.

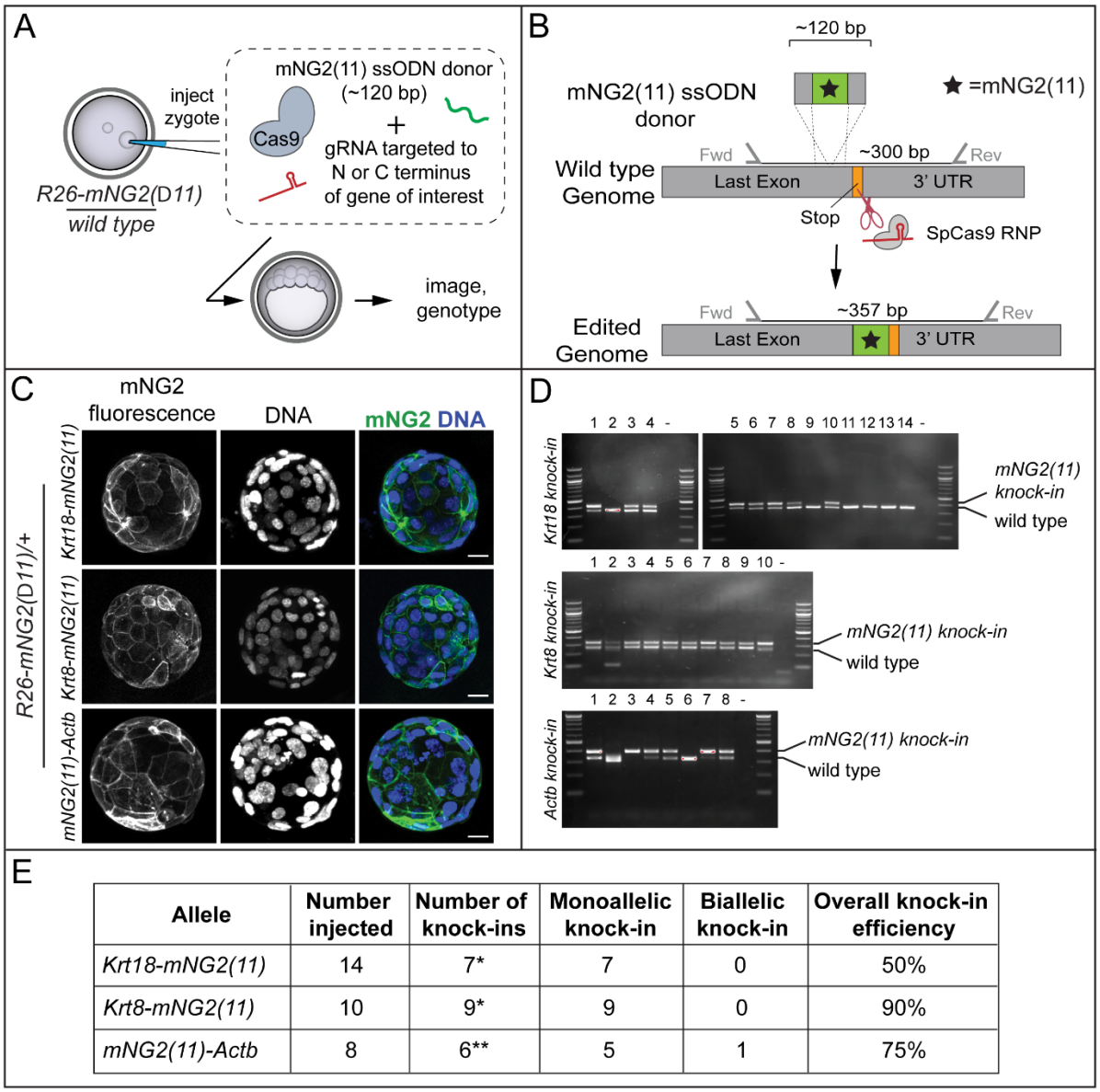

E

Allele	Number injected	Number of knock-ins	Monoallelic knock-in	Biallelic knock-in	Overall knock-in efficiency
Krt18-mNG2(11)	14	7*	7	0	50%
Krt8-mNG2(11)	10	9*	9	0	90%
mNG2(11)-Actb	8	6**	5	1	75%

Figure 5.3. The GOGREEN system enables detection of endogenous proteins. (A) Experimental design: *R26-mGN2(Δ11)/+* knock-in zygotes (generated per cross shown in Fig. 5.2A) are injected with CRISPR/Cas9 targeting reagents to knock *mNG2(11)* into loci of interest, in frame with target proteins. Embryos are then cultured *ex vivo*, imaged and genotyped to evaluate the efficiency of *mNG2(11)* knock-in. gRNA, guide RNA; ssODN, single-stranded oligodeoxyribonucleotide. (B) Overview of strategy for targeting *mNG2(11)* to genomic loci to produce fusion proteins. (C) The GOGREEN system enables detection of endogenous cytoskeletal proteins including intermediate filaments KRT18, KRT8 and ACTB. Note that 100% of embryos inherited *R26-mNG2(Δ11)*. Scale bars: 20 μm. Sample sizes in E. (D) PCR genotyping of embryos, including those shown in C, to identify which embryos were successful *mNG2(11)* knock-ins.(E) Summary of *mNG2(11)* knock-in results observed for the three loci shown. *, one additional embryo presented the knock-in genotype, but not the expected fluorescent phenotype; **, one additional embryo presented the fluorescent phenotype, but not the expected genotype.

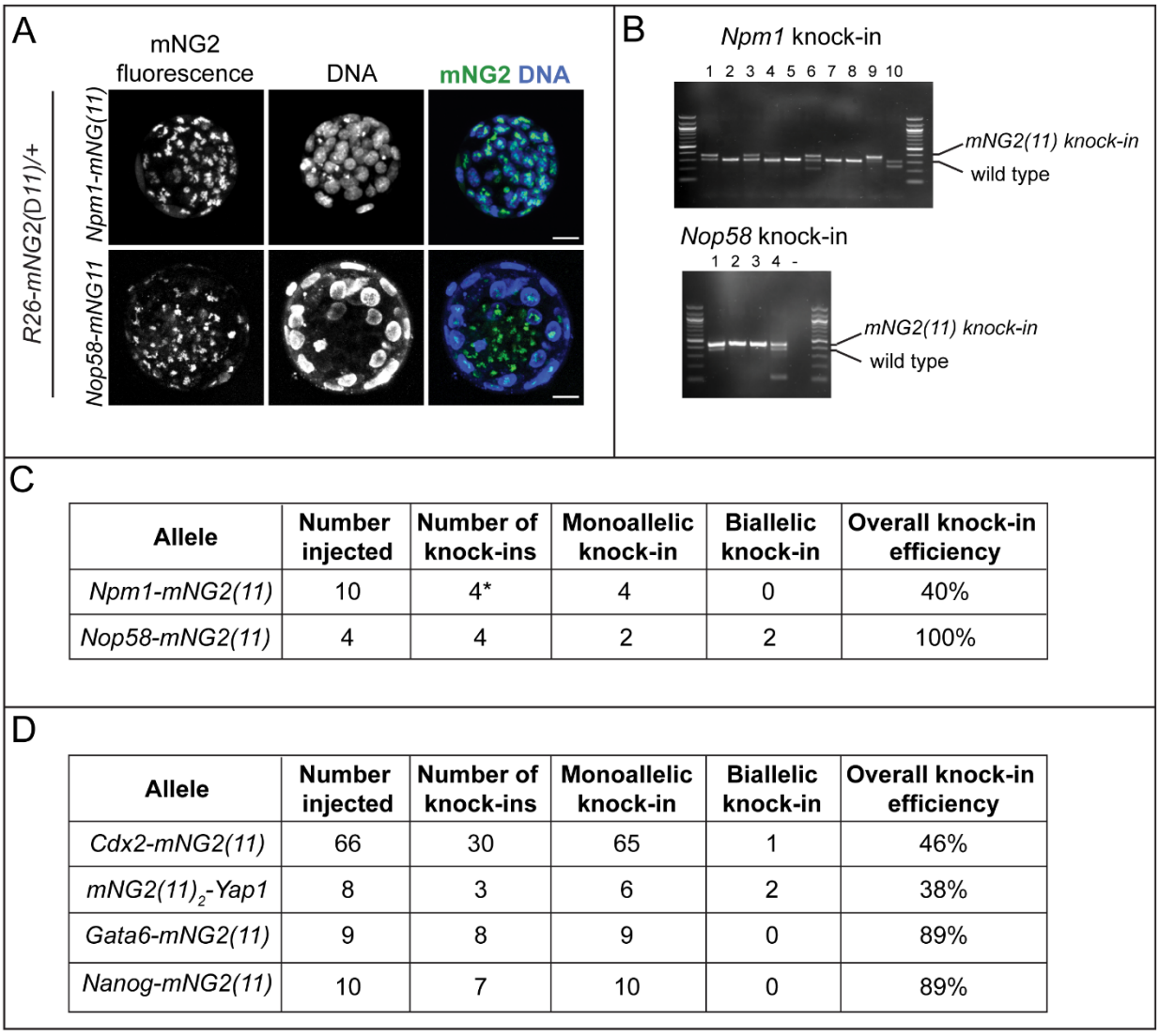

C

Allele	Number injected	Number of knock-ins	Monoallelic knock-in	Biallelic knock-in	Overall knock-in efficiency
Npm1-mNG2(11)	10	4*	4	0	40%
Nop58-mNG2(11)	4	4	2	2	100%

D

Allele	Number injected	Number of knock-ins	Monoallelic knock-in	Biallelic knock-in	Overall knock-in efficiency
Cdx2-mNG2(11)	66	30	65	1	46%
mNG2(11)$_2$-Yap1	8	3	6	2	38%
Gata6-mNG2(11)	9	8	9	0	89%
Nanog-mNG2(11)	10	7	10	0	89%

Figure 5.4. The GOGREEN system can report endogenous protein localization in the nucleus. (A) In the *R26-mNG2(Δ11)* background, knock-in of *mNG2(11)* in frame with the coding regions of two different nuclear proteins demonstrates fluorescent reconstitution of mNG2 and localization within nuclei. Scale bars: 20 μm. Sample sizes in C and D. (B) PCR genotyping to confirm knock-in of *mNG2(11)* into indicated loci for individual embryos, including those shown in A. (C) Efficient knock-in of nuclear proteins shown in A and B. *, one additional embryo presented the fluorescent phenotype but not the expected genotype. (D) Summary of *mNG2(11)* knock-in efficiencies, as determined by PCR genotyping, that were undetectable using the GOGREEN system.

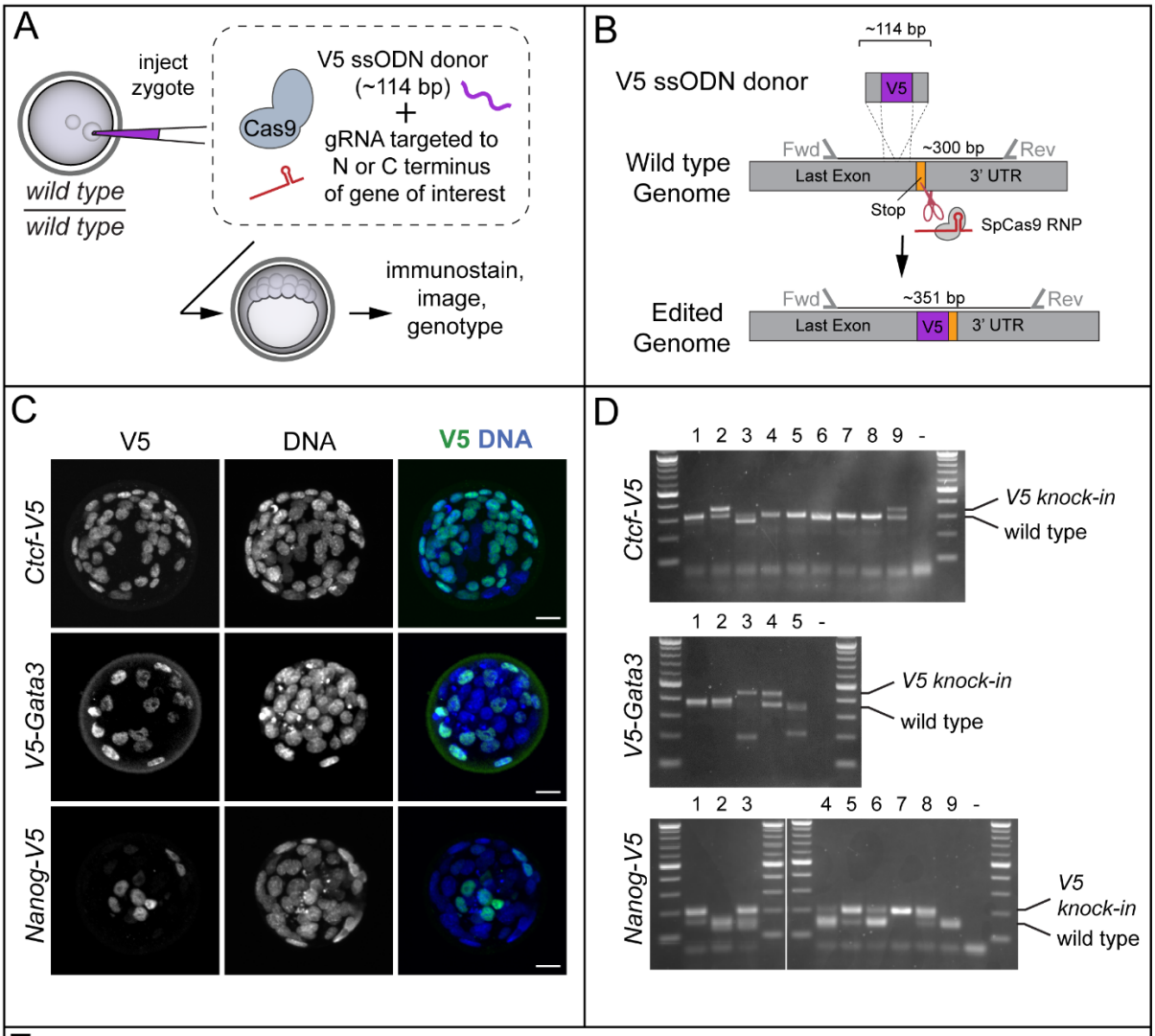

E

Allele	Number injected	Number of knock-ins	Monoallelic knock-in	Biallelic knock-in	Overall knock-in efficiency
Ctcf-V5	9	2	2	0	22%
V5-Gata3	5	2	2	0	40%
Nanog-V5	9	6*	5	1	66%

Figure 5.5. A V5-based system for the detection of diverse transcription factors with a single antibody. (A) Strategy for knocking the V5-encoding gene into loci of interest in wild-type zygotes, to enable streamlined detection of diverse endogenous proteins with a monoclonal anti-V5 antibody. (B) Overview of V5 targeting strategy. (C) Examples of proteins detected as V5 fusion proteins, following knock-in as illustrated in A and B. Scale bars: 20 μm. Sample sizes in E. (D) PCR genotyping of embryos to confirm V5 knock-in at indicated genomic loci, including those shown in C. (E) Summary of V5 knock-in efficiency at indicated loci. *, one additional embryo presented the knock-in genotype, but not the expected fluorescent phenotype.

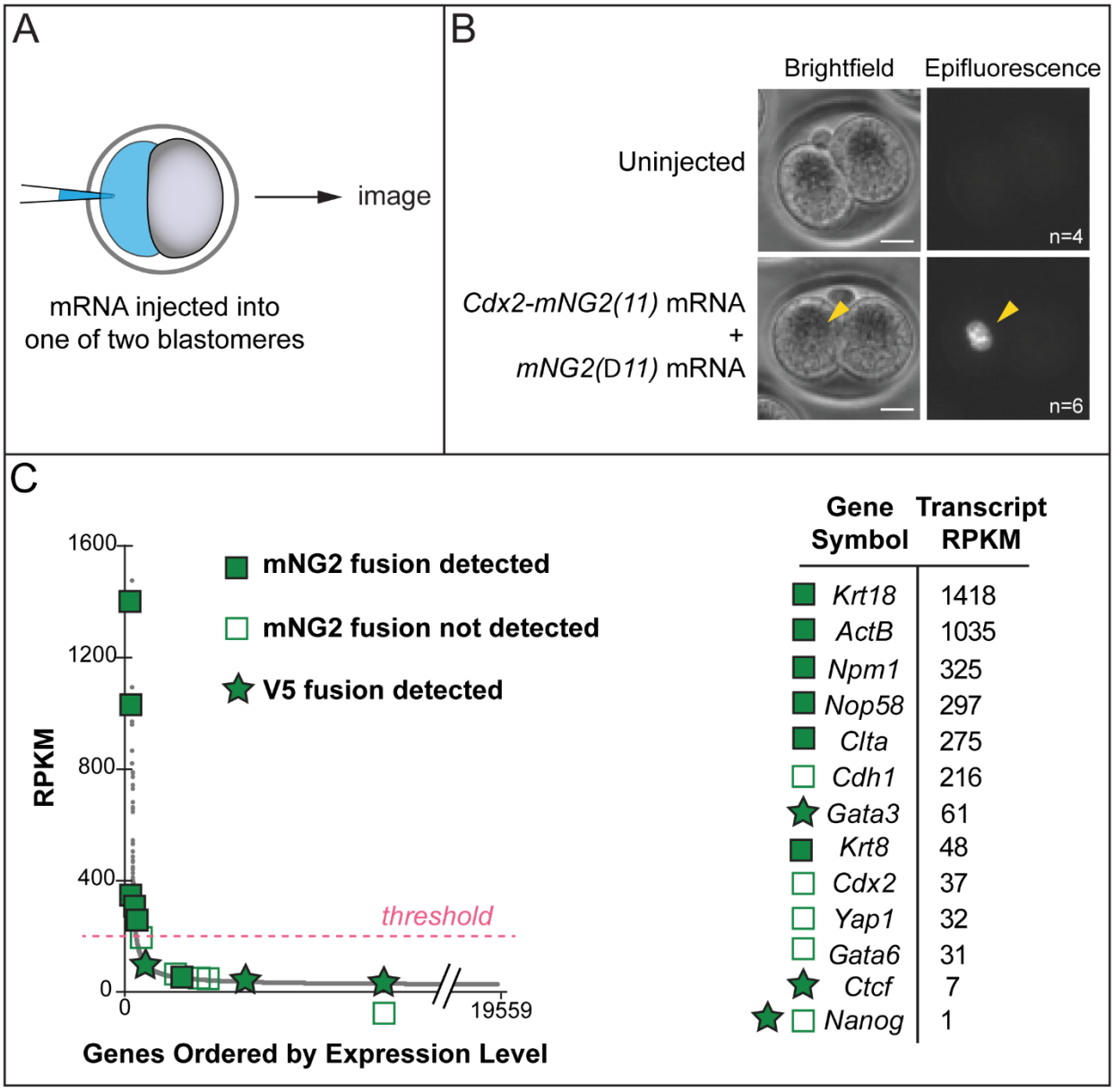

Figure 5.6. Complementary systems enable detection of endogenous proteins over a range of expression levels. (A) Overview of experimental design: mRNA injection into one of two blastomeres of the early mouse embryo, followed by imaging. (B) Overexpression of mRNAs encoding *mNG2(Δ11)* and *Cdx2-mNG2(11)* leads to reconstituted fluorescence in the nucleus of the injected blastomere. n, number of embryos presenting the phenotype shown. Scale bars: 20 μm. (C) Relative abundance of endogenous mRNAs encoding tagged proteins, as measured by RNA-seq (Aksoy et al., 2013), and detection results using GOGREEN or V5 systems. Each gray dot indicates a unique gene transcript. RPKM, reads per kilobase per million reads. For all genes shown, *mNG2(11)* or V5 knock-in was confirmed by PCR.

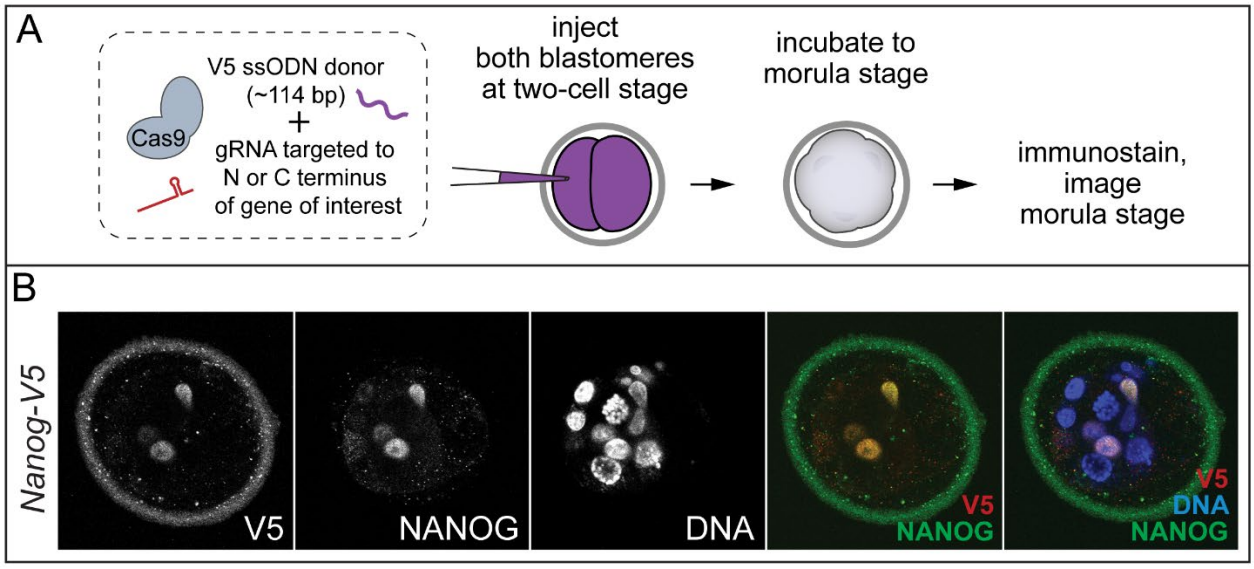

Supplemental Figure 5.1. NANOG-V5 is detected in NANOG-expressing cells. A) Experimental design. **B)** Immunofluorescent detection of V5 and NANOG in embryos prior to the blastocyst stage (n =3).

CHAPTER 6.

FLUORESCENT REPORTERS DISTINGUISH STEM CELL COLONY SUBTYPES DURING SOMATIC CELL REPROGRAMMING

Alexandra Moauro[1,2], Robin E. Kruger[3,4], Daniel O'Hagan[5], and Amy Ralston[4,5].

1) Molecular, Cellular and Integrative Physiology Ph.D. Program, Michigan State University, East Lansing, MI, 48824

2) D.O.-Ph.D. Program, Michigan State University, East Lansing, MI, 48824

3) Cell and Molecular Biology Ph.D. Program, Michigan State University, East Lansing, MI, 48824

4) Reproductive and Developmental Sciences Program, Michigan State University, East Lansing, MI, 48824

5) Department of Biochemistry and Molecular Biology, Michigan State University, East Lansing, MI, 48824

This chapter is modified from Moauro *et al.,* published in *Cellular Reprogramming* on December 12, 2022.

This study was supported by the National Institutes of Health R35 GM131759 and T32 HD087166.

Section 6.1. Abstract

Somatic cell reprogramming was first developed to create induced pluripotent stem (iPS) cells. Since that time, the highly dynamic and heterogeneous nature of the reprogramming process has come to be appreciated. Remarkably, a distinct type of stem cell, called induced extraembryonic endoderm stem (iXEN) cells, also form during reprogramming of mouse somatic cells by ectopic expression of the transcription factors OCT4, SOX2, KLF4, and MYC (OSKM). The mechanisms leading somatic cells to adopt differing stem cell fates are challenging to resolve given that formation of either stem cell type is slow, stochastic, and rare. For these reasons, fluorescent gene expression reporters have provided an invaluable tool for revealing the path from the somatic state to pluripotency. However, no such reporters have been established for comparable studies of iXEN cell formation. In this study we examined the expression of multiple fluorescent reporters, including *Nanog*, *Oct4*, and the endodermal genes *Gata4*, and *Gata6* – alone, and in combination, during reprogramming. We show that only the simultaneous evaluation of *Nanog* and *Gata4* reliably distinguishes iPS and iXEN cell colonies during reprogramming.

Section 6.2. Introduction

Since the initial report that somatic cells can be reprogrammed to induced pluripotent stem (iPS) cells (Takahashi & Yamanaka, 2006), much interest has focused on how to distinguish iPS cell colonies from undesirable colonies, such as partially reprogrammed cell colonies (Buganim et al., 2012; E. M. Chan et al., 2009; Mikkelsen et al., 2008; Sridharan et al., 2009; Velychko et al., 2019). We and others have reported that cells

expressing endodermal genes arise during reprogramming of mouse and human somatic cells (Guan et al., 2022; He et al., 2020; Parenti et al., 2016; Schiebinger et al., 2019; Y. Zhao et al., 2015). Moreover, viral transduction of pluripotency transcription factors *Oct4*, *Sox2*, *Klf4*, and *Myc* (*OSKM*) leads to formation of stable induced extraembryonic endoderm (iXEN) stem cell lines in murine and canine fibroblasts (Nishimura et al., 2017; Parenti et al., 2016). Unlike partially reprogrammed cells, iXEN cells are capable of unlimited proliferation and lineage-specific differentiation, and therefore meet both criteria of authentic stem cell lines. However, little is known regarding the mechanisms that guide alternative reprogramming outcomes, nor how to distinguish iPS cells and iXEN cells during the reprogramming process.

Fluorescent reporters, such as knock-in reporters of endogenous *Oct4* or *Nanog* expression, are commonly used for quantifying reprogramming efficiencies (Brambrink et al., 2008; Buganim et al., 2012; Dos Santos et al., 2014; Huangfu et al., 2008; Judson et al., 2009; Pour et al., 2015; Y. Shi et al., 2008; Tsubooka et al., 2009; Xiao et al., 2016; X. Y. Zhao et al., 2009). In this application, the number or proportion of fluorescent colonies is often reported. However, the expression of these reporters has not been evaluated in the context of iXEN cells. This seems important especially given that *Oct4* is associated with both pluripotent and extraembryonic endodermal lineages during embryogenesis (Frum et al., 2013; Le Bin et al., 2014; Palmieri et al., 1994) and is a component of the transcription factor cocktails that produce iXEN cells (Nishimura et al., 2017; Parenti et al., 2016). Conversely, a fluorescent reporter that specifically labels iXEN cell colonies during reprogramming has not been identified.

The identification of fluorescent reporters to reliably distinguish iPS and iXEN cell colonies would enable new approaches to the discovery of the mechanisms underlying the reprogramming process. To identify specific fluorescent reporters requires a more systematic evaluation of the expression and co-expression of pluripotency and endodermal gene expression reporters over the course of somatic cell reprogramming. We therefore evaluated the expression dynamics of fluorescent reporters of the transcription factors important for pluripotency (OCT4 and NANOG) and extraembryonic endoderm (GATA6 and GATA4), in conjunction with colony morphology, during mouse somatic cell reprogramming. We chose to focus on these transcription factors because they are all involved in the earliest stages of segregating pluripotent and endodermal cell fates during development (Artus & Hadjantonakis, 2012; Bassalert et al., 2018; Frum & Ralston, 2015).

Section 6.3. Materials and Methods

Mouse Lines

All animal research was conducted in accordance with the guidelines of the Michigan State University Institutional Animal Care and Use Committee. The following alleles were maintained in a CD-1 background: *Gata4*$^{H2B\text{-}eGFP}$ (Simon et al., 2018), *Gata6*^{tm1Hadj} (Freyer et al., 2015), *Pou5f1*^{tm2Jae} (Lengner et al., 2007), and *Nanog*^{mCherry} (reported here).

The *Nanog*^{mCherry} mouse was created via a CRISPR/Cas9-mediated knock-in of *mCherry* immediately downstream of, and in frame with, the *Nanog* coding region using

a published donor plasmid (Addgene 59995) (H. Yang et al., 2013). CAS9 protein and guide RNA (5'CGTAAGTCTCATATTTCACC-3') (50-200 ng/µl), and circular donor plasmid (5-20 ng/µl) were injected into C57Bl/6 zygotes, which were then transferred to pseudo-pregnant female mice. Offspring were then screened by *Nanog* locus-specific PCR ('5-TACCACCATGCCAGGCTGAGAATGT-3' and 5'-TCAACAGGGAGAAGTTAGTGGCGCT-3'). Using this approach, a 2,105 bp PCR product can only be generated if homologous recombination has occurred between the donor plasmid's upstream homology arm and the Nanog locus and 9 of 22 offspring were positive using this criterion, for an overall knock-in efficiency of ~40%. The *Nanog* locus of a single founder mouse was confirmed by sequencing. The *Nanog*^{mCherry} mouse line was maintained in a CD-1 background.

Immunofluorescence and Confocal Microscopy

Mice carrying *Nanog*^{mCherry} were naturally mated, and then embryos were obtained from pregnant moms around embryonic day (E) E3.75. Embryos were then processed for immunofluorescence as previously described (O'Hagan et al., 2021), using the following reagents: goat-anti-SOX17 (1:2000, R&D, AF1924), goat-anti-SOX2 (1:2000, Neuromics, GT15098), donkey-anti-goat Alexa488 (1:400, Invitrogen, A-11055), and DRAQ5 (1:400, Cell Signaling Technology, 4084). Embryos were imaged using an Olympus FluoView FV1000 Confocal Laser Scanning Microscope system with a 20x UPlanFLN objective (0.5 NA) and 3x digital zoom. For each embryo, z-stacks were collected with 5-µm intervals between optical sections. Optical sections are displayed as an intensity projection over the z-axis.

Cell lines and cellular reprogramming

R1 ES cell lines (ATCC, SCRC-1011) and XEN cell lines (derived in-house from CD-1 blastocysts) were cultured in the presence of MEFs and Leukemia Inhibitory Factor (LIF) as previously described (Blij et al., 2015; Moauro & Ralston, 2022; Parenti et al., 2016). To derive MEF lines, mice carrying one or more fluorescent reporter alleles were naturally mated, and then embryos were collected from pregnant females at E13.5. MEF lines were established and genotyped from individual E13.5 embryos as previously described (Moauro & Ralston, 2022). Cellular reprogramming was achieved using the modified Moloney Murine Leukemia Virus (MMLV) retrovirus as previously described (Moauro & Ralston, 2022). pMXs plasmids expressing *Oct4*, *Klf4*, *Sox2* or *Myc* cDNAs were obtained from Addgene (13366, 13367, 13370, and 13375). Throughout reprogramming, expression of fluorescent markers was detected using a Lumen Prior 200 camera and Leica microscope. Our reprogramming efficiency ranged from 0.44-0.63% +/- 0.025% (total colonies per MEFs plated).

The Nanog-mCherry knock-in ES cell line was generated by electroporation of ES cells with a plasmid carrying *Nanog-2A-mCherry* (Addgene, p59995) and pSpCas9(BB)-2A-Puro (Addgene, pX459), which was modified to carry the *Nanog* guide RNA and then cultured in the presence of 1.25 µg/mL puromycin (Gibco A1113803). Fluorescent colonies were isolated, expanded, and then PCR screened as described above.

RNA isolation and qPCR

RNA was harvested using 1:6 chloroform to Trizol (Invitrogen), and then 1 µg RNA was reverse transcribed to create cDNA using QuantiTect Reverse Transcription Kit (Qiagen), following manufacturer instructions. For qPCR, cDNA was amplified in quadruplicate using transcript-specific primers (Table 6.1) and quantified on Lightcycler 480 (Roche). Primer amplification efficiencies were determined empirically by generating a standard curve using extraembryonic endoderm (XEN) cells and embryonic stem (ES) cell cDNA libraries.

Section 6.4. Results

The making of a *Nanog-2A-mCherry* fluorescent reporter mouse line

Our goal was to determine whether *Nanog*, together with other reporters, reliably distinguish iPS and iXEN cells during reprogramming (Fig. 6.1A). Because only *GFP*-like reporters of many different genes are available, we first created a new *Nanog-mCherry* mouse line (Supp. Fig. 6.1) that would enable the simultaneous evaluation of multiple fluorescent reporters. To evaluate the specificity of this reporter for the pluripotent lineage, we examined blastocysts carrying *Nanog-mCherry* at embryonic day E3.75. At this stage, embryos possess pluripotent and non-pluripotent cell types, including the pluripotent epiblast and the primitive endoderm (progenitors of XEN cells) (Chazaud et al., 2006; Kunath et al., 2005). Indeed, we observed expression of NANOG-mCherry only in epiblast cells, and not within the non-pluripotent cell types (Supp. Fig. 6.1C). Moreover, NANOG-mCherry was detected in embryonic stem (ES)

cells, but not in differentiated ES cells (Supp. Fig. 6.1D). We therefore conclude that the *Nanog*^{mCherry} allele is a faithful reporter of endogenous *Nanog* expression.

Nanog-mCherry and *Oct4-eGFP* do not reliably identify iPS cell colonies

Next, we evaluated the expression of NANOG-mCherry during reprogramming. We reprogrammed mouse embryonic fibroblasts (MEFs) carrying one allele of *Nanog-mCherry* by retroviral delivery of OSKM, and then tracked colony morphology and fluorescence. During reprogramming, presumptive iPS cell colonies appear as round, compact colonies with smooth borders (Meissner et al., 2007). Using these criteria, we first determined that around 20% of all observable colonies possessed morphological features of iPS cell colonies staring around day 8, and at three-day intervals until day 20 (Fig. 6.1B). We next quantified the proportion of colonies expressing NANOG-mCherry, with the expectation that if *Nanog* is a specific reporter of iPS cell colonies, then the proportion of fluorescent colonies should be equivalent to the proportion of morphologically-apparent iPS cell colonies. However, at several points, the proportion of NANOG-mCherry-expressing colonies appeared to be greater than the proportion of colonies that morphologically resembled iPS cell colonies (Fig. 6.1B), suggesting that *Nanog* is expressed in non-iPS cell colonies during reprogramming. We therefore evaluated the expression of NANOG-mCherry in non-iPS cell colonies, including iXEN colonies.

As we previously reported, presumptive iXEN colonies appear flatter and more spread, with less defined borders than iPS cells (Moauro & Ralston, 2022; Parenti et al., 2016).

Additionally, we observed a third type of colony that displayed morphological features of both iPS and iXEN cell colonies, which we termed Mixed colonies. Mixed colonies possessed domed, smooth-edged, iPS cell-like clusters, which cascaded into flatter, rough-edged, iXEN cell-like colonies (Fig. 6.1C). Consistent with our prior observations, we observed that NANOG-mCherry expression was not always restricted to presumptive iPS cell colonies, but was also observed in presumptive iXEN and Mixed colonies (Fig. 6.1C-D) during reprogramming. However, NANOG-mCherry was expressed evenly throughout presumptive iPS cell colonies, while NANOG-mCherry was observed in diffuse patches of presumptive iXEN cell and Mixed colonies (Fig. 6.1D). Moreover, expression of NANOG-mCherry was largely restricted to iPS cell-like regions of the Mixed colonies during reprogramming. To evaluate the expression of NANOG-mCherry within stable iPS and iXEN cell lines, we manually picked presumptive iPS and iXEN colonies and derived stable cell lines as previously described (Parenti et al., 2016; Takahashi & Yamanaka, 2006). Ultimately, iPS cell lines expressed NANOG-mCherry, while iXEN cell lines did not (Fig. 6.1E). These stem cell lines also expressed appropriate markers (Fig. 6.1F), authenticating their identities as iPS or iXEN cell lines, and confirming the validity of our morphological criteria for selecting stem cell colony subtypes. Taken together, these observations indicate that while *Nanog*-mCherry is detected in established iPS cell lines, it is also detected in cells that do not appear to be part of iPS cell colonies during reprogramming. This observation underscores the importance of using both morphology and fluorescence to identify emerging iPS cell colonies.

Finally, we asked whether the combined use of two pluripotency reporters could more reliably identify iPS cell colonies during reprograming than *Nanog*^{mCherry} alone. We reprogrammed MEFs carrying alleles of both *Oct4-eGFP* (Lengner et al., 2007), and *Nanog-mCherry* as before. Overall, we observed concordance between the proportion of morphologically apparent iPS cells and eGFP/mCherry double-positive colonies (Fig. 6.2A). However, closer examination revealed that double-positive cells were present in all three colony types (Fig. 6.2B-C). Interestingly, OCT4-eGFP and NANOG-mCherry appeared to be coexpressed within individual cells of the double-positive colonies (Fig. 6.2B). Our observations indicate that these pluripotency markers label cells that are not part of presumptive iPS cells colonies and/or that colony subtypes are potentially highly heterogeneous.

Gata6-H2B-Venus is expressed in multiple colony subtypes during reprogramming

Because our previous results suggested that pluripotency reporters alone are not sufficient to distinguish iPS and iXEN cell colonies during reprogramming, we next sought to identify a reliable reporter for iXEN cell fate. In the embryo, GATA6 is considered to be one of the earliest-acting regulators of extraembryonic endoderm development (Artus et al., 2011; Chazaud et al., 2006; Koutsourakis et al., 1999; Morrisey et al., 1996; Schrode et al., 2014). Additionally, GATA6 is sufficient to induce an extraembryonic endoderm phenotype in ES cells (Capo-Chichi et al., 2005; Fujikura et al., 2002; Shimosato et al., 2007; Wamaitha et al., 2015). These observations suggest that GATA6 could be a marker of XEN cell fate during somatic cell

reprogramming. A mouse knock-in line carrying *Gata6-H2B-Venus* has been established, and Venus was observed within extraembryonic endoderm lineages (Freyer et al., 2015). We therefore evaluated the expression of GATA6-H2B-Venus during reprogramming of MEFs carrying *Gata6-H2B-Venus*.

We began by quantifying the proportion of presumptive iXEN colonies present throughout reprogramming, using morphological criteria defined above (Fig. 6.3A). Next, we quantified the proportion of all colonies in which GATA6-H2B-Venus was detected. Starting around day 14, we observed expression of GATA6-H2B-Venus in 10-20% of all colonies (Fig. 6.3A), suggesting that not all presumptive iXEN cell colonies express GATA6-H2B-Venus.

We next evaluated the expression of GATA6-H2B-Venus within iPS, Mixed, and iXEN cell colonies. Surprisingly, GATA6-H2B-Venus was expressed diffusely in all three colony types (iPS, iXEN and Mixed), localizing to subsets of cells within each colony subtype (Fig. 6.3B-C). To test whether GATA6-H2B-Venus eventually becomes restricted to iXEN cell lines, presumptive iPS and iXEN cell colonies were picked and passaged to create stable cell lines. After passaging, all cell lines maintained appropriate morphologies (Fig. 6.3D) and expression of key lineage-determining genes (Fig. 6.3E). Notably, GATA6-H2B-Venus was only expressed in some iXEN cell lines, despite qPCR evidence of *Gata6* expression (Fig. 6.3D-E). These observations are consistent with the observation that *Gata6-H2B-Venus* was not detected in all extraembryonic endoderm cells during development (Freyer et al., 2015). For these

reasons, we conclude that *Gata6-H2B-Venus* may not be useful for distinguishing stem cell colony subtypes during reprogramming.

Gata4-H2B-eGFP is expressed in iXEN and not iPS cell colonies

Like GATA6, the closely-related factor GATA4 is also thought to play an essential and instructional role in extraembryonic endoderm development *in vivo* and in ES cell lines (Artus et al., 2011; Capo-Chichi et al., 2005; Fujikura et al., 2002; Kuo et al., 1997; Molkentin et al., 1997; Shimosato et al., 2007). The *Gata4-H2B-eGFP* reporter has been shown to faithfully recapitulate expression of *Gata4* during development (Simon et al., 2018). During reprogramming of MEFs carrying the *Gata4-H2B-eGFP* allele, we observed expression of GATA4-H2B-eGFP in very few colonies (Fig. 6.4A). However, GATA4-H2B-eGFP was only detected in presumptive iXEN and Mixed colonies, and not in iPS cell colonies (Fig. 6.4B-C), indicating that GATA4-H2B-eGFP may be more informative than GATA6-H2B-Venus for identifying presumptive iXEN cells during reprogramming.

However, like GATA6-H2B-Venus, GATA4-H2B-eGFP was detected non-uniformly throughout presumptive iXEN and Mixed colonies, raising questions about the fidelity of this marker and the identity of the GATA4-H2B-eGFP-positive cells within these colonies. To investigate this further, presumptive iXEN colonies were picked and passaged to create stable cell lines. Encouragingly, all iXEN cell lines expressed GATA4-H2B-eGFP in conjunction with appropriate morphology and gene expression (Fig. 6.4D-E). Moreover, all iXEN cell lines carrying an allele of *Gata4-H2B-eGFP*

expressed GATA4-H2B-eGFP by passage 5, regardless of whether *Gata4* had been expressed initially, unlike iXEN cell lines carrying an allele of *Gata6-H2B-Venus* (Fig. 6.4F). We conclude that Gata4-H2B-Venus is expressed in iXEN and not iPS cell colonies.

We next sought to examine the expression of GATA4-H2B-eGFP and NANOG-mCherry simultaneously. As expected, based on their individual expression patterns, these two reporters were co-expressed in very few colonies during reprogramming (Fig. 6.4G). Strikingly, however, only Mixed colonies co-expressed both GATA4-H2B-eGFP and NANOG-mCherry (Fig. 6.4H). In addition, these two reporters exhibited complementary expression patterns within the Mixed colonies, consistent with cell type-specific expression of these two genes in embryos (Artus et al., 2011; Chazaud et al., 2006; Niakan & Eggan, 2013). We therefore propose that the combined use of GATA4-H2B-eGFP and NANOG-mCherry can be used to resolve specific stem cell colony subtypes during reprogramming.

Section 6.5. Discussion

Although transcription factor-mediated somatic cell reprogramming has been possible for over a decade, we still have only a rough understanding of the molecular events that each cell undergoes as it acquires iPS or iXEN cell fates. As single cell genomic approaches become more commonplace, we are beginning to understand the stages of the reprogramming process. However, most genomic approaches do not permit the long-term evaluation of cellular changes over time in real time. For these reasons,

fluorescent reporters, which permit live imaging, individual cell tracking, and readout of gene expression, are an appealing complement to genomic studies of somatic cell reprogramming.

We have identified a combination of two mouse gene expression fluorescent reporter lines that can reliably distinguish colonies of presumptive iPS and iXEN cells. One limitation of this approach is the need to derive MEF lines from mice carrying multiple distinct reporter alleles. However, the reliable identification of early iXEN and iPS cell lines will lead to discovery of more facile approaches for cell isolation, such as unique cell surface markers that label live iXEN and iPS cells early in their formation. Nevertheless, the ability to select cells on the basis of the expression of potent developmental regulators of pluripotent and extraembryonic endoderm cell fate provides additional advantages.

First, we note that, while *Gata4* was detected within presumptive iXEN cell colonies, it did not appear to be expressed in all cells of those colonies. The reasons for the limited expression of *Gata4* within iXEN cell colonies is not yet clear. One possibility is that *Gata4* expression is dynamically regulated in nascent iXEN cells, giving the illusion, in snapshots, that *Gata4* is only expressed in a subset of iXEN cells. Similarly, expression of *Gata4* may be progressive, consistent with the gradual adoption of iXEN cell fate. Another possibility is that the *Gata4* reporter labels a unique subtype of iXEN cells. These possibilities could be investigated using live imaging and fluorescent cell sorting in future studies.

Second, we were surprised that the *Nanog* reporter was detected within non-iPS cell colony subtypes, including iXEN and Mixed colonies. While this pattern could raise some concern for the fidelity of *Nanog* as a marker for the emergence of pluripotency, we do not yet understand the dynamics of *Nanog* expression outside of iPS cell colonies. One possibility is that *Nanog* is expressed very transiently in most cells that undergo reprogramming – regardless of their ultimate fates. Another possibility is that *bona fide*, *Nanog*-expressing iPS cells arise within Mixed and iXEN cell colonies. These possibilities could again be addressed using live imaging and fluorescent cell sorting in future studies, which could reveal whether *Nanog* expression is stable or transient and whether *Nanog*-expressing cells give rise to iPS, iXEN, Mixed, or failed cell lines.

Lastly, we observed a significant number of Mixed colonies in all of our reprogramming experiments. These colonies could be considered to have failed or stalled during reprogramming. However, it is intriguing that Mixed colonies possess characteristics of both iPS and iXEN colonies, including morphology and fluorescent marker expression. Therefore, is tempting to speculate that Mixed colonies also give rise to bona fide iPS and iXEN cells. However, the quality and properties of stem cell lines that can be derived specifically from the Mixed colonies awaits further investigation. Similarly, these reporters can be used to determine when and how iXEN and iPS cell fates first diverge from each other in future studies because they will enable identification of differences in transcriptional signature and developmental potential in single-cell studies. Ultimately, the use of fluorescent gene expression reporters will likely enable us to address these and other exciting questions about how and why reprogramming works.

Section 6.6. Acknowledgements

We would like to thank Anna-Katerina Hadjantonakis and her lab for providing *Gata4*$^{H2B\text{-}eGFP}$ and *Gata6*^{tm1Hadj}/J mice and the Michigan State University Transgenic Core for assistance creating the *Nanog-mCherry* mouse line.

TABLES

Gene Target	Forward Primer	Reverse Primer
Oct4	GTTGGAGAAGGTGGAACCAA	CCAAGGTGATCCTCTTCTGC
Nanog	ATGCCTGCAGTTTTTCATCC	GAGGCAGGTCTTCAGAGGAA
Sox2	GCGGAGTGGAAACTTTTGTCC	CGGGAAGCGTGTACTTATCCTT
Gata6	ATGCTTGCGGGCTCTATATG	GGTTTTCGTTTCCTGGTTTG
Gata4	CTGGAAGACACCCCAATCTC	ACAGCGTGGTGGTGGTAGT
Sox7	GGCCAAGGATGAGAGGAAAC	TCTGCCTCATCCACATAGGG
Sox17	CTTTATGGTGTGGGCCAAAG	GCTTCTCTGCCAAGGTCAAC
ActinB	CTGAACCCTAAGGCCAACC	CCAGAGGCATACAGGGACAG

Table 6.1. Quantitative Polymerase Chain Reaction Primers for Detecting Endogenous Transcripts for Chapter 6.

Gene Target	Forward Primer	Reverse Primer
Nanog^{mCherry}	CCACTAGGGAAAGCCATGCGCATTT	GGAAGAAGGAAGGAACCTGGCTTTGC
mCherry	AGGACGGCGAGTTCATCTAC	TGGTGTAGTCCTCGTTGTGG
Pou5f1^{eGFP}	CCAAAAGACGGCAATATGGT	CAAGGCAAGGGAGGTAGACA
Pou5f1 wild-type allele	TGCCAGACAATGGCTATGAG	CAAGGCAAGGGAGGTAGACA
Gata6$^{H2B\text{-}Venus}$	CCAGGGAGCTCTGAGAAAAAG	CCTTAGTCACCGCCTTCTTG
Gata6 wild-type allele	CCAGGGAGCTCTGAGAAAAAG	GTCAGTGAAGAGCAACAGGT
Gata4$^{H2B\text{-}eGFP}$	GTTTCTGCTTTGATGCTGGA	TGCTCAGGTAGTGGTTGT
Gata4 wild-type allele	GTTTCTGCTTTGATGCTGGA	CGGAGTGGGCACGTAGAC

Table 6.2. Genotyping Primers for Chapter 6.

FIGURES

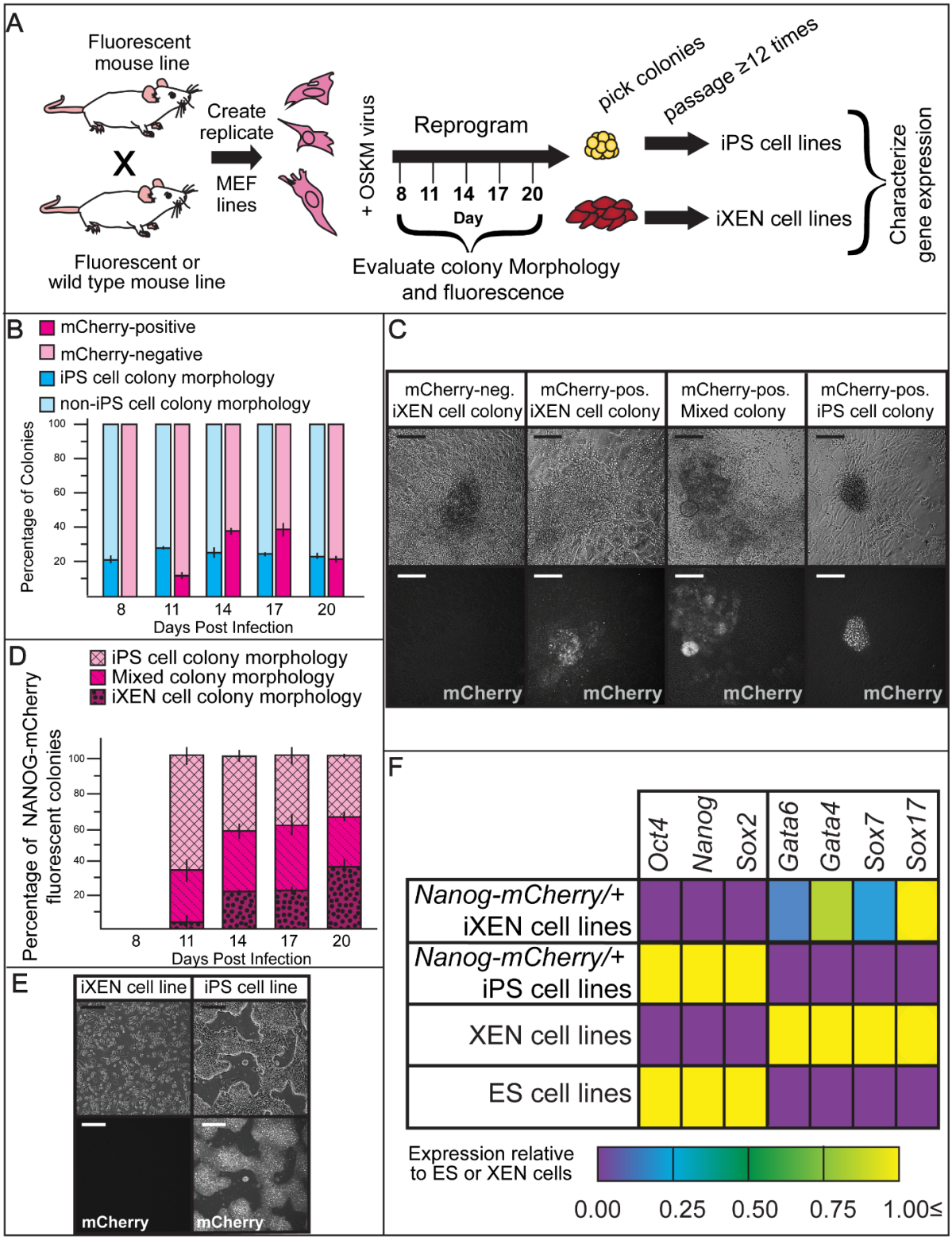

Figure 6.1. NANOG-mCherry expression is detected in colonies bearing non-iPS cell colony morphology during reprogramming.

Figure 6.1 (cont'd).
A) Workflow for all experiments described in this study, including the derivation of MEF lines carrying one or more fluorescent reporter, evaluation of colonies during the 21-day reprogramming process, and isolation of colonies at the end of reprogramming to derive stable stem cell lines. **B)** The proportion of iPS cell colonies is not equivalent to the proportion of mCherry-positive colonies during days 11–17 of reprogramming, error bar = standard error (n = 3 MEF lines reprogrammed). **C)** Representative images of NANOG-mCherry expression among colony subtypes during reprogramming (scale bar = 200 μm). **D)** Expression of NANOG-mCherry is observed in all three colony subtypes throughout reprogramming, error bar = standard error (n = 3 MEF lines reprogrammed). **E)** Expression of NANOG-mCherry expression is observed in established iPS, and not iXEN, cell lines (scale bar = 200 μm). **F)** Heat map summary of qPCR analysis of established iXEN and iPS cell lines (n = 3 biological replicates each), relative to positive control cell lines: XEN or ES cell lines (n = 3 replicate wells per cell line), confirms expected expression patterns of key lineage markers. Scale bar = 200 μm. ES, embryonic stem; iPS, induced pluripotent stem; iXEN, induced extraembryonic endoderm; MEF, mouse embryonic fibroblast; qPCR, quantitative polymerase chain reaction; XEN, extraembryonic endoderm.

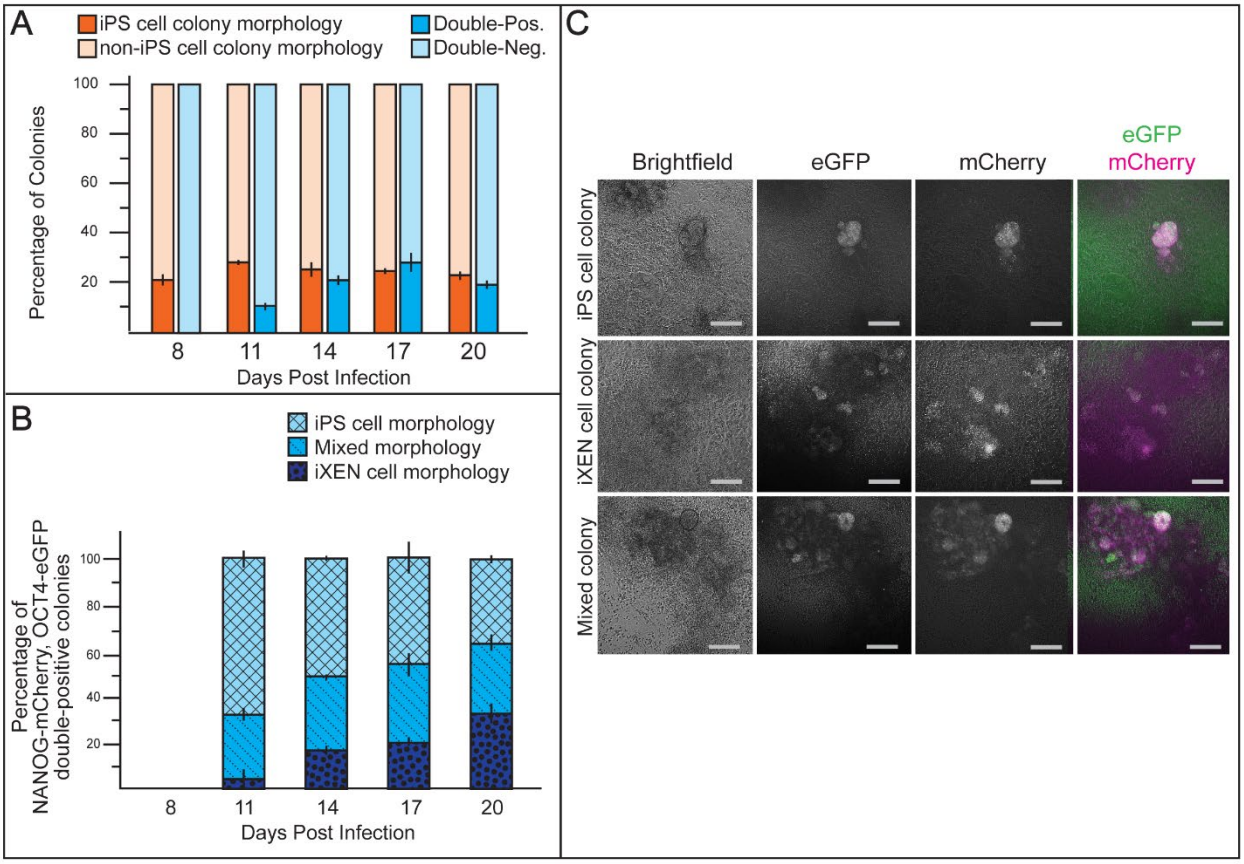

Figure 6.2. NANOG-mCherry and OCT4-eGFP are coexpressed in multiple colony subtypes during reprogramming. A) The proportion of iPS cell colonies is roughly equivalent to the proportion of NANOG-mCherry and OCT4-eGFP double-positive colonies during reprogramming, error bar = standard error (n = 3 MEF lines reprogrammed). **B)** Expression of NANOG-mCherry and OCT4-eGFP is observed in all three colony subtypes during reprogramming, error bar = standard error (n = 3 MEF lines reprogrammed). **C)** Representative images of NANOG-mCherry and OCT4-eGFP expression during reprogramming, scale bar = 200 μm.

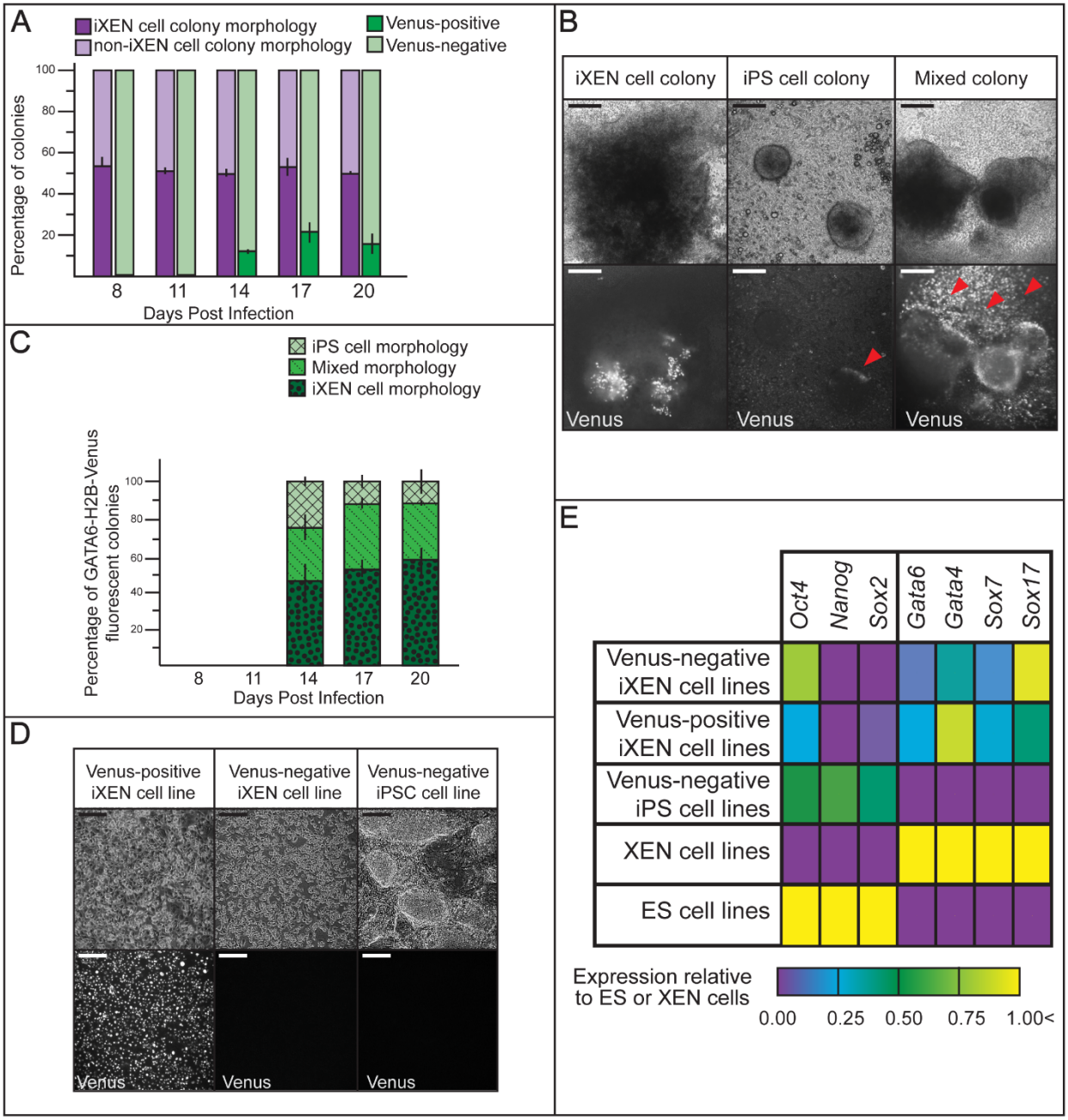

Figure 6.3. GATA6-H2B-Venus expression is detected in colonies bearing non-iXEN cell colony morphology during reprogramming. A) The proportion of GATA6-H2B-Venus-positive colonies is low relative to the proportion of colonies exhibiting iXEN cell morphology during reprogramming, error bar = standard error (n = 3 MEF lines reprogrammed). **B)** Expression of GATA6-H2B-Venus is observed in all three colony subtypes during reprogramming, scale bar = 200 μm. **C)** Expression of GATA6-H2B-Venus is observed in all three colony subtypes during reprogramming, error bar = standard error (n = 3 MEF lines reprogrammed). **D)** Expression of GATA6-H2B-Venus is restricted to established iXEN, and not iPS, cell lines, but is not expressed in all iXEN lines.

Figure 6.3 (cont'd).
E) Heat map summary of qPCR analysis of established iXEN and iPS cell lines (n = 3 biological replicates each), relative to positive control cell lines: XEN or ES cell lines (n = 3 replicate wells per cell line), confirms expected expression patterns of key lineage markers.

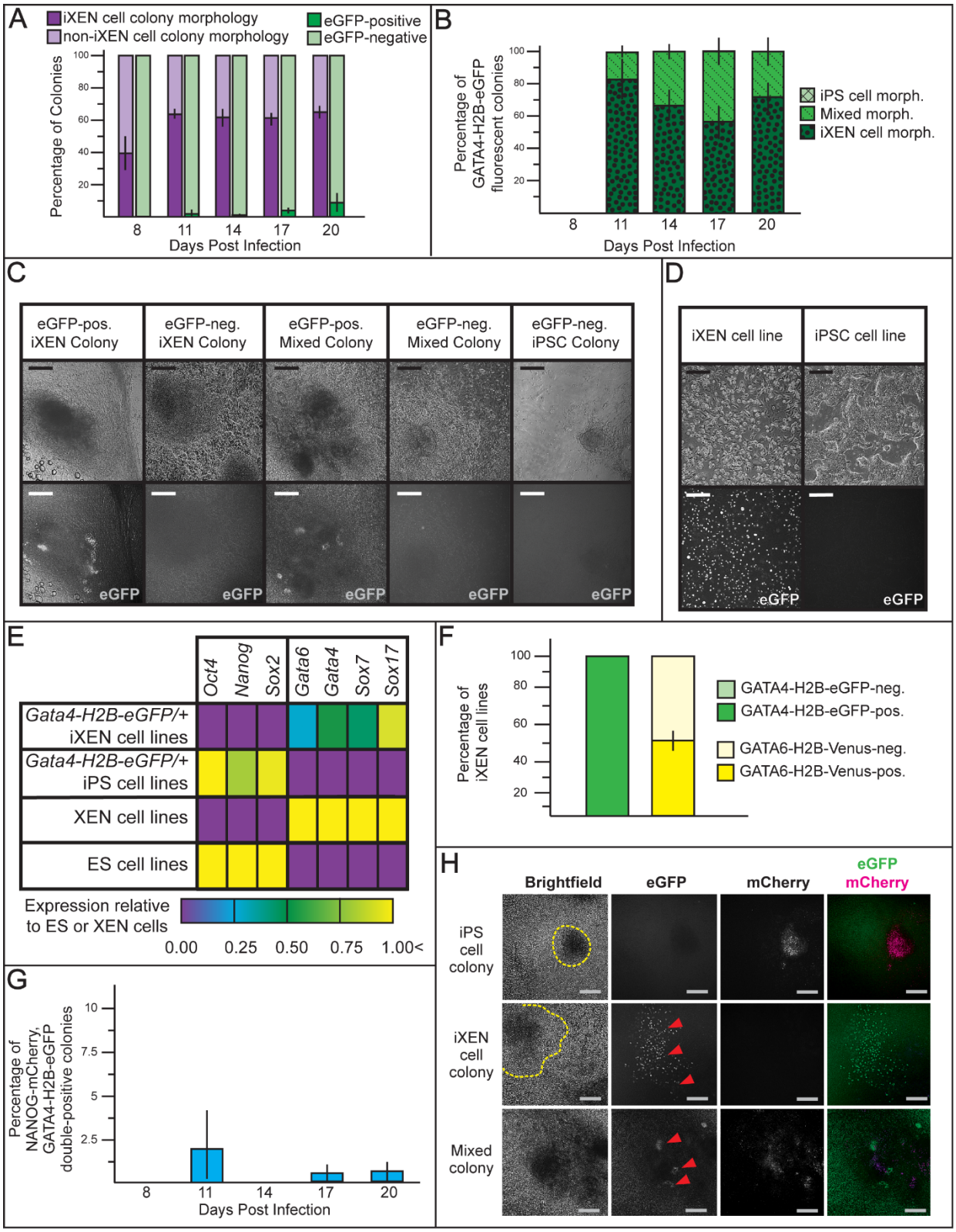

Figure 6.4. GATA4-H2B-eGFP, in combination with NANOG-mCherry, distinguishes iPS and iXEN cell colonies during reprogramming.

Figure 6.4 (cont'd).
A) The proportion of GATA4-H2B-eGFP-positive colonies is low relative to the proportion of iXEN cell colonies observed during reprogramming, error bar = standard error (n = 3 MEF lines reprogrammed). **B)** Expression of GATA4B-H2B-eGFP is observed in iXEN and Mixed, but not iPS, cell colonies during reprogramming, error bar = standard error (n = 3 MEF lines reprogrammed). **C)** Expression of GATA4B-H2B-eGFP is observed in iXEN and Mixed, but not iPS, cell colonies during reprogramming, scale bar = 200 μm. **D)** Expression of GATA4B-H2B-eGFP is observed in established iXEN, and not iPS, cell lines, scale bar = 200 μm. **E)** Heat map summary of qPCR analysis of established iXEN and iPS cell lines (n = 3 biological replicates each), relative to positive control cell lines: XEN or ES cell lines (n = 3 replicate wells per cell line), confirms expected expression patterns of key lineage markers. **F)** All established iXEN cell lines carrying the Gata4-H2B-eGFP allele expressed eGFP, whereas only half of the iXEN cell lines carrying Gata6-H2B-Venus expressed Venus, error bar = standard error (n = 6 and 8 iXEN cell lines, respectively). **G)** Percentage of all colonies in which expression of both NANOG-mCherry and GATA4-H2B-eGFP was observed during reprogramming, error bar = standard error (n = 3 MEF lines reprogrammed). **H)** Expression of both NANOG-mCherry and GATA4-H2B-eGFP is observed only in Mixed colonies, scale bar = 200 μm.

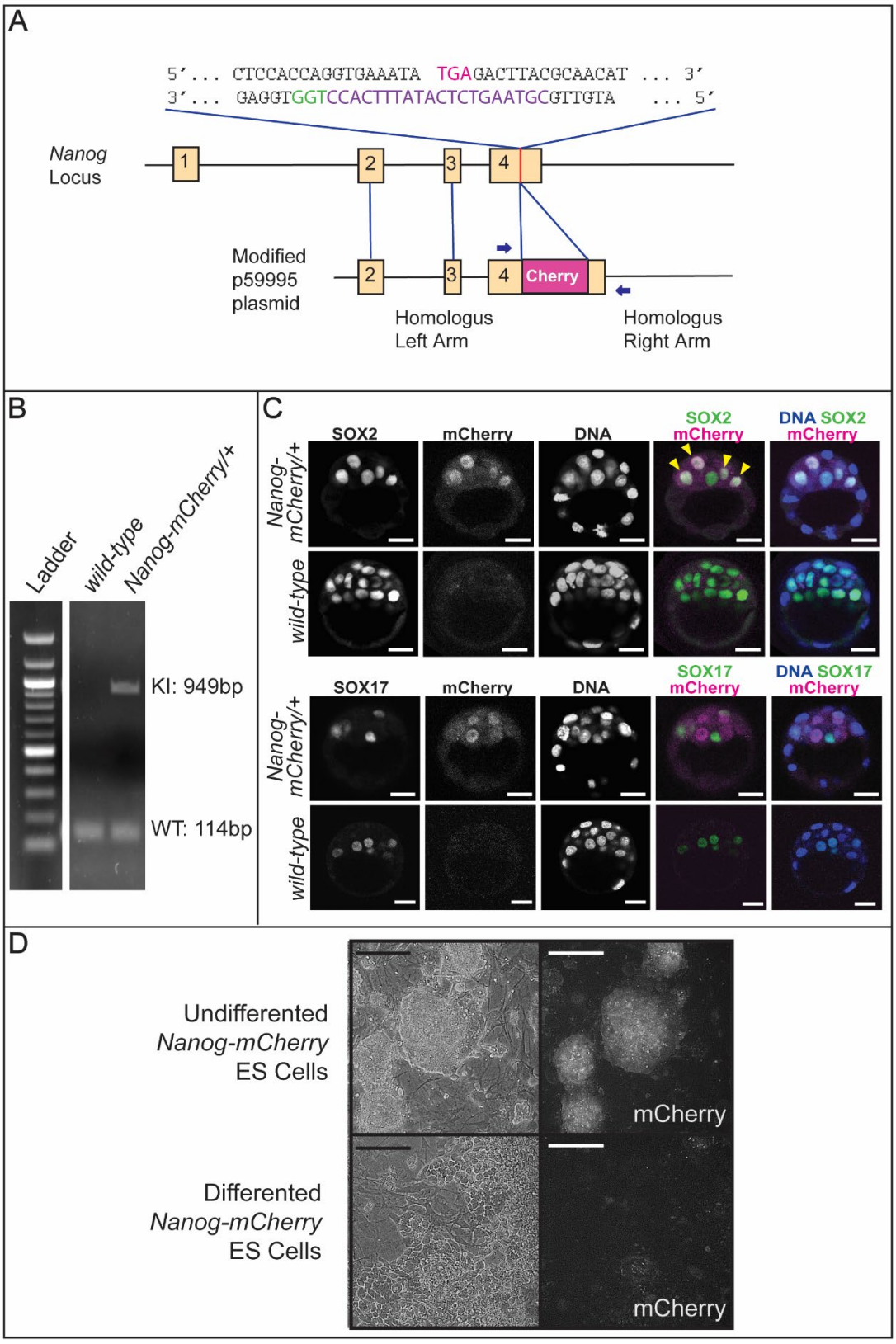

Supplemental Figure 6.1. Genetic engineering and characterization of *Nanog-mCherry* knock-in in early embryos and ES cell lines.

Supplemental Figure 6.1 (cont'd).
A) Targeting scheme to generate mice expressing a NANOG-mCherry fusion protein. Schematic shows *mCherry* inserted in frame near the stop codon (magenta TGA) of the *Nanog* locus. The protospacer-adjacent motif (PAM) sequence (green GGT) and the sgRNA target sequence (purple) are also highlighted. Arrows represent the genotyping primer locations. **B)** Genotypes of ear punches of wild-type and *Nanog-mCherry*/+ distinguished by PCR using locus-specific primers (as shown in panel A and Table 6.2). **C)** Confocal cross-sections of *Nanog-mCherry* and wild type E3.75 blastocysts immunofluorescently stained with antibodies specific for pluripotent epiblast (SOX2) or primitive endoderm (SOX17) cells, demonstrate that SOX2 and NANOG are coexpressed (yellow arrows), while SOX17 and NANOG are complementary in expression. Scale bar = 25 μm. **D)** Expression of *Nanog-mCherry* in undifferentiated mouse ES cells and in ES cells following withdrawal of MEFs and LIF. Scale bar = 100 μm.

CHAPTER 7.

IDENTIFICATION OF OCT4 BINDING SITES IN ICM CELLS BY uliCUT&RUN

Robin E. Kruger[1,2], Sarah Hainer[3], and Amy Ralston[2,4]

1) Cell and Molecular Biology Ph.D. Program, Michigan State University, East Lansing, MI, 48824, USA

2) Reproductive and Developmental Sciences Training Program, Michigan State University, East Lansing, MI, 48824, USA

3) Department of Biological Sciences, University of Pittsburgh, Pittsburgh, PA, 15260, USA

4) Department of Biochemistry and Molecular Biology, Michigan State University, East Lansing, MI, 48824, USA

This study was supported by the National Institutes of Health R35 GM131759 and T32 HD087166.

Section 7.1. Abstract

The transcription factor OCT4 is necessary for the specification of both epiblast (EPI) cells and primitive endoderm (PrE) cells in the inner cell mass of the mouse blastocyst. However, it is unknown how the same transcription factor promotes the emergence of a pluripotent cell type and a non-pluripotent cell type in the same tissue. I hypothesize that OCT4 binds different *cis*-regulatory elements in these two different cell types. To investigate OCT4 binding sites in EPI and PrE cells, I performed ultra-low-input CUT&RUN for OCT4 in blastocyst-stage embryos enriched for either EPI or PrE cells. I was able to identify unique peaks of OCT4 binding locations in EPI-enriched and PrE-enriched blastocysts, demonstrating the effectiveness of this technique to identify transcription factor binding sites in samples with limited genetic material.

Section 7.2. Introduction

The transcription factor OCT4 is generally considered to be a marker of pluripotency (Frum et al., 2013; Le Bin et al., 2014; Palmieri et al., 1994). OCT4 is expressed in early mouse embryos beginning at the 8-cell stage, and becomes restricted to the pluripotent inner cell mass after blastocyst formation (Palmieri et al., 1994). *Oct4*-knockout embryos die at ~E4.5 with severe inner cell mass (ICM) defects (Nichols et al., 1998). It is also considered one of the key factors that maintain pluripotency in embryonic stem cells, forming a network with NANOG and SOX2 (M. Li & Belmonte, 2017; Masui et al., 2007; Mitsui et al., 2003). When ESCs are differentiated and lose their pluripotency, OCT4 is rapidly downregulated. Altogether, these observations demonstrate that this transcription factor plays a key role in maintaining pluripotent cells.

However, more recent studies have shown that OCT4 does not solely promote pluripotency in preimplantation mouse embryos. Rather, OCT4 is essential for the specification of a non-pluripotent cell type, primitive endoderm (PrE). PrE cells are specified in the second cell fate decision, when the ICM differentiates into pluripotent epiblast (EPI), which forms the fetus, and multipotent PrE, which contributes mostly to the extraembryonic yolk sac (Cockburn & Rossant, 2010, see Chapter 1). Interestingly, knockouts of *Oct4* do not express PrE markers such as *Sox17* (Frum et al., 2013; Le Bin et al., 2014), and reprogrammed XEN cells, the *in vitro* stem cell model of PrE, also express OCT4 (Moauro et al., 2022). Therefore, it appears that OCT4 promotes both EPI and PrE cell fate in the ICM. How a single transcription factor can promote two different cell fates within the same tissue remains an open question.

Genomic analyses are capable of providing extremely rich information about transcription and protein-DNA interactions down to the single cell level (Wen & Tang, 2022). Knowing where a transcription factor or chromatin modifier is bound on the DNA – be that on a promotor, enhancer, or silencer sequence – can help us build gene regulatory networks to determine how *trans*-acting factors ultimately affect the actions of a cell. Chromatin immunoprecipitation followed by sequencing (ChIP-seq) is a commonly used technique to map transcription factor binding sites. However, this technique has some shortcomings (Dahl & Gilfillan, 2018). ChIP-seq and its variations generally require protein crosslinking, which may introduce artifacts in the data (Baranello et al., 2016). More importantly, ChIP-seq involves shearing the entire genomic chromatin and the precipitating out the bound chromatin, which leads to loss of

material and a high background. For this reason, ChIP-seq techniques are not effective or reproducible with small (<10,000 cells) or highly heterogeneous samples (Hainer et al., 2019; Jakobsen et al., 2015). As preimplantation mouse embryos are typically fewer than 100 cells, the inefficiency of ChIP-seq based techniques has thus far prevented effective mapping of transcription factor binding sites in these rare samples.

As an alternative to ChIP-seq, Cleavage Under Targets and Release Using Nuclease (CUT&RUN) uses a different approach that is far more compatible with small sample sizes (Skene & Henikoff, 2017). In CUT&RUN, an antibody against the protein-of-interest first detects the protein bound to the DNA. A fusion protein A-micrococcal nuclease (MNase) binds to the antibodies and the nuclease cleaves the chromatin precisely on either side of the bound protein. Once released from the protein complex, these short DNA fragments go into solution while the bulk chromatin remains insoluble, allowing it to be easily removed. This drastically improves the signal-to-noise ratio, decreasing the requirement for high reads and large samples to overcome the background. An adaptation to this method, called ultra-low-input (uli) CUT&RUN, has been shown to be effective in profiling transcription factor binding sites specifically in preimplantation mouse embryos, even at the single-cell level (Hainer et al., 2019; Hainer & Fazzio, 2019; Patty & Hainer, 2021).

Here, I used uliCUT&RUN to generate a dataset of OCT4 binding sites in mid-blastocyst stage mouse embryos. To compare OCT4 binding sites between EPI and PrE cells, I pooled embryos enriched for either EPI or PrE cells in the ICM. These two pools of

embryos produced different lists of OCT4-bound genes, providing evidence for the hypothesis that OCT4 regulates different targets in EPI and PrE cells.

Section 7.3. Materials and Methods

Mouse Strains and Genotyping

All animal research was conducted in accordance with the guidelines of the Michigan State University Institutional Animal Care and Use Committee under approved protocol 202300108. Wild type embryos were obtained from CD-1 mice (Charles River). Mice were maintained on a 12 hour light/dark cycle.

Embryo Collection and Culture

Preimplantation (E2.5 or E3.75) embryos were collected by flushing the oviduct or uterus with M2 medium (Sigma M7167). For embryo culture, KSOM medium (Millipore MR-121-D) was equilibrated overnight prior to embryo collection. E2.75 embryos were collected and cultured at 37°C in a 5% CO_2 incubator under light mineral oil (Millipore ES-005-C). To enrich for PrE cells, 1 µg/mL recombinant FGF4 in PBS with 0.1% BSA (R&D 235-F4) + 1 µg/mL heparin (Sigma H3149) was added to the culture media. To enrich for EPI cells, 1 µM PD173074 in DMSO (Selleckchem S1264) + 5 µM PD0325901 in DMSO (Stemgent 04-0006) was added to the culture media. 0.2% DMSO (New England BioLabs B0515A) was added to the culture media in control samples.

Immunofluorescence and Confocal Microscopy

Preimplantation embryos were fixed with 4% formaldehyde (Polysciences 04018) for 10 minutes, permeabilized with 0.5% Triton X-100 (Sigma Aldrich X100) for 30 minutes, and then blocked with blocking solution (10% Fetal Bovine Serum (HyClone SH30396.02), 0.1% Triton X-100) overnight at 4°C. Embryos were incubated with primary antibody overnight at 4°C. The next day, embryos were washed in blocking solution for 30 minutes, incubated in secondary antibody diluted in blocking solution for 1 hour, washed in blocking solution for 30 minutes, then stained with nuclear stain diluted in block for 10 minutes or overnight. Antibodies used are listed in Table 1. Embryos were imaged using an Olympus FluoView FV1000 Confocal Laser Scanning Microscope system with 60X PlanApoN oil (NA 1.42) objective. For each embryo, z-stacks were collected, with 5 μm intervals between optical sections.

Embryo Analysis

For each embryo, z-stacks were analyzed using Fiji (ImageJ), which enabled the labeling, based on DNA stain, of all individual cell nuclei. Statistical analysis was performed using GraphPad Prism (v. 9.5.1). Figure images were assembled using Adobe Illustrator.

Embryo Preparation for uliCUT&RUN

Wild-type mouse embryos were collected at E3.75 or collected at E2.75 and cultured 36 hours in the treatment conditions described above. The zona pellucida was removed by Acid Tyrode’s treatment. Embryos were transferred into Nuclear Extraction buffer (20

mM HEPES-KOH, pH 7.9; 10 mM KCl; 0.5 mM Spermidine; 0.1% Triton X-100; 20% glycerol; 1X HALT protease inhibitors (ThermoFisher 78439)) and incubated on ice for 10 minutes. Samples were then centrifuged at 600xg for 10 minutes at 4°C to pellet the nuclei. Once completed, the supernatant was removed. After nuclear extraction, samples were either flash-frozen in liquid nitrogen and stored at -80°C, or the nuclei were fixed for 10 minutes in formaldehyde solution (1.5 mL 37% formaldehyde, 0.1mL 5M NaCl, 0.01mL 0.5M EDTA, 0.25mL 1M HEPES 7.6, and up to 5mL water), then quenched in 0.25M glycine for 5 minutes. Crosslinked nuclei were stored in quenched fix at 4°C for up to 2 weeks.

uliCUT&RUN on Embryo Nuclei

Prepared samples were shipped on ice to Dr. Sarah Hainer, who performed uliCUT&RUN for CTCF and OCT4 as described in Hainer & Fazzio, 2019. Briefly, each sample of frozen or fixed nuclei was affixed to concanavalin A beads. The samples were then treated for 2 hours with a primary antibody against either CTCF or OCT4. One or more negative control samples were not treated with primary antibody (no Ab control) and washed. All samples were then treated with pA-MNase fusion protein and washed. The MNase activity was then activated by treatment with calcium chloride for 30 minutes. The DNA digestion was stopped by treatment with Stop buffer (see Hainer & Fazzio, 2019), including a known concentration of *S. cerevisiae* spike-in DNA as a positive control. The samples were incubated at 37 °C for 10 minutes to release the fragments of DNA into solution. After incubation, the samples were centrifuged at 16,000xg for 2 minutes, then placed on a magnetic rack to separate the intact

chromatin. The supernatant containing the enriched, fragmented samples was transferred to new microcentrifuge tubes. Then, in fixed samples, the crosslinking was reversed by treatment with 10% SDS and Proteinase K. Input chromatin was then fragmented by sonification and purified by DNA spin column. Sample library construction and multiplexing was performed using DNA Library Prep Kit for Illumina (ChIP-seq, CUT&RUN) with Multiplex Oligos for Illumina (ChIP-seq, CUT&RUN), according to the manufacturer's protocol for CUT&RUN DNA. Before multiplexing, proper library construction was confirmed using 5 µL of each sample for analysis by agarose gel electrophoresis.

Bioinformatic Analyses

Bioinformatic analyses were performed as described in Hainer & Fazzio, 2019. Briefly, sample sequences were aligned to the mouse or *S. cerevisiae* genomes using bowtie2. Low-quality reads (MAPQ<10) and PCR duplicates were removed. The remaining aligned sequences were filtered for size between 1-120 bp. To assess peak enrichment over known genomic loci, deepTools was used to compare aligned sequences to known binding sites in embryonic stem cells for either CTCF (X. Chen et al., 2008) or OCT4 (Marson et al., 2008). To identify all binding sites of interest, peaks located within 2kb of transcriptional start sites were called using the algorithm Sparse Enrichment Analysis for CUT&RUN (SEACR, Meers et al., 2019).

Section 7.4. Results and Conclusions

Our goal for these experiments was to map OCT4 binding sites in EPI and PrE cells in preimplantation mouse embryos. However, to optimize the protocol for isolating nuclei and performing uliCUT&RUN on embryos, we first tried mapping the binding sites for CTCF, using an antibody already validated for uliCUT&RUN (Hainer et al., 2019). To determine the optimal number of embryos per sample, we performed uliCUT&RUN on samples of E3.75 wild-type embryos from single embryos, pools of five embryos, and pools of ten embryos. The resulting peaks were tested for enrichment over known CTCF and OCT4 binding sites in embryonic stem cells (X. Chen et al., 2008; Marson et al., 2008). We were successful in using uliCUT&RUN to detect CTCF enrichment over known binding sites in 100% of samples from 5- or 10-embryo pools, but only 50% of samples from single embryos (Fig. 7.1A). This suggested that pools of 5 embryos would maximize success in later experiments. However, we were unable to map OCT4 binding sites in any samples using frozen nuclei, regardless of embryo number (Fig. 7.1B).

We hypothesized that the failure to detect OCT4 binding sites may be due to thawing of flash-frozen nuclei during shipping; therefore, we repeated the experiment to map OCT4 binding sites in wild-type E3.75 embryos using fixed nuclei instead of frozen. We also tested the efficiency of two different anti-OCT4 antibodies. We were able to detect enrichment of OCT4 peaks over ESC OCT4-binding sites in all fixed samples, regardless of the antibody used (Fig. 7.2). Similar to our results from the first experiment, larger embryo pools resulted in the detection of more OCT4 binding sites, likely due to increased read depth (Fig. 7.2). This helped us determine that OCT4

binding sites could be mapped in preimplantation mouse embryos, and that crosslinking the nuclei would give us the best outcome for later experiments.

Finally, we were able to examine OCT4 binding sites in EPI- and PrE-enriched embryos. Treatment with exogenous FGF4 promotes differentiation of the ICM to a PrE fate in mouse embryos, while inhibiting FGF signaling in mouse embryos promotes EPI cell fate (Yamanaka et al., 2010). I used this protocol to generate pools of embryos which were enriched for either EPI or PrE cells (see Methods). I performed immunofluorescence for markers of EPI and PrE on a separate group of treated embryos to confirm the effectiveness of the treatments (Fig. 7.3A). The Hainer lab performed uliCUT&RUN in triplicate on fixed nuclei from pools of 5 embryos from each treatment group. Both the FGF4-treated samples and FGF inhibitor-treated samples showed excellent peak enrichment over known OCT4 binding sites compared to no-antibody controls (Fig. 7.3B). In analysis of called peaks (see Methods), FGF4-treated embryos showed 170 total OCT4-binding peaks, while FGF-inhibited embryos showed 11,994 (Fig. 7.4B). Unfortunately, the no-treatment control samples had much sparser read depth and did not show high peak enrichment compared to no-antibody controls (Fig. 7.3B). This prevented more in-depth analysis of the called peaks, since there was no positive control to validate that the sites identified in the treated embryos were also bound by OCT4 in wild-type embryos. We were able to ascertain that all samples (even the poor quality control samples) showed peak profiling over the *Pou5f1* promoter, the gene which encodes OCT4 (Fig. 7.4A). Since OCT4 is known to bind its own promoter in mouse embryonic stem cells (Chew et al., 2005; Loh et al., 2006), this provides some

quality control evidence that the uliCUT&RUN detected true OCT4-binding sites in the treated samples.

The generation of this dataset shows that this technique can be used efficiently to detect transcription factor binding sites in preimplantation embryos. It also suggests that this dataset could be a useful starting point in helping to determine how OCT4 may regulate both EPI and PrE cell fate within the ICM. Future studies will want to optimize the protocol further to get a reliable high read depth to be able to test useful hypotheses from these data.

TABLES

Antibody/Stain	Source	Identifiers	Dilution	Fluorophore
Goat-anti-SOX17	R&D Systems	AF1924	1:2000	
Rabbit-anti-NANOG	Reprocell	RCAB002P-F	1:400	
Donkey-anti-goat IgG	Invitrogen	A-11055	1:400	Alexa488
Donkey-anti-rabbit IgG	Jackson Immuno Research	711-165-152	1:400	Cy3
DRAQ5	Cell Signaling	4084	1:400	

Table 7.1. Antibody Table for Chapter 7.

FIGURES

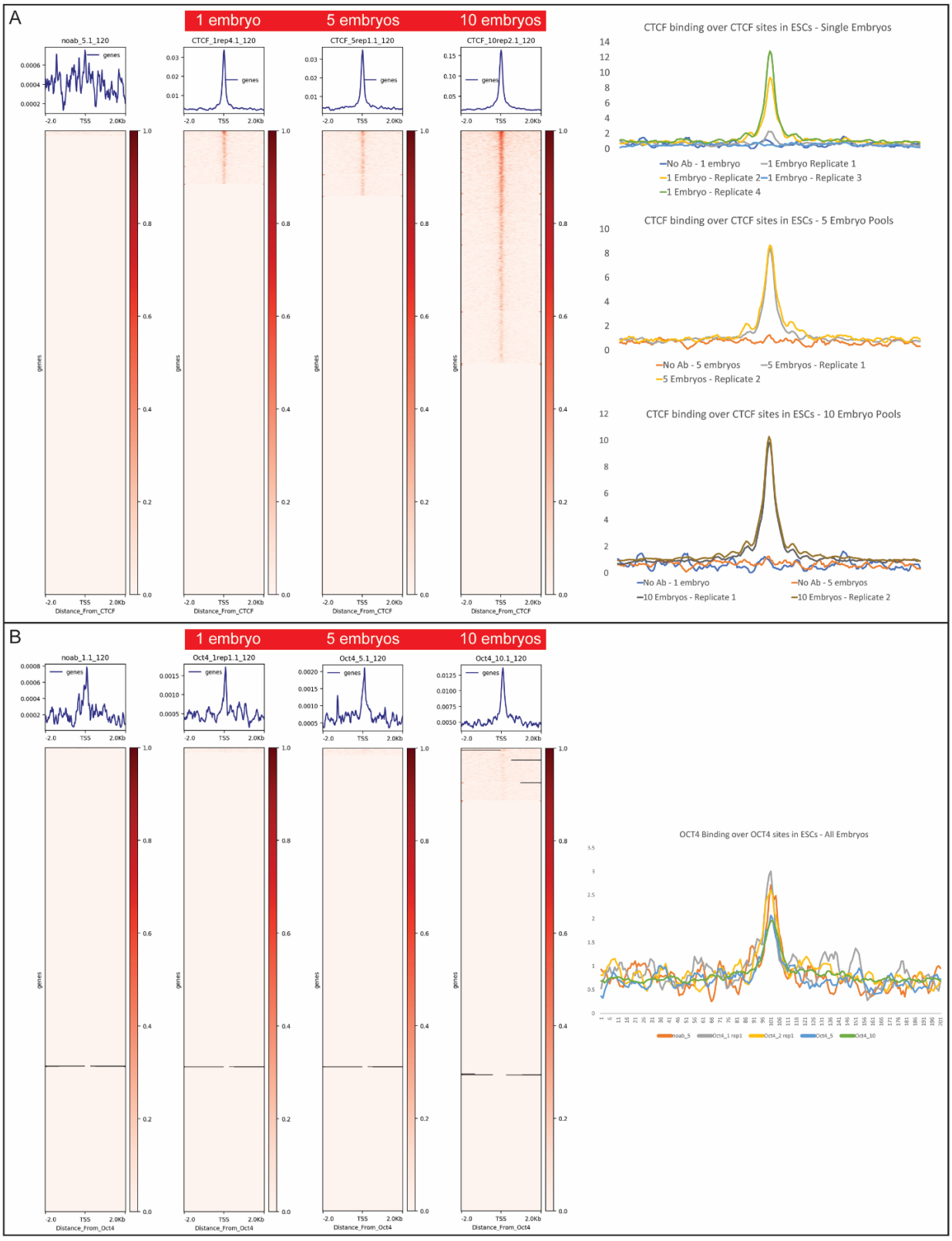

Figure 7.1. Pools of five embryos maximize successful uliCUT&RUN experiments.

Figure 7.1 (cont'd).
A) uliCUT&RUN for CTCF was performed on nuclei extracted from wild-type E3.75 embryos and flash-frozen in liquid nitrogen. The heat maps show CTCF binding between 2kb upstream and 2kb downstream of CTCF binding sites mapped in embryonic stem cells (X. Chen et al., 2008). Graphs show average signal across the same region. A darker line in the center of the heat map shows peak enrichment over background at the known CTCF binding site. Heat maps display data from a representative single experiment performed in 2-4 replicates (No-antibody control (N=2); Single embryos (N=4); Pools of 5 embryos (N=2); Pools of 10 embryos (N=2)). No-antibody control represents background detected without enrichment from a primary antibody. 50% of single-embryo and 100% of pooled embryo experiments show enrichment over no-antibody control. **B)** uliCUT&RUN for OCT4 was performed on nuclei extracted from wild-type E3.75 embryos and flash-frozen in liquid nitrogen. Heat maps display data from representative single experiments of each type of sample (No-antibody control (N=1); Single embryos (N=2); Pools of 5 embryos (N=1); Pools of 10 embryos (N=1)). No experimental samples show enrichment over no-antibody control.

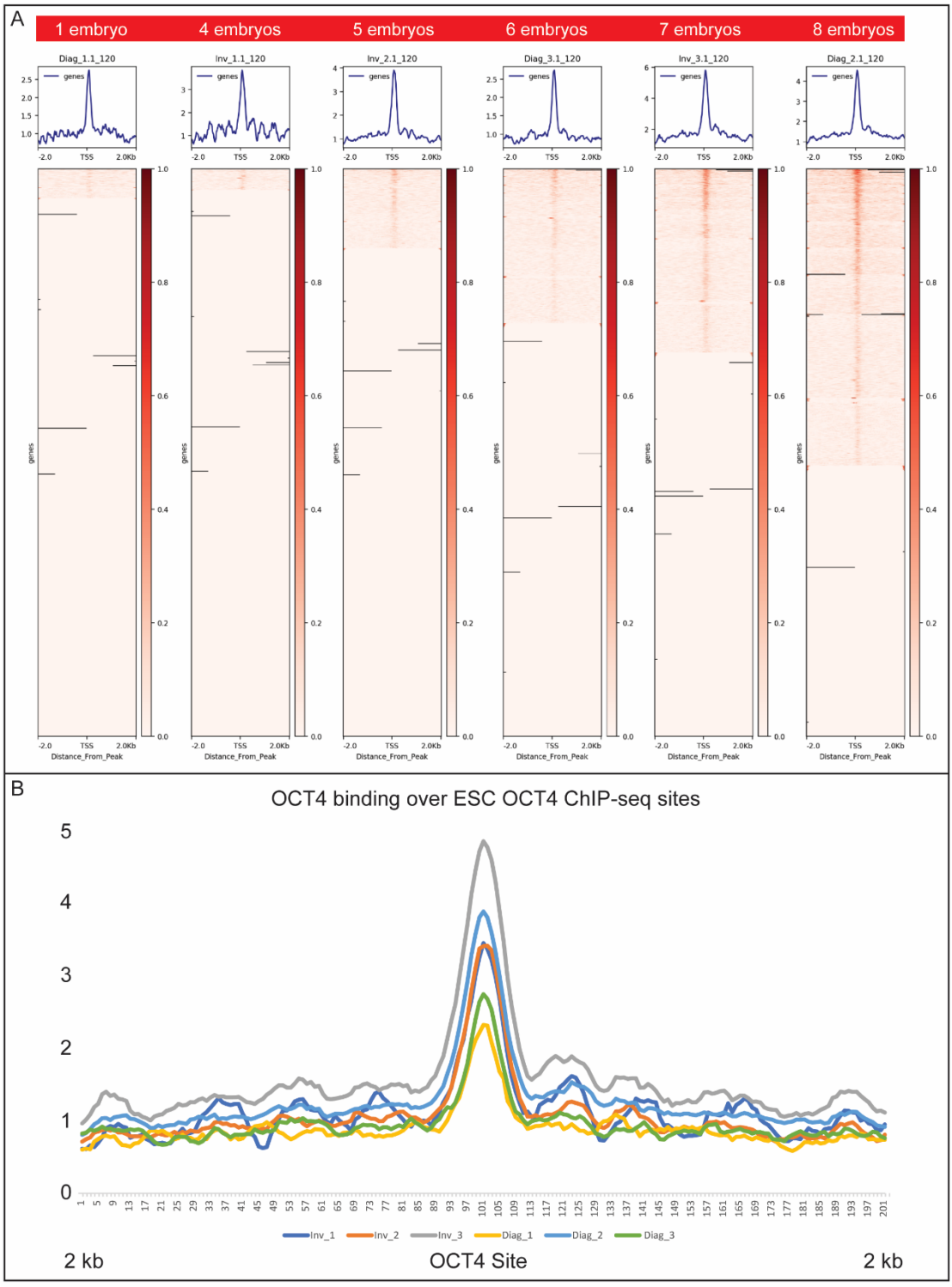

Figure 7.2. Crosslinking nuclei improves successful mapping of OCT4 binding sites. uliCUT&RUN for OCT4 was performed on nuclei extracted from wild-type E3.75 embryos and crosslinked. Heat maps represent single samples of each experiment (N=1 for all). All experimental samples show enrichment over no-antibody control. Inv=anti-OCT4 antibody from Invitrogen, Diag=anti-OCT4 antibody from Diagenode.

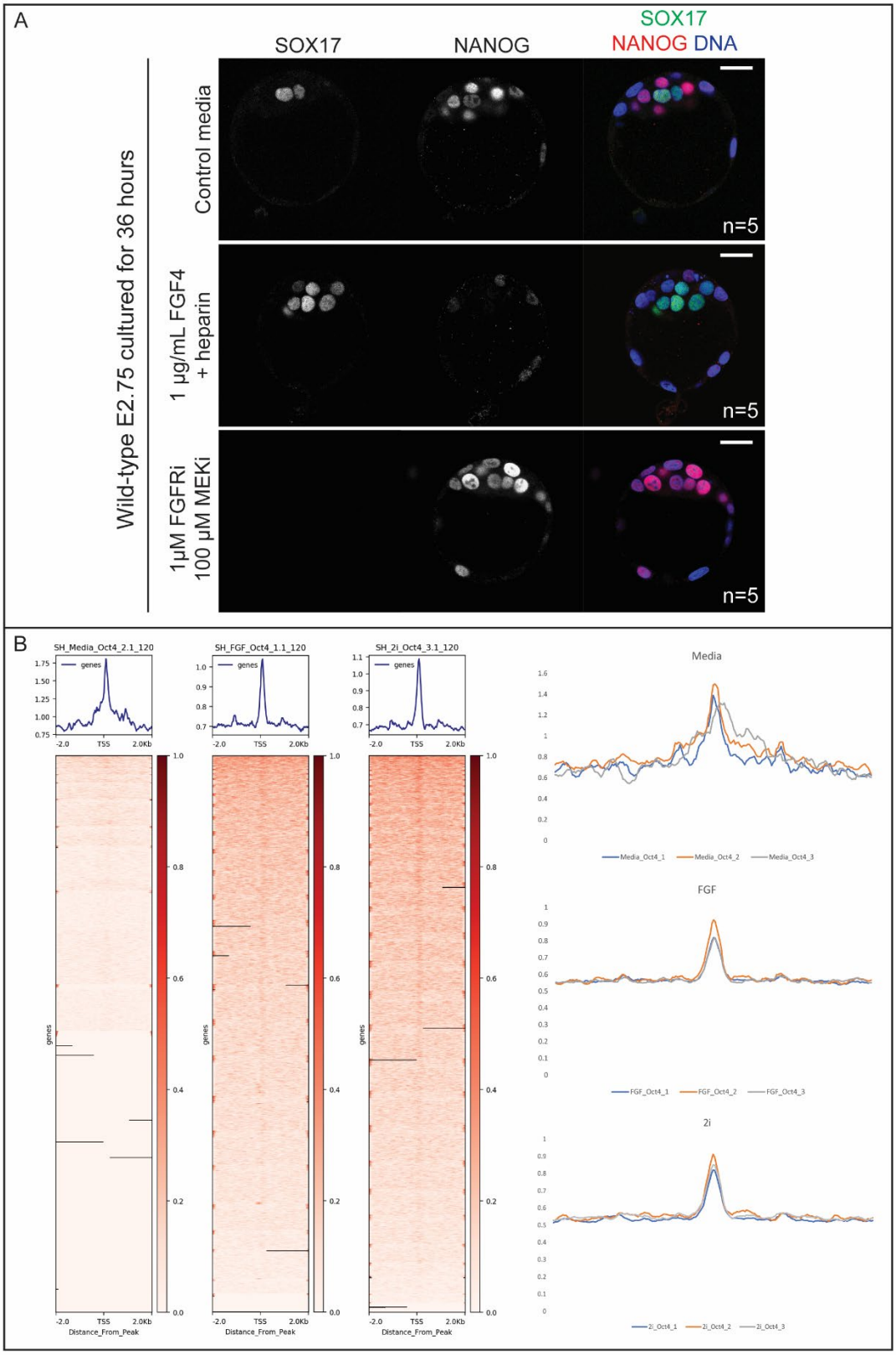

Figure 7.3. Detection of OCT4 binding sites in EPI-enriched and PrE-enriched blastocysts.

Figure 7.3 (cont'd).
A) Wild-type embryos were collected at E2.75 and cultured for 36 hours in either unsupplemented media, media containing 1 µg/mL FGF4 + 1 µg/mL heparin, or media containing 1 µM FGFR inhibitor + 5 µM MEK inhibitor (2i, Yamanaka et al., 2010). Changes in ICM composition were confirmed by immunofluorescence for EPI marker NANOG and PrE marker SOX17. **B)** uliCUT&RUN for OCT4 was performed on nuclei extracted from pools of 5 embryos cultured according to the conditions in A and crosslinked. Heat maps present data from representative single experiments from each sample (No-antibody control (N=1); Control media embryo pools (N=3); FGF4-treated embryo pools (N=3); FGF inhibitor-treated embryo pools (N=3)). FGF4-treated and FGF inhibitor-treated samples show enrichment over no-antibody control.

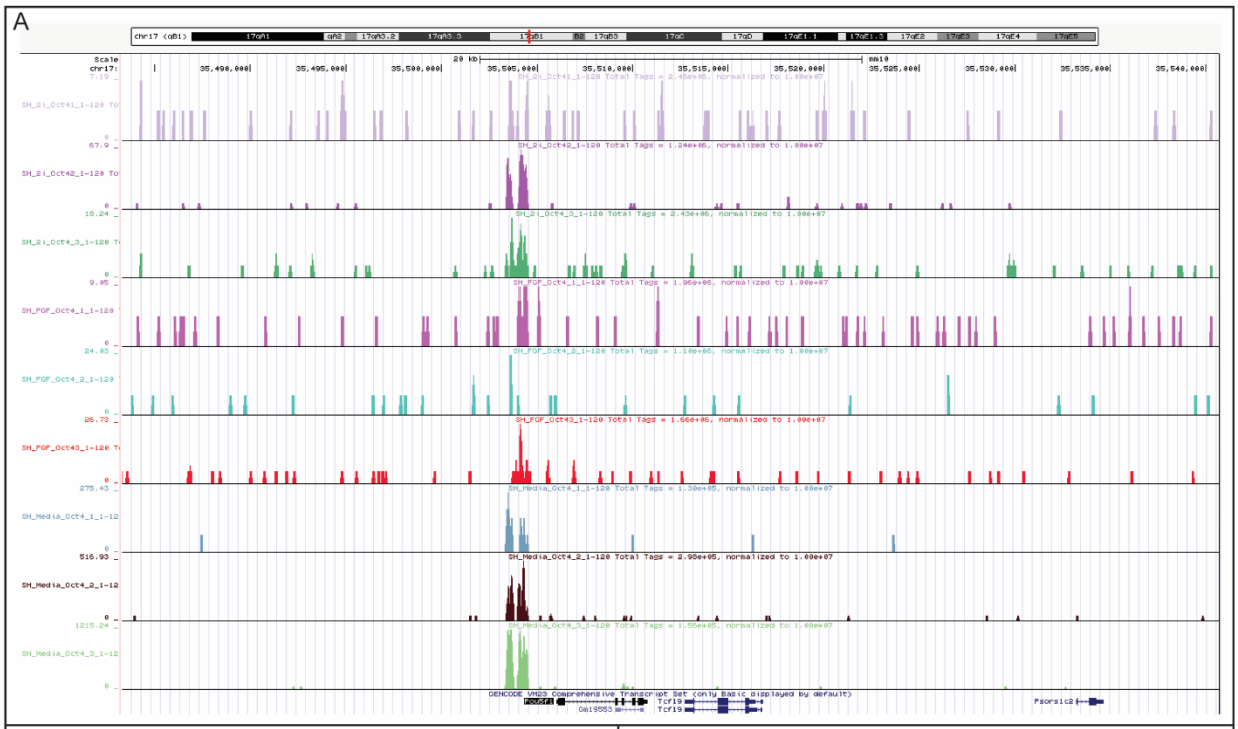

B

	2i	FGF
TOTAL PEAKS	11994	170
3UTR	133	2
RNA	0	0
miRNA	1	0
ncRNA	14	0
TTS	129	1
LINE	1277	13
SINE	1040	13
tRNA	2	0
pseudo	3	0
Exon	188	7
Intron	3554	59
Intergenic	3567	40
Promoter	168	2
5UTR	14	0
snoRNA	0	0
scRNA	5	0
CpG-Island	4	0
Low_complexity	19	1
LTR	1607	24
Simple_repeat	44	2
snRNA	1	0
Satellite	7	3
rRNA	4	0

C

% of peaks	2i	FGF
3UTR	1.10888778	1.17647059
RNA	0	0
miRNA	0.0083375	0
ncRNA	0.11672503	0
TTS	1.07553777	0.58823529
LINE	10.6469902	7.64705882
SINE	8.67100217	7.64705882
tRNA	0.016675	0
pseudo	0.02501251	0
Exon	1.56745039	4.11764706
Intron	29.6314824	34.7058824
Intergenic	29.7398699	23.5294118
Promoter	1.40070035	1.17647059
5UTR	0.11672503	0
snoRNA	0	0
scRNA	0.04168751	0
CpG-Island	0.03335001	0
Low_complexity	0.15841254	0.58823529
LTR	13.3983658	14.1176471
Simple_repeat	0.36685009	1.17647059
snRNA	0.0083375	0
Satellite	0.05836251	1.76470588
rRNA	0.03335001	0

Figure 7.4. Analysis of OCT4-bound peaks from EPI-enriched and PrE-enriched blastocysts. A) Profiles of peaks for each sample from Figure 7.3 over the *Pou5f1* promoter region from the UCSC Genome Browser. All samples show expected enrichment on the *Pou5f1* promoter. **B)** Number of OCT4-bound peaks in FGF4-treated and FGF inhibitor treated embryos, sorted by genome location type. **C)** Percentage of total peaks from B by genome location type.

CONCLUSION

This work presents several advancements in the fields of embryology and stem cell biology (Fig. 8.1). Firstly, I identify novel regulatory mechanisms of embryonic development by intercellular molecular signaling. Conflicting reports in the literature have made the role of BMP signaling in mouse embryonic development unclear. My work shows that BMP signaling is not required for preimplantation development in mouse embryos. However, my studies uncovered a previously unknown role for SMAD4-mediated signaling immediately after implantation, in which SMAD4 attenuates FGF signaling to promote proper epiblast scaling and morphogenesis. This role for SMAD4 does not depend on BMP signaling activity; therefore, identification of the exact mechanism by which SMAD4 interacts with FGF signaling and how unknown factors downstream of these pathways regulate epiblast morphogenesis will be of particular interest in future studies. I also demonstrate that Hippo effectors YAP1 and WWTR1 are essential for maintaining blastomere polarization during preimplantation development, but that these factors are dispensable for initiating blastomere polarization. Future studies are needed to determine the mechanisms which regulate the timing of Hippo signaling dependence in blastomere polarization. Finally, I present three novel techniques for studying early embryonic development. The GOGREEN system provides an efficient technique for generating fluorescently-tagged proteins in early embryos. A combination of fluorescent reporters more accurately distinguished iPSC and iXEN colonies during cellular reprogramming. uliCUT&RUN can be used to detect transcription factor binding sites in preimplantation mouse embryos. Altogether, my work

addresses many previously outstanding questions in the field of mammalian embryology and provides new technical tools for future studies in this fascinating field of research.

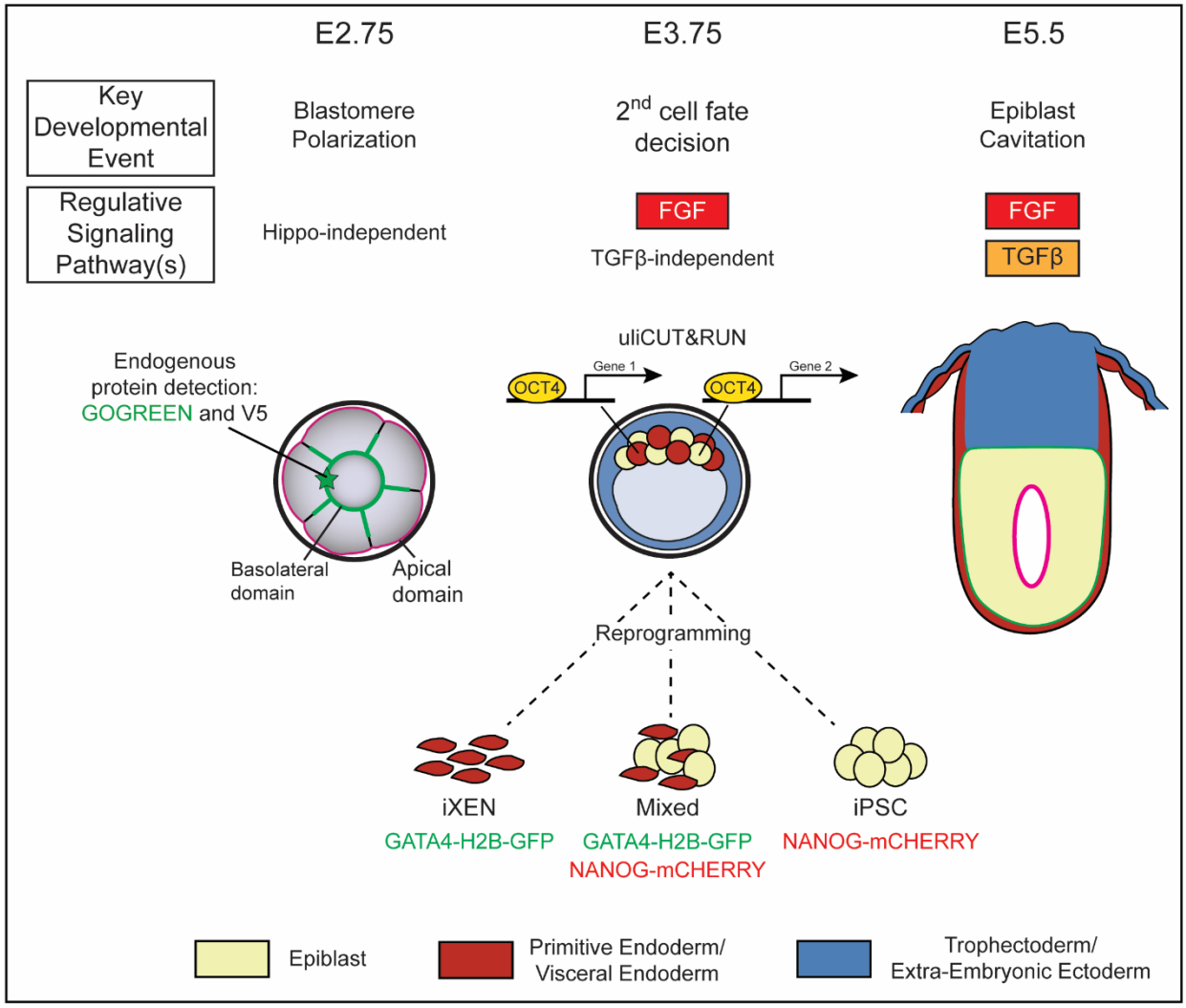

Figure 8.1. Summary of Findings. My work presents several advancements in the study of early embryonic development. I newly identify several molecular regulatory mechanisms in murine development at several early embryonic stages. In Chapter 4, I show that initial blastomere polarization at E2.75 is independent of Hippo signaling. In Chapter 2, I show that the second cell fate decision at E3.75 is independent of TGFβ signaling, but that epiblast cavitation after implantation depends on the interaction between TGFβ and FGF signaling. I also developed novel techniques for the study of embryonic development at these stages, including tagging endogenous proteins for detection (Chapter 5), identifying more accurate fluorescent reporters to distinguish iPSC and iXEN colonies during reprogramming (Chapter 6), and detecting sites of transcription factor binding in embryonic stem cell progenitors by uliCUT&RUN (Chapter 7).

REFERENCES

Abbassi, L., Malki, S., Cockburn, K., Macaulay, A., Robert, C., Rossant, J., & Clarke, H. J. (2016). Multiple Mechanisms Cooperate to Constitutively Exclude the Transcriptional Co-Activator YAP from the Nucleus During Murine Oogenesis1. *Biology of Reproduction*, *94*(5). https://doi.org/10.1095/biolreprod.115.137968

Abou Nader, N., Levasseur, A., Zhang, X., Boerboom, D., Nagano, M. C., & Boyer, A. (2019). Yes-associated protein expression in germ cells is dispensable for spermatogenesis in mice. *Genesis*, *57*(10), 1–7. https://doi.org/10.1002/dvg.23330

Abou Nader, N., Ménard, A., Levasseur, A., St-Jean, G., Boerboom, D., Zamberlam, G., & Boyer, A. (2022). Targeted Disruption of Lats1 and Lats2 in Mice Impairs Testis Development and Alters Somatic Cell Fate. *International Journal of Molecular Sciences*, *23*(21). https://doi.org/10.3390/ijms232113585

Aksoy, I., Jauch, R., Chen, J., Dyla, M., Divakar, U., Bogu, G. K., Teo, R., Leng Ng, C. K., Herath, W., Lili, S., Hutchins, A. P., Robson, P., Kolatkar, P. R., & Stanton, L. W. (2013). Oct4 switches partnering from Sox2 to Sox17 to reinterpret the enhancer code and specify endoderm. *EMBO J*, *32*(7), 938–953. https://doi.org/10.1038/emboj.2013.31

Alarcon, V. B. (2010). Cell polarity regulator PARD6B is essential for trophectoderm formation in the preimplantation mouse embryo. *Biology of Reproduction*, *83*(3), 347–358. https://doi.org/10.1095/biolreprod.110.084400

Alarcon, V. B., & Marikawa, Y. (2018). *Chromatin Regulation of Early Embryonic Lineage Specification* (Vol. 229). http://link.springer.com/10.1007/978-3-319-63187-5

Anani, S., Bhat, S., Honma-Yamanaka, N., Krawchuk, D., & Yamanaka, Y. (2014). Initiation of Hippo signaling is linked to polarity rather than to cell position in the pre-implantation mouse embryo. *Development (Cambridge)*, *141*(14), 2813–2824. https://doi.org/10.1242/dev.107276

Antoniazzi, A. Q., Webb, B. T., Romero, J. J., Ashley, R. L., Smirnova, N. P., Henkes, L. E., Bott, R. C., Oliveira, J. F., Niswender, G. D., Bazer, F. W., & Hansen, T. R. (2013). Endocrine delivery of interferon tau protects the corpus luteum from prostaglandin F2 alpha-induced luteolysis in ewes. *Biology of Reproduction*, *88*(6), 1–12. https://doi.org/10.1095/biolreprod.112.105684

Arman, E., Haffner-Krausz, R., Chen, Y., Heath, J. K., & Lonai, P. (1998). Targeted disruption of fibroblast growth factor (FGF) receptor 2 suggests a role for FGF signaling in pregastrulation mammalian development. *Proceedings of the National Academy of Sciences of the United States of America*, *95*(9), 5082–5087.

https://doi.org/10.1073/pnas.95.9.5082

Arnold, S. J., Maretto, S., Islam, A., Bikoff, E. K., & Robertson, E. J. (2006). Dose-dependent Smad1, Smad5 and Smad8 signaling in the early mouse embryo. *Developmental Biology*, *296*(1), 104–118. https://doi.org/10.1016/j.ydbio.2006.04.442

Arnold, S. J., & Robertson, E. J. (2009). Making a commitment: Cell lineage allocation and axis patterning in the early mouse embryo. *Nature Reviews Molecular Cell Biology*, *10*(2), 91–103. https://doi.org/10.1038/nrm2618

Artus, J., Douvaras, P., Piliszek, A., Isern, J., Baron, M. H., & Hadjantonakis, A. K. (2012). BMP4 signaling directs primitive endoderm-derived XEN cells to an extraembryonic visceral endoderm identity. *Developmental Biology*, *361*(2), 245–262. https://doi.org/10.1016/j.ydbio.2011.10.015

Artus, J., & Hadjantonakis, A. K. (2012). Troika of the mouse blastocyst: lineage segregation and stem cells. *Curr Stem Cell Res Ther*, *7*(1), 78–91. http://www.ncbi.nlm.nih.gov/pubmed/22023624

Artus, J., Piliszek, A., & Hadjantonakis, A. K. (2011). The primitive endoderm lineage of the mouse blastocyst: Sequential transcription factor activation and regulation of differentiation by Sox17. *Developmental Biology*, *350*(2), 393–404. https://doi.org/10.1016/j.ydbio.2010.12.007

Azami, T., Bassalert, C., Allègre, N., Estrella, L. V., Pouchin, P., Ema, M., & Chazaud, C. (2019). Regulation of the erk signalling pathway in the developing mouse blastocyst. *Development (Cambridge)*, *146*(14). https://doi.org/10.1242/dev.177139

Bai, R., Kusama, K., Nakamura, K., Sakurai, T., Kimura, K., Ideta, A., Aoyagi, Y., & Imakawa, K. (2018). Down-regulation of transcription factor OVOL2 contributes to epithelial–mesenchymal transition in a noninvasive type of trophoblast implantation to the maternal endometrium. *The FASEB Journal*, *32*(6), 3371–3384. https://doi.org/10.1096/fj.201701131RR

Baranello, L., Kouzine, F., Sanford, S., & Levens, D. (2016). ChIP bias as a function of cross-linking time. *Chromosome Research*, *24*(2), 175–181. https://doi.org/10.1007/s10577-015-9509-1

Bassalert, C., Valverde-Estrella, L., & Chazaud, C. (2018). Chapter Five - Primitive Endoderm Differentiation: From Specification to Epithelialization. In B. Plusa & A.-K. Hadjantonakis (Eds.), *Current Topics in Developmental Biology* (Vol. 128, pp. 81–104). Academic Press. https://doi.org/10.1016/bs.ctdb.2017.12.001

Beddington, R. S. P., & Robertson, E. J. (1999). Axis development and early asymmetry

in mammals. *Cell*, *96*(2), 195–209. https://doi.org/10.1016/S0092-8674(00)80560-7

Bedzhov, I., & Zernicka-Goetz, M. (2014). Self-organizing properties of mouse pluripotent cells initiate morphogenesis upon implantation. *Cell*, *156*(5), 1032–1044. https://doi.org/10.1016/j.cell.2014.01.023

Ben-Haim, N., Lu, C., Guzman-Ayala, M., Pescatore, L., Mesnard, D., Bischofberger, M., Naef, F., Robertson, E. J. J., & Constam, D. B. (2006). The Nodal Precursor Acting via Activin Receptors Induces Mesoderm by Maintaining a Source of Its Convertases and BMP4. *Developmental Cell*, *11*(3), 313–323. https://doi.org/10.1016/j.devcel.2006.07.005

Beppu, H., Kawabata, M., Hamamoto, T., Chytil, A., Minowa, O., Noda, T., & Miyazono, K. (2000). BMP type II receptor is required for gastrulation and early development of mouse embryos. *Developmental Biology*, *221*(1), 249–258. https://doi.org/10.1006/dbio.2000.9670

Bessonnard, S., Coqueran, S., Vandormael-Pournin, S., Dufour, A., Artus, J., & Cohen-Tannoudji, M. (2017). ICM conversion to epiblast by FGF/ERK inhibition is limited in time and requires transcription and protein degradation. *Scientific Reports*, *7*(1), 1–12. https://doi.org/10.1038/s41598-017-12120-0

Blij, S., Frum, T., Akyol, A., Fearon, E., & Ralston, A. (2012). Maternal Cdx2 is dispensable for mouse development. *Development (Cambridge)*, *139*(21), 3969–3972. https://doi.org/10.1242/dev.086025

Blij, S., Parenti, A., Tabatabai-Yazdi, N., & Ralston, A. (2015). Cdx2 efficiently induces trophoblast stem-like cells in naïve, but not primed, pluripotent stem cells. *Stem Cells and Development*, *24*(11), 1352–1365. https://doi.org/10.1089/scd.2014.0395

Boergermann, J. H., Kopf, J., Yu, P. B., & Knaus, P. (2010). Dorsomorphin and LDN-193189 inhibit BMP-mediated Smad, p38 and Akt signalling in C2C12 cells. *International Journal of Biochemistry and Cell Biology*, *42*(11), 1802–1807. https://doi.org/10.1016/j.biocel.2010.07.018

Boroviak, T., Loos, R., Lombard, P., Okahara, J., Behr, R., Sasaki, E., Nichols, J., Smith, A., & Bertone, P. (2015). Lineage-Specific Profiling Delineates the Emergence and Progression of Naive Pluripotency in Mammalian Embryogenesis. *Developmental Cell*, *35*(3), 366–382. https://doi.org/10.1016/j.devcel.2015.10.011

Bosman, E. A., Lawson, K. A., Debruyn, J., Beek, L., Francis, A., Schoonjans, L., Huylebroek, D., & Zwijsen, A. (2006). Smad5 determines murine amnion fate through the control of bone morphogenetic protein expression and signalling levels. *Development*, *133*(17), 3399–3409. https://doi.org/10.1242/dev.02497

Bragdon, B., Moseychuk, O., Saldanha, S., King, D., Julian, J., & Nohe, A. (2011). Bone Morphogenetic Proteins: A critical review. *Cellular Signalling*, *23*(4), 609–620. https://doi.org/10.1016/j.cellsig.2010.10.003

Brambrink, T., Foreman, R., Welstead, G. G., Lengner, C. J., Wernig, M., Suh, H., & Jaenisch, R. (2008). Sequential Expression of Pluripotency Markers during Direct Reprogramming of Mouse Somatic Cells. *Cell Stem Cell*, *2*(2), 151–159. https://doi.org/10.1016/j.stem.2008.01.004

Brennan, J., Lu, C. C., Norris, D. P., Rodriguez, T. A., Beddington, R. S. P., & Robertson, E. J. (2001). Nodal signalling in the epiblast patterns the early mouse embryo. *Nature*, *411*(2000), 965–969.

Brewer, J. R., Mazot, P., & Soriano, P. (2016). Genetic insights into the mechanisms of Fgf signaling. *Genes and Development*, *30*(7), 751–771. https://doi.org/10.1101/gad.277137.11

Buganim, Y., Faddah, D. A., Cheng, A. W., Itskovich, E., Markoulaki, S., Ganz, K., Klemm, S. L., van Oudenaarden, A., & Jaenisch, R. (2012). Single-Cell Expression Analyses during Cellular Reprogramming Reveal an Early Stochastic and a Late Hierarchic Phase. *Cell*, *150*(6), 1209–1222. https://doi.org/10.1016/j.cell.2012.08.023

Cabantous, S., Terwilliger, T. C., & Waldo, G. S. (2005). Protein tagging and detection with engineered self-assembling fragments of green fluorescent protein. *Nature Biotechnology*, *23*(1), 102–107. https://doi.org/10.1038/nbt1044

Cao, Z., Carey, T. S., Ganguly, A., Wilson, C. A., Paul, S., & Knott, J. G. (2015). Transcription factor AP-2 induces early Cdx2 expression and represses HIPPO signaling to specify the trophectoderm lineage. *Development*, *142*(9), 1606–1615. https://doi.org/10.1242/dev.120238

Capo-Chichi, C. D., Rula, M. E., Smedberg, J. L., Vanderveer, L., Parmacek, M. S., Morrisey, E. E., Godwin, A. K., & Xu, X. X. (2005). Perception of differentiation cues by GATA factors in primitive endoderm lineage determination of mouse embryonic stem cells. *Dev Biol*, *286*(2), 574–586. https://doi.org/10.1016/j.ydbio.2005.07.037

Carbognin, E., Carlini, V., Panariello, F., Chieregato, M., Guerzoni, E., Benvegnù, D., Perrera, V., Malucelli, C., Cesana, M., Grimaldi, A., Mutarelli, M., Carissimo, A., Tannenbaum, E., Kugler, H., Hackett, J. A., Cacchiarelli, D., & Martello, G. (2023). Esrrb guides naive pluripotent cells through the formative transcriptional programme. *Nature Cell Biology*, *25*(5), 643–657. https://doi.org/10.1038/s41556-023-01131-x

Chan, C. J., Costanzo, M., Ruiz-Herrero, T., Mönke, G., Petrie, R. J., Bergert, M., Diz-

Muñoz, A., Mahadevan, L., & Hiiragi, T. (2019). Hydraulic control of mammalian embryo size and cell fate. *Nature*, *571*(7763), 112–116. https://doi.org/10.1038/s41586-019-1309-x

Chan, E. M., Ratanasirintrawoot, S., Park, I. H., Manos, P. D., Loh, Y. H., Huo, H., Miller, J. D., Hartung, O., Rho, J., Ince, T. A., Daley, G. Q., & Schlaeger, T. M. (2009). Live cell imaging distinguishes bona fide human iPS cells from partially reprogrammed cells. *Nat Biotechnol*, *27*(11), 1033–1037. https://doi.org/10.1038/nbt.1580

Chang, C. (2016). Agonists and Antagonists of TGF-β Family Ligands. *Cold Spring Harbor Perspectives in Biology*, *8*(8), a021923. https://doi.org/10.1101/cshperspect.a021923

Chang, H., Huylebroeck, D., Verschueren, K., Guo, Q., Matzuk, M. M., & Zwijsen, A. (1999). Smad5 knockout mice die at mid-gestation due to multiple embryonic and extraembryonic defects. *Development*, *126*(8), 1631–1642.

Chazaud, C., & Yamanaka, Y. (2016). Lineage specification in the mouse preimplantation embryo. *Development (Cambridge)*, *143*(7), 1063–1074. https://doi.org/10.1242/dev.128314

Chazaud, C., Yamanaka, Y., Pawson, T., & Rossant, J. (2006). Early Lineage Segregation between Epiblast and Primitive Endoderm in Mouse Blastocysts through the Grb2-MAPK Pathway. *Developmental Cell*, *10*(5), 615–624. https://doi.org/10.1016/j.devcel.2006.02.020

Chen, D., Zhao, M., & Mundy, G. R. (2004). Bone morphogenetic proteins. *Growth Factors*, *22*(4), 233–241. https://doi.org/10.1080/08977190412331279890

Chen, F., Ma, B., Lin, Y., Luo, X., Xu, T., Zhang, Y., Chen, F., Li, Y., Zhang, Y., Luo, B., Zhang, Q., & Xie, X. (2022). Comparative maternal protein profiling of mouse biparental and uniparental embryos. *GigaScience*, *11*, 1–19. https://doi.org/10.1093/gigascience/giac084

Chen, H., Song, Y., Yang, S., Fu, J., Feng, X., & Huang, W. (2017). YAP mediates human decidualization of the uterine endometrial stromal cells. *Placenta*, *53*, 30–35. https://doi.org/10.1016/j.placenta.2017.03.013

Chen, Q., Chen, H., Zheng, D., Kuang, C., Fang, H., Zou, B., Zhu, W., Bu, G., Jin, T., Wang, Z., Zhang, X., Chen, J., Field, L. J., Rubart, M., Shou, W., & Chen, Y. (2009). Smad7 is required for the development and function of the heart. *Journal of Biological Chemistry*, *284*(1), 292–300. https://doi.org/10.1074/jbc.M807233200

Chen, X., Xu, H., Yuan, P., Fang, F., Huss, M., Vega, V. B., Wong, E., Orlov, Y. L.,

Zhang, W., Jiang, J., Loh, Y. H., Yeo, H. C., Yeo, Z. X., Narang, V., Govindarajan, K. R., Leong, B., Shahab, A., Ruan, Y., Bourque, G., … Ng, H. H. (2008). Integration of External Signaling Pathways with the Core Transcriptional Network in Embryonic Stem Cells. *Cell*, *133*(6), 1106–1117. https://doi.org/10.1016/j.cell.2008.04.043

Cheng, Y., Feng, Y., Jansson, L., Sato, Y., Deguchi, M., Kawamura, K., & Hsueh, A. J. (2015). Actin polymerization-enhancing drugs promote ovarian follicle growth mediated by the Hippo signaling effector YAP. *FASEB Journal*, *29*(6), 2423–2430. https://doi.org/10.1096/fj.14-267856

Chew, J.-L., Loh, Y.-H., Zhang, W., Chen, X., Tam, W.-L., Yeap, L.-S., Li, P., Ang, Y.-S., Lim, B., Robson, P., & Ng, H.-H. (2005). Reciprocal Transcriptional Regulation of Pou5f1 and Sox2 via the Oct4/Sox2 Complex in Embryonic Stem Cells . *Molecular and Cellular Biology*, *25*(14), 6031–6046. https://doi.org/10.1128/mcb.25.14.6031-6046.2005

Chisholm, J. C., & Houliston, E. (1987). Cytokeratin filament assembly in the preimplantation mouse embryo. *Development*, *101*(3), 565–582. http://www.ncbi.nlm.nih.gov/entrez/query.fcgi?cmd=Retrieve&db=PubMed&dopt=Citation&list_uids=2458899

Choudhary, S., & Satija, R. (2022). Comparison and evaluation of statistical error models for scRNA-seq. *Genome Biology*, *23*(1), 27. https://doi.org/10.1186/s13059-021-02584-9

Chu, G. C., Dunn, N. R., Anderson, D. C., Oxburgh, L., & Robertson, E. J. (2004). Differential requirements for Smad4 in TGFβ-dependent patterning of the early mouse embryo. *Development*, *131*(15), 3501–3512. https://doi.org/10.1242/dev.01248

Chu, V. T., Weber, T., Graf, R., Sommermann, T., Petsch, K., Sack, U., Volchkov, P., Rajewsky, K., & Kühn, R. (2016). Efficient generation of Rosa26 knock-in mice using CRISPR/Cas9 in C57BL/6 zygotes. *BMC Biotechnology*, *16*(1), 4. https://doi.org/10.1186/s12896-016-0234-4

Chuva De Sousa Lopes, S. M., Roelen, B. A. J., Monteiro, R. M., Emmens, R., Lin, H. Y., Li, E., Lawson, K. A., & Mummery, C. L. (2004). BMP signaling mediated by ALK2 in the visceral endoderm is necessary for the generation of primordial germ cells in the mouse embryo. *Genes and Development*, *18*(15), 1838–1849. https://doi.org/10.1101/gad.294004

Clark, K. L., George, J. W., Przygrodzka, E., Plewes, M. R., Hua, G., Wang, C., & Davis, J. S. (2022). Hippo Signaling in the Ovary: Emerging Roles in Development, Fertility, and Disease. *Endocrine Reviews*, *43*(6), 1074–1096.

https://doi.org/10.1210/endrev/bnac013

Cockburn, K., Biechele, S., Garner, J., & Rossant, J. (2013). The hippo pathway member nf2 is required for inner cell mass specification. *Current Biology*, *23*(13), 1195–1201. https://doi.org/10.1016/j.cub.2013.05.044

Cockburn, K., & Rossant, J. (2010). Making the blastocyst: Lessons from the mouse. *Journal of Clinical Investigation*, *120*(4), 995–1003. https://doi.org/10.1172/JCI41229

Coonen, E., Dumoulin, J. C. M., & Ramaekers, F. C. S. (1993). Intermediate filament protein expression in early developmental stages of the mouse - A confocal scanning laser microscopy study of in vitro fertilized and in vitro cultured pre-implanation mouse embryos. *Histochemistry*, *99*(2), 141–149. https://doi.org/10.1007/BF00571875

Corson, L. B., Yamanaka, Y., Venus Lai, K. M., & Rossant, J. (2003). Spatial and temporal patterns of ERK signalling during mouse embryogenesis. *Development*, *130*(19), 4527–4537. https://doi.org/10.1242/dev.00669

Costa, M. A. (2016). The endocrine function of human placenta: An overview. *Reproductive BioMedicine Online*, *32*(1), 14–43. https://doi.org/10.1016/j.rbmo.2015.10.005

Coucouvanis, E., & Martin, G. R. (1995). Signals for death and survival: A two-step mechanism for cavitation in the vertebrate embryo. *Cell*, *83*(2), 279–287. https://doi.org/10.1016/0092-8674(95)90169-8

Coucouvanis, E., & Martin, G. R. (1999). BMP signaling plays a role in visceral endoderm differentiation and cavitation in the early mouse embryo. *Development*, *126*(3), 535–546.

Cross, J. C., Werb, Z., & Fisher, S. J. (1994). Implantation and the Placenta: Key Pieces of the Development Puzzle. *Science*, *266*(5190), 1508–1518. https://doi.org/10.1126/science.7985020

Dahl, J. A., & Gilfillan, G. D. (2018). How low can you go? Pushing the limits of low-input ChIP-seq. *Briefings in Functional Genomics*, *17*(2), 89–95. https://doi.org/10.1093/bfgp/elx037

Das, P., Maduzia, L. L., Wang, H., Finelli, A. L., Cho, S. H., Smith, M. M., & Padgettt, R. W. (1998). The Drosophila gene Medea demonstrates the requirement for different classes of Smads in dpp signaling. *Development*, *125*(8), 1519–1528. https://doi.org/10.1242/dev.125.8.1519

Davis, J. R., & Tapon, N. (2019). Hippo signalling during development. *Development*, *146*(18). https://doi.org/10.1242/dev.167106

De Robertis, E. M., & Sasai, Y. (1996). A common plan for dorsoventral patterning in Bilateria. *Nature*, *380*, 37–40.

De Roo, C., Lierman, S., Tilleman, K., & De Sutter, P. (2020). In-vitro fragmentation of ovarian tissue activates primordial follicles through the Hippo pathway . *Human Reproduction Open*, *2020*(4), 1–16. https://doi.org/10.1093/hropen/hoaa048

De Vries, W. N., Binns, L. T., Fancher, K. S., Dean, J., Moore, R., Kemler, R., & Knowles, B. B. (2000). Expression of Cre recombinase in mouse oocytes: A means to study maternal effect genes. *Genesis*, *26*(2), 110–112. https://doi.org/10.1002/(SICI)1526-968X(200002)26:2<110::AID-GENE2>3.0.CO;2-8

Di-Gregorio, A., Sancho, M., Stuckey, D. W., Crompton, L. A., Godwin, J., Mishina, Y., & Rodriguez, T. A. (2007). BMP signalling inhibits premature neural differentiation in the mouse embryo. *Development*, *134*(18), 3359–3369. https://doi.org/10.1242/dev.005967

Dijke, P. T., & Hill, C. S. (2004). New insights into TGF-β-Smad signalling. *Trends in Biochemical Sciences*, *29*(5), 265–273. https://doi.org/10.1016/j.tibs.2004.03.008

Dorey, K., & Amaya, E. (2010). FGF signalling: Diverse roles during early vertebrate embryogenesis. *Development*, *137*(22), 3731–3742. https://doi.org/10.1242/dev.037689

Dorfman, R., & Shilo, B. Z. (2001). Biphasic activation of the BMP pathway patterns the Drosophila embryonic dorsal region. *Development (Cambridge, England)*, *128*(6), 965–972. https://doi.org/10.1242/dev.128.6.965

Dos Santos, R. L., Tosti, L., Radzisheuskaya, A., Caballero, I. M., Kaji, K., Hendrich, B., & Silva, J. C. R. (2014). MBD3/NuRD facilitates induction of pluripotency in a context-dependent manner. *Cell Stem Cell*, *15*(1), 102–110. https://doi.org/10.1016/j.stem.2014.04.019

Dumortier, J. G., Le Verge-Serandour, M., Tortorelli, A. F., Mielke, A., De Plater, L., Turlier, H., & Maître, J. L. (2019). Hydraulic fracturing and active coarsening position the lumen of the mouse blastocyst. *Science*, *365*(6452), 465–468. https://doi.org/10.1126/science.aaw7709

Faure, S., Lee, M. A., Keller, T., Dijke, P. ten, & Whitman, M. (2000). Endogenous patterns of TGFbeta superfamily signaling during early Xenopus. *Development*, *127*(13), 2917–2931.

http://dev.biologists.org/content/127/13/2917%5Cnhttp://dev.biologists.org/content/127/13/2917.long%5Cnhttp://www.ncbi.nlm.nih.gov/pubmed/10851136

Feldman, B., Poueymirou, W., Papaioannou, V. E., M., T., DeChiara, & Goldfarb, M. (1995). Requirement of FGF-4 for postimplantation mouse. *Science*, *Vol. 267,*(January), 13–17.

Feng, S., Sekine, S., Pessino, V., Li, H., Leonetti, M. D., & Huang, B. (2017). Improved split fluorescent proteins for endogenous protein labeling. *Nature Communications*, *8*(1), 370. https://doi.org/10.1038/s41467-017-00494-8

Fernandes, M. G., Dries, R., Roost, M. S., Semrau, S., De Melo Bernardo, A., Davis, R. P., Ramakrishnan, R., Szuhai, K., Maas, E., Umans, L., Abon Escalona, V., Salvatori, D., Deforce, D., Van Criekinge, W., Huylebroeck, D., Mummery, C., Zwijsen, A., & Chuva De Sousa Lopes, S. M. (2016). BMP-SMAD Signaling Regulates Lineage Priming, but Is Dispensable for Self-Renewal in Mouse Embryonic Stem Cells. *Stem Cell Reports*, *6*(1), 85–94. https://doi.org/10.1016/j.stemcr.2015.11.012

Filimonow, K., & de la Fuente, R. (2022). Specification and role of extraembryonic endoderm lineages in the periimplantation mouse embryo. *Theriogenology*, *180*, 189–206. https://doi.org/10.1016/j.theriogenology.2021.12.021

Fisher, S. J. (2015). Why is placentation abnormal in preeclampsia? *American Journal of Obstetrics and Gynecology*, *213*(4), S115–S122. https://doi.org/10.1016/j.ajog.2015.08.042

Frankenberg, S., Gerbe, F., Bessonnard, S., Belville, C., Pouchin, P., Bardot, O., & Chazaud, C. (2011). Primitive Endoderm Differentiates via a Three-Step Mechanism Involving Nanog and RTK Signaling. *Developmental Cell*, *21*(6), 1005–1013. https://doi.org/10.1016/j.devcel.2011.10.019

Freyer, L., Schröter, C., Saiz, N., Schrode, N., Nowotschin, S., Martinez-Arias, A., & Hadjantonakis, A. K. (2015). A loss-of-function and H2B-Venus transcriptional reporter allele for Gata6 in mice. *BMC Dev Biol*, *15*, 38. https://doi.org/10.1186/s12861-015-0086-5

Friedrich, G., & Soriano, P. (1991). Promoter traps in embryonic stem cells: a genetic screen to identify and mutate developmental genes in mice. *Genes & Development*, *5*(9), 1513–1523. https://doi.org/10.1101/gad.5.9.1513

Frum, T., Halbisen, M. A., Wang, C., Amiri, H., Robson, P., & Ralston, A. (2013). Oct4 Cell-autonomously promotes primitive endoderm development in the mouse blastocyst. *Developmental Cell*, *25*(6), 610–622. https://doi.org/10.1016/j.devcel.2013.05.004

Frum, T., Murphy, T. M., & Ralston, A. (2018). HIPPO signaling resolves embryonic cell fate conflicts during establishment of pluripotency in vivo. *ELife*, *7*, 1–21. https://doi.org/10.7554/elife.42298

Frum, T., & Ralston, A. (2015). Cell signaling and transcription factors regulating cell fate during formation of the mouse blastocyst. *Trends Genet*, *31*(7), 402–410. https://doi.org/10.1016/j.tig.2015.04.002

Frum, T., & Ralston, A. (2020). Culture conditions antagonize lineage-promoting signaling in the mouse blastocyst. *Reproduction*, *160*(1), V5–V7. https://doi.org/10.1530/REP-20-0107

Frum, T., Watts, J. L., & Ralston, A. (2019). TEAD4, YAP1 and WWTR1 prevent the premature onset of pluripotency prior to the 16-cell stage. *Development (Cambridge)*, *146*(17), 1–7. https://doi.org/10.1242/dev.179861

Fu, D., Lv, X., Hua, G., He, C., Dong, J., Lele, S. M., Li, D. W. C., Zhai, Q., Davis, J. S., & Wang, C. (2014). YAP regulates cell proliferation, migration, and steroidogenesis in adult granulosa cell tumors. *Endocrine-Related Cancer*, *21*(2), 297–310. https://doi.org/10.1530/ERC-13-0339

Fu, M., Hu, Y., Lan, T., Guan, K. L., Luo, T., & Luo, M. (2022). The Hippo signalling pathway and its implications in human health and diseases. *Signal Transduction and Targeted Therapy*, *7*(1). https://doi.org/10.1038/s41392-022-01191-9

Fujikura, J., Yamato, E., Yonemura, S., Hosoda, K., Masui, S., Nakao, K., Miyazaki Ji, J., & Niwa, H. (2002). Differentiation of embryonic stem cells is induced by GATA factors. *Genes Dev*, *16*(7), 784–789. http://www.ncbi.nlm.nih.gov/entrez/query.fcgi?cmd=Retrieve&db=PubMed&dopt=Citation&list_uids=11937486

Fujiwara, T., Dehart, D. B., Sulik, K. K., & Hogan, B. L. M. (2002). Distinct requirements for extra-embryonic and embryonic bone morphogenetic protein 4 in the formation of the node and primitive streak and coordination of left-right asymmetry in the mouse. *Development*, *129*(20), 4685–4696. https://doi.org/10.1242/dev.129.20.4685

Fujiwara, T., Dunn, N. R., & Hogan, B. L. M. (2001). Bone morphogenetic protein 4 in the extraembryonic mesoderm is required for allantois development and the localization and survival of primordial germ cells in the mouse. *Proceedings of the National Academy of Sciences of the United States of America*, *98*(24), 13739–13744. https://doi.org/10.1073/pnas.241508898

Goissis, M. D., Bradshaw, B., Posfai, E., & Rossant, J. (2023). *FGF2 and BMP4 influence on FGFR2 dynamics during the segregation of 2 epiblast and primitive*

endoderm cells in the pre-implantation mouse embryo. 1–14. https://doi.org/10.1371/journal.pone.0279515

Goldman-Wohl, D., & Yagel, S. (2002). Regulation of trophoblast invasion: From normal implantation to pre-eclampsia. *Molecular and Cellular Endocrinology*, *187*(1–2), 233–238. https://doi.org/10.1016/S0303-7207(01)00687-6

Grabarek, J. B., Zyzyńska, K., Saiz, N., Piliszek, A., Frankenberg, S., Nichols, J., Hadjantonakis, A. K., & Plusa, B. (2012). Differential plasticity of epiblast and primitive endoderm precursors within the ICM of the early mouse embryo. *Development*, *139*(1), 129–139. https://doi.org/10.1242/dev.067702

Graham, S. J. L., Wicher, K. B., Jedrusik, A., Guo, G., Herath, W., Robson, P., & Zernicka-Goetz, M. (2014). BMP signalling regulates the pre-implantation development of extra-embryonic cell lineages in the mouse embryo. *Nature Communications*, *5*(May). https://doi.org/10.1038/ncomms6667

Grosbois, J., & Demeestere, I. (2018). Dynamics of PI3K and Hippo signaling pathways during in vitro human follicle activation. *Human Reproduction (Oxford, England)*, *33*(9), 1705–1714. https://doi.org/10.1093/humrep/dey250

Gu, B., Posfai, E., & Rossant, J. (2018). Efficient generation of targeted large insertions by microinjection into two-cell-stage mouse embryos. *Nature Biotechnology*, *36*(7), 632–637. https://doi.org/10.1038/nbt.4166

Gu, Z., Reynolds, E. M., Song, J., Lei, H., Feijen, A., Yu, L., He, W., MacLaughlin, D. T., Van Den Eijnden-Van Raaij, J., Donahoe, P. K., & Li, E. (1999). The type I serine/threonine kinase receptor ActRIA (ALK2) is required for gastrulation of the mouse embryo. *Development*, *126*(11), 2551–2561.

Guan, J., Wang, G., Wang, J., Zhang, Z., Fu, Y., Cheng, L., Meng, G., Lyu, Y., Zhu, J., Li, Y., Wang, Y., Liuyang, S., Liu, B., Yang, Z., He, H., Zhong, X., Chen, Q., Zhang, X., Sun, S., … Deng, H. (2022). Chemical reprogramming of human somatic cells to pluripotent stem cells. *Nature*, *605*(7909), 325–331. https://doi.org/10.1038/s41586-022-04593-5

Gupta, A., Lutolf, M. P., Hughes, A. J., & Sonnen, K. F. (2021). Bioengineering in vitro models of embryonic development. *Stem Cell Reports*, *16*(5), 1104–1116. https://doi.org/10.1016/j.stemcr.2021.04.005

Hafemeister, C., & Satija, R. (2019). Normalization and variance stabilization of single-cell RNA-seq data using regularized negative binomial regression. *Genome Biology*, *20*(1), 296. https://doi.org/10.1186/s13059-019-1874-1

Hainer, S. J., Bošković, A., McCannell, K. N., Rando, O. J., & Fazzio, T. G. (2019).

Profiling of Pluripotency Factors in Single Cells and Early Embryos. *Cell*, *177*(5), 1319-1329.e11. https://doi.org/10.1016/j.cell.2019.03.014

Hainer, S. J., & Fazzio, T. G. (2019). High-Resolution Chromatin Profiling Using CUT&RUN. *Current Protocols in Molecular Biology*, *126*, 1–22. https://doi.org/10.1002/cpmb.85

Halimi, R., Levin-Zaidman, S., Levin-Salomon, V., Bialik, S., & Kimchi, A. (2022). Epiblast fragmentation by shedding—a novel mechanism to eliminate cells in post-implantation mouse embryos. *Cell Death and Differentiation*, *29*(6), 1255–1266. https://doi.org/10.1038/s41418-021-00918-5

Hansen, T. R., Austin, K. J., Perry, D. J., Pru, J. K., Teixeira, M. G., & Johnson, G. A. (1999). Mechanism of action of interferon-tau in the uterus during early pregnancy. *Journal of Reproduction and Fertility. Supplement*, *54*, 329–339.

Hao, Y., Hao, S., Andersen-Nissen, E., Mauck, W. M., Zheng, S., Butler, A., Lee, M. J., Wilk, A. J., Darby, C., Zager, M., Hoffman, P., Stoeckius, M., Papalexi, E., Mimitou, E. P., Jain, J., Srivastava, A., Stuart, T., Fleming, L. M., Yeung, B., … Satija, R. (2021). Integrated analysis of multimodal single-cell data. *Cell*, *184*(13), 3573-3587.e29. https://doi.org/10.1016/j.cell.2021.04.048

Hari Reddi, A. (2003). Bone morphogenetic proteins. *The Cytokine Handbook*, 1179–1185. https://doi.org/10.1016/B978-012689663-3/50055-7

Harvey, K. F., Pfleger, C. M., & Hariharan, I. K. (2003). The Drosophila Mst ortholog, hippo, restricts growth and cell proliferation and promotes apoptosis. *Cell*, *114*(4), 457–467. https://doi.org/10.1016/S0092-8674(03)00557-9

Hayashi, K., Kobayashi, T., Umino, T., Goitsuka, R., Matsui, Y., & Kitamura, D. (2002). SMAD1 signaling is critical for initial commitment of germ cell lineage from mouse epiblast. *Mechanisms of Development*, *118*(1–2), 99–109. https://doi.org/10.1016/S0925-4773(02)00237-X

He, X., Chi, G., Li, M., Xu, J., Zhang, L., Song, Y., Wang, L., & Li, Y. (2020). Characterisation of extraembryonic endoderm-like cells from mouse embryonic fibroblasts induced using chemicals alone. *Stem Cell Research \& Therapy*, *11*(1), 157. https://doi.org/10.1186/s13287-020-01664-0

Hefel, A., & Smolikove, S. (2019). Tissue-Specific Split sfGFP System for Streamlined Expression of GFP Tagged Proteins in the Caenorhabditis elegans Germline. *G3 (Bethesda, Md.)*, *9*(6), 1933–1943. https://doi.org/10.1534/g3.119.400162

Hill, C. S. (2016). Transcriptional control by the SMADs. *Cold Spring Harbor Perspectives in Biology*, *8*(10). https://doi.org/10.1101/cshperspect.a022079

Hirate, Y., Hirahara, S., Inoue, K. I., Suzuki, A., Alarcon, V. B., Akimoto, K., Hirai, T., Hara, T., Adachi, M., Chida, K., Ohno, S., Marikawa, Y., Nakao, K., Shimono, A., & Sasaki, H. (2013). Polarity-dependent distribution of angiomotin localizes hippo signaling in preimplantation embryos. *Current Biology*, *23*(13), 1181–1194. https://doi.org/10.1016/j.cub.2013.05.014

Hirate, Y., Hirahara, S., Inoue, K. ichi, Kiyonari, H., Niwa, H., & Sasaki, H. (2015). Par-aPKC-dependent and -independent mechanisms cooperatively control cell polarity, Hippo signaling, and cell positioning in 16-cell stage mouse embryos. *Development Growth and Differentiation*, *57*(8), 544–556. https://doi.org/10.1111/dgd.12235

Hirate, Y., & Sasaki, H. (2014). The role of angiomotin phosphorylation in the Hippo pathway during preimplantation mouse development. *Tissue Barriers*, *2*(1). https://doi.org/10.4161/tisb.28127

Home, P., Ray, S., Dutta, D., Bronshteyn, I., Larson, M., & Paul, S. (2009). GATA3 is selectively expressed in the trophectoderm of peri-implantation embryo and directly regulates Cdx2 gene expression. *J Biol Chem*, *284*(42), 28729–28737. https://doi.org/10.1074/jbc.M109.016840

Home, P., Saha, B., Ray, S., Dutta, D., Gunewardena, S., Yoo, B., Pal, A., Vivian, J. L., Larson, M., Petroff, M., Gallagher, P. G., Schulz, V. P., White, K. L., Golos, T. G., Behr, B., & Paul, S. (2012). Altered subcellular localization of transcription factor TEAD4 regulates first mammalian cell lineage commitment. *Proceedings of the National Academy of Sciences of the United States of America*, *109*(19), 7362–7367. https://doi.org/10.1073/pnas.1201595109

Hossain, Z., Ali, S. M., Ko, H. L., Xu, J., Ng, C. P., Guo, K., Qi, Z., Ponniah, S., Hong, W., & Hunziker, W. (2007). Glomerulocystic kidney disease in mice with a targeted inactivation of Wwtr1. *Proceedings of the National Academy of Sciences*, *104*(5), 1631–1636. https://doi.org/10.1073/pnas.0605266104

Hsueh, A. J. W., Kawamura, K., Cheng, Y., & Fauser, B. C. J. M. (2015). Intraovarian control of early folliculogenesis. *Endocrine Reviews*, *36*(1), 1–24. https://doi.org/10.1210/er.2014-1020

Hu, L. L., Su, T., Luo, R. C., Zheng, Y. H., Huang, J., Zhong, Z. S., Nie, J., & Zheng, L. P. (2019). Hippo pathway functions as a downstream effector of AKT signaling to regulate the activation of primordial follicles in mice. *Journal of Cellular Physiology*, *234*(2), 1578–1587. https://doi.org/10.1002/jcp.27024

Hu, M., Zheng, Y., Liao, J., Wen, L., Cheng, J., Huang, J., Huang, B., Lin, L., Long, Y., Wu, Y., Ye, X., Fu, Y., Qi, H., Baker, P. N., & Tong, C. (2022). miR21 modulates the Hippo signaling pathway via interference with PP2A Bβ to inhibit trophoblast invasion and cause preeclampsia. *Molecular Therapy - Nucleic Acids*,

30(December), 143–161. https://doi.org/10.1016/j.omtn.2022.09.006

Huangfu, D., Maehr, R., Guo, W., Eijkelenboom, A., Snitow, M., Chen, A. E., & Melton, D. A. (2008). Induction of pluripotent stem cells by defined factors is greatly improved by small-molecule compounds. *Nature Biotechnology*, *26*(7), 795–797. https://doi.org/10.1038/nbt1418

Huminiecki, L., Goldovsky, L., Freilich, S., Moustakas, A., Ouzounis, C., & Heldin, C. H. (2009). Emergence, development and diversification of the TGF- signalling pathway within the animal kingdom. *BMC Evolutionary Biology*, *9*(1), 1–17. https://doi.org/10.1186/1471-2148-9-28

Imakawa, K., Anthony, R. V, Kazemi, M., & Marotti, K. R. (1987). Interferon-like sequence of ovine trophoblast protein secreted by embryonic trophectoderm. *Nature*, *330*, 377–379.

Israel, S., Ernst, M., Psathaki, O. E., Drexler, H. C. A., Casser, E., Suzuki, Y., Makalowski, W., Boiani, M., Fuellen, G., & Taher, L. (2019). An integrated genome-wide multi-omics analysis of gene expression dynamics in the preimplantation mouse embryo. *Scientific Reports*, *9*(1), 1–15. https://doi.org/10.1038/s41598-019-49817-3

Jakobsen, J. S., Bagger, F. O., Hasemann, M. S., Schuster, M. B., Frank, A. K., Waage, J., Vitting-Seerup, K., & Porse, B. T. (2015). Amplification of pico-scale DNA mediated by bacterial carrier DNA for small-cell-number transcription factor ChIP-seq. *BMC Genomics*, *16*(1), 1–12. https://doi.org/10.1186/s12864-014-1195-4

Jedrusik, A., Parfitt, D. E., Guo, G., Skamagki, M., Grabarek, J. B., Johnson, M. H., Robson, P., & Zernicka-Goetz, M. (2008). Role of Cdx2 and cell polarity in cell allocation and specification of trophectoderm and inner cell mass in the mouse embryo. *Genes and Development*, *22*(19), 2692–2706. https://doi.org/10.1101/gad.486108

Ji, S. Y., Liu, X. M., Li, B. T., Zhang, Y. L., Liu, H. Bin, Zhang, Y. C., Chen, Z. J., Liu, J., & Fan, H. Y. (2017). The polycystic ovary syndrome-associated gene Yap1 is regulated by gonadotropins and sex steroid hormones in hyperandrogenism-induced oligo-ovulation in mouse. *Molecular Human Reproduction*, *23*(10), 698–707. https://doi.org/10.1093/molehr/gax046

Jiang, L.-L., Xie, J.-K., Cui, J.-Q., Wei, D., Yin, B.-L., Zhang, Y.-N., Chen, Y.-H., Han, X., Wang, Q., & Zhang, C.-L. (2017). Promoter methylation of yes-associated protein (YAP1) gene in polycystic ovary syndrome. *Medicine*, *96*(2), e5768. https://doi.org/10.1097/MD.0000000000005768

Johnson, M. H., & Ziomek, C. A. (1981). The foundation of two distinct cell lineages

within the mouse morula. *Cell*, *24*(1), 71–80. https://doi.org/10.1016/0092-8674(81)90502-X

Joris, H., Nagy, Z., Van De Velde, H., De Vos, A., & Van Steirteghem, A. (1998). Intracytoplasmic sperm injection: Laboratory set-up and injection procedure. *Human Reproduction*, *13*(SUPPL. 1), 76–86. https://doi.org/10.1093/humrep/13.suppl_1.76

Judson, R. L., Babiarz, J. E., Venere, M., & Blelloch, R. (2009). Embryonic stem cell-specific microRNAs promote induced pluripotency. *Nature Biotechnology*, *27*(5), 459–461. https://doi.org/10.1038/nbt.1535

Kamiyama, D., Sekine, S., Barsi-Rhyne, B., Hu, J., Chen, B., Gilbert, L. A., Ishikawa, H., Leonetti, M. D., Marshall, W. F., Weissman, J. S., & Huang, B. (2016). Versatile protein tagging in cells with split fluorescent protein. *Nature Communications*, *7*(1), 11046. https://doi.org/10.1038/ncomms11046

Kang, M., Garg, V., & Hadjantonakis, A. K. (2017). Lineage Establishment and Progression within the Inner Cell Mass of the Mouse Blastocyst Requires FGFR1 and FGFR2. *Developmental Cell*, *41*(5), 496-510.e5. https://doi.org/10.1016/j.devcel.2017.05.003

Kang, M., Piliszek, A., Artus, J., & Hadjantonakis, A. K. (2013). FGF4 is required for lineage restriction and salt-and-pepper distribution of primitive endoderm factors but not their initial expression in the mouse. *Development (Cambridge)*, *140*(2), 267–279. https://doi.org/10.1242/dev.084996

Karasek, C., Ashry, M., Driscoll, C. S., & Knott, J. G. (2020). A tale of two cell-fates: Role of the Hippo signaling pathway and transcription factors in early lineage formation in mouse preimplantation embryos. *Molecular Human Reproduction*, *26*(9), 653–664. https://doi.org/10.1093/molehr/gaaa052

Kawamura, K., Cheng, Y., Suzuki, N., Deguchi, M., Sato, Y., Takae, S., Ho, C., Kawamura, N., Tamura, M., Hashimoto, S., Sugishita, Y., Morimoto, Y., Hosoi, Y., Yoshioka, N., Ishizuka, B., & Hsueh, A. J. (2013). Hippo signaling disruption and Akt stimulation of ovarian follicles for infertility treatment. *Proceedings of the National Academy of Sciences of the United States of America*, *110*(43), 17474–17479. https://doi.org/10.1073/pnas.1312830110

Kim, J., Zhao, T., Petralia, R. S., Yu, Y., Peng, H., Myers, E., & Magee, J. C. (2012). mGRASP enables mapping mammalian synaptic connectivity with light microscopy. *Nature Methods*, *9*(1), 96–102. https://doi.org/10.1038/nmeth.1784

Knöfler, M., Haider, S., Saleh, L., Pollheimer, J., Gamage, T. K. J. B., & James, J. (2019). Human placenta and trophoblast development: key molecular mechanisms

and model systems. *Cellular and Molecular Life Sciences*, *76*(18), 3479–3496. https://doi.org/10.1007/s00018-019-03104-6

Korotkevich, E., Niwayama, R., Courtois, A., Friese, S., Berger, N., Buchholz, F., & Hiiragi, T. (2017). The Apical Domain Is Required and Sufficient for the First Lineage Segregation in the Mouse Embryo. *Developmental Cell*, *40*(3), 235-247.e7. https://doi.org/10.1016/j.devcel.2017.01.006

Koutsourakis, M., Langeveld, A., Patient, R., Beddington, R., & Grosveld, F. (1999). The transcription factor GATA6 is essential for early extraembryonic development. *Development*, *126*(4), 723–732. http://www.ncbi.nlm.nih.gov/pubmed/9895320

Kramer, C., Mayr, T., Nowak, M., Schumacher, J., Runke, G., Bauer, H., Wagner, D. S., Schmid, B., Imai, Y., Talbot, W. S., Mullins, M. C., & Hammerschmidt, M. (2002). Maternally Supplied Smad5 Is Required for Ventral Specification in Zebrafish Embryos Prior to Zygotic Bmp Signaling. *Developmental Biology*, *250*(2), 263–279. https://doi.org/10.1006/dbio.2002.0805

Krawchuk, D., Honma-Yamanaka, N., Anani, S., & Yamanaka, Y. (2013). FGF4 is a limiting factor controlling the proportions of primitive endoderm and epiblast in the ICM of the mouse blastocyst. *Developmental Biology*, *384*(1), 65–71. https://doi.org/10.1016/j.ydbio.2013.09.023

Kunath, T., Arnaud, D., Uy, G. D., Okamoto, I., Chureau, C., Yamanaka, Y., Heard, E., Gardner, R. L., Avner, P., & Rossant, J. (2005). Imprinted X-inactivation in extra-embryonic endoderm cell lines from mouse blastocysts. *Development*, *132*(7), 1649–1661. https://doi.org/10.1242/dev.01715

Kuo, C. T., Morrisey, E. E., Anandappa, R., Sigrist, K., Lu, M. M., Parmacek, M. S., Soudais, C., & Leiden, J. M. (1997). GATA4 transcription factor is required for ventral morphogenesis and heart tube formation. *Genes Dev*, *11*(8), 1048–1060. http://www.ncbi.nlm.nih.gov/pubmed/9136932

Kurotaki, Y., Hatta, K., Nakao, K., Nabeshima, Y. I., & Fujimori, T. (2007). Blastocyst axis is specified independently of early cell lineage but aligns with the ZP shape. *Science*, *316*(5825), 719–723. https://doi.org/10.1126/science.1138591

Kusama, K., Bai, R., Sakurai, T., Bai, H., Ideta, A., Aoyagi, Y., & Imakawa, K. (2016). A transcriptional cofactor YAP regulates IFNT expression via transcription factor TEAD in bovine conceptuses. *Domestic Animal Endocrinology*, *57*, 21–30. https://doi.org/10.1016/j.domaniend.2016.05.002

Kwon, G. S., Viotti, M., & Hadjantonakis, A. K. (2008). The Endoderm of the Mouse Embryo Arises by Dynamic Widespread Intercalation of Embryonic and Extraembryonic Lineages. *Developmental Cell*, *15*(4), 509–520.

https://doi.org/10.1016/j.devcel.2008.07.017

Lanner, F., & Rossant, J. (2010). The role of FGF/Erk signaling in pluripotent cells. *Development*, *137*(20), 3351–3360. https://doi.org/10.1242/dev.050146

Lanza, D. G., Gaspero, A., Lorenzo, I., Liao, L., Zheng, P., Wang, Y., Deng, Y., Cheng, C., Zhang, C., Seavitt, J. R., DeMayo, F. J., Xu, J., Dickinson, M. E., Beaudet, A. L., & Heaney, J. D. (2018). Comparative analysis of single-stranded DNA donors to generate conditional null mouse alleles. *BMC Biology*, *16*(1), 69. https://doi.org/10.1186/s12915-018-0529-0

Lawson, K. A., Dunn, N. R., Roelen, B. A. J., Zeinstra, L. M., Davis, A. M., Wright, C. V. E., Korving, J. P. W. F. M., & Hogan, B. L. M. (1999). Bmp4 is required for the generation of primordial germ cells in the mouse embryo. *Genes and Development*, *13*(4), 424–436. https://doi.org/10.1101/gad.13.4.424

Le Bin, G. C., Muñoz-Descalzo, S., Kurowski, A., Leitch, H., Lou, X., Mansfield, W., Etienne-Dumeau, C., Grabole, N., Mulas, C., Niwa, H., Hadjantonakis, A. K., & Nichols, J. (2014). Oct4 is required for lineage priming in the developing inner cell mass of the mouse blastocyst. *Development (Cambridge)*, *141*(5), 1001–1010. https://doi.org/10.1242/dev.096875

Lee, M. T., Bonneau, A. R., & Giraldez, A. J. (2014). Zygotic genome activation during the maternal-to-zygotic transition. *Annual Review of Cell and Developmental Biology*, *30*, 581–613. https://doi.org/10.1146/annurev-cellbio-100913-013027

Lengner, C. J., Camargo, F. D., Hochedlinger, K., Welstead, G. G., Zaidi, S., Gokhale, S., Scholer, H. R., Tomilin, A., & Jaenisch, R. (2007). Oct4 expression is not required for mouse somatic stem cell self-renewal. *Cell Stem Cell*, *1*(4), 403–415. https://doi.org/10.1016/j.stem.2007.07.020

Leonetti, M. D., Sekine, S., Kamiyama, D., Weissman, J. S., & Huang, B. (2016). A scalable strategy for high-throughput GFP tagging of endogenous human proteins. *Proceedings of the National Academy of Sciences of the United States of America*, *113*(25), E3501--8. https://doi.org/10.1073/pnas.1606731113

Leung, C. Y., & Zernicka-Goetz, M. (2013). Angiomotin prevents pluripotent lineage differentiation in mouse embryos via Hippo pathway-dependent and-independent mechanisms. *Nature Communications*, *4*. https://doi.org/10.1038/ncomms3251

Levasseur, A., Paquet, M., Boerboom, D., & Boyer, A. (2017). Yes-associated protein and WW-containing transcription regulator 1 regulate the expression of sex-determining genes in Sertoli cells, but their inactivation does not cause sex reversal†. *Biology of Reproduction*, *97*(1), 162–175. https://doi.org/10.1093/biolre/iox057

Li, C., Li, Y.-P., Fu, X.-Y., & Deng, C. X. (2010). Anterior Visceral Endoderm SMAD4 Signaling Specifies Anterior Embryonic Patterning and Head Induction in Mice. *International Journal of Biological Sciences*, *6*(6), 569–583.

Li, J., Zhou, F., Zheng, T., Pan, Z., Liang, X., Huang, J., Zheng, L., & Zheng, Y. (2015). Ovarian Germline Stem Cells (OGSCs) and the Hippo Signaling Pathway Association with Physiological and Pathological Ovarian Aging in Mice. *Cellular Physiology and Biochemistry*, *36*(5), 1712–1724. https://doi.org/10.1159/000430144

Li, L., Zheng, P., & Dean, J. (2010). Maternal control of early mouse development. *Development*, *137*(6), 859–870. https://doi.org/10.1242/dev.039487

Li, M., & Belmonte, J. C. I. (2017). Ground rules of the pluripotency gene regulatory network. *Nature Reviews Genetics*, *18*(3), 180–191. https://doi.org/10.1038/nrg.2016.156

Li, S., Edgar, D., Fässler, R., Wadsworth, W., & Yurchenco, P. D. (2003). The role of laminin in embryonic cell polarization and tissue organization. *Developmental Cell*, *4*(5), 613–624. https://doi.org/10.1016/S1534-5807(03)00128-X

Li, T., Zhao, H., Zhao, X., Zhang, B., Cui, L., Shi, Y., Li, G., Wang, P., & Chen, Z. J. (2012). Identification of YAP1 as a novel susceptibility gene for polycystic ovary syndrome. *Journal of Medical Genetics*, *49*(4), 254–257. https://doi.org/10.1136/jmedgenet-2011-100727

Liang, X., Zhou, Q., Li, X., Sun, Y., Lu, M., Dalton, N., Ross, J., & Chen, J. (2005). PINCH1 Plays an Essential Role in Early Murine Embryonic Development but Is Dispensable in Ventricular Cardiomyocytes. *Molecular and Cellular Biology*, *25*(8), 3056–3062. https://doi.org/10.1128/mcb.25.8.3056-3062.2005

Lim, H. Y. G., Alvarez, Y. D., Gasnier, M., Wang, Y., Tetlak, P., Bissiere, S., Wang, H., Biro, M., & Plachta, N. (2020). Keratins are asymmetrically inherited fate determinants in the mammalian embryo. *Nature*, *585*(7825), 404–409. https://doi.org/10.1038/s41586-020-2647-4

Lim, H. Y. G., & Plachta, N. (2021). Cytoskeletal control of early mammalian development. *Nature Reviews Molecular Cell Biology*, *22*(8), 548–562. https://doi.org/10.1038/s41580-021-00363-9

Liu, C. Y., Zha, Z. Y., Zhou, X., Zhang, H., Huang, W., Zhao, D., Li, T., Chan, S. W., Lim, C. J., Hong, W., Zhao, S., Xiong, Y., Lei, Q. Y., & Guan, K. L. (2010). The hippo tumor pathway promotes TAZ degradation by phosphorylating a phosphodegron and recruiting the SCFβ-TrCP E3 ligase. *Journal of Biological Chemistry*, *285*(48), 37159–37169. https://doi.org/10.1074/jbc.M110.152942

Liu, W., Selever, J., Wang, D., Lu, M. F., Mosest, K. A., Schwartz, R. J., & Martin, J. F. (2004). Bmp4 signaling is required for outflow-tract septation and branchial-arch artery remodeling. *Proceedings of the National Academy of Sciences of the United States of America*, *101*(13), 4489–4494. https://doi.org/10.1073/pnas.0308466101

Loh, Y. H., Wu, Q., Chew, J. L., Vega, V. B., Zhang, W., Chen, X., Bourque, G., George, J., Leong, B., Liu, J., Wong, K. Y., Sung, K. W., Lee, C. W. H., Zhao, X. D., Chiu, K. P., Lipovich, L., Kuznetsov, V. A., Robson, P., Stanton, L. W., … Ng, H. H. (2006). The Oct4 and Nanog transcription network regulates pluripotency in mouse embryonic stem cells. *Nature Genetics*, *38*(4), 431–440. https://doi.org/10.1038/ng1760

Lorthongpanich, C., & Issaragrisil, S. (2015). Emerging Role of the Hippo Signaling Pathway in Position Sensing and Lineage Specification in Mammalian Preimplantation Embryos1. *Biology of Reproduction*, *92*(6), 1–10. https://doi.org/10.1095/biolreprod.114.127803

Lorthongpanich, C., Messerschmidt, D. M., Chan, S. W., Hong, W., Knowles, B. B., & Solter, D. (2013). Temporal reduction of LATS kinases in the early preimplantation embryo prevents ICM lineage differentiation. *Genes and Development*, *27*(13), 1441–1446. https://doi.org/10.1101/gad.219618.113

Lowery, J. W., Brookshire, B., & Rosen, V. (2016). A survey of strategies to modulate the bone morphogenetic protein signaling pathway: Current and future perspectives. *Stem Cells International*, *2016*. https://doi.org/10.1155/2016/7290686

Lu, C. C., Brennan, J., & Robertson, E. J. (2001). From fertilization to gastrulation: Axis formation in the mouse embryo. *Current Opinion in Genetics and Development*, *11*(4), 384–392. https://doi.org/10.1016/S0959-437X(00)00208-2

Lv, X., He, C., Huang, C., Hua, G., Chen, X., Timm, B. K., Maclin, V. M., Haggerty, A. A., Aust, S. K., Golden, D. M., Dave, B. J., Tseng, Y. A., Chen, L., Wang, H., Chen, P., Klinkebiel, D. L., Karpf, A. R., Dong, J., Drapkin, R. I., … Wang, C. (2020). Reprogramming of ovarian granulosa cells by YAP1 leads to development of high-grade cancer with mesenchymal lineage and serous features. *Science Bulletin*, *65*(15), 1281–1296. https://doi.org/10.1016/j.scib.2020.03.040

Lv, X., He, C., Huang, C., Wang, H., Hua, G., Wang, Z., Zhou, J., Chen, X., Ma, B., Timm, B. K., Maclin, V., Dong, J., Rueda, B. R., Davis, J. S., & Wang, C. (2019). Timely expression and activation of YAP1 in granulosa cells is essential for ovarian follicle development. *FASEB Journal : Official Publication of the Federation of American Societies for Experimental Biology*, *33*(9), 10049–10064. https://doi.org/10.1096/fj.201900179RR

Ma, M., Zhang, L., Liu, Z., Teng, Y., Li, M., Peng, X., & An, L. (2024). Effect of

blastocyst development on hatching and embryo implantation. *Theriogenology*, *214*(October 2023), 66–72. https://doi.org/10.1016/j.theriogenology.2023.10.011

Maas, K., Mirabal, S., Penzias, A., Sweetnam, P. M., Eggan, K. C., & Sakkas, D. (2018). Hippo signaling in the ovary and polycystic ovarian syndrome. *Journal of Assisted Reproduction and Genetics*, *35*(10), 1763–1771. https://doi.org/10.1007/s10815-018-1235-0

Maître, J. L., Turlier, H., Illukkumbura, R., Eismann, B., Niwayama, R., Nédélec, F., & Hiiragi, T. (2016). Asymmetric division of contractile domains couples cell positioning and fate specification. *Nature*, *536*(7616), 344–348. https://doi.org/10.1038/nature18958

Marcho, C., Bevilacqua, A., Tremblay, K. D., & Mager, J. (2015). Tissue-specific regulation of Igf2r/Airn imprinting during gastrulation. *Epigenetics \& Chromatin*, *8*(1), 10. https://doi.org/10.1186/s13072-015-0003-y

Marson, A., Levine, S. S., Cole, M. F., Frampton, G. M., Brambrink, T., Johnstone, S., Guenther, M. G., Johnston, W. K., Wernig, M., Newman, J., Calabrese, J. M., Dennis, L. M., Volkert, T. L., Gupta, S., Love, J., Hannett, N., Sharp, P. A., Bartel, D. P., Jaenisch, R., & Young, R. A. (2008). Connecting microRNA Genes to the Core Transcriptional Regulatory Circuitry of Embryonic Stem Cells. *Cell*, *134*(3), 521–533. https://doi.org/10.1016/j.cell.2008.07.020

Massagué, J., & Sheppard, D. (2023). TGF-β signaling in health and disease. *Cell*, *186*(19), 4007–4037. https://doi.org/10.1016/j.cell.2023.07.036

Masui, S., Nakatake, Y., Toyooka, Y., Shimosato, D., Yagi, R., Takahashi, K., Okochi, H., Okuda, A., Matoba, R., Sharov, A. A., Ko, M. S. H., & Niwa, H. (2007). Pluripotency governed by Sox2 via regulation of Oct3/4 expression in mouse embryonic stem cells. *Nature Cell Biology*, *9*(6), 625–635. https://doi.org/10.1038/ncb1589

Matsui, Y., & Lai, Z. C. (2013). Mutual regulation between Hippo signaling and actin cytoskeleton. *Protein and Cell*, *4*(12), 904–910. https://doi.org/10.1007/s13238-013-3084-z

Matsuo, I., & Hiramatsu, R. (2017). Mechanical perspectives on the anterior-posterior axis polarization of mouse implanted embryos. *Mechanisms of Development*, *144*, 62–70. https://doi.org/10.1016/j.mod.2016.09.002

McDole, K., Xiong, Y., Iglesias, P. A., & Zheng, Y. (2011). Lineage mapping the pre-implantation mouse embryo by two-photon microscopy, new insights into the segregation of cell fates. *Dev Biol*, *355*(2), 239–249. https://doi.org/10.1016/j.ydbio.2011.04.024

Meers, M. P., Tenenbaum, D., & Henikoff, S. (2019). Peak calling by Sparse Enrichment Analysis for CUT&RUN chromatin profiling. *Epigenetics and Chromatin*, *12*(1), 1–11. https://doi.org/10.1186/s13072-019-0287-4

Meinhardt, G., Haider, S., Kunihs, V., Saleh, L., Pollheimer, J., Fiala, C., Hetey, S., Feher, Z., Szilagyi, A., Than, N. G., & Knöfler, M. (2020). Pivotal role of the transcriptional co-activator YAP in trophoblast stemness of the developing human placenta. *Proceedings of the National Academy of Sciences of the United States of America*, *117*(24), 13562–13570. https://doi.org/10.1073/pnas.2002630117

Meissner, A., Wernig, M., & Jaenisch, R. (2007). Direct reprogramming of genetically unmodified fibroblasts into pluripotent stem cells. *Nat Biotechnol*, *25*(10), 1177–1181. https://doi.org/nbt1335 [pii] 10.1038/nbt1335

Meng, Y., Cai, K. Q., Moore, R., Tao, W., Tse, J. D., Smith, E. R., & Xu, X. X. (2017). Pten facilitates epiblast epithelial polarization and proamniotic lumen formation in early mouse embryos. *Developmental Dynamics*, *246*(7), 517–530. https://doi.org/10.1002/dvdy.24503

Mesnard, D., Guzman-Ayala, M., & Constam, D. B. (2006). Nodal specifies embryonic visceral endoderm and sustains pluripotent cells in the epiblast before overt axial patterning. *Development*, *133*(13), 2497–2505. https://doi.org/10.1242/dev.02413

Messerschmidt, D. M., & Kemler, R. (2010). Nanog is required for primitive endoderm formation through a non-cell autonomous mechanism. *Developmental Biology*, *344*(1), 129–137. https://doi.org/10.1016/j.ydbio.2010.04.020

Mihajlović, A. I., & Bruce, A. W. (2016). Rho-associated protein kinase regulates subcellular localisation of Angiomotin and Hippo-signalling during preimplantation mouse embryo development. *Reproductive BioMedicine Online*, *33*(3), 381–390. https://doi.org/10.1016/j.rbmo.2016.06.028

Mikkelsen, T. S., Hanna, J., Zhang, X., Ku, M., Wernig, M., Schorderet, P., Bernstein, B. E., Jaenisch, R., Lander, E. S., & Meissner, A. (2008). Dissecting direct reprogramming through integrative genomic analysis. *Nature*, *454*(7200), 49–55. https://doi.org/10.1038/nature07056

Mishina, Y., Suzuki, A., Ueno, N., & Behringer, R. R. (1995). Bmpr encodes a type I bone morphogenetic protein receptor that is essential for gastrulation during mouse embryogenesis. *Genes and Development*, *9*(24), 3027–3037. https://doi.org/10.1101/gad.9.24.3027

Misra, J. R., & Irvine, K. D. (2018). The Hippo Signaling Network and Its Biological Functions. *Annual Review of Genetics*, *52*(1), 65–87. https://doi.org/10.1146/annurev-genet-120417-031621

Mistri, T. K., Arindrarto, W., Ng, W. P., Wang, C., Lim, L. H., Sun, L., Chambers, I., Wohland, T., & Robson, P. (2018). Dynamic changes in Sox2 spatio-temporal expression promote the second cell fate decision through Fgf4/Fgfr2 signaling in preimplantation mouse embryos. *Biochemical Journal*, *475*(6), 1075–1089. https://doi.org/10.1042/BCJ20170418

Mitsui, K., Tokuzawa, Y., Itoh, H., Segawa, K., Murakami, M., Takahashi, K., Maruyama, M., Maeda, M., & Yamanaka, S. (2003). The homeoprotein nanog is required for maintenance of pluripotency in mouse epiblast and ES cells. *Cell*, *113*(5), 631–642. https://doi.org/10.1016/S0092-8674(03)00393-3

Miyanaga, Y., Torregroza, I., & Evans, T. (2002). A Maternal Smad Protein Regulates Early Embryonic Apoptosis in Xenopus laevis. *Molecular and Cellular Biology*, *22*(5), 1317–1328. https://www.ncbi.nlm.nih.gov/pmc/articles/PMC134692/

Moauro, A., Kruger, R. E., O'Hagan, D., & Ralston, A. (2022). Fluorescent Reporters Distinguish Stem Cell Colony Subtypes During Somatic Cell Reprogramming. *Cellular Reprogramming*, *24*(6), 353–362. https://doi.org/10.1089/cell.2022.0071

Moauro, A., & Ralston, A. (2022). Distinguishing Between Endodermal and Pluripotent Stem Cell Lines During Somatic Cell Reprogramming. *Methods in Molecular Biology*, *2429*, 41–55. https://doi.org/10.1007/978-1-0716-1979-7_4

Molkentin, J. D., Lin, Q., Duncan, S. A., & Olson, E. N. (1997). Requirement of the transcription factor GATA4 for heart tube formation and ventral morphogenesis. *Genes Dev*, *11*(8), 1061–1072. http://www.ncbi.nlm.nih.gov/pubmed/9136933

Molotkov, A., Mazot, P., Brewer, J. R., Cinalli, R. M., & Soriano, P. (2017). Distinct Requirements for FGFR1 and FGFR2 in Primitive Endoderm Development and Exit from Pluripotency. *Developmental Cell*, *41*(5), 511-526.e4. https://doi.org/10.1016/j.devcel.2017.05.004

Monsivais, D., Nagashima, T., Prunskaite-Hyyryläinen, R., Nozawa, K., Shimada, K., Tang, S., Hamor, C., Agno, J. E., Chen, F., Masand, R. P., Young, S. L., Creighton, C. J., DeMayo, F. J., Ikawa, M., Lee, S. J., & Matzuk, M. M. (2021). Endometrial receptivity and implantation require uterine BMP signaling through an ACVR2A-SMAD1/SMAD5 axis. *Nature Communications*, *12*(1), 1–17. https://doi.org/10.1038/s41467-021-23571-5

Morgani, S. M., & Hadjantonakis, A. K. (2020). Signaling regulation during gastrulation: Insights from mouse embryos and in vitro systems. In *Current Topics in Developmental Biology* (1st ed., Vol. 137). Elsevier Inc. https://doi.org/10.1016/bs.ctdb.2019.11.011

Morgani, S. M., Saiz, N., Garg, V., Raina, D., Simon, C. S., Kang, M., Arias, A. M.,

Nichols, J., Schröter, C., & Hadjantonakis, A. K. (2018). A Sprouty4 reporter to monitor FGF/ERK signaling activity in ESCs and mice. *Developmental Biology*, *441*(1), 104–126. https://doi.org/10.1016/j.ydbio.2018.06.017

Morrisey, E. E., Ip, H. S., Lu, M. M., & Parmacek, M. S. (1996). GATA-6: a zinc finger transcription factor that is expressed in multiple cell lineages derived from lateral mesoderm. *Dev Biol*, *177*(1), 309–322. http://www.ncbi.nlm.nih.gov/entrez/query.fcgi?cmd=Retrieve&db=PubMed&dopt=Citation&list_uids=8660897

Motosugi, N., Bauer, T., Polanski, Z., Solter, D., & Hiiragi, T. (2005). Polarity of the mouse embryo is established at blastocyst and is not prepatterned. *Genes and Development*, *19*(9), 1081–1092. https://doi.org/10.1101/gad.1304805

Moya, I. M., & Halder, G. (2016). The Hippo pathway in cellular reprogramming and regeneration of different organs. *Curr Opin Cell Biol*, *43*, 62–68. https://doi.org/10.1016/j.ceb.2016.08.004

Murray, S. A., Morgan, J. L., Kane, C., Sharma, Y., Heffner, C. S., Lake, J., & Donahue, L. R. (2010). Mouse gestation length is genetically determined. *PLoS ONE*, *5*(8). https://doi.org/10.1371/journal.pone.0012418

Nagy, A., Gertsenstein, M., Vintersten, K., & Behringer, R. (2003). *Manipulating the Mouse Embryo*. Cold Spring Harbor Laboratory Press.

Ni, F. Da, Hao, S. L., & Yang, W. X. (2019). Multiple signaling pathways in Sertoli cells: recent findings in spermatogenesis. *Cell Death and Disease*, *10*(8). https://doi.org/10.1038/s41419-019-1782-z

Niakan, K. K., & Eggan, K. (2013). Analysis of human embryos from zygote to blastocyst reveals distinct gene expression patterns relative to the mouse. *Developmental Biology*, *375*(1), 54–64. https://doi.org/10.1016/j.ydbio.2012.12.008

Niakan, K. K., Ji, H., Maehr, R., Vokes, S. A., Rodolfa, K. T., Sherwood, R. I., Yamaki, M., Dimos, J. T., Chen, A. E., Melton, D. A., McMahon, A. P., & Eggan, K. (2010). Sox17 promotes differentiation in mouse embryonic stem cells by directly regulating extraembryonic gene expression and indirectly antagonizing self-renewal. *Genes and Development*, *24*(3), 312–326. https://doi.org/10.1101/gad.1833510

Nichols, J., Silva, J., Roode, M., & Smith, A. (2009). Suppression of Erk signalling promotes ground state pluripotency in the mouse embryo. *Development*, *136*(19), 3215–3222. https://doi.org/10.1242/dev.038893

Nichols, J., & Smith, A. (2009). Naive and Primed Pluripotent States. *Cell Stem Cell*, *4*(6), 487–492. https://doi.org/10.1016/j.stem.2009.05.015

Nichols, J., Zevnik, B., Anastassiadis, K., Niwa, H., Klewe-Nebenius, D., Chambers, I., Schöler, H., & Smith, A. (1998). Formation of pluripotent stem cells in the mammalian embryo depends on the POU transcription factor Oct4. *Cell*, *95*(3), 379–391. https://doi.org/10.1016/S0092-8674(00)81769-9

Nishimura, T., Unezaki, N., Kanegi, R., Wijesekera, D. P. H., Hatoya, S., Sugiura, K., Kawate, N., Tamada, H., Imai, H., & Inaba, T. (2017). Generation of Canine Induced Extraembryonic Endoderm-Like Cell Like That Forms Both Extraembryonic and Embryonic Endoderm Derivatives. *Stem Cells and Development*, *26*(15), 1111–1120. https://doi.org/10.1089/scd.2017.0026

Nishioka, N., Inoue, K. ichi, Adachi, K., Kiyonari, H., Ota, M., Ralston, A., Yabuta, N., Hirahara, S., Stephenson, R. O., Ogonuki, N., Makita, R., Kurihara, H., Morin-Kensicki, E. M., Nojima, H., Rossant, J., Nakao, K., Niwa, H., & Sasaki, H. (2009). The Hippo Signaling Pathway Components Lats and Yap Pattern Tead4 Activity to Distinguish Mouse Trophectoderm from Inner Cell Mass. *Developmental Cell*, *16*(3), 398–410. https://doi.org/10.1016/j.devcel.2009.02.003

Nishioka, N., Yamamoto, S., Kiyonari, H., Sato, H., Sawada, A., Ota, M., Nakao, K., & Sasaki, H. (2008). Tead4 is required for specification of trophectoderm in pre-implantation mouse embryos. *Mechanisms of Development*, *125*(3–4), 270–283. https://doi.org/10.1016/j.mod.2007.11.002

Nowotschin, S., & Hadjantonakis, A. K. (2014). Live imaging mouse embryonic development: seeing is believing and revealing. *Methods Mol Biol*, *1092*, 405–420. https://doi.org/10.1007/978-1-60327-292-6_24

Nowotschin, S., Setty, M., Kuo, Y. Y., Liu, V., Garg, V., Sharma, R., Simon, C. S., Saiz, N., Gardner, R., Boutet, S. C., Church, D. M., Hoodless, P. A., Hadjantonakis, A. K., & Pe'er, D. (2019). The emergent landscape of the mouse gut endoderm at single-cell resolution. *Nature*, *569*(7756), 361–367. https://doi.org/10.1038/s41586-019-1127-1

O'Connor, M. B., Umulis, D., Othmer, H. G., & Blair, S. S. (2006). Shaping BMP morphogen gradients in the Drosophila embryo and pupal wing. *Development*, *133*(2), 183–193. https://doi.org/10.1242/dev.02214

O'Hagan, D., Kruger, R. E., Gu, B., & Ralston, A. (2021). Efficient generation of endogenous protein reporters for mouse development. *Development (Cambridge)*, *148*(13). https://doi.org/10.1242/DEV.197418

Ohnishi, Y., Huber, W., Tsumura, A., Kang, M., Xenopoulos, P., Kurimoto, K., Oleå, A. K., Araúzo-Bravo, M. J., Saitou, M., Hadjantonakis, A. K., & Hiiragi, T. (2014). Cell-to-cell expression variability followed by signal reinforcement progressively segregates early mouse lineages. *Nature Cell Biology*, *16*(1), 27–37.

https://doi.org/10.1038/ncb2881

Okada, H., Tsuzuki, T., & Murata, H. (2018). Decidualization of the human endometrium. *Reproductive Medicine and Biology*, *17*(3), 220–227. https://doi.org/10.1002/rmb2.12088

Paca, A., Séguin, C. A., Clements, M., Ryczko, M., Rossant, J., Rodriguez, T. A., & Kunath, T. (2012). BMP signaling induces visceral endoderm differentiation of XEN cells and parietal endoderm. *Developmental Biology*, *361*(1), 90–102. https://doi.org/10.1016/j.ydbio.2011.10.013

Palmieri, S. L., Peter, W., Hess, H., & Scholer, H. R. (1994). Oct-4 Transcription Factor Is Differentially Expressed in the Mouse Embryo during Establishment of the First Two Extraembryonic Cell Lineages Involved in Implantation. *Developmental Biology*, *166*, 259–267.

Parenti, A., Halbisen, M. A., Wang, K., Latham, K., & Ralston, A. (2016). OSKM Induce Extraembryonic Endoderm Stem Cells in Parallel to Induced Pluripotent Stem Cells. *Stem Cell Reports*, *6*(4), 447–455. https://doi.org/10.1016/j.stemcr.2016.02.003

Patty, B. J., & Hainer, S. J. (2021). Transcription factor chromatin profiling genome-wide using uliCUT&RUN in single cells and individual blastocysts. *Nature Protocols*, *16*(5), 2633–2666. https://doi.org/10.1038/s41596-021-00516-2

Pei, T., Huang, X., Long, Y., Duan, C., Liu, T., Li, Y., & Huang, W. (2019). Increased expression of YAP is associated with decreased cell autophagy in the eutopic endometrial stromal cells of endometriosis. *Molecular and Cellular Endocrinology*, *491*(April), 110432. https://doi.org/10.1016/j.mce.2019.04.012

Pei, T., Luo, B., Huang, W., Liu, D., Li, Y., Xiao, L., Huang, X., Ouyang, Y., & Zhu, H. (2022). Increased Expression of YAP Inhibited the Autophagy Level by Upregulating mTOR Signal in the Eutopic ESCs of Endometriosis. *Frontiers in Endocrinology*, *13*(January), 1–13. https://doi.org/10.3389/fendo.2022.813165

Perea-Gomez, A., Rhinn, M., & Ang, S. L. (2001). Role of the anterior visceral endoderm in restricting posterior signals in the mouse embryo. *International Journal of Developmental Biology*, *45*(1), 311–320.

Perez-Garcia, V., Fineberg, E., Wilson, R., Murray, A., Mazzeo, C. I., Tudor, C., Sienerth, A., White, J. K., Tuck, E., Ryder, E. J., Gleeson, D., Siragher, E., Wardle-Jones, H., Staudt, N., Wali, N., Collins, J., Geyer, S., Busch-Nentwich, E. M., Galli, A., … Hemberger, M. (2018). Placentation defects are highly prevalent in embryonic lethal mouse mutants. *Nature*, *555*(7697), 463–468. https://doi.org/10.1038/nature26002

Piotrowska-Nitsche, K., Perea-Gomez, A., Haraguchi, S., & Zernicka-Goetz, M. (2005). Four-cell stage mouse blastomeres have different developmental properties. *Development*, *132*(3), 479–490. https://doi.org/10.1242/dev.01602

Piotrowska, K., Wianny, F., Pedersen, R. A., & Zernicka-Goetz, M. (2001). Blastomeres arising from the first cleavage division have distinguishable fates in normal mouse development. *Development*, *3748*, 3739–3748.

Plachta, N., Bollenbach, T., Pease, S., Fraser, S. E., & Pantazis, P. (2011). Oct4 kinetics predict cell lineage patterning in the early mammalian embryo. *Nat Cell Biol*, *13*(2), 117–123. https://doi.org/ncb2154 [pii] 10.1038/ncb2154

Plewes, M. R., Hou, X., Zhang, P., Liang, A., Hua, G., Wood, J. R., Cupp, A. S., Lv, X., Wang, C., & Davis, J. S. (2019). Yes-associated protein 1 is required for proliferation and function of bovine granulosa cells in vitro. *Biology of Reproduction*, *101*(5), 1001–1017. https://doi.org/10.1093/biolre/ioz139

Plouhinec, J. L., & De Robertis, E. M. (2009). Systems biology of the self-regulating morphogenetic gradient of the Xenopus gastrula. *Cold Spring Harbor Perspectives in Biology*, *1*(2). https://doi.org/10.1101/cshperspect.a001701

Plouhinec, J. L., Zakin, L., Moriyama, Y., & De Robertis, E. M. (2013). Chordin forms a self-organizing morphogen gradient in the extracellular space between ectoderm and mesoderm in the Xenopus embryo. *Proceedings of the National Academy of Sciences of the United States of America*, *110*(51), 20372–20379. https://doi.org/10.1073/pnas.1319745110

Plusa, B., Frankenberg, S., Chalmers, A., Hadjantonakis, A. K., Moore, C. A., Papalopulu, N., Papaioannou, V. E., Glover, D. M., & Zernicka-Goetz, M. (2005). Downregulation of Par3 and aPKC function directs cells towards the ICM in the preimplantation mouse embryo. *Journal of Cell Science*, *118*(3), 505–515. https://doi.org/10.1242/jcs.01666

Plusa, B., Piliszek, A., Frankenberg, S., Artus, J., & Hadjantonakis, A. K. (2008). Distinct sequential cell behaviours direct primitive endoderm formation in the mouse blastocyst. *Development*, *135*(18), 3081–3091. https://doi.org/10.1242/dev.021519

Posfai, E., Petropoulos, S., de Barros, F. R. O., Schell, J. P., Jurisica, I., Sandberg, R., Lanner, F., & Rossant, J. (2017). Position- and Hippo signaling-dependent plasticity during lineage segregation in the early mouse embryo. *ELife*, *6*, e22906. https://doi.org/10.7554/eLife.22906

Pour, M., Pilzer, I., Rosner, R., Smith, Z. D., Meissner, A., & Nachman, I. (2015). Epigenetic predisposition to reprogramming fates in somatic cells. *EMBO Reports*, *16*(3), 370–378. https://doi.org/10.15252/embr.201439264

PrabhuDas, M., Bonney, E., Caron, K., Dey, S., Erlebacher, A., Fazleabas, A., Fisher, S., Golos, T., Matzuk, M., McCune, J. M., Mor, G., Schulz, L., Soares, M., Spencer, T., Strominger, J., Way, S. S., & Yoshinaga, K. (2015). Immune mechanisms at the maternal-fetal interface: perspectives and challenges. *Nature Immunology*, *16*(4), 328–334. https://www.nature.com/articles/ni.3131

Ralston, A., Cox, B. J., Nishioka, N., Sasaki, H., Chea, E., Rugg-Gunn, P., Guo, G., Robson, P., Draper, J. S., & Rossant, J. (2010). Gata3 regulates trophoblast development downstream of Tead4 and in parallel to Cdx2. *Development*, *137*(3), 395–403. https://doi.org/10.1242/dev.038828

Ralston, A., & Rossant, J. (2008). Cdx2 acts downstream of cell polarization to cell-autonomously promote trophectoderm fate in the early mouse embryo. *Developmental Biology*, *313*(2), 614–629. https://doi.org/10.1016/j.ydbio.2007.10.054

Ramel, M. C., & Hill, C. S. (2013). The ventral to dorsal BMP activity gradient in the early zebrafish embryo is determined by graded expression of BMP ligands. *Developmental Biology*, *378*(2), 170–182. https://doi.org/10.1016/j.ydbio.2013.03.003

Rankin, T., Soyal, S., & Dean, J. (2000). The mouse zona pellucida: Folliculogenesis, fertility and pre- implantation development. *Molecular and Cellular Endocrinology*, *163*(1–2), 21–25. https://doi.org/10.1016/S0303-7207(99)00236-1

Rappolee, D. A., Basilico, C., Patel, Y., & Werb, Z. (1994). Expression and function of FGF-4 in peri-implantation development in mouse embryos. *Development*, *120*(8), 2259–2269.

Ray, S., Saha, A., Ghosh, A., Roy, N., Kumar, R. P., Meinhardt, G., Mukerjee, A., Gunewardena, S., Kumar, R., Knofler, M., & Paul, S. (2022). Hippo signaling cofactor, WWTR1, at the crossroads of human trophoblast progenitor self-renewal and differentiation. *Proceedings of the National Academy of Sciences of the United States of America*, *119*(36), 1–12. https://doi.org/10.1073/pnas.2204069119

Rayon, T., Menchero, S., Nieto, A., Xenopoulos, P., Crespo, M., Cockburn, K., Cañon, S., Sasaki, H., Hadjantonakis, A. K., de la Pompa, J. L., Rossant, J., & Manzanares, M. (2014). Notch and Hippo Converge on Cdx2 to Specify the Trophectoderm Lineage in the Mouse Blastocyst. *Developmental Cell*, *30*(4), 410–422. https://doi.org/10.1016/j.devcel.2014.06.019

Reddi, A. H. (2003). Bone morphogenetic proteins. *The Cytokine Handbook*, 1179–1185. https://doi.org/10.1016/B978-012689663-3/50055-7

Reddy, P., Deguchi, M., Cheng, Y., & Hsueh, A. J. W. (2013). Actin cytoskeleton

regulates Hippo signaling. *PloS One*, *8*(9). https://doi.org/10.1371/journal.pone.0073763

Reim, G., & Brand, M. (2006). Maternal control of vertebrate dorsoventral axis formation and epiboly by the POU domain protein Spg/Pou2/Oct4. *Development*, *133*(14), 2757–2770. https://doi.org/10.1242/dev.02391

Reima, I., & Lehtonen, E. (1985). Localization of nonerythroid spectrin and actin in mouse oocytes and preimplantation embryos. *Differentiation*, *30*, 68–75. http://www.ncbi.nlm.nih.gov/pubmed/4092865

Reyes de Mochel, N. S., Luong, M., Chiang, M., Javier, A. L., Luu, E., Toshihiko, F., MacGregor, G. R., Cinquin, O., & Cho, K. W. Y. (2015). BMP signaling is required for cell cleavage in preimplantation-mouse embryos. *Developmental Biology*, *397*(1), 45–55. https://doi.org/10.1016/j.ydbio.2014.10.001

Rinkenberger, J. L., Cross, J. C., & Werb, Z. (1997). Molecular genetics of implantation in the mouse. *Developmental Genetics*, *21*(1), 6–20. https://doi.org/10.1002/(SICI)1520-6408(1997)21:1<6::AID-DVG2>3.0.CO;2-B

Roberts, R. M., Cross, J. C., & Leaman, D. W. (1992). Interferons as Hormones of Pregnancy. *Endocrine Reviews*, *13*(3), 432–452. https://doi.org/10.1210/edrv-13-3-432

Robertson, E. J. (2014). Dose-dependent nodal/smad signals pattern the early mouse embryo. *Seminars in Cell and Developmental Biology*, *32*, 73–79. https://doi.org/10.1016/j.semcdb.2014.03.028

Rosner, M., Reithofer, M., Fink, D., & Hengstschläger, M. (2021). Human embryo models and drug discovery. *International Journal of Molecular Sciences*, *22*(2), 1–17. https://doi.org/10.3390/ijms22020637

Rossant, J. (2001). Stem Cells from the Mammalian Blastocyst. *Stem Cells*, *19*(6), 477–482. https://doi.org/10.1634/stemcells.19-6-477

Rossant, J., & Cross, J. C. (2001). Placental development: Lessons from mouse mutants. *Nature Reviews Genetics*, *2*(7), 538–548. https://doi.org/10.1038/35080570

Rossant, J., & Tam, P. P. L. (2009). Blastocyst lineage formation, early embryonic asymmetries and axis patterning in the mouse. *Development*, *136*(5), 701–713. https://doi.org/10.1242/dev.017178

Rushlow, C., Frasch, M., Doyle, H., & Levine, M. (1987). Maternal regulation of zerknüllt: A homoeobox gene controlling differentiation of dorsal tissues in

Drosophila. *Nature*, *330*(6148), 583–586. https://doi.org/10.1038/330583a0

Saha, B., Ganguly, A., Home, P., Bhattacharya, B., Ray, S., Ghosh, A., Karim Rumi, M. A., Marsh, C., French, V. A., Gunewardena, S., & Paul, S. (2020). TEAD4 ensures postimplantation development by promoting trophoblast self-renewal: An implication in early human pregnancy loss. *Proceedings of the National Academy of Sciences of the United States of America*, *117*(30), 17864–17875. https://doi.org/10.1073/pnas.2002449117

Saitou, M., & Yamaji, M. (2012). Primordial germ cells in mice. *Cold Spring Harbor Perspectives in Biology*, *4*(11), 1–20. https://doi.org/10.1101/cshperspect.a008375

Saiz, N., Grabarek, J. B., Sabherwal, N., Papalopulu, N., & Plusa, B. (2013). Atypical protein kinase C couples cell sorting with primitive endoderm maturation in the mouse blastocyst. *Development*, *140*(21), 4311–4322. https://doi.org/10.1242/dev.093922

Saiz, N., Plusa, B., & Hadjantonakis, A. K. (2015). Single cells get together: High-resolution approaches to study the dynamics of early mouse development. *Semin Cell Dev Biol*, *47–48*, 92–100. https://doi.org/10.1016/j.semcdb.2015.06.004

Sakai, T., Li, S., Docheva, D., Grashoff, C., Sakai, K., Kostka, G., Braun, A., Pfeifer, A., Yurchenco, P. D., & Fässler, R. (2003). Integrin-linked kinase (ILK) is required for polarizing the epiblast, cell adhesion, and controlling actin accumulation. *Genes and Development*, *17*(7), 926–940. https://doi.org/10.1101/gad.255603

Sasai, Y., Lu, B., Steinbeisser, H., Geissert, D., Gont, L. K., & De Robertis, E. M. (1994). Xenopus chordin: A novel dorsalizing factor activated by organizer-specific homeobox genes. *Cell*, *79*(5), 779–790. https://doi.org/10.1016/0092-8674(94)90068-X

Sasaki, H. (2015). Position- and polarity-dependent Hippo signaling regulates cell fates in preimplantation mouse embryos. *Seminars in Cell and Developmental Biology*, *47–48*, 80–87. https://doi.org/10.1016/j.semcdb.2015.05.003

Sasaki, H. (2017). Roles and regulations of Hippo signaling during preimplantation mouse development. *Development Growth and Differentiation*, *59*(1), 12–20. https://doi.org/10.1111/dgd.12335

Schiebinger, G., Shu, J., Tabaka, M., Cleary, B., Subramanian, V., Solomon, A., Gould, J., Liu, S., Lin, S., Berube, P., Lee, L., Chen, J., Brumbaugh, J., Rigollet, P., Hochedlinger, K., Jaenisch, R., Regev, A., & Lander, E. S. (2019). Optimal-Transport Analysis of Single-Cell Gene Expression Identifies Developmental Trajectories in Reprogramming. *Cell*, *176*(4), 928--943.e22. https://doi.org/10.1016/j.cell.2019.01.006

Schohl, A., & Fagotto, F. (2002). β-catenin, MAPK and Smad signaling during early Xenopus development. *Development*, *129*, 37–52. https://doi.org/10.1242/dev.02841

Schrode, N., Saiz, N., Di Talia, S., & Hadjantonakis, A. K. (2014). GATA6 Levels Modulate Primitive Endoderm Cell Fate Choice and Timing in the Mouse Blastocyst. *Dev Cell*, *29*(4), 454–467. https://doi.org/10.1016/j.devcel.2014.04.011

Schwarz, N., Windoffer, R., Magin, T. M., & Leube, R. E. (2015). Dissection of keratin network formation, turnover and reorganization in living murine embryos. *Scientific Reports*, *5*, 9007. https://doi.org/10.1038/srep09007

Sen Sharma, S., & Majumdar, S. S. (2017). Transcriptional co-activator YAP regulates cAMP signaling in Sertoli cells. *Molecular and Cellular Endocrinology*, *450*, 64–73. https://doi.org/10.1016/j.mce.2017.04.017

Sen Sharma, S., Vats, A., & Majumdar, S. (2019). Regulation of Hippo pathway components by FSH in testis. *Reproductive Biology*, *19*(1), 61–66. https://doi.org/10.1016/j.repbio.2019.01.003

Senft, A. D., Bikoff, E. K., Robertson, E. J., & Costello, I. (2019). Genetic dissection of Nodal and Bmp signalling requirements during primordial germ cell development in mouse. *Nature Communications*, *10*(1), 1–11. https://doi.org/10.1038/s41467-019-09052-w

Shahbazi, M. N., Scialdone, A., Skorupska, N., Weberling, A., Recher, G., Zhu, M., Jedrusik, A., Devito, L. G., Noli, L., MacAulay, I. C., Buecker, C., Khalaf, Y., Ilic, D., Voet, T., Marioni, J. C., & Zernicka-Goetz, M. (2017). Pluripotent state transitions coordinate morphogenesis in mouse and human embryos. *Nature*, *552*(7684), 239–243. https://doi.org/10.1038/nature24675

Shaner, N. C., Lambert, G. G., Chammas, A., Ni, Y., Cranfill, P. J., Baird, M. A., Sell, B. R., Allen, J. R., Day, R. N., Israelsson, M., Davidson, M. W., & Wang, J. (2013). A bright monomeric green fluorescent protein derived from Branchiostoma lanceolatum. *Nature Methods*, *10*(5), 407–409. https://doi.org/10.1038/nmeth.2413

Sharma, J., Antenos, M., & Madan, P. (2021). A comparative analysis of hippo signaling pathway components during murine and bovine early mammalian embryogenesis. *Genes*, *12*(2), 1–11. https://doi.org/10.3390/genes12020281

Shi, W. H., Zhou, Z. Y., Ye, M. J., Qin, N. X., Jiang, Z. R., Zhou, X. Y., Xu, N. X., Cao, X. L., Chen, S. C., Huang, H. F., & Xu, C. M. (2023). Sperm morphological abnormalities in autosomal dominant polycystic kidney disease are associated with the Hippo signaling pathway via PC1. *Frontiers in Endocrinology*, *14*(April), 1–11. https://doi.org/10.3389/fendo.2023.1130536

Shi, Y., Desponts, C., Do, J. T., Hahm, H. S., Schöler, H. R., & Ding, S. (2008). Induction of Pluripotent Stem Cells from Mouse Embryonic Fibroblasts by Oct4 and Klf4 with Small-Molecule Compounds. *Cell Stem Cell*, *3*(5), 568–574. https://doi.org/10.1016/j.stem.2008.10.004

Shimosato, D., Shiki, M., & Niwa, H. (2007). Extra-embryonic endoderm cells derived from ES cells induced by GATA factors acquire the character of XEN cells. *BMC Dev Biol*, *7*, 80. http://www.ncbi.nlm.nih.gov/entrez/query.fcgi?cmd=Retrieve&db=PubMed&dopt=Citation&list_uids=17605826

Shiratori, H., & Hamada, H. (2006). The left-right axis in the mouse: From origin to morphology. *Development*, *133*(11), 2095–2104. https://doi.org/10.1242/dev.02384

Shirayoshi, Y., Okada, T. S., & Takeichi, M. (1983). The calcium-dependent cell-cell adhesion system regulates inner cell mass formation and cell surface polarization in early mouse development. *Cell*, *35*(3 PART 2), 631–638. https://doi.org/10.1016/0092-8674(83)90095-8

Sidi, S., Goutel, C., Peyriéras, N., & Rosa, F. M. (2003). Maternal induction of ventral fate by zebrafish radar. *Proceedings of the National Academy of Sciences of the United States of America*, *100*(6), 3315–3320. https://doi.org/10.1073/pnas.0530115100

Simmons, D. G., Fortier, A. L., & Cross, J. C. (2007). Diverse subtypes and developmental origins of trophoblast giant cells in the mouse placenta. *Dev Biol*, *304*(2), 567–578. https://doi.org/10.1016/j.ydbio.2007.01.009

Simon, C. S., Zhang, L., Wu, T., Cai, W., Saiz, N., Nowotschin, S., Cai, C.-L., & Hadjantonakis, A.-K. (2018). A Gata4 nuclear GFP transcriptional reporter to study endoderm and cardiac development in the mouse. *Biology Open*, *7*(12), bio036517. https://doi.org/10.1242/bio.036517

Sirard, C., De La Pompa, J. L., Elia, A., Itie, A., Mirtsos, C., Cheung, A., Hahn, S., Wakeham, A., Schwartz, L., Kern, S. E., Rossant, J., & Mak, T. W. (1998). The tumor suppressor gene Smad4/Dpc4 is required for gastrulation and later for anterior development of the mouse embryo. *Genes and Development*, *12*(1), 107–119. https://doi.org/10.1101/gad.12.1.107

Skene, P. J., & Henikoff, S. (2017). An efficient targeted nuclease strategy for high-resolution mapping of DNA binding sites. *ELife*, *6*, 1–35. https://doi.org/10.7554/eLife.21856

Smith, W. C., & Harland, R. M. (1992). Expression cloning of noggin, a new dorsalizing factor localized to the Spemann organizer in Xenopus embryos. *Cell*, *70*(5), 829–

840. https://doi.org/10.1016/0092-8674(92)90316-5

Smyth, N., Vatansever, H. S., Murray, P., Meyer, M., Frie, C., Paulsson, M., & Edgar, D. (1999). Absence of Basement Membranes after Targeting the. *J Cell Biol*, *144*(1), 151–160.

Song, Y., Fu, J., Zhou, M., Xiao, L., Feng, X., Chen, H., & Huang, W. (2016). Activated Hippo/Yes-associated protein pathway promotes cell proliferation and anti-apoptosis in endometrial stromal cells of endometriosis. *Journal of Clinical Endocrinology and Metabolism*, *101*(4), 1552–1561. https://doi.org/10.1210/jc.2016-1120

Soszyńska, A., Klimczewska, K., & Suwińska, A. (2019). FGF/ERK signaling pathway: How it operates in mammalian preimplantation embryos and embryo-derived stem cells. *International Journal of Developmental Biology*, *63*(3–5), 171–186. https://doi.org/10.1387/ijdb.180408as

Sozen, B., Can, A., & Demir, N. (2014). Cell fate regulation during preimplantation development: A view of adhesion-linked molecular interactions. *Developmental Biology*, *395*(1), 73–83. https://doi.org/10.1016/j.ydbio.2014.08.028

Spemann, H., & Mangold, H. (1923). Induction of Embryonic Primordia by Implantation of Organizers from a Different Species. *International Journal of Developmental Biology*, *45*, 13–38.

Sridharan, R., Tchieu, J., Mason, M. J., Yachechko, R., Kuoy, E., Horvath, S., Zhou, Q., & Plath, K. (2009). Role of the murine reprogramming factors in the induction of pluripotency. *Cell*, *136*(2), 364–377. https://doi.org/10.1016/j.cell.2009.01.001

St-Jean, G., Tsoi, M., Abedini, A., Levasseur, A., Rico, C., Morin, M., Djordjevic, B., Miinalainen, I., Kaarteenaho, R., Paquet, M., Gévry, N., Boyer, A., Vanderhyden, B., & Boerboom, D. (2019). Lats1 and Lats2 are required for the maintenance of multipotency in the Müllerian duct mesenchyme. *Development*, *146*(20), 1–12. https://doi.org/10.1242/dev.180430

St John, M. A. R., Tao, W., Fei, X., Fukumoto, R., Carcangiu, M. L., Brownstein, D. G., Parlow, A. F., McGrath, J., & Xu, T. (1999). Mice deficient of Lats1 develop soft-tissue sarcomas, ovarian tumours and pituitary dysfunction. *Nature Genetics*, *21*(2), 182–186. https://doi.org/10.1038/5965

Stephens, L. E., Sutherland, A. E., Klimanskaya, I. V., Andrieux, A., Meneses, J., Pedersen, R. A., & Damsky, C. H. (1995). Deletion of β1 integrins in mice results in inner cell mass failure and peri-implantation lethality. *Genes and Development*, *9*(15), 1883–1895. https://doi.org/10.1101/gad.9.15.1883

Stephenson, R. O., Yamanaka, Y., & Rossant, J. (2010). Disorganized epithelial polarity and excess trophectoderm cell fate in preimplantation embryos lacking E-cadherin. *Development*, *137*(20), 3383–3391. https://doi.org/10.1242/dev.050195

Stower, M. J., & Srinivas, S. (2018). The Head's Tale: Anterior-Posterior Axis Formation in the Mouse Embryo. In *Current Topics in Developmental Biology* (1st ed., Vol. 128). Elsevier Inc. https://doi.org/10.1016/bs.ctdb.2017.11.003

Strakova, Z., Reed, J., & Ihnatovych, I. (2010). Human transcriptional coactivator with PDZ-binding motif (TAZ) is downregulated during decidualization. *Biology of Reproduction*, *82*(6), 1112–1118. https://doi.org/10.1095/biolreprod.109.081844

Strumpf, D., Mao, C. A., Yamanaka, Y., Ralston, A., Chawengsaksophak, K., Beck, F., & Rossant, J. (2005). Cdx2 is required for correct cell fate specification and differentiation of trophectoderm in the mouse blastocyst. *Development*, *132*(9), 2093–2102. https://doi.org/10.1242/dev.01801

Stuart, H. T., Stirparo, G. G., Lohoff, T., Bates, L. E., Kinoshita, M., Lim, C. Y., Sousa, E. J., Maskalenka, K., Radzisheuskaya, A., Malcolm, A. A., Alves, M. R. P., Lloyd, R. L., Nestorowa, S., Humphreys, P., Mansfield, W., Reik, W., Bertone, P., Nichols, J., Göttgens, B., & Silva, J. C. R. (2019). Distinct Molecular Trajectories Converge to Induce Naive Pluripotency. *Cell Stem Cell*, *25*(3), 388-406.e8. https://doi.org/10.1016/j.stem.2019.07.009

Sudol, M., Bork, P., Einbond, A., Kastury, K., Druck, T., Negrini, M., Huebner, K., & Lehman, D. (1995). Characterization of the mammalian YAP (Yes-associated protein) gene and its role in defining a novel protein module, the WW domain. *Journal of Biological Chemistry*, *270*(24), 14733–14741. https://doi.org/10.1074/jbc.270.24.14733

Sun, M., Na, Q., Huang, L., Song, G., Jin, F., Li, Y., Hou, Y., Kang, D., & Qiao, C. (2018). YAP Is Decreased in Preeclampsia and Regulates Invasion and Apoptosis of HTR-8/SVneo. *Reproductive Sciences (Thousand Oaks, Calif.)*, *25*(9), 1382–1393. https://doi.org/10.1177/1933719117746784

Sun, S. C., Wang, Q. L., Gao, W. W., Xu, Y. N., Liu, H. L., Cui, X. S., & Kim, N. H. (2013). Actin nucleator Arp2/3 complex is essential for mouse preimplantation embryo development. *Reproduction, Fertility and Development*, *25*(4), 617–623. https://doi.org/10.1071/RD12011

Sun, S., Reddy, B. V. V. G., & Irvine, K. D. (2015). Localization of Hippo signalling complexes and Warts activation in vivo. *Nature Communications*, *6*. https://doi.org/10.1038/ncomms9402

Sun, S., Zhao, S., & Wang, Z. (2008). Genes of Hippo signaling network act

unconventionally in the control of germline proliferation in Drosophila. *Developmental Dynamics*, *237*(1), 270–275. https://doi.org/10.1002/dvdy.21411

Sun, T., & Diaz, F. J. (2019). Ovulatory signals alter granulosa cell behavior through YAP1 signaling. *Reproductive Biology and Endocrinology*, *17*(1), 9–12. https://doi.org/10.1186/s12958-019-0552-1

Suzuki, A., Chang, C., Yingling, J. M., Wang, X. F., & Hemmati-Brivanlou, A. (1997). Smad5 induces ventral fates in Xenopus embryo. *Developmental Biology*, *184*(2), 402–405. https://doi.org/10.1006/dbio.1997.8548

Taft, R. A. (2008). Virtues and limitations of the preimplantation mouse embryo as a model system. *Theriogenology*, *69*(1), 10–16. https://doi.org/10.1016/j.theriogenology.2007.09.032

Takahashi, K., & Yamanaka, S. (2006). Induction of Pluripotent Stem Cells from Mouse Embryonic and Adult Fibroblast Cultures by Defined Factors. *Cell*, *126*(4), 663–676. https://doi.org/10.1016/j.cell.2006.07.024

Takaoka, K., & Hamada, H. (2012). Cell fate decisions and axis determination in the early mouse embryo. *Development*, *139*(1), 3–14. https://doi.org/10.1242/dev.060095

Tang, S. J., Hoodless, P. A., Lu, Z., Breitman, M. L., McInnes, R. R., Wrana, J. L., & Buchwald, M. (1998). The Tlx-2 homeobox gene is a downstream target of BMP signalling and is required for mouse mesoderm development. *Development*, *125*(10), 1877–1887. https://doi.org/10.1242/dev.125.10.1877

Tarkowski, A. K., & Wróblewska, J. (1967). Development of blastomeres of mouse eggs isolated at the 4- and 8-cell stage. *Journal of Embryology and Experimental Morphology*, *18*(1), 155–180. https://doi.org/10.1242/dev.18.1.155

To, T.-L., Schepis, A., Ruiz-González, R., Zhang, Q., Yu, D., Dong, Z., Coughlin, S. R., & Shu, X. (2016). Rational Design of a GFP-Based Fluorogenic Caspase Reporter for Imaging Apoptosis In Vivo. *Cell Chemical Biology*, *23*(7), 875–882. https://doi.org/10.1016/j.chembiol.2016.06.007

Torres-Padilla, M. E., Parfitt, D. E., Kouzarides, T., & Zernicka-Goetz, M. (2007). Histone arginine methylation regulates pluripotency in the early mouse embryo. *Nature*, *445*(7124), 214–218. https://doi.org/10.1038/nature05458

Tremblay, K. D., Dunn, N. R., & Robertson, E. J. (2001). Mouse embryos lacking Smad1 signals display defects in extra-embryonic tissues and germ cell formation. *Development*, *128*(18), 3609–3621. https://doi.org/10.1242/dev.128.18.3609

Tsoi, M., Morin, M., Rico, C., Johnson, R. L., Paquet, M., Gevry, N., & Boerboom, D. (2019). Lats1 and Lats2 are required for ovarian granulosa cell fate maintenance. *FASEB Journal : Official Publication of the Federation of American Societies for Experimental Biology*, fj201900609R. https://doi.org/10.1096/fj.201900609R

Tsubooka, N., Ichisaka, T., Okita, K., Takahashi, K., Nakagawa, M., & Yamanaka, S. (2009). Roles of Sall4 in the generation of pluripotent stem cells from blastocysts and fibroblasts. *Genes to Cells*, *14*(6), 683–694. https://doi.org/10.1111/j.1365-2443.2009.01301.x

Tucker, J. A., Mintzer, K. A., & Mullins, M. C. (2008). The BMP Signaling Gradient Patterns Dorsoventral Tissues in a Temporally Progressive Manner along the Anteroposterior Axis. *Developmental Cell*, *14*(1), 108–119. https://doi.org/10.1016/j.devcel.2007.11.004

Varelas, X., Samavarchi-Tehrani, P., Narimatsu, M., Weiss, A., Cockburn, K., Larsen, B. G., Rossant, J., & Wrana, J. L. (2010). The Crumbs Complex Couples Cell Density Sensing to Hippo-Dependent Control of the TGF-β-SMAD Pathway. *Developmental Cell*, *19*(6), 831–844. https://doi.org/10.1016/j.devcel.2010.11.012

Velychko, S., Adachi, K., Kim, K.-P., Hou, Y., MacCarthy, C. M., Wu, G., & Schöler, H. R. (2019). Excluding Oct4 from Yamanaka Cocktail Unleashes the Developmental Potential of iPSCs. *Cell Stem Cell*, *25*(6), 737--753.e4. https://doi.org/10.1016/J.STEM.2019.10.002

Vinot, S., Le, T., Ohno, S., Pawson, T., Maro, B., & Louvet-Vallée, S. (2005). Asymmetric distribution of PAR proteins in the mouse embryo begins at the 8-cell stage during compaction. *Developmental Biology*, *282*(2), 307–319. https://doi.org/10.1016/j.ydbio.2005.03.001

Vogt, E. J., Meglicki, M., Hartung, K. I., Borsuk, E., & Behr, R. (2012). Importance of the pluripotency factor LIN28 in the mammalian nucleolus during early embryonic development. *Development*, *139*(24), 4514–4523. https://doi.org/10.1242/dev.083279

Vogt, J., Traynor, R., & Sapkota, G. P. (2011). The specificities of small molecule inhibitors of the TGFß and BMP pathways. *Cellular Signalling*, *23*(11), 1831–1842. https://doi.org/10.1016/j.cellsig.2011.06.019

Waldrip, W. R., Bikoff, E. K., Hoodless, P. A., Wrana, J. L., & Robertson, E. J. (1998). Smad2 signaling in extraembryonic tissues determines anterior-posterior polarity of the early mouse embryo. *Cell*, *92*(6), 797–808. https://doi.org/10.1016/S0092-8674(00)81407-5

Wallingford, J. B. (2019). We Are All Developmental Biologists. *Developmental Cell*,

50(2), 132–137. https://doi.org/10.1016/j.devcel.2019.07.006

Walsh, D. W., Godson, C., Brazil, D. P., & Martin, F. (2010). Extracellular BMP-antagonist regulation in development and disease: Tied up in knots. *Trends in Cell Biology*, *20*(5), 244–256. https://doi.org/10.1016/j.tcb.2010.01.008

Wamaitha, S. E., del Valle, I., Cho, L. T., Wei, Y., Fogarty, N. M., Blakeley, P., Sherwood, R. I., Ji, H., & Niakan, K. K. (2015). Gata6 potently initiates reprograming of pluripotent and differentiated cells to extraembryonic endoderm stem cells. *Genes Dev*, *29*(12), 1239–1255. https://doi.org/10.1101/gad.257071.114

Wang, E. A., Rosen, V., Cordes, P., Hewick, R. M., Kriz, M. J., Luxenberg, D. P., Sibley, B. S., & Wozney, J. M. (1988). Purification and characterization of other distinct bone-inducing factors. *Proceedings of the National Academy of Sciences of the United States of America*, *85*(24), 9484–9488. https://doi.org/10.1073/pnas.85.24.9484

Wang, R. N., Green, J., Wang, Z., Deng, Y., Qiao, M., Peabody, M., Zhang, Q., Ye, J., Yan, Z., Denduluri, S., Idowu, O., Li, M., Shen, C., Hu, A., Haydon, R. C., Kang, R., Mok, J., Lee, M. J., Luu, H. L., & Shi, L. L. (2014). Bone Morphogenetic Protein (BMP) signaling in development and human diseases. *Genes and Diseases*, *1*(1), 87–105. https://doi.org/10.1016/j.gendis.2014.07.005

Weiss, A., & Attisano, L. (2013). The TGFbeta superfamily signaling pathway. *Wiley Interdisciplinary Reviews: Developmental Biology*, *2*(1), 47–63. https://doi.org/10.1002/wdev.86

Wen, L., & Tang, F. (2022). Recent advances in single-cell sequencing technologies. *Precision Clinical Medicine*, *5*(1). https://doi.org/10.1093/pcmedi/pbac002

Wicklow, E., Blij, S., Frum, T., Hirate, Y., Lang, R. A., Sasaki, H., & Ralston, A. (2014). HIPPO Pathway Members Restrict SOX2 to the Inner Cell Mass Where It Promotes ICM Fates in the Mouse Blastocyst. *PLoS Genetics*, *10*(10). https://doi.org/10.1371/journal.pgen.1004618

Wigger, M., Kisielewska, K., Filimonow, K., Plusa, B., Maleszewski, M., & Suwińska, A. (2017). Plasticity of the inner cell mass in mouse blastocyst is restricted by the activity of FGF/MAPK pathway. *Scientific Reports*, *7*(1), 1–13. https://doi.org/10.1038/s41598-017-15427-0

Winnier, G., Blessing, M., Labosky, P. A., & Hogan, B. L. M. (1995). Bone morphogenetic protein-4 is required for mesoderm formation and patterning in the mouse. *Genes and Development*, *9*(17), 2105–2116. https://doi.org/10.1101/gad.9.17.2105

Wu, D., & Dean, J. (2020). Maternal factors regulating preimplantation development in mice. *Current Topics in Developmental Biology*, *140*, 317–340. https://doi.org/10.1016/bs.ctdb.2019.10.006

Wu, Z., & Guan, K. L. (2021). Hippo Signaling in Embryogenesis and Development. *Trends in Biochemical Sciences*, *46*(1), 51–63. https://doi.org/10.1016/j.tibs.2020.08.008

Xia, L. J., & Du, J. (2022). Mechanical stress-induced Hippo signaling in respect to primordial follicle development and polycystic ovary syndrome pathogenesis. *Reproductive and Developmental Medicine*, *6*(2), 121–128. https://doi.org/10.1097/RD9.0000000000000009

Xiang, C., Li, J., Hu, L., Huang, J., Luo, T., Zhong, Z., Zheng, Y., & Zheng, L. (2015). Hippo signaling pathway reveals a spatio-temporal correlation with the size of primordial follicle pool in mice. *Cellular Physiology and Biochemistry*, *35*(3), 957–968. https://doi.org/10.1159/000369752

Xiao, X., Li, N., Zhang, D., Yang, B., Guo, H., & Li, Y. (2016). Generation of Induced Pluripotent Stem Cells with Substitutes for Yamanaka's Four Transcription Factors. *Cellular Reprogramming*, *18*(5), 281–297. https://doi.org/10.1089/cell.2016.0020

Xie, D., Chen, C. C., Ptaszek, L. M., Xiao, S., Cao, X., Fang, F., Ng, H. H., Lewin, H. A., Cowan, C., & Zhong, S. (2010). Rewirable gene regulatory networks in the preimplantation embryonic development of three mammalian species. *Genome Research*, *20*(6), 804–815. https://doi.org/10.1101/gr.100594.109

Xin, M., Kim, Y., Sutherland, L. B., Murakami, M., Qi, X., McAnally, J., Porrello, E. R., Mahmoud, A. I., Tan, W., Shelton, J. M., Richardson, J. A., Sadek, H. A., Bassel-Duby, R., & Olson, E. N. (2013). Hippo pathway effector Yap promotes cardiac regeneration. *Proceedings of the National Academy of Sciences of the United States of America*, *110*(34), 13839–13844. https://doi.org/10.1073/pnas.1313192110

Xin, M., Kim, Y., Sutherland, L. B., Qi, X., McAnally, J., Schwartz, R. J., Richardson, J. A., Bassel-Duby, R., & Olson, E. N. (2011). Development: Regulation of insulin-like growth factor signaling by Yap governs cardiomyocyte proliferation and embryonic heart size. *Science Signaling*, *4*(196), 1–8. https://doi.org/10.1126/scisignal.2002278

Xu, J., Liu, H., Lan, Y., Adam, M., Clouthier, D. E., Potter, S., & Jiang, R. (2019). Hedgehog signaling patterns the oralaboral axis of the mandibular arch. *ELife*, *8*, 1–26. https://doi.org/10.7554/eLife.40315

Yagi, R., Kohn, M. J., Karavanova, I., Kaneko, K. J., Vullhorst, D., DePamphilis, M. L., &

Buonanno, A. (2007). Transcription factor TEAD4 specifies the trophectoderm lineage at the beginning of mammalian development. *Development*, *134*(21), 3827–3836. https://doi.org/10.1242/dev.010223

Yamagata, K., Yamazaki, T., Yamashita, M., Hara, Y., Ogonuki, N., & Ogura, A. (2005). Noninvasive visualization of molecular events in the mammalian zygote. *Genesis*, *43*(2), 71–79. https://doi.org/10.1002/gene.20158

Yamagata, M., & Sanes, J. R. (2012). Transgenic strategy for identifying synaptic connections in mice by fluorescence complementation (GRASP). *Frontiers in Molecular Neuroscience*, *5*, 18. https://doi.org/10.3389/fnmol.2012.00018

Yamamoto, M., Beppu, H., Takaoka, K., Meno, C., Li, E., Miyazono, K., & Hamada, H. (2009). Antagonism between Smad1 and Smad2 signaling determines the site of distal visceral endoderm formation in the mouse embryo. *Journal of Cell Biology*, *184*(2), 323–334. https://doi.org/10.1083/jcb.200808044

Yamamura, S., Goda, N., Akizawa, H., Kohri, N., Balboula, A. Z., Kobayashi, K., Bai, H., Takahashi, M., & Kawahara, M. (2020). Yes-associated protein 1 translocation through actin cytoskeleton organization in trophectoderm cells. *Developmental Biology*, *468*(1–2), 14–25. https://doi.org/10.1016/j.ydbio.2020.09.004

Yamanaka, Y., Lanner, F., & Rossant, J. (2010). FGF signal-dependent segregation of primitive endoderm and epiblast in the mouse blastocyst. *Development*, *137*(5), 715–724. https://doi.org/10.1242/dev.043471

Yang, H., Wang, H., Shivalila, C. S., Cheng, A. W., Shi, L., & Jaenisch, R. (2013). One-step generation of mice carrying reporter and conditional alleles by CRISPR/Cas-mediated genome engineering. *Cell*, *154*(6), 1370–1379. https://doi.org/10.1016/j.cell.2013.08.022

Yang, X., Li, C., Herrera, P. L., & Deng, C. X. (2002). Generation of Smad4/Dpc4 conditional knockout mice. *Genesis*, *32*(2), 80–81. https://doi.org/10.1002/gene.10029

Yang, X., Li, C., Xu, X., & Deng, C. (1998). The tumor suppressor SMAD4/DPC4 is essential for epiblast proliferation and mesoderm induction in mice. *Proceedings of the National Academy of Sciences of the United States of America*, *95*(7), 3667–3672. https://doi.org/10.1073/pnas.95.7.3667

Ye, H., Li, X., Zheng, T., Hu, C., Pan, Z., Huang, J., Li, J., Li, W., & Zheng, Y. (2017). The Hippo Signaling Pathway Regulates Ovarian Function via the Proliferation of Ovarian Germline Stem Cells. *Cellular Physiology and Biochemistry*, *41*(3), 1051–1062. https://doi.org/10.1159/000464113

Yildirim, E., Bora, G., Onel, T., Talas, N., & Yaba, A. (2021). Cell fate determination and Hippo signaling pathway in preimplantation mouse embryo. *Cell and Tissue Research*, *386*(3), 423–444. https://doi.org/10.1007/s00441-021-03530-8

Ying, Y., Liu, X. M., Marble, A., Lawson, K. A., & Zhao, G. Q. (2000). Requirement of Bmp8b for the generation of primordial germ cells in the mouse. *Molecular Endocrinology*, *14*(7), 1053–1063. https://doi.org/10.1210/mend.14.7.0479

Ying, Y., Qi, X., & Zhao, G. Q. (2001). Induction of primordial germ cells from murine epiblasts by synergistic action of BMP4 and BMP8B signaling pathways. *Proceedings of the National Academy of Sciences of the United States of America*, *98*(14), 7858–7862. https://doi.org/10.1073/pnas.151242798

Ying, Y., & Zhao, G. Q. (2001). Cooperation of endoderm-derived BMP2 and extraembryonic ectoderm-derived BMP4 in primordial germ cell generation in the mouse. *Developmental Biology*, *232*(2), 484–492. https://doi.org/10.1006/dbio.2001.0173

Yoon, Y., Wang, D., Tai, P. W. L., Riley, J., Gao, G., & Rivera-Pérez, J. A. (2018). Streamlined ex vivo and in vivo genome editing in mouse embryos using recombinant adeno-associated viruses. *Nature Communications*, *9*(1), 412. https://doi.org/10.1038/s41467-017-02706-7

Yu, C., Ji, S.-Y., Dang, Y.-J., Sha, Q.-Q., Yuan, Y.-F., Zhou, J.-J., Yan, L.-Y., Qiao, J., Tang, F., & Fan, H.-Y. (2016). Oocyte-expressed yes-associated protein is a key activator of the early zygotic genome in mouse. *Cell Research*, *26*(3), 275–287. https://doi.org/10.1038/cr.2016.20

Yuan, G., Yang, G., Zheng, Y., Zhu, X., Chen, Z., Zhang, Z., & Chen, Y. (2015). The non-canonical BMP and Wnt/β-catenin signaling pathways orchestrate early tooth development. *Development (Cambridge)*, *142*(1), 128–139. https://doi.org/10.1242/dev.117887

Zenker, J., White, M. D., Gasnier, M., Alvarez, Y. D., Lim, H. Y. G., Bissiere, S., Biro, M., & Plachta, N. (2018). Expanding Actin Rings Zipper the Mouse Embryo for Blastocyst Formation. *Cell*, *173*(3), 776-791.e17. https://doi.org/10.1016/j.cell.2018.02.035

Zhang, F., Li, X., He, M., Ye, D., Xiong, F., Amin, G., Zhu, Z., & Sun, Y. (2020). Efficient generation of zebrafish maternal-zygotic mutants through transplantation of ectopically induced and Cas9/gRNA targeted primordial germ cells. *Journal of Genetics and Genomics*, *47*(1), 37–47. https://doi.org/10.1016/j.jgg.2019.12.004

Zhang, G.-M., Zhang, T.-T., An, S.-Y., El-Samahy, M. A., Yang, H., Wan, Y.-J., Meng, F.-X., Xiao, S.-H., Wang, F., & Lei, Z.-H. (2019). Expression of Hippo signaling

pathway components in Hu sheep male reproductive tract and spermatozoa. *Theriogenology*, *126*, 239–248. https://doi.org/10.1016/j.theriogenology.2018.12.029

Zhang, H., & Bradley, A. (1996). Mice deficient for BMP2 are nonviable and have defects in amnion/chorion and cardiac development. *Development*, *122*(10), 2977–2986. https://doi.org/10.1242/dev.122.10.2977

Zhang, H., Ji, S., Zhang, K., Chen, Y., Ming, J., Kong, F., Wang, L., Wang, S., Zou, Z., Xiong, Z., Xu, K., Lin, Z., Huang, B., Liu, L., Fan, Q., Jin, S., Deng, H., & Xie, W. (2023). Stable maternal proteins underlie distinct transcriptome, translatome, and proteome reprogramming during mouse oocyte-to-embryo transition. *Genome Biology*, *24*(1), 1–25. https://doi.org/10.1186/s13059-023-02997-8

Zhang, Y. E. (2009). Non-Smad pathways in TGF-β signaling. *Cell Research*, *19*(1), 128–139. https://doi.org/10.1038/cr.2008.328

Zhao, X. Y., Li, W., Lv, Z., Liu, L., Tong, M., Hai, T., Hao, J., Guo, C. L., Ma, Q. W., Wang, L., Zeng, F., & Zhou, Q. (2009). IPS cells produce viable mice through tetraploid complementation. *Nature*, *461*(7260), 86–90. https://doi.org/10.1038/nature08267

Zhao, Y., Zhao, T., Guan, J., Zhang, X., Fu, Y., Ye, J., Zhu, J., Meng, G., Ge, J., Yang, S., Cheng, L., Du, Y., Zhao, C., Wang, T., Su, L., Yang, W., & Deng, H. (2015). A XEN-like State Bridges Somatic Cells to Pluripotency during Chemical Reprogramming. *Cell*, *163*(7), 1678–1691. https://doi.org/10.1016/j.cell.2015.11.017

Zheng, Y., & Pan, D. (2019). The Hippo Signaling Pathway in Development and Disease. *Developmental Cell*, *50*(3), 264–282. https://doi.org/10.1016/j.devcel.2019.06.003

Zhou, F., Sun, Y., Gao, Q., & Wang, H. (2020). microRNA-21 regulates the proliferation of placental cells via FOXM1 in preeclampsia. *Experimental and Therapeutic Medicine*, 1871–1878. https://doi.org/10.3892/etm.2020.8930

Zhu, H., Pan, Y., Jiang, Y., Li, J., Zhang, Y., & Zhang, S. (2019). Activation of the Hippo/TAZ pathway is required for menstrual stem cells to suppress myofibroblast and inhibit transforming growth factor β signaling in human endometrial stromal cells. *Human Reproduction*, *34*(4), 635–645. https://doi.org/10.1093/humrep/dez001

Zhu, M., Cornwall-Scoones, J., Wang, P., Handford, C. E., Na, J., Thomson, M., & Zernicka-Goetz, M. (2020). Developmental clock and mechanism of de novo polarization of the mouse embryo. *Science*, *370*(6522).

https://doi.org/10.1126/science.abd2703

Zhu, M., Leung, C. Y., Shahbazi, M. N., & Zernicka-Goetz, M. (2017). Actomyosin polarisation through PLC-PKC triggers symmetry breaking of the mouse embryo. *Nature Communications*, *8*(1). https://doi.org/10.1038/s41467-017-00977-8

Zhu, M., Xu, M., Zhang, J., & Zheng, C. (2023). The role of Hippo pathway in ovarian development. *Frontiers in Physiology*, *14*(June), 1–15. https://doi.org/10.3389/fphys.2023.1198873

Zhu, M., & Zernicka-Goetz, M. (2020). Principles of Self-Organization of the Mammalian Embryo. *Cell*, *183*(6), 1467–1478. https://doi.org/10.1016/j.cell.2020.11.003

Zinski, J., Tajer, B., & Mullins, M. C. (2018). TGF-β Family Signaling in Early Vertebrate Development. *Cold Spring Harbor Perspectives in Biology*, *10*(6), a033274. https://doi.org/10.1101/cshperspect.a033274